A multilevel assessment of the drivers of fish contribution to the inorganic carbon cycle on coral reefs

Universität Bremen

Mattia Ghilardi

Faculty 2 Biology and Chemistry
Universität Bremen

A dissertation
in partial fulfillment of the requirements for the degree of

Doctor of Natural Sciences
- Der. rer. nat. -

March 2023, Bremen

The work contained within this dissertation was conducted between July 2019 and March 2023 at the Leibniz Centre for Tropical Marine Research (ZMT) in Bremen, Germany.

Supervisors:

Dr. Sonia Bejarano (Primary supervisor)

Prof. Dr. Christian Wild (Official supervisor)

Prof. Dr. Valeriano Parravicini

Dr. Sebastian C. A. Ferse

PD Dr. Tim Rixen

Reviewers:

Prof. Dr. Grace K. Saba

Prof. Dr. Alastair R. Harborne

Prof. Dr. Martin Grosell

Examination committee:

Prof. Dr. Marko Rohlfs (Chair)

Prof. Dr. Christian Wild

Prof. Dr. Grace K. Saba

Prof. Dr. Alastair R. Harborne

Additional committee members:

Dr. Sonia Bejarano

Viktoria Sturm

Date of PhD Colloquium: 24th May 2023

In memoria di nonno Gianni e nonna Angela.

Acknowledgements

There are many people I would like to thank, without whom the completion of this thesis would not have been possible. First and foremost, a big thanks goes to Sonia, who gave me this opportunity and the privilege of being the first PhD student under her supervision. Despite my limited experience at the time, you saw potential in me. You invited me to take part in a large international project, holding a position with several responsibilities. Despite this you have given me full freedom to manage myself and to develop and pursue my ideas. This has allowed me to mature deeply as a person and as a researcher. Thank you for your guidance, advice, continued encouragement and support. Thank you for your constant availability, I have always been able to count on you when I needed it. I am looking forward to continue our collaboration for a long time.

Christian, Sebastian, Tim and Vale, thank you for your continued support and guidance. You have always encouraged me, but at the same time you have also taught me to be more realistic in my goals and expectations. This is a lesson that I will always carry with me and without which this thesis would not have finished yet. Grazie Vale per aver accettato di ospitarmi come tirocinante in un momento complicato per me, avermi insegnato molto in poco tempo ed avermi aperto le porte a questa opportunità di tesi. So di aver sempre potuto contare su di te quando ne avessi avuto bisogno.

Thanks to all the members of the examination committee who kindly accepted to be part of it. A particular thanks goes to the three reviewers, Alastair Harborne, Grace Saba, and Martin Grosell, for accepting the invitation to read and evaluate this thesis.

I would like to thank the great support I received from the ZMT labs in analysing my samples in the midst of the pandemic. Two people in particular, Matthias Birkicht, who spent considerable time developing a specific protocol for my project and was always open to discussion and knowledge exchange, and Sebastian Flotow, who introduced me to SEM and EDX analysis and always waited patiently for me to complete my work.

There are many other people who have contributed directly to this thesis. Special thanks to Michael Salter, Rod Wilson, and Chris Perry, who agreed to contribute to this project by generously sharing their data and expertise on fish

Abstract

Marine fish play important functional roles within the carbon cycle, including the production and excretion of intestinal carbonates. With fish accounting for at least 3-15% of total marine carbonate production, the global significance of this process is clear. A comprehensive assessment of the drivers of fish carbonate excretion rate and mineralogy is however lacking. Closing this gap is imperative to fully understand the role of fish in the inorganic carbon cycle and to predict how it may change in future. Focusing on tropical and subtropical reefs, this thesis assessed the drivers of fish contributions to the inorganic carbon cycle at different ecological levels and spatial scales. At the individual level, this project compiled intestinal traits for 142 species and carbonate excretion rates and mineralogy for 85 species. A comprehensive modelling approach then identified the species traits and environmental factors that influence individual excretion rates and mineralogy. At the community level and at the global scale, a novel analysis of >1,400 reefs mapped distribution patterns in fish carbonate excretion and mineralogy. A causal inference analysis identified the major ecological, environmental, and socio-economic factors driving these community-level patterns. At the regional scale (i.e., in the Australian coral reefs context), structural equation models disentangled the indirect effects of human gravity (i.e., a proxy for human pressure) and fisheries management on fish contributions to inorganic carbon cycling. Findings at the individual level confirmed the long-assumed direct link between fish carbonate excretion and metabolic rate and showed that diet strongly influences intestinal morphology. Relative intestinal length was uncovered as a strong driver of carbonate excretion rates and mineralogy, as were taxonomic identity and temperature. Current global patterns of fish contribution to the inorganic carbon cycle are primarily driven by fish community structure, sea surface temperature, and human gravity. Carbonate excretion rates peaked in highly productive areas supporting high fish biomass, especially within the upper trophic levels, and where human gravity is low. Globally, fish communities predominantly excrete the more soluble carbonates and their proportion increases with increasing temperature. On Australian reefs, fish carbonate excretion was strongly affected by human impact through reduced fish biomass despite the region's relatively low fishing pressure. In this particular geographic context, current fisheries management is not sufficient to maintain fish carbonate

excretion, despite positive effects on fish biodiversity. This thesis advances our understanding of the role of fish in inorganic carbon cycling from the physiological, ecological, biogeographic, chemical, mineralogical, and conservation perspectives. It unravels the complex variability of this function across ecological levels and spatial scales. Coupled with predictive models, this information could yield solid predictions of the future levels of this function in light of anthropogenic impacts and climate-driven range shifts. While fish carbonate excretion may increase with climate change, excreted carbonates will dissolve faster and/or at shallower water depths, thereby changing their influence on seawater chemistry and reducing their sedimentation potential. Protecting large predators would promote inorganic carbonate production and other fish roles within the carbon cycle. However, fisheries management has in places limited capacity to sustain fish inorganic carbon cycling. The need for effective, context-tailored management approaches that address socio-economic factors beyond fishing pressure is strongly emphasised.

Zusammenfassung

Meeresfische spielen im Kohlenstoffkreislauf eine wichtige Rolle, unter anderem bei der Produktion und Ausscheidung von Darmkarbonaten. Da Fische für mindestens 3-15 % der gesamten marinen Karbonatproduktion verantwortlich sind, ist die globale Bedeutung dieses Prozesses offensichtlich. Eine umfassende Bewertung der Faktoren, die für die Ausscheidungsrate von Fischkarbonat und die Mineralogie verantwortlich sind, steht jedoch noch aus. Diese Lücke muss unbedingt geschlossen werden, um die Rolle der Fische im anorganischen Kohlenstoffkreislauf vollständig zu verstehen und um vorauszusagen, wie sie sich in Zukunft verändern könnte. Im Rahmen dieser Arbeit, die sich auf tropische und subtropische Riffe konzentriert, wurden die Einflussfaktoren für den Beitrag der Fische zum anorganischen Kohlenstoffkreislauf auf verschiedenen ökologischen Ebenen und räumlichen Maßstäben untersucht. Auf der organismischen Ebene wurden im Rahmen dieser Arbeit Merkmale für 142 Arten sowie Karbonatausscheidungsraten und Mineralogie für 85 Arten zusammengestellt. Mit Hilfe eines umfassenden Modellierungsansatzes wurden dann die Arteneigenschaften und Umweltfaktoren ermittelt, die die individuellen Ausscheidungsraten und die Mineralogie beeinflussen. Auf Gemeinschaftsebene und auf globaler Ebene wurden in einer neuartigen Analyse von mehr als 1 400 Riffen Verteilungsmuster der Karbonatausscheidung und Mineralogie von Fischen kartiert. Durch eine Kausalanalyse wurden die wichtigsten ökologischen, ökologischen und sozioökonomischen Faktoren ermittelt, die diese Muster auf Gemeinschaftsebene beeinflussen. Auf regionaler Ebene (d. h. im Kontext der australischen Korallenriffe) wurden mit Hilfe von Strukturgleichungsmodellen die indirekten Auswirkungen des menschlichen Drucks und des Fischereimanagements auf den Beitrag der Fische zum anorganischen Kohlenstoffkreislauf aufgeschlüsselt. Die Ergebnisse auf der orgnismischen Ebene bestätigten die seit langem angenommene direkte Verbindung zwischen der Karbonatausscheidung der Fische und ihrer Stoffwechselrate und zeigten, dass die Ernährung die Darmmorphologie stark beeinflusst. Die relative Darmlänge erwies sich als starker Einflussfaktor auf die Karbonatausscheidungsrate und die Mineralogie, ebenso wie die taxonomische Identität und die Temperatur. Die derzeitigen globalen Muster des Beitrags der Fische zum anorganischen Kohlenstoffkreislauf in erster Linie von der Struktur der Fischgemeinschaft, der Meeresoberflächentemperatur und des menschlichen Drucks

bestimmt werden. Die Karbonatausscheidungsraten erreichten ihren Höhepunkt in hochproduktiven Gebieten, die eine hohe Fischbiomasse aufweisen, insbesondere in den oberen trophischen Ebenen, und wo der menschliche Druck gering war. Weltweit scheiden Fischgemeinschaften überwiegend die löslicheren Karbonate aus, und ihr Anteil nimmt mit steigender Temperatur zu. In den australischen Riffen wurde die Karbonatausscheidung der Fische trotz des relativ geringen Fischereidrucks in der Region durch den menschlichen Einfluss stark beeinträchtigt, da die Fischbiomasse abnahm. In diesem besonderen geografischen Kontext reicht das derzeitige Fischereimanagement nicht aus, um die Karbonatausscheidung von Fischen aufrechtzuerhalten, trotz der positiven Auswirkungen auf die biologische Vielfalt der Fische. Diese Arbeit verbessert unser Verständnis der Rolle von Fischen im anorganischen Kohlenstoffkreislauf aus physiologischer, ökologischer, biogeografischer, chemischer, mineralogischer und naturschutzfachlicher Sicht. Sie entschlüsselt die komplexe Variabilität dieser Funktion über ökologische Ebenen und räumliche Maßstäbe hinweg. In Verbindung mit Vorhersagemodellen könnten diese Informationen solide Vorhersagen über das künftige Ausmaßdieser Funktion angesichts der anthropogenen Einflüsse und der klimabedingten Arealverschiebung liefern. Während die Karbonatausscheidung von Fischen mit dem Klimawandel zunehmen könnte, werden sich die ausgeschiedenen Karbonate schneller und/oder in geringerer Wassertiefe auflösen, wodurch sich ihr Einfluss auf die Meerwasserchemie verändert und ihr Sedimentationspotenzial verringert. Der Schutz großer Raubfische würde die anorganische Karbonatproduktion und andere Funktionen der Fische im Kohlenstoffkreislauf fördern. Das Fischereimanagement ist jedoch nur begrenzt in der Lage, den anorganischen Kohlenstoffkreislauf der Fische zu unterstützen. Es wird nachdrücklich auf die Notwendigkeit wirksamer, kontextbezogener Managementansätze hingewiesen, die neben dem Fischereidruck auch sozioökonomische Faktoren berücksichtigen.

Contents

Contents

Introduction

Ecosystem functions, services, and conservation

Ecosystem functioning describes the collective activities of all life forms and their effects on the physical conditions of their environment. Biodiversity is thus an integral part of ecosystem functioning and vice versa. A myriad of species and their interactions enable ecosystems to function, but it is also true that functioning ecosystems are needed for biodiversity to thrive. The functioning of ecosystems is based on an efficient flow of energy and resources through the biosphere, which defines the structure and dynamics of ecosystems. Within an ecosystem, the movement and storage of energy and material is what defines ecosystem functions (also referred to as ecosystem processes) (Bellwood et al. 2019b), such as primary and secondary production, decomposition of dead matter, and nutrient recycling.

These functions provide humanity with a variety of services, such as food provision, oxygen production and buffering against extreme climate events, that directly or indirectly contribute to human well-being (Costanza et al. 1997). These ecosystem services can be classified into four broad categories as proposed by the Millennium Ecosystem Assessment (2005):

- *Provisioning services* provide humans with material benefits such as food, water, wood and other raw materials.
- *Regulating services* help maintain the quality of air, soil and water, and include climate regulation, carbon sequestration, pest control and pollination.
- *Supporting services*, such as habitat provision, primary productivity and nutrient cycling, are the basic ecosystem processes that contribute indirectly to human well-being by supporting biodiversity and the other ecosystem

services. This category is sometimes replaced by *Habitat services* (TEEB 2010).

- *Cultural services* provide non-material benefits such as aesthetic inspiration, cultural identity, recreational and spiritual experiences.

Certain ecosystem services, especially provisioning services, are easily understood and quantified. Others operate beyond peoples' perception (e.g., many supporting services) and thus are unnoticed or undervalued. Cultural services such as aesthetic appreciation and inspiration for culture, art and innovation are less tangible and inherently difficult to quantify. Valuing ecosystems is however useful for incentivising industry and governments towards more sustainable policies and improved management (Costanza et al. 2017). In 1997, ecosystems were estimated to provide an average of US$33 trillion per year in services, about twice as much as the global gross national product at the time (Costanza et al. 1997). Since this seminal publication, a great amount of research has increased our understanding of ecosystem services and nature's worth (Costanza et al. 2017). However, ecosystems globally are degrading rapidly, thus jeopardizing ecosystem services.

Virtually every ecosystem on land and in the ocean is facing profound changes in response to climate change and increasing disturbance activity (Keith et al. 2022; Stuart-Smith et al. 2022; Lapola et al. 2023). The oceans are however experiencing faster rates of species turnover and biodiversity reorganisation (Blowes et al. 2019; Eriksson and Hillebrand 2019). Ecosystems are rapidly transforming into novel configurations (Hughes et al. 2017a; Hughes et al. 2018a; Stuart-Smith et al. 2018; Benedetti et al. 2021; Seidl and Turner 2022). This has wide-reaching implications for ecosystem functioning, the ecosystem service supply, and ultimately human well-being (Williams and Graham 2019; Woodhead et al. 2019; Bianchi et al. 2021; Cavan and Hill 2021; Eddy et al. 2021; Hicks et al. 2021). Climate-related erosion of ecosystem services in the Amazon may cost US$ 7.7 trillion to the regional economy in a period of 30 years (Lapola et al. 2018), while economic losses from mangroves deforestation are estimated to be up to US$42 billion annually (UNEP 2014).

Sustaining ecosystem services requires knowledge regarding the mechanisms that drive changes in ecosystem functioning (Keith et al. 2015). Identifying the drivers of ecosystem functions at multiple scales is not only a central task in ecology, but also critical to predict the functioning and service supply of future ecosystems. Coupled with modelling approaches that integrate the plausible socio-economic and climate change scenarios (Shared Socioeconomic Pathway-Representative Concentration Pathway, SSP-RCP, van Vuuren et al. 2014), this knowledge provide convincing evidence to influence policy responses.

Of the many processes that occur within and across ecosystems, the carbon cycle is particularly important for maintaining a stable climate and sustaining life on Earth. This cycle underpins the vast majority of services provided by nature. Comprehensive accounts of how carbon cycles through ecosystems marking its sinks and sources, are thus crucial to guide actions aimed at climate change mitigation and safeguarding ecosystem services supply.

The global and marine carbon cycles

As one of the primary building blocks of all organic molecules, carbon is essential to life. In the atmosphere, it plays a key role in setting Earth's temperature. As an energy source, it has fuelled technological innovation and economic growth. The carbon cycle is the biogeochemical cycle that describes the flow of carbon between the biotic (biosphere) and abiotic (atmosphere, hydrosphere and geosphere) systems of Earth. Many biological, chemical, geological and physical processes are involved in the exchange of carbon between these compartments. These include long-term processes of carbon sequestration to, and release from, carbon sinks.

The carbon cycle can be seen as two interconnected subcycles, one where carbon moves rapidly through the biosphere ('fast' carbon cycle) and the other involving medium to long-term geological processes ('slow' carbon cycle). The fast carbon cycle is characterised by the uptake of carbon by autotrophs, which enters the biosphere and is recycled through the food web. This organic carbon

is then released back to the atmosphere through respiration and decomposition on annual and decadal timescales. The slow carbon cycle includes the formation and weathering of sedimentary rock over millions of years. The subduction (i.e., the movement of a tectonic plate under another) of ocean's carbon sediments into the Earth's mantle generates carbon dioxide (CO_2) that can be released into the atmosphere through volcanic eruptions (Burton et al. 2013). Medium-term processes include the exchange of carbon between the ocean and atmosphere which can take centuries (Heinze and Maier-Reimer 1991).

The ocean plays a central role in the global carbon cycle and exerts a major control on climate through the absorption and sequestration of atmospheric CO_2. In the last decade, 2.9 billion metric tons of carbon, equivalent to 26% of the global anthropogenic CO_2 emissions, were absorbed by the ocean each year (Friedlingstein et al. 2022). The marine carbon cycle can regulate the partial pressure of atmospheric CO_2 ($p$$CO_2$) through three well established mechanisms: the solubility pump, the organic carbon pump (also known as biological pump) and the inorganic carbonate pump (Figure 1) (Heinze and Maier-Reimer 1991). The solubility pump is a physico-chemical process by which dissolved inorganic carbon (DIC) is transported from the ocean's surface to depth and favours the CO_2 uptake of the ocean. This mostly occurs at high latitudes where deep waters are formed and CO_2 is more soluble, due to higher solubility in seawater at low temperature and salinity (Weiss 1974). Conversely, the reduced solubility in warmer waters causes CO_2 to be released into the atmosphere where cold deep water upwells at low latitudes (Feely et al. 1999). The organic carbon pump and inorganic carbonate pump are driven by biological processes and export particulate organic carbon (POC) and particulate inorganic carbon (PIC), respectively, from surface waters.

The organic carbon pump is characterised by the fixation of dissolved CO_2 into organic carbon by photosynthetic organisms, such as phytoplankton, in the euphotic zone. The process is thus limited by availability of light and nutrients. This organic carbon is then transported to the deeper ocean through passive sinking of particles, active vertical migration of metazoans (zooplankton and fish), or

Figure 1: Schematic diagram of the three ocean carbon pumps that regulate the partial pressure of atmospheric CO_2. Redrawn from Heinze and Maier-Reimer (1991).

physical mechanisms (Boyd et al. 2019). This process drives carbon sequestration in the deep ocean and increases CO_2 uptake at the surface. A small proportion of the organic matter reaches the seafloor where it can be incorporated within sediments or used by benthic organisms. However, most is remineralised back to CO_2 as particles sink below the euphotic zone and are fragmented into smaller, slower-sinking particles and consumed by microbes, zooplankton, and fishes (Giering et al. 2014; Guidi et al. 2015; Briggs et al. 2020). Upwelling and ocean mixing bring the released DIC and nutrients back to the surface leading to CO_2 release into the atmosphere and promoting new primary production. The depth at which organic carbon is remineralised directly impacts atmospheric CO_2 concentrations (Kwon et al. 2009).

The inorganic carbonate pump is characterised by the production of calcium carbonate ($CaCO_3$) by marine calcifying organisms in surface waters. Marine calcifiers include planktonic (e.g., coccolithophores, foraminifera, pteropods) and benthic

or sessile (e.g., corals, coralline algae, molluscs, crustaceans) organisms which precipitate $CaCO_3$ with different crystalline forms, mostly aragonite and calcite, to construct their skeletons and shells. They produce $CaCO_3$ by actively promoting the reaction of calcium (Ca^{2+}) and bicarbonate (HCO_3^-) ions from seawater:

$$Ca^{2+} + 2\,HCO_3^- \rightleftharpoons CaCO_3 + CO_2 + H_2O, \tag{1}$$
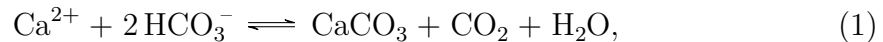
thereby consuming alkalinity and producing CO_2. This process contrasts with the other two carbon pumps in that it acts as a source of CO_2 in surface waters, enhancing ocean acidification.

Biogenic $CaCO_3$ production is also a sink of carbon. The $CaCO_3$ skeletons and shells produced by marine calcifiers may have two different fates when these organisms die. Those of benthic and sessile organisms likely become part of the local sediments as they already live in contact with the sea-bottom and in conditions favourable to calcification. Carbonates derived from pelagic organisms sink rapidly into deeper waters due to their high density. Here, they can contribute to the formation of sediments (Morse et al. 2007) or dissolve (due to higher pressure and lower temperature, Millero 2007) thus releasing alkalinity and decreasing CO_2 (Equation (1) from right to left). The depth at which carbonates dissolve depends on their mineralogy and local water chemistry (Millero 2007; Sulpis et al. 2021). Some, such as high-magnesium calcite (HMC), dissolve at relatively shallow depth where they can contribute to increase alkalinity and pH (Sulpis et al. 2021). Aragonite and low-magnesium calcite (LMC) dissolve at greater depth where they act as a negative feedback on the CO_2 brought in the deep ocean by the solubility pump. Recent evidence suggests that a large portion of pelagic $CaCO_3$ may dissolve within the euphotic zone, potentially caused by dissolution within the guts of grazers or by microbial respiration of organic carbon within aggregates containing $CaCO_3$ (Ziveri et al. 2023). Upwelling and vertical mixing (a slow process taking 500-1000 years, Millero 2007) bring the HCO_3^- ions released by carbonate dissolution to surface waters, favouring CO_2 uptake of the ocean.

Fish contribution to the marine carbon cycle

Fish are the most abundant vertebrates in the ocean and contribute to the carbon cycle through multiple mechanisms. They directly and indirectly affect the organic carbon pump, but they also have a significant role in the inorganic carbonate pump (Wilson et al. 2009). Based on the high abundance and biomass of fish in epipelagic and mesopelagic ecosystems, these vertebrates provide a substantial downward flux of (organic and inorganic) carbon. This has been estimated at ~16% of total carbon flux out of the euphotic zone, with sequestration time of 10 years to >50 years (Saba et al. 2021). Yet, this estimate exhibits high uncertainty due to limited data availability (Saba et al. 2021).

Marine fish directly and indirectly influence the organic carbon pump by consuming and recycling primary or secondary producers (Figure 2). The ingested carbon is recycled in four ways (Schiettekatte et al. 2020): 1) used for metabolic process and respired CO_2 is released through the gills, 2) used to build new body mass in which carbon is stored, 3) egested into faecal material (POC), 4) excreted as dissolved organic carbon (DOC). Through their diet, fish also recycle other elements, such as nitrogen and phosphorous, thereby contributing to their biogeochemical cycles (Allgeier et al. 2017; Schiettekatte et al. 2020). Excreted dissolved organic and inorganic nitrogen and phosphorous, together with respired CO_2, sustain the organic carbon pump by promoting primary production (Allgeier et al. 2017).

Carbon and nutrients stored in fish bodies can be recycled through the food web or sink towards the sea bottom when fish die. Carcasses of fish can be consumed while sinking or when they reach the benthos, and some can be buried within sediments. This process could thus provide an important but yet unquantified export of carbon to the deep ocean, particularly through sinking of large-bodied fishes (Mariani et al. 2020). Carbon sequestration through carcasses deadfall is however hampered by ocean fisheries which have prevented the export of 21.8 million metric tons of carbon through sinking of fish bodies since 1950 (Mariani et al. 2020).
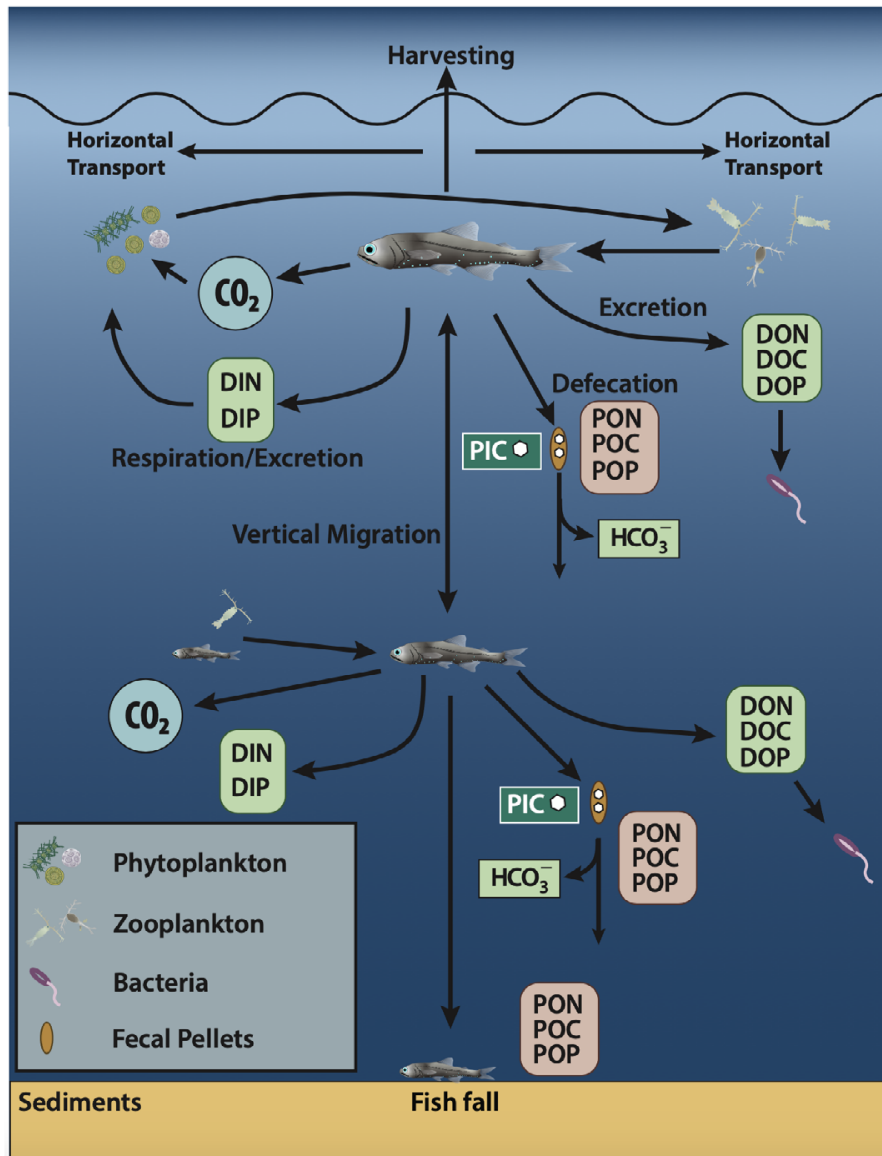
Figure 2: Conceptual diagram showing the mechanisms by which fish contribute to carbon and nutrient cycling. A diel vertically migrating midwater myctophid fish is used as a model organism. Arrows between different types of organisms infer predation from a prey item to a predator (arrow pointing to the predator; e.g., zooplankton feeding on phytoplankton in the upper water column, myctophids feeding on zooplankton in the upper water column, myctophid feeding on zooplankton and small fishes in mid-water). From Saba et al. (2021).

In addition to carcasses deadfall, fish contribute to the passive organic carbon flux through egestion of fast-sinking faecal material (Staresinic et al. 1983; Saba and Steinberg 2012). Faecal pellets produced by epipelagic fish reach the benthos in <1 day in most coastal habitats (Saba and Steinberg 2012), or sink to the mesopelagic zone where they are remineralised. Carbon sequestration time is <100 years for an export to <400 m (Saba et al. 2021). Faecal pellets produced by mesopelagic fish, the most abundant fish and vertebrates on Earth (Irigoien et al. 2014), can reach a depth of thousands of metres thus sequestering carbon for hundreds of years (Huffard et al. 2020; Saba et al. 2021).

Mesopelagic fish also contribute to the ocean carbon pump by performing diel vertical migrations to feed near the surface at night (Davison et al. 2013). Here, they excrete respired CO_2 and are fed upon by predators. Returning to deeper waters at night they actively transport organic carbon which is released through egestion of POC and excretion of DOC and CO_2 (Davison et al. 2013). Fish not only transport carbon vertically, they can also transport it horizontally. Many species, for instance, undergo seasonal migrations related to spawning and ontogenetic cycles. Fish also perform daily movements cycles between foraging and resting areas, transporting carbon between these areas (e.g., Currey et al. 2015; Papastamatiou et al. 2018). Fish larvae are transported by currents and upwelling filaments, moving carbon from coastal environments into offshore waters (Santana-Falcón et al. 2020). Through their movements fish also contribute to small- to regional-scale turbulent mixing which could drive new primary production by bringing nutrients into shallow depths (Fernández Castro et al. 2022).

Further, all marine bony fishes contribute to the inorganic carbonate pump through the continuous excretion of intestinal carbonates (PIC) as a byproduct of osmoregulation (Walsh et al. 1991; Wilson et al. 2002; Wilson et al. 2009). This process has been identified as a significant source of $CaCO_3$ in surface oceans and plays an important role in seawater acid-base chemistry (Wilson et al. 2009). As fish carbonates are generally more soluble than most biogenic carbonates (Wilson et al. 2009; Woosley et al. 2012; Foran et al. 2013; Salter et al. 2017), they are

hypothesised to dissolve at shallower depths (<1 km), replenishing surface ocean alkalinity and decreasing CO_2 (Wilson et al. 2009). This would partially explain the widespread increase in seawater alkalinity over the upper kilometre (Wilson et al. 2009; Sulpis et al. 2021). However, the fate of fish carbonates once excreted remains unresolved, preventing the estimation of their net impact on seawater chemistry. In shallow areas they can rapidly reach the benthos and accumulate within sediments (Perry et al. 2011; Salter et al. 2014). This results in both carbon sink and net acidification of seawater due to CO_2 release during calcification (Equation (1)). The relatively high solubility of fish-generated carbonate sediments also suggests that they would be the first to dissolve as carbonate saturation state decreases due to ocean acidification (Morse et al. 2006; Roberts et al. 2017). This could partially buffer the impact of acidification on benthic calcifiers.

Mesopelagic fish are a source of $CaCO_3$ in deeper waters, but they could also produce carbonates at depth during the day and excrete them near the surface at night. Their dissolution would result in a net removal of CO_2 from surface waters and corresponding increase in alkalinity. Therefore, it has been hypothesised that they may drive an upward alkalinity pump which can buffer surface ocean acidification (Roberts et al. 2017). Fish carbonates are excreted as mucus-coated pellets or incorporated within faeces when fish are feeding (Walsh et al. 1991; Wilson et al. 2002). They indirectly affect organic carbon by adding a dense ballast to faecal pellets or other sinking organic particles. The PIC/POC ratio of particles thus determines their sinking rate and the depth to which organic carbon is exported.

Fish carbonate excretion and composition

Carbonate precipitation and excretion

Marine bony fish precipitate carbonate crystals within their intestines as a result of their need to continuously drink seawater (Figure 3) (Wilson et al. 2002). Indeed,

they live in a hyperosmotic environment as their internal osmotic pressure (~310-350 mOsm) is approximately one-third that of ambient seawater (~1000 mOsm) (Shehadeh and Gordon 1969). This causes substantial osmotic loss of water through the gills and other permeable surfaces, which is replaced by the ingestion of relatively large volumes of seawater (Smith 1930; Shehadeh and Gordon 1969; Wilson et al. 1996; Grosell et al. 2004). However, ensuring intestinal water absorption to maintain body hydration requires lowering the luminal osmotic pressure to or below that of the blood (Genz et al. 2011). Fish achieve this primarily through absorption of sodium (Na^+) and chloride (Cl^-) ions through the water-impermeable esophagous and the anterior intestine (Hirano and Mayer-Gostan 1976; Parmelee and Renfro 1983; Nagashima and Ando 1994; Grosell et al. 2007; Whittamore 2012). These are then actively excreted via the gills (Larsen et al. 2014). Further, the alkaline (pH up to 9.2) and HCO_3^--rich (50-100 mM) intestinal fluid promotes the precipitation of seawater calcium (Ca^{2+}) and magnesium (Mg^{2+}) ions as $Ca(Mg)CO_3$ crystals, which are then excreted at high rates either within mucus-coated pellets or faeces (Shehadeh and Gordon 1969; Walsh et al. 1991; Wilson et al. 1996; Wilson et al. 2002). The HCO_3^- ions that react with Ca^{2+} and Mg^{2+} derive from metabolic CO_2 and are secreted into the intestinal lumen (Grosell et al. 2005; Grosell et al. 2009). The calcification process is governed by a proteinaceous matrix (Schauer et al. 2016) and reduces the luminal osmotic pressure by 70-100 mOsm (Wilson et al. 2002; Grosell et al. 2009). This reduction in osmotic pressure is critical to promote intestinal water absorption and thus a successful osmoregulation (Genz et al. 2011). Intestinal calcification also plays an important role in the sh's calcium homeostasis (Whittamore 2012) and prevents intestinal calcium being absorbed into the blood reducing the risk of renal stone formation (Wilson and Grosell 2003).

The mechanisms of carbonate precipitation in fishes and their physiological importance are now well understood. Further, we know relatively little about the drivers of carbonate excretion rate, even though this knowledge is critical for a more complete understanding of the role fish play in the inorganic carbon cycle. Carbonate precipitation depends on the amount of calcium and magnesium imbibed
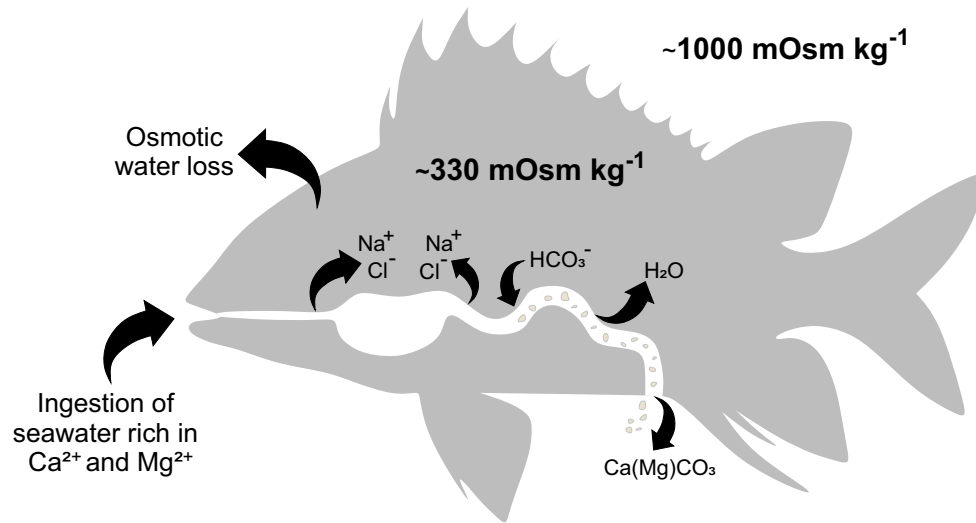
Figure 3: Schematic presentation of carbonate precipitation in the intestine of a marine bony fish and its excretion. Ca^{2+} and Mg^{2+} imbibed with seawater combine with HCO_3^- secreted by the intestine in a precipitation reaction governed by a proteinaceous matrix (not shown) to form precipitates in the intestinal lumen.

with seawater, thus higher drinking rates lead to higher carbonate precipitation and excretion rates (Genz et al. 2008). As drinking rate is directly related to metabolic rate (Takei and Tsukada 2001), it is assumed that carbonate excretion rate increases proportionally with metabolic rate (Jennings and Wilson 2009; Wilson et al. 2009). This assumption was adopted within a global modelling study that estimated fish to account for 3 to 15% (0.04-0.11 x 10^{15} g of $CaCO_3$-C year^{-1}) of the total global new carbonate production in the surface oceans (Wilson et al. 2009). Less conservative estimates suggest that their contribution can reach up to 45% (Wilson et al. 2009). However, the assumption remains untested. Carbonate excretion rate per unit of body mass was later found to decrease with increasing body mass in reef fishes (Perry et al. 2011; Salter et al. 2018), and to increase with increasing temperature in the sheepshead minnow (*Cyprinodon variegatus*) (Wilson et al. 2009) and Gulf toadfish (*Opsanus beta*) (Heuer et al. 2016). These results are consistent with metabolic theory (Brown et al. 2004), but a rigorous investigation to confirm a direct relationship between carbonate excretion rate and metabolic rate across species is lacking.

Fish contribution to total oceanic carbonate production is predicted to increase in response to climate change (Wilson et al. 2009). The formation of carbonate precipitates increases with temperature due to an increase in metabolic rate and metabolic CO_2 production (Wilson et al. 2009). Temperature also affects drinking rate indirectly, as fish respond to seawater warming by increasing gill ventilation, resulting in an increased osmotic loss of water. Furthermore, unlike other marine calcifiers which decrease carbonate production rates as dissolved CO_2 increases (Feely et al. 2004; Orr et al. 2005), fish are predicted to increase carbonate excretion rates. Indeed, increases in $p\mathrm{CO_2}$ within fish blood, driven by rising levels of ambient CO_2 (Pörtner et al. 2004), will stimulate further production of HCO_3^- by the intestinal cells (Grosell et al. 2005; Gregório et al. 2019). This suggests that an increase in carbonate precipitation can be expected with increasing seawater $p\mathrm{CO_2}$ (Grosell 2019). Although these predictions have been tested on a few species (Perry et al. 2010; Heuer et al. 2012; Rogers 2015; Heuer et al. 2016; Gregório et al. 2019), evidence of rising carbonate excretion rates at CO_2 levels expected through climate change is limited (Grosell 2019).

In addition to metabolism, carbonate excretion rate may be influenced by other factors that determine calcium and magnesium ingestion rates. Drinking rates increase with salinity due to higher osmotic water loss (Maetz and Skadhauge 1968; Shehadeh and Gordon 1969; Tytler and Ireland 1994; Genz et al. 2008). Indeed, a positive relationship between salinity and carbonate excretion rate has been demonstrated in several fish species (Genz et al. 2008; Mekuchi et al. 2010; Schauer et al. 2018). The Japanese eel (*Anguilla japonica*), for instance, did not precipitate carbonates in freshwater but it did after acclimation to seawater in a salinity-dependent manner (Mekuchi et al. 2010). The efficiency of intestinal water absorption may indirectly affect drinking rate and thus carbonate excretion rate. To replace lost water, fish should require lower drinking rates if they absorb water more efficiently. Water absorption efficiency has been measured in several species and ranges between 38.5 and 85% (Smith 1930; Hickman 1968; Shehadeh and Gordon 1969; Fletcher 1978; Sleet and Weber 1982; Wilson et al. 1996; Wilson et al. 2002;

Genz et al. 2008; Whittamore et al. 2010; Whittamore 2012). This high variability may be related to variability in intestinal morphology, and its potential influence on carbonate excretion has yet to be investigated. Fish also ingest large amounts of calcium (and in minor measure magnesium) with food. This leads to high luminal concentrations of these ions which directly affect carbonate precipitation (Wilson and Grosell 2003; Mekuchi et al. 2010).

Carbonate excretion rates have been estimated for a range of tropical and subtropical species (Perry et al. 2011; Salter et al. 2017; Salter et al. 2018). The carbonate excretion rate-body mass relationship obtained from this data was used to produce regional-level estimates of fish-mediated carbonate production in The Bahamas and Australia (Perry et al. 2011; Salter et al. 2017; Salter et al. 2018). However, the range of families, body sizes, trophic levels and environmental conditions considered should be broadened through new data collection. This would allow to investigate the drivers of interspecific variation in carbonate excretion rate, to produce more robust estimates of community-level carbonate production and to better predict how this would change in response to increasing disturbances.

Carbonate morphology and mineralogy

Fish account for a significant proportion of the carbonate in surface oceans, but the significance of this function within the carbon cycle lies not only in the quantity but also in the mineralogical composition of the excreted carbonates (Wilson et al. 2009). Initially fish were assumed to excrete only high-Mg calcite (HMC) (Walsh et al. 1991; Wilson et al. 2009), which is more soluble than both aragonite and low-Mg calcite (LMC), and has a shallower saturation horizon (Woosley et al. 2012; Sulpis et al. 2021). This led to the hypothesis that fish can strongly influence alkalinity depth profiles in the ocean (Wilson et al. 2009). However, several studies have now demonstrated that fish produce a remarkable variety of crystalline morphologies and carbonate polymorphs (Figure 4) (Perry et al. 2011; Salter et al. 2012; Foran et al. 2013; Salter et al. 2017; Salter et al. 2018; Salter et al. 2019). These include LMC, HMC, aragonite, monohydrocalcite (MHC), and amorphous calcium magnesium
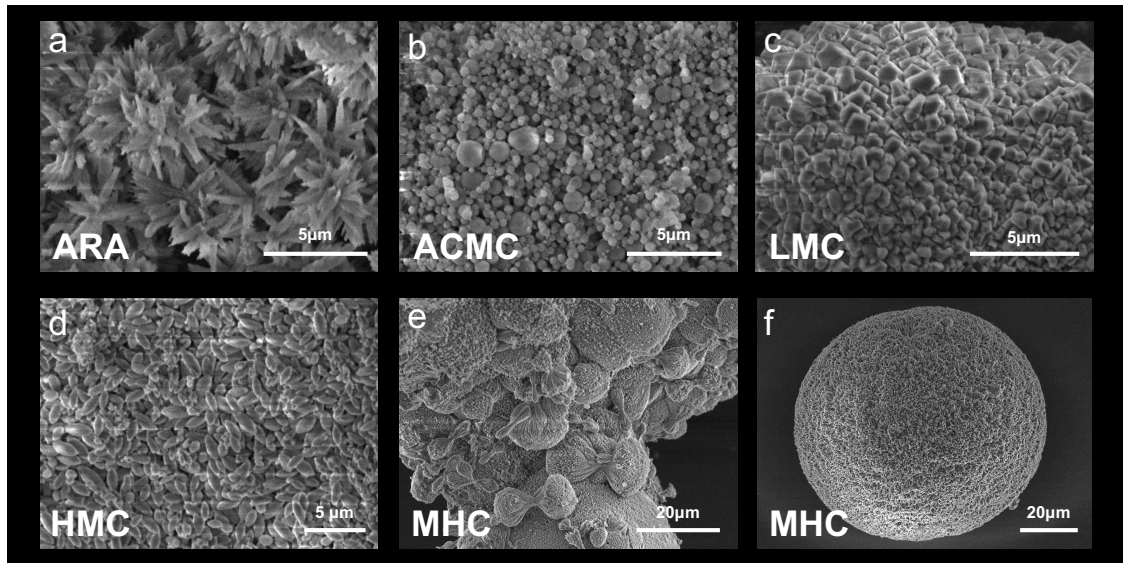
Figure 4: Scanning electron microscope images showing representative morphologies for the main carbonate polymorphs produced by fish. **a**: aragonite (ARA) needles. **b**: amorphous calcium magnesium carbonate (ACMC) nanospheres. **c**: low-magnesium calcite (LMC) rhombohedra. **d**: high-magnesium calcite (HMC) ellipsoids. **e,f**: monohydrocalcite (MHC) dumbbells and spheres.

carbonate (ACMC). The known solubility rates of these carbonate polymorphs in seawater (i.e., in order of increasing solubility: LMC < aragonite < HMC < MHC < ACMC, Plummer and Busenberg 1982; Breevi and Nielsen 1989; Fukushi et al. 2011; Woosley et al. 2012) span several orders of magnitude. This suggests that they will undergo different fates post-excretion, with highly unstable ACMC and metastable MHC likely dissolving rapidly (Foran et al. 2013). The role of fish carbonates in the inorganic carbon cycle and their influence on seawater chemistry will thus depend on the type of polymorphs produced and their relative proportions.

The mineralogical composition of fish carbonates has now been characterised for a wide range of tropical, subtropical, and temperate species (Salter et al. 2012; Salter et al. 2017; Salter et al. 2018; Salter et al. 2019). These studies have found that species within the same family typically produce the same carbonate polymorphs (Salter et al. 2017; Salter et al. 2018; Salter et al. 2019). This family-level consistency was also confirmed across biogeographic regions and large thermal gradients, with a few exceptions (Salter et al. 2018; Salter et al. 2019). These findings are particularly important as they facilitate quantification of polymorph-

specific production rates at the community-level. However, a comprehensive analysis of the drivers of the mineralogical composition of fish carbonates is lacking, yet essential to understand the contribution of fish to carbonate sediment cycling and inorganic carbon cycling.

Taking advantage of the strong family-level consistency, the first community-level estimates of carbonate mineralogy were produced for coral reef systems in The Bahamas and Australia (Salter et al. 2017; Salter et al. 2018). Carbonates excreted in The Bahamas were dominated by HMC, whereas ACMC was the dominant polymorph in Australia (Salter et al. 2018). These differences were driven by variation in fish community composition and highlighted important regional variations in the preservation potential of fish carbonates. Incorporating carbonate mineralogy within production models is therefore important for assessing the current role of fish in the inorganic carbon cycle. Furthermore, a better understanding of the environmental and socio-economic factors influencing spatial patterns in the excretion rate and mineralogical composition of fish carbonates is critical to predict how these will change under different global change scenarios.

Objectives and outline of the thesis

The goal of this dissertation is to advance our understanding of the role fish play in the marine inorganic carbon cycle. The physiological aspects underlying the precipitation and excretion of carbonates by marine fish are reasonably well understood. Intense empirical data collection efforts have expanded the database of carbonate excretion rates and mineralogical composition over the last decade, particularly for tropical and subtropical species (Perry et al. 2011; Salter et al. 2012; Salter et al. 2017; Salter et al. 2018; Salter et al. 2019). As of 2019 (the starting year of this project), we have excretion rate data from 270 fishes encompassing 39 species across 21 families collected in The Bahamas and Australia (Perry et al. 2011; Salter et al. 2017; Salter et al. 2018). Mineralogical data have also been collected in temperate settings and include >70 species (Salter et al. 2012; Salter

et al. 2017; Salter et al. 2018; Salter et al. 2019). These data have increased our understanding of the mineralogical diversity of fish carbonates and the importance of incorporating it within production models. We lack, however, a detailed and comprehensive assessment of the drivers of fish carbonate excretion rate and mineralogical composition at multiple levels, from the individual to the community. This is essential to: 1) refine current regional and global estimates of carbonate excretion and composition, 2) anticipate the impacts of anthropogenic disturbances and climate change on this ecosystem function, 3) predict future changes in the contribution of fish to the marine carbon cycle, and 4) inform appropriate policy responses to these changes.

In light of this important knowledge gap, the overarching scientific question addressed in this thesis was:

> What are the drivers of fish contribution to the marine inorganic carbon cycle?

To address this question, three specific research questions (RQs) were asked:

- RQ1) Which fish traits and environmental variables determine carbonate excretion rate and mineralogical composition in individual fishes? (*Chapters 1* and *2*)
- RQ2) What are the ecological, environmental and socio-economic factors shaping global spatial patterns in carbonate excretion and mineralogy? (*Chapter 3*)
- RQ3) How do human pressure and fisheries management affect fish inorganic carbon cycling? (*Chapter 4*)

This thesis focused on tropical and subtropical reef fish as they make up almost entirely the carbonate excretion rate database available for this project. Although they occupy a small fraction of the ocean, they represent most of marine vertebrate biodiversity (Kulbicki et al. 2013). Further, the huge amount of standardised and detailed data on reef fish communities (e.g., Edgar and Stuart-Smith 2014;

Barneche et al. 2019; Edgar et al. 2020) and associated ecological, environmental, and socio-economic data (e.g., Mora et al. 2011; Duffy et al. 2016; Cinner et al. 2016; Cinner et al. 2018) makes them the best subject to address the above mentioned questions.

The three research questions were addressed through the compilation of large databases and the application of a variety of statistical approaches (predictive models, causal inference, and structural equation models). A two-step approach was applied to answer RQ1 (Figure 5). First, a large database of fish intestinal traits (i.e., intestinal length, diameter and surface area) was compiled and Bayesian phylogenetic models were built to predict these traits. These models identified the key factors shaping fish intestinal morphology (*Chapter 1*). Second, field research was carried out in Palau to expand the existing carbonate database. Species-level relative intestinal length was predicted from *Chapter 1* and input into predictive models to identify the fish traits and environmental variables that determine the excretion rate and mineralogical composition of fish carbonates (*Chapter 2*). To address RQ2, refined community-level estimates of carbonate excretion and mineralogy at the global scale (>1,400 tropical and subtropical reef sites) were obtained combining the newly created predictive models with a standardised reef fish survey database (Reef Life Survey, www.reeflifesurvey.com). Bayesian causal inference was then applied to identify the underlying ecological, environmental and socio-economic drivers (*Chapter 3*). While causal inference is a great tool to quantify total causal effects, it fails to identify underlying mechanisms when multiple potential mediators are present. Therefore, to answer RQ3 structural equation models were used to investigate the indirect effects of human pressure and fisheries management on fish carbonate excretion through changes in fish community structure and composition. To this aim Australian reefs were used as a case study (*Chapter 4*). The findings of all chapters are finally summarised in a general discussion and future research opportunities towards a more complete understanding of the role of fish in the carbon cycle are discussed.
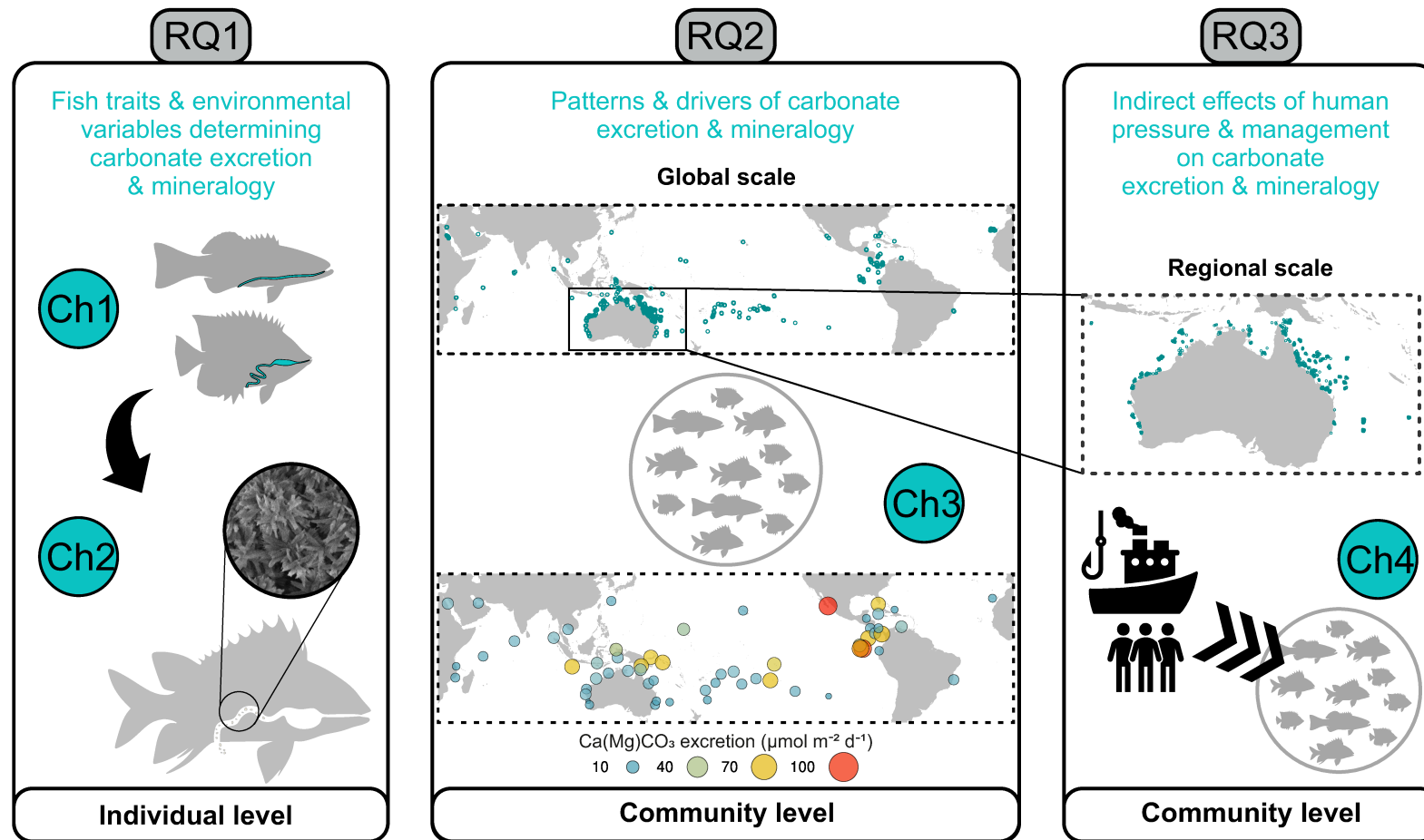
Figure 5: Thesis structure divided by research questions (RQs), which are synthesised at the top of each panel. The ecological level (i.e., individual or community) and spatial scale (i.e., regional or global) of the analyses within each chapter (Ch) is displayed. To address RQ1, large databases of fish intestinal morphology and carbonate excretion rates and mineralogy were compiled through field research and lab analyses (Ch1 and Ch2, respectively). To address RQ2, predictive models built in Ch2 were combined with an existing fish survey database of >1,400 tropical and subtropical reef sites (top map) to obtain refined estimates of carbonate excretion and mineralogy (bottom map) (Ch3). To address RQ3, Australian reefs were used as a case study (Ch4).

Author's contributions

Table 1: Contributions of the PhD candidate to tasks within each chapter (%).

Chapter	Concept / design	Data collection/ compilation	Data analysis/ interpretation	Figures/ tables	Drafting of manuscript	State of publication
1	50	50	90	100	95	Published in *Ecology and Evolution* (DOI: 10.1002/ece3.8045)
2	90	50	100	100	100	Published in *Nature Communications* (DOI: 10.1038/s41467-023-36617-7)
3	70	30	80	100	100	In preparation for *Nature Ecology & Evolution*
4	50	30	60	95	90	In preparation for *Journal of Applied Ecology*

References

Allgeier, Jacob E., Deron E. Burkepile, and Craig A. Layman (2017). "Animal pee in the sea: consumer-mediated nutrient dynamics in the world's changing oceans". In: *Global Change Biology* 23.6, pp. 2166–2178. DOI: 10.1111/gcb.13625.

Barneche, D. R. et al. (2019). "Body size, reef area and temperature predict global reef-fish species richness across spatial scales". In: *Global Ecology and Biogeography* 28.3, pp. 315–327. DOI: 10.1111/geb.12851.

Bellwood, David R. et al. (2019b). "The meaning of the term function' in ecology: A coral reef perspective". In: *Functional Ecology* 33, pp. 948–961. DOI: 10.1111/1365-2435.13265.

Benedetti, Fabio et al. (2021). "Major restructuring of marine plankton assemblages under global warming". In: *Nature Communications* 12, p. 5226. DOI: 10.1038/s41467-021-25385-x.

Bianchi, Daniele et al. (2021). "Estimating global biomass and biogeochemical cycling of marine fish with and without fishing". In: *Science Advances* 7, eabd7554. DOI: 10.1126/sciadv.abd7554.

Blowes, Shane A. et al. (2019). "The geography of biodiversity change in marine and terrestrial assemblages". In: *Science* 366.6463, pp. 339–345. DOI: 10.1126/science.aaw1620.

Boyd, Philip W. et al. (2019). "Multi-faceted particle pumps drive carbon sequestration in the ocean". In: *Nature* 568.7752, pp. 327–335. DOI: 10.1038/s41586-019-1098-2.

Breevi, Ljerka and Arne Erik Nielsen (1989). "Solubility of amorphous calcium carbonate". In: *Journal of Crystal Growth* 98, pp. 504–510.

Briggs, Nathan, Giorgio Dall'Olmo, and Hervé Claustre (2020). "Major role of particle fragmentation in regulating biological sequestration of CO2 by the oceans". In: *Science* 367.6479, pp. 791–793. DOI: 10.1126/science.aay1790.

Brown, J. H. et al. (2004). "Toward a metabolic theory of ecology". In: *Ecology* 85.7, pp. 1771–1789. DOI: 10.1007/978-3-030-84771-5_8.

Burton, Michael R., Georgina M. Sawyer, and Domenico Granieri (2013). "Deep carbon emissions from volcanoes". In: *Reviews in Mineralogy and Geochemistry* 75, pp. 323–354. DOI: 10.2138/rmg.2013.75.11.

Cavan, Emma L. and Simeon L. Hill (2021). "Commercial fishery disturbance of the global ocean biological carbon sink". In: *Global Change Biology* 28.4, pp. 1212–1221. DOI: 10.1111/gcb.16019.

Cinner, Joshua E et al. (2016). "Bright spots among the world's coral reefs". In: *Nature* 535.7612, pp. 416–419. DOI: 10.1038/nature18607.

Cinner, Joshua E. et al. (2018). "Gravity of human impacts mediates coral reef conservation gains". In: *Proceedings of the National Academy of Sciences of the United States of America* 115.27, E6116–E6125. DOI: 10.1073/pnas.1708001115.

Costanza, Robert et al. (1997). "The value of the world's ecosystem services and natural capital". In: *Nature* 387.6630, pp. 253–260. DOI: 10.1038/387253a0.

Costanza, Robert et al. (2017). "Twenty years of ecosystem services: How far have we come and how far do we still need to go?" In: *Ecosystem Services* 28, pp. 1–16. DOI: 10.1016/j.ecoser.2017.09.008.

Currey, Leanne M. et al. (2015). "Assessing fine-scale diel movement patterns of an exploited coral reef fish". In: *Animal Biotelemetry* 3, p. 41. DOI: 10.1186/s40317-015-0072-5.

Davison, P. C. et al. (2013). "Carbon export mediated by mesopelagic fishes in the northeast Pacific Ocean". In: *Progress in Oceanography* 116, pp. 14–30. DOI: 10.1016/j.pocean.2013.05.013.

Duffy, J. Emmett et al. (2016). "Biodiversity enhances reef fish biomass and resistance to climate change". In: *Proceedings of the National Academy of Sciences of the United States of America* 113.22, pp. 6230–6235. DOI: 10.1073/pnas.1524465113.

Eddy, Tyler D. et al. (2021). "Global decline in capacity of coral reefs to provide ecosystem services". In: *One Earth* 4.9, pp. 1278–1285. DOI: 10.1016/j.oneear.2021.08.016.

Edgar, Graham J. and Rick D. Stuart-Smith (2014). "Systematic global assessment of reef fish communities by the Reef Life Survey program". In: *Scientific Data* 1, p. 140007. DOI: 10.1038/sdata.2014.7.

Edgar, Graham J. et al. (2020). "Reef Life Survey: Establishing the ecological basis for conservation of shallow marine life". In: *Biological Conservation* 252.June, p. 108855. DOI: 10.1016/j.biocon.2020.108855.

Eriksson, Britas Klemens and Helmut Hillebrand (2019). "Rapid reorganization of global biodiversity". In: *Science* 366.6463, pp. 308–309. DOI: 10.1126/science.aaz4520.

Feely, R A et al. (1999). "Influence os El Nino on the Equatorial Pacific contribution to atmospheric CO2 accounts". In: *Nature* 398.April, pp. 597–601. DOI: 10.1038/19273.

Feely, Richard A. et al. (2004). "Impact of anthropogenic CO2 on the CaCO3 system in the oceans". In: *Science* 305.5682, pp. 362–366. DOI: 10.1126/science.1097329.

Fernández Castro, Bieito et al. (2022). "Intense upper ocean mixing due to large aggregations of spawning fish". In: *Nature Geoscience* 15.4, pp. 287–292. DOI: `10.1038/s41561-022-00916-3`.

Fletcher, C. R. (1978). "Osmotic and ionic regulation in the cod (*Gadus callarias* L.) - I. Water Balance". In: *Journal of Comparative Physiology* 124, pp. 149–155. DOI: `10.1007/BF00689176`.

Foran, Elizabeth, Steve Weiner, and Maoz Fine (2013). "Biogenic fish-gut calcium carbonate is a stable amorphous phase in the gilt-head seabream, sparus aurata". In: *Scientific Reports* 3, p. 1700. DOI: `10.1038/srep01700`.

Friedlingstein, Pierre et al. (2022). "Global Carbon Budget 2022". In: *Earth System Science Data* 14.11, pp. 4811–4900.

Fukushi, Keisuke et al. (2011). "Monohydrocalcite: A promising remediation material for hazardous anions". In: *Science and Technology of Advanced Materials* 12.6, p. 064702. DOI: `10.1088/1468-6996/12/6/064702`.

Genz, J., J. R. Taylor, and M. Grosell (2008). "Effects of salinity on intestinal bicarbonate secretion and compensatory regulation of acid-base balance in *Opsanus beta*". In: *Journal of Experimental Biology* 211.14, pp. 2327–2335. DOI: `10.1242/jeb.016832`.

Genz, Janet, M. Danielle McDonald, and Martin Grosell (2011). "Concentration of MgSO4 in the intestinal lumen of Opsanus beta limits osmoregulation in response to acute hypersalinity stress". In: *American Journal of Physiology - Regulatory Integrative and Comparative Physiology* 300.4. DOI: `10.1152/ajpregu.00299.2010`.

Giering, Sarah L.C. et al. (2014). "Reconciliation of the carbon budget in the ocean's twilight zone". In: *Nature* 507.7493, pp. 480–483. DOI: `10.1038/nature13123`.

Gregório, Sílvia F. et al. (2019). "Increased intestinal carbonate precipitate abundance in the sea bream (Sparus aurata L.) in response to ocean acidification". In: *PLoS ONE* 14.6, pp. 1–18. DOI: `10.1371/journal.pone.0218473`.

Grosell, Martin (2019). "CO2 and calcification processes in fish". In: *Fish Physiology*. Ed. by Martin Grosell et al. 1st ed. Vol. 37. Elsevier Inc., pp. 133–159. DOI: `10.1016/bs.fp.2019.07.002`.

Grosell, Martin, Katie M. Gilmour, and Steven F. Perry (2007). "Intestinal carbonic anhydrase, bicarbonate, and proton carriers play a role in the acclimation of rainbow trout to seawater". In: *American Journal of Physiology - Regulatory Integrative and Comparative Physiology* 293.5, pp. 2099–2111. DOI: `10.1152/ajpregu.00156.2007`.

Grosell, Martin et al. (2004). "Effects of prolonged copper exposure in the marine gulf toadfish (Opsanus beta) II: Copper accumulation, drinking rate and Na+/K +-ATPase activity in osmoregulatory tissues". In: *Aquatic Toxicology* 68.3, pp. 263–275. DOI: `10.1016/j.aquatox.2004.03.007`.

Grosell, Martin et al. (2005). "Bicarbonate secretion plays a role in chloride and water absorption of the European flounder intestine". In: *American Journal of Physiology-Regulatory, Integrative and Comparative Physiology* 288.4, R936–R946. DOI: `10.1152/ajpregu.00684.2003`.

Grosell, Martin et al. (2009). "The involvement of H+-ATPase and carbonic anhydrase in intestinal HCO3- secretion in seawater-acclimated rainbow trout". In: *Journal of Experimental Biology* 212.12, pp. 1940–1948. DOI: `10.1242/jeb.026856`.

Guidi, Lionel et al. (2015). "A new look at ocean carbon remineralization for estimating deepwater sequestration". In: *Global biogeochemical cycles*, pp. 1044–1059. DOI: `10.1002/2014GB005063`.

Heinze, C. and E. Maier-Reimer (1991). "Glacial pCO2 reduction by the world ocean: experiments with the Hamburg carbon cycle model". In: *Paleoceanography* 6.4, pp. 395–430.

Heuer, Rachael M., Andrew J. Esbaugh, and Martin Grosell (2012). " Ocean Acidification Leads to Counterproductive Intestinal Base Loss in the Gulf Toadfish (Opsanus beta) ". In: *Physiological and Biochemical Zoology* 85.5, pp. 450–459. DOI: `10.1086/667617`.

Heuer, Rachael M. et al. (2016). "Changes to intestinal transport physiology and carbonate production at various CO2 levels in a marine teleost, the Gulf Toadfish (*Opsanus beta*)". In: *Physiological and Biochemical Zoology* 89.5, pp. 402–416. DOI: `10.1086/688235`.

Hickman, C. P. (1968). "Ingestion, intestinal absorption, and elimination of seawater and salts in the southern flounder, *Paralichthys lethostigma*." In: *Canadian journal of zoology* 46.3, pp. 457–466. DOI: `10.1139/z68-063`.

Hicks, Christina C. et al. (2021). "Secure local aquatic food systems in the face of declining coral reefs". In: *One Earth* 4.9, pp. 1214–1216. DOI: `10.1016/j.oneear.2021.08.023`.

Hirano, T. and N. Mayer-Gostan (1976). "Eel esophagus as an osmoregulatory organ". In: *Proceedings of the National Academy of Sciences of the United States of America* 73.4, pp. 1348–1350. DOI: `10.1073/pnas.73.4.1348`.

Huffard, Christine L. et al. (2020). "Temporally-resolved mechanisms of deep-ocean particle flux and impact on the seafloor carbon cycle in the northeast Pacific". In: *Deep-Sea Research Part II: Topical Studies in Oceanography* 173, p. 104763. DOI: `10.1016/j.dsr2.2020.104763`.

Hughes, Terry P. et al. (2017a). "Coral reefs in the Anthropocene". In: *Nature* 546.7656, pp. 82–90. DOI: `10.1038/nature22901`.

Hughes, Terry P. et al. (2018a). "Global warming transforms coral reef assemblages". In: *Nature* 556, pp. 492–496. DOI: `10.1038/s41586-018-0041-2`.

Irigoien, Xabier et al. (2014). "Large mesopelagic fishes biomass and trophic efficiency in the open ocean". In: *Nature communications* 5, p. 3271. DOI: `10.1038/ncomms4271`.

Jennings, Simon and Rod W. Wilson (2009). "Fishing impacts on the marine inorganic carbon cycle". In: *Journal of Applied Ecology* 46.5, pp. 976–982. DOI: `10.1111/j.1365-2664.2009.01682.x`.

Keith, David A. et al. (2015). "The IUCN red list of ecosystems: Motivations, challenges, and applications". In: *Conservation Letters* 8.3, pp. 214–226. DOI: `10.1111/conl.12167`.

Keith, David A. et al. (2022). "A function-based typology for Earth's ecosystems". In: *Nature* 610, pp. 513–518. DOI: `10.1038/s41586-022-05318-4`.

Kulbicki, Michel et al. (2013). "Global biogeography of reef fishes: A hierarchical quantitative delineation of regions". In: *PLoS ONE* 8.12, e81847. DOI: `10.1371/journal.pone.0081847`.

Kwon, Eun Young, François Primeau, and Jorge L. Sarmiento (2009). "The impact of remineralization depth on the air-sea carbon balance". In: *Nature Geoscience* 2.9, pp. 630–635. DOI: `10.1038/ngeo612`.

Lapola, David M et al. (2023). "The drivers and impacts of Amazon forest degradation". In: *Science* 379.6630, eabp8622. DOI: `10.1126/science.abp8622`.

Lapola, David M. et al. (2018). "Limiting the high impacts of Amazon forest dieback with no-regrets science and policy action". In: *Proceedings of the National Academy*

of Sciences of the United States of America 115.46, pp. 11671–11679. DOI: 10.1073/pnas.1721770115.

Larsen, Erik Hviid et al. (2014). "Osmoregulation and excretion". In: *Comprehensive Physiology* 4.2, pp. 405–573. DOI: 10.1002/cphy.c130004.

Maetz, J. and E. Skadhauge (1968). "Drinking rates and gill ionic turnover in relation to external salinities in the eel". In: *Nature* 217.5126, pp. 371–373. DOI: 10.1038/217371a0.

Mariani, Gaël et al. (2020). "Let more big fish sink: Fisheries prevent blue carbon sequestration-half in unprofitable areas". In: *Science Advances* 6.44, pp. 1–9. DOI: 10.1126/sciadv.abb4848.

Mekuchi, Miyuki, Tamao Hatta, and Toyoji Kaneko (2010). "Mg-calcite, a carbonate mineral, constitutes Ca precipitates produced as a byproduct of osmoregulation in the intestine of seawater-acclimated Japanese eel *Anguilla japonica*". In: *Fisheries Science* 76.2, pp. 199–205. DOI: 10.1007/s12562-009-0199-5.

Millennium Ecosystem Assessment (2005). *Ecosystems and Human Well- Being: Synthesis.* Tech. rep.

Millero, Frank J. (2007). "The marine inorganic carbon cycle". In: *Chemical Reviews* 107.2, pp. 308–341. DOI: 10.1021/cr0503557.

Mora, Camilo et al. (2011). "Global human footprint on the linkage between biodiversity and ecosystem functioning in reef fishes". In: *PLoS Biology* 9.4, e1000606. DOI: 10.1371/journal.pbio.1000606.

Morse, John W., Andreas J. Andersson, and Fred T. Mackenzie (2006). "Initial responses of carbonate-rich shelf sediments to rising atmospheric pCO2 and "ocean acidification": Role of high Mg-calcites". In: *Geochimica et Cosmochimica Acta* 70, pp. 5814–5830. DOI: 10.1016/j.gca.2006.08.017.

Morse, John W., Rolf S. Arvidson, and Andreas Lüttge (2007). "Calcium carbonate formation and dissolution". In: *Chemical Reviews* 107.2, pp. 342–381. DOI: 10.1021/cr050358j.

Nagashima, K. and M. Ando (1994). "Characterization of esophageal desalination in the seawater eel, *Anguilla japonica*". In: *Journal of Comparative Physiology B* 164.1, pp. 47–54. DOI: 10.1007/BF00714570.

Orr, James C. et al. (2005). "Anthropogenic ocean acidification over the twenty-first century and its impact on calcifying organisms". In: *Nature* 437.7059, pp. 681–686. DOI: 10.1038/nature04095.

Papastamatiou, Yannis P. et al. (2018). "Activity seascapes highlight central place foraging strategies in marine predators that never stop swimming". In: *Movement Ecology* 6, p. 9. DOI: 10.1186/s40462-018-0127-3.

Parmelee, J. T. and J. L. Renfro (1983). "Esophageal desalination of seawater in flounder: Role of active sodium transport". In: *American Journal of Physiology - Regulatory Integrative and Comparative Physiology* 245.6, R888–R893. DOI: 10.1152/ajpregu.1983.245.6.r888.

Perry, Chris T. et al. (2011). "Fish as major carbonate mud producers and missing components of the tropical carbonate factory". In: *Proceedings of the National Academy of Sciences* 108.10, pp. 3865–3869. DOI: 10.1073/pnas.1015895108.

Perry, Steve F. et al. (2010). "Acid-base regulation in the plainfin midshipman (Porichthys notatus): An aglomerular marine teleost". In: *Journal of Comparative Physiology B: Biochemical, Systemic, and Environmental Physiology* 180.8, pp. 1213–1225. DOI: 10.1007/s00360-010-0492-8.

Plummer, L. Niel and Eurybiades Busenberg (1982). "The solubilities of calcite, aragonite and vaterite in CO2-H2O solutions between 0 and 90řC, and an evaluation of the aqueous model for the system CaCO3-CO2-H2O". In: *Geochimica et Cosmochimica Acta* 46.6, pp. 1011–1040. DOI: 10.1016/0016-7037(82)90056-4.

Pörtner, Hans O, Martina Langenbuch, and Anke Reipschlager (2004). "Biological Impact of Elevated Ocean CO 2 Concentrations : Lessons from Animal Physiology and Earth History". In: *Journal of Oceanography* 60, pp. 705–718.

Roberts, Callum M. et al. (2017). "Marine reserves can mitigate and promote adaptation to climate change". In: *Proceedings of the National Academy of Sciences* 114.24, pp. 6167–6175. DOI: 10.1073/pnas.1701262114.

Rogers, Nicholas John (2015). "The Respiratory and Gut Physiology of Fish : Responses to Environmental Change". PhD thesis. University of Exeter, p. 218.

Saba, Grace K. and Deborah K. Steinberg (2012). "Abundance, composition, and sinking rates of fish fecal pellets in the santa barbara channel". In: *Scientific Reports* 2, p. 716. DOI: 10.1038/srep00716.

Saba, Grace K. et al. (2021). "Toward a better understanding of fish-based contribution to ocean carbon flux". In: *Limnology and Oceanography* 66.5, pp. 1639–1664. DOI: 10.1002/lno.11709.

Salter, Michael A., Chris T. Perry, and Abigail M. Smith (2019). "Calcium carbonate production by fish in temperate marine environments". In: *Limnology and Oceanography* 64.6, pp. 2755–2770. DOI: 10.1002/lno.11339.

Salter, Michael A., Chris T. Perry, and Rod W. Wilson (2014). "Size fraction analysis of fish-derived carbonates in shallow sub-tropical marine environments and a potentially unrecognised origin for peloidal carbonates". In: *Sedimentary Geology* 314, pp. 17–30. DOI: 10.1016/j.sedgeo.2014.10.005.

Salter, Michael A., Christopher T. Perry, and Rod W. Wilson (2012). "Production of mud-grade carbonates by marine fish: Crystalline products and their sedimentary significance". In: *Sedimentology* 59.7, pp. 2172–2198. DOI: 10.1111/j.1365-3091.2012.01339.x.

Salter, Michael A. et al. (2017). "Phase heterogeneity in carbonate production by marine fish influences their roles in sediment generation and the inorganic carbon cycle". In: *Scientific Reports* 7.1, pp. 1–15. DOI: 10.1038/s41598-017-00787-4.

Salter, Michael A. et al. (2018). "Reef fish carbonate production assessments highlight regional variation in sedimentary significance". In: *Geology* 46.8, pp. 699–702. DOI: 10.1130/G45286.1.

Santana-Falcón, Yeray, Evan Mason, and Javier Arístegui (2020). "Offshore transport of organic carbon by upwelling filaments in the Canary Current System". In: *Progress in Oceanography* 186.April, p. 102322. DOI: 10.1016/j.pocean.2020.102322.

Schauer, Kevin L. et al. (2016). "A proteinaceous organic matrix regulates carbonate mineral production in the marine teleost intestine". In: *Scientific Reports* 6.July, pp. 1–14. DOI: 10.1038/srep34494.

Schauer, Kevin L. et al. (2018). "Interrogation of the Gulf toadfish intestinal proteome response to hypersalinity exposure provides insights into osmoregulatory mechanisms and regulation of carbonate mineral precipitation". In: *Comparative Biochemistry and Physiology - Part D: Genomics and Proteomics* 27.June, pp. 66–76. DOI: 10.1016/j.cbd.2018.06.004.

Schiettekatte, Nina M.D. et al. (2020). "Nutrient limitation, bioenergetics and stoichiometry: A new model to predict elemental fluxes mediated by fishes". In: *Functional Ecology* 34.9, pp. 1857–1869. DOI: 10.1111/1365-2435.13618.

Seidl, Rupert and Monica G. Turner (2022). "Post-disturbance reorganization of forest ecosystems in a changing world". In: *Proceedings of the National Academy of Sciences of the United States of America* 119.28, e2202190119. DOI: 10.1073/pnas.2202190119.

Shehadeh, Ziad H. and Malcolm S. Gordon (1969). "The role of the intestine in salinity adaptation of the rainbow trout, *Salmo gairdneri*". In: *Comparative Biochemistry And Physiology* 30.3, pp. 397–418. DOI: 10.1016/0010-406X(69)92011-8.

Sleet, R. B. and L. J. Weber (1982). "The rate and manner of seawater ingestion by a marine teleost and corresponding seawater modification by the gut". In: *Comparative Biochemistry and Physiology – Part A: Physiology* 72.3, pp. 469–475. DOI: 10.1016/0300-9629(82)90110-4.

Smith, Homer W. (1930). "The absorption and excretion of water and salts by marine teleosts". In: *American Journal of Physiology* 93, pp. 480–505.

Staresinic, Nick et al. (1983). "Downward transport of particulate matter in the Peru coastal upwelling: Role of the anchoveta, *Engraulis ringens*". In: *Coastal upwelling: Its sediment record. Part A. Responses of the sedimentary regime to present coastal upwelling.* Ed. by E. Suess and J. Theide. New York: Plenum Publishing Corporation, pp. 225–240. DOI: 10.1007/978-1-4615-6651-9_12.

Stuart-Smith, Rick D et al. (2018). "Ecosystem restructuring along the Great Barrier Reef following mass coral bleaching". In: *Nature* 560, pp. 92–96. DOI: 10.1038/s41586-018-0359-9.

Stuart-Smith, Rick D. et al. (2022). "Tracking widespread climate-driven change on temperate and tropical reefs". In: *Current Biology* 32.19, 4128–4138.e3. DOI: 10.1016/j.cub.2022.07.067.

Sulpis, Olivier et al. (2021). "Calcium carbonate dissolution patterns in the ocean". In: *Nature Geoscience* 14.6, pp. 423–428. DOI: 10.1038/s41561-021-00743-y.

Takei, Yoshio and Takehiro Tsukada (2001). "Ambient temperature regulates drinking and arterial pressure in eels". In: *Zoological Science* 18.7, pp. 963–967. DOI: 10.2108/zsj.18.963.

TEEB (2010). *The Economics of Ecosystems & Biodiversity: Mainstreaming the Economics of Nature: A synthesis of the approach, conclusions and recommendations of TEEB.* Tech. rep. Malta.

Tytler, P. and J. Ireland (1994). "Drinking and water absorption by the larvae of herring (Clupea harengus) and turbot (Scophthalmus maximus)". In: *Journal of Fish Biology* 44, pp. 103–116. DOI: 10.1111/j.1095-8649.1994.tb01588.x.

UNEP (2014). *The importance of mangroves to people: A call to action.* Ed. by J. van Bochove, E. Sullivan, and T. Nakamura. Cambridge: United Nations Environment Programme World Conservation Monitoring Centre, 128 pp.

Van Vuuren, Detlef P et al. (2014). "A new scenario framework for Climate Change Research : scenario matrix architecture". In: *Climate Change* 122, pp. 373–386. DOI: 10.1007/s10584-013-0906-1.

Walsh, Patrick J. et al. (1991). "Carbonate deposits in marine fish intestines: A new source of biomineralization". In: *Limnology and Oceanography* 36.6, pp. 1227–1232. DOI: 10.4319/lo.1991.36.6.1227.

Weiss, R. F. (1974). "Carbon dioxide in water and seawater: the solubility of a non-ideal gas". In: *Marine Chemistry1* 2.3, pp. 203–215. DOI: 10.5194/bg-13-841-2016.

Whittamore, Jonathan M. (2012). "Osmoregulation and epithelial water transport: Lessons from the intestine of marine teleost fish". In: *Journal of Comparative Physiology B: Biochemical, Systemic, and Environmental Physiology* 182.1, pp. 1–39. DOI: 10.1007/s00360-011-0601-3.

Whittamore, Jonathan M., Christopher A. Cooper, and Rod W. Wilson (2010). "HCO3- secretion and CaCO3 precipitation play major roles in intestinal water absorption in marine teleost fish in vivo". In: *American Journal of Physiology - Regulatory Integrative and Comparative Physiology* 298.4, pp. 877–886. DOI: 10.1152/ajpregu.00545.2009.

Williams, Gareth J. and Nicholas A.J. Graham (2019). "Rethinking coral reef functional futures". In: *Functional Ecology* 33.6, pp. 942–947. DOI: 10.1111/1365-2435.13374.

Wilson, Rod W. and Martin Grosell (2003). "Intestinal bicarbonate secretion in marine teleost fish - Source of bicarbonate, pH sensitivity, and consequences for whole animal acid-base and calcium homeostasis". In: *Biochimica et Biophysica Acta - Biomembranes* 1618.2, pp. 163–174. DOI: 10.1016/j.bbamem.2003.09.014.

Wilson, Rod W., Jonathan M. Wilson, and Martin Grosell (2002). "Intestinal bicarbonate secretion by marine teleost fish-why and how?" In: *Biochimica et Biophysica Acta* 1566, pp. 182–193. DOI: 10.1016/s0005-2736(02)00600-4.

Wilson, Rod W. et al. (1996). "Intestinal base excretion in the seawater-adapted rainbow trout: a role in acid-base balance?" In: *The Journal of experimental biology* 199.Pt 10, pp. 2331–43. DOI: 10.1242/jeb.199.10.2331.

Wilson, Rod W. et al. (2009). "Contribution of fish to the marine inorganic carbon cycle". In: *Science* 323.January, pp. 359–362. DOI: 10.1126/science.1157972.

Woodhead, Anna J. et al. (2019). "Coral reef ecosystem services in the Anthropocene". In: *Functional Ecology* 33.6, pp. 1023–1034. DOI: 10.1111/1365-2435.13331.

Woosley, Ryan J., Frank J. Millero, and Martin Grosell (2012). "The solubility of fish-produced high magnesium calcite in seawater". In: *Journal of Geophysical Research: Oceans* 117.4, pp. 1–5. DOI: 10.1029/2011JC007599.

Ziveri, Patrizia et al. (2023). "Pelagic calcium carbonate production and shallow dissolution in the North Pacific Ocean". In: *Nature Communications* 14, p. 805. DOI: 10.1038/s41467-023-36177-w.

1

Phylogeny, body morphology, and trophic level shape intestinal traits in coral reef fishes

Mattia Ghilardi[1,2,3,4]*, Nina M. D. Schiettekatte[3,4], Jordan M. Casey[3,4,5], Simon J. Brandl[3,4,5,6], Samuel Degregori[7], Alexandre Mercière[3,4], Fabien Morat[3,4], Yves Letourneur[4,8], Sonia Bejarano[1], Valeriano Parravicini[3,4,9]

1. Reef Systems Research Group, Department of Ecology, Leibniz Centre for Tropical Marine Research (ZMT), FahrenheitstraSSe 6, 28359 Bremen, Germany

2. Department of Marine Ecology, Faculty of Biology and Chemistry, University of Bremen, Leobener StraSSe UFT, 28359 Bremen, Germany

3. PSL Université Paris: EPHE-UPVD-CNRS, USR3278 CRIOBE, 66860 Perpignan, France

4. Laboratoire d'Excellence "CORAIL", Perpignan, France

5. Department of Marine Science, Marine Science Institute, University of Texas at Austin, 750 Channel View Drive, Port Aransas, Texas 78383, United States

6. CESAB, Centre for the Synthesis and Analysis of Biodiversity, Institut Bouisson Bertrand, 34000 Montpellier, France

7. Department of Ecology and Evolutionary Biology, University of California Los Angeles, Los Angeles, United States

8. UMR ENTROPIE (UR-IRD-CNRS-IFREMER-UNC), Université de la Nouvelle-Calédonie, BP R4, 98851 Nouméa Cedex, New Caledonia

9. Institut Universitaire de France, Paris, France

***Correspondence:** M. Ghilardi (`mattia.ghilardi@leibniz-zmt.de`)

Abstract

1. Trait-based approaches are increasingly used to study species assemblages and understand ecosystem functioning. The strength of these approaches lies in the appropriate choice of functional traits that relate to the functions of interest. However, trait-function relationships are often supported by weak empirical evidence.

2. Processes related to digestion and nutrient assimilation are particularly challenging to integrate into trait-based approaches. In fishes, intestinal length is commonly used to describe these functions. Although there is broad consensus concerning the relationship between fish intestinal length and diet, evolutionary and environmental forces have shaped a diversity of intestinal morphologies that is not captured by length alone.

3. Focusing on coral reef fishes, we investigate how evolutionary history and ecology shape intestinal morphology. Using a large dataset encompassing 142 species across 31 families collected in French Polynesia, we test how phylogeny, body morphology, and diet relate to three intestinal morphological traits: intestinal length, diameter, and surface area.

4. We demonstrate that phylogeny, body morphology, and trophic level explain most of the interspecific variability in fish intestinal morphology. Despite the high degree of phylogenetic conservatism, taxonomically unrelated herbivorous fishes exhibit similar intestinal morphology due to adaptive convergent evolution. Furthermore, we show that stomachless, durophagous species have the widest intestines to compensate for the lack of a stomach and allow passage of relatively large undigested food particles.

5. Rather than traditionally applied metrics of intestinal length, intestinal surface area may be the most appropriate trait to characterise intestinal morphology in functional studies.

1.1   Introduction

Characterising the relationship between form and function provides information on the evolutionary history of species, their potential to adapt to new environmental conditions, and their role within ecosystems. Form and function are often closely related (Wainwright 1988), as is evident across a wide variety of taxonomic groups, such as invertebrates (Griffen and Mosblack 2011; Wang et al. 1997) and large mammals (Ekdale 2016; Hutchinson et al. 2011). However, determining whether the relationship between form and function is driven by evolutionary processes (Banavar et al. 2014; Westneat 1995) or environmental conditions (Herrel et al. 2008; Naya et al. 2014) remains difficult to pinpoint.

Intestinal morphology is central to one of the most important organismal processes–the digestion of prey sourced from the environment–and as such likely to have tight links to functional roles. Indeed, characteristics of the intestine and other digestive organs are associated with energy assimilation (Battley and Piersma 2005; Cleveland and Montgomery 2003) and thus the persistence of populations (Brewster et al. 2020). Further, intestinal morphology is strongly related to diet in both vertebrate and invertebrate groups (Griffen and Mosblack 2011; Steinberg 2018). For instance, intestinal length is negatively correlated with trophic level in mammals (Korn 1992; Wang De-Hua et al. 2003), birds (Al-Dabbagh et al. 1987; Battley and Piersma 2005; Ricklefs 1996), reptiles (O'Grady et al. 2005), amphibians (Naya et al. 2009) and fishes (Elliott and Bellwood 2003; Kramer and Bryant 1995b; reviewed in Steinberg 2018). Primary consumers generally require long intestines because they need to acquire energy and nutrients from plants with low nutritional value and high fibre content (Horn 1989). However, building and maintaining a long intestine has high evolutionary and physiological costs (Cant et al. 1996). Intestinal morphology therefore represents a trade-off between the benefits of nutrient acquisition and the costs of maintaining a large organ.

Beyond diet, evolutionary processes also play a role in shaping intestinal morphology (Lauder 1981). Phylogenetic conservatism has been identified across sev-

eral taxa (Davis et al. 2013; German et al. 2010; Hunt et al. 2019), suggesting that evolution can constrain intestinal morphological variation within certain size ranges. However, species can overcome phylogenetic conservatism through phenotypic flexibility, which allows organisms to adapt to local environmental conditions (Piersma and Lindström 1997). For example, some vertebrates can respond to changing environmental conditions by adjusting the structure and physiology of their gastro-intestinal tracts (Battley and Piersma 2005; Dala-Corte et al. 2017; Herrel et al. 2008; Starck 2003). Intestinal structural flexibility has been observed in response to fasting (Starck and Beese 2002; Zaldúa and Naya 2014), increased food intake (Dykstra and Karasov 1992; Starck and Beese 2001), changes in diet (Naya et al. 2007; Olsson et al. 2007), and through ontogenetic development (Kramer and Bryant 1995a).

Coral reefs host an extraordinary diversity of species. Among these species, fishes are the most diverse and prominent vertebrates, exhibiting a wide array of morphologies and trophic strategies (Alfaro et al. 2007; Cowman et al. 2009; Floeter et al. 2018; Parravicini et al. 2020; Price et al. 2011; Price et al. 2013; Siqueira et al. 2020) (Alfaro et al., 2007; Cowman et al. , 2009; Price et al., 2011, 2013; Floeter et al., 2018; Parravicini et al. 2020; Siqueira et al., 2020). Given this multitude of feeding behaviours, reef fishes represent an ideal group to study how evolutionary and ecological mechanisms influence intestinal morphology.

Reef fish intestinal morphology has been related to the quality of their diet (Al-Hussaini 1947; Elliott and Bellwood 2003; Emery 1973). However, several limitations have hampered a full understanding of the nature and strength of this relationship. First, previous studies are often limited to single taxonomic families (Berumen et al. 2011; Wagner et al. 2009). Second, most studies focus on intestinal length, which, alone, does not fully describe intestinal morphology (Elliott and Bellwood 2003). Third, evolutionary constraints on intestinal morphology have only been considered across a limited number of taxonomic groups (Davis et al. 2013; Wagner et al. 2009). Fourth, while intestinal traits have always been corrected for allometry, no study has accounted for body shape. Lastly, other digestive

organs, such as the stomach, may impact this relationship, but this has never been investigated. Thus, a better understanding of the digestive traits and trophic roles of reef fishes may come from a broader, more diverse, and multifaceted assessment of digestive traits in reef fishes.

Here, we assess the main drivers of variability in the intestinal morphology of coral reef fishes. We investigate differences in intestinal length, diameter, and surface area of 1,208 individuals belonging to 142 species and 31 families collected in Mo'orea, French Polynesia. Specifically, we use Bayesian phylogenetic hierarchical analysis to disentangle the relationship among intestinal morphological traits and phylogeny, body size, body shape, diet, and the presence of the stomach. Further, we investigate the body size relationship at both the inter and intraspecific level.

1.2 Methods

1.2.1 Data collection

A total of 1,208 individuals from 142 species were collected from reefs around Mo'orea, French Polynesia, in the lagoon, pass, and outer reef slope (Supplementary Table 1.1), between 2018 and 2019. We primarily targeted adult fishes, but a wider size range was collected for a subset of species. The selection of species cover all the major trophic guilds of coral reef fishes (i.e. corallivores, herbivores, invertivores, piscivores, planktivores). All individuals were collected by spearfishing between 10:00 and 15:00 and transferred to the laboratory on ice. In the laboratory, each individual was measured and weighed, and the intestine was unravelled and photographed on a tray, using a ruler for a size reference. A minimum of three individuals per species were examined. The collection of fishes for this project was approved by the Ministry of the Environment of French Polynesia (permit #681/MCE/ENV).

We measured the length and the external diameter of the intestine using the software Fiji/ImageJ (Schindelin et al. 2012). The length was measured from the pyloric outlet to the anus in the presence of a stomach, and from the oesophagus to

the anus in stomachless fishes (Elliott and Bellwood 2003; Karachle and Stergiou 2010a; Kramer and Bryant 1995a; Kramer and Bryant 1995b). The average diameter was calculated with measurements taken at ten equal intervals along the entire length of the intestine (Elliott and Bellwood 2003). The external intestinal surface area (IS) was used as a proxy for mucosal surface area (Cleveland and Montgomery 2003; Lassuy 1984; Montgomery 1977), and it was estimated using the following formula:

$$\text{IS} = 2\pi\text{r} \cdot \text{IL}, \tag{1.1}$$

where r is the mean outer radius of the intestine and IL is the intestinal length. Notably, scraping and excavating species of parrotfishes (genera *Chlorurus* and *Scarus*, $n = 10$ species) have ileal sacculations (Clements and Choat 2018), leading to a potential underestimation of their intestinal surface area by this formula; yet, all other species examined in this study have a smooth external intestinal surface, suggesting accurate quantifications via the applied formula. Thus, while our calculation is a coarse estimation of mucosal surface area that does not account for mucosal folding, it can be considered a valid indicator of general intestinal surface area across most species (Cleveland and Montgomery 2003; Lassuy 1984; Montgomery 1977).

Each species was classified based on the presence or absence of a functional stomach. We considered both gastric and muscular (gizzard-like, $n = 5$) stomachs to be functional stomachs because they contribute to food digestion. In contrast, sac-like stomachs (e.g. Tetraodontidae) were considered non-functional stomachs. Furthermore, species were classified as either durophagous or not durophagous depending on whether their diet consisted of hard-shelled prey items (e.g. corals, crabs, molluscs, sea urchins). We compiled this dataset according to the literature (Fagundes et al. 2016; Koide and Sakai 2021; Ray and Ringø 2014; Sorenson et al. 2013; Wilson and Castro 2010), authors' knowledge, and direct observation of the dissected fishes.

We used trophic level as a continuous measure of diet. Data were retrieved from FishBase using the R package *rfishbase* version 3.0.4 (Boettiger et al. 2012). In FishBase, a species' trophic level is calculated by adding one to the mean trophic level of all food items consumed, weighted by their contribution (Froese and Pauly 2000). Two estimates of trophic level are available: one based on diet composition and the other based on food items. The diet-based index is only available for a few of our species, so the food item-based index was used as a measure of trophic level and, when unavailable, the mean value of the genus ($n = 14$) or family level ($n = 1$) was used.

Since food item-based trophic levels reflect temporal snapshots of gut contents, they may not represent a species' entire dietary breath. To assess whether trophic levels of our species were indicative of their diet in Mo'orea, we investigated the relationship between trophic level and nitrogen stable isotope ratio (δ^{15}N), which represents diet over longer periods of time (Hesslein et al. 1993). Using δ^{15}N values available for a subset of species ($n = 83$) from Mo'orea we found a strong positive relationship between δ^{15}N and trophic level after accounting for body size and phylogenetic relationships (see Supplementary Methods). These results are consistent with previous observations (Kline and Pauly 1998) and suggest that food item-based trophic level is a reasonable indicator of diet, thus supporting its use in our analysis.

FishBase was also used to retrieve species-level data on body elongation (i.e. standard length divided by maximum body depth). Similar to trophic level, when elongation was unavailable, the mean value of the genus ($n = 1$) was used. We used body elongation to account for body shape as it is the major axis of body shape variation among reef fishes (Claverie and Wainwright 2014). Moreover, body elongation is strongly related to abdominal cavity depth and the space available to accommodate the intestine and other organs (Burns 2021).

1.2.2   Data analysis

To investigate the relative contribution of phylogeny, body morphology, and diet in determining intestinal traits, we fitted Bayesian phylogenetic hierarchical linear models. We extracted the phylogeny for the 142 species sampled in Mo'orea from the Fish Tree of Life (Rabosky et al. 2018) using the R package *fishtree* version 0.3.2 (Chang et al. 2019). For species without verified phylogenetic information (n = 3), we used the *fishtree_complete_phylogeny()* function to retrieve the pseudo-posterior distribution of 100 synthetic stochastically-resolved phylogenies, with missing species placed using stochastic polytomy resolution.

Using this phylogenetic information, we constructed a phylogenetic relatedness matrix (Hadfield and Nakagawa 2010) and we tested whether phylogeny, body size, trophic level, body elongation, the presence/absence of the stomach, and a durophagous diet explain intestinal traits using Bayesian phylogenetic hierarchical linear models. To account for both inter and intraspecific scaling, we included a fixed slope on the average measured standard length (SL) per species (i.e., the interspecific variance of SL) and a random slope on the species-mean-centred SL (i.e., the individual SL minus the average SL of the species; the intraspecific variance of SL). We also included an interaction term between stomach and durophagy to obtain an estimate for each of the four possible combinations. Thus, the intestinal trait of the ith individual of the jth species is estimated as follows:

$$\ln(y)_{ij} = \beta_{0j} + \beta_1 \overline{\ln(\text{SL})_j} + \beta_2 \text{TL}_j + \beta_{3j}(\ln(\text{SL})_{ij} - \overline{\ln(\text{SL})_j})$$
$$+ \beta_4 \ln(\text{EL})_j + \beta_5 \text{ST}_j + \beta_6 \text{DU}_j + \beta_7 \text{ST} \times \text{DU}_j, \tag{1.2}$$

with β_{0j} and β_{3j} defined as:

$$\beta_{0j} = \gamma_{00} + u_{0\text{phy}} + u_{0j}, \tag{1.3}$$

$$\beta_{3j} = \gamma_{30} + u_{3j}, \tag{1.4}$$

where γ_{00} is the estimated average intercept, $u_{0\text{phy}}$ and u_{0j} represent deviations from the model intercept attributable to species-level variation related and unrelated to the phylogeny, respectively, β_1 and β_2 are the slopes of the species-mean

SL and trophic level (TL), respectively, γ_{30} is the average slope for the species-mean-centered SL, u_{3j} represents deviations from γ_{30} attributable to species-level variation, β_4 , β_5 , and β_6 are the slopes for the body elongation (EL), stomach presence (ST), and durophagous diet (DU), respectively, and β_7 is the slope of the interaction between stomach and durophagy. All intestinal traits , fish SL, and elongation were natural-log-transformed prior to the analyses. All continuous predictors were centred and scaled to provide a meaningful interpretation of the intercept (i.e., it represents the intestinal trait at the mean body size, trophic level, and elongation for stomachless, non-durophagous species) and allow comparison between the slopes.

For each intestinal trait, we mapped the predicted mean values onto a phylogenetic tree, including the 139 species with verified phylogenetic positions, using the R package *ggtree* version 2.2.4 (Yu et al. 2017). We further visualised the predicted intestinal traits in two-dimensional morphospace to characterise the length and diameter of fish intestines and observe the partitioning of intestinal morphology among reef fish families and trophic guilds, which were determined using an unbiased, reproducible trophic categorisation scheme (Parravicini et al. 2020). In both the phylogenetic tree and morphospace, parrotfishes (Labridae: tribe Scarini) are depicted separately from other Labridae species since they occupy distinct trophic niches.

To assess the phylogenetic signal (i.e., the tendency of traits in related species to resemble each other more than in species drawn at random from the same tree), we calculated the phylogenetic heritability index, H^2, which is defined as the ratio of the phylogenetic component to the total variance (Lynch 1991) and is equivalent to Pagel's λ (Pagel 1999). As such, values can vary between zero, for traits that have no phylogenetic component, and one, for traits evolving according to a Brownian motion (random walk) process (Nakagawa and Santos 2012).

To investigate the intraspecific scaling of intestinal traits, we extracted the random effects on the slopes from our models, which describe their relationship with body size for each species. From the 142 species-specific slopes for each intestinal

trait, we retained those with a 95% credible interval (CI) above zero that belong to species with a minimum of ten sampled individuals whose size range covered at least 25% of the reported maximum body size (retrieved from FishBase). This threshold is necessary to provide reliable estimates of scaling parameters. Isometric scaling (i.e., a proportional relationship with body size during growth) for intestinal length and diameter is defined by a slope of $\beta = 1$ and for intestinal surface area the slope is $\beta = 2$. Conversely, slopes that deviate from isometry represent allometric relationships. Thus, slopes below these defined values have negative allometry and slopes above them have positive allometry.

To assess the robustness of the results despite intraspecific variability in morphological traits, we used a sensitivity procedure. All analyses were repeated using two subsets of the complete dataset: (1) 122 species with a minimum of five sampled individuals per species and (2) 69 species with a minimum of eight sampled individuals per species.

1.2.3 Model specifications

We fitted equation (1.2) using the R package *brms* version 2.14.4 (Bürkner 2017) to derive posterior distributions and associated 95% CIs for the fitted parameters. We used a Student-t error distribution and weakly informative, normally distributed priors with means of zero: $N(0, 10)$ for the intercept and $N(0, 5)$ for fixed effects and species-level deviations from model intercept and species-mean-centred SL mean slope. The posterior distributions of model parameters were estimated using Markov chain Monte Carlo (MCMC) methods by constructing four chains of 8,000 steps with a warm-up of 2,000 steps. For all models we inspected the MCMC chains for convergence and model fit (Supplementary Fig. 1.6). We used Bayesian R^2 to estimate the amount of explained variation from each model (Gelman et al. 2019). All analyses were performed in the software program R (version 4.0.2; R Core Team (2020)).

1.3   Results

1.3.1   Phylogenetic conservatism

We detected evidence for phylogenetic signal for all intestinal traits. However, phylogeny accounted for a higher variability in intestinal length and surface area (H^2 = 0.90 [0.80, 0.94] and H^2 = 0.76 [0.50, 0.90], respectively, mean and 95% CI) than intestinal diameter (H^2 = 0.34 [0.12, 0.59]). Intestinal morphology varies markedly across the phylogenetic tree, with increases in intestinal length and/or diameter, and, consequently, in surface area, occurring across different lineages (Fig. 1.1). For example, long intestines evolved independently in Acanthuridae, Chaetodontidae, Pomacanthidae, and the tribe Scarini in the Labridae.

1.3.2   Partitioning of intestinal morphology

The distribution of species based on intestinal morphology (Fig. 1.2) marks a continuum that ranges from short and narrow intestines (piscivores; e.g., *Cephalopholis argus*, Serranidae: 14.26 cm and 0.25 cm, mean estimates of intestinal length and diameter at SL = 15 cm) to long and wide intestines (herbivores; e.g., *Acanthurus guttatus*, Acanthuridae: 95.55 cm and 0.72 cm, mean estimates of intestinal length and diameter at SL = 15 cm). Some species also have short and wide intestines (e.g., invertivorous wrasses, Labridae) or long and narrow intestines (e.g., corallivorous butterflyfishes, Chaetodontidae).

Fish families vary in their distribution across the intestine morphospace and the clearest separation occurs between Acanthuridae, Chaetodontidae, Serranidae, and Labridae (non-Scarini) which have four distinct intestinal morphologies (i.e., each of these families occupy one of the four quadrants of morphospace; Fig. 1.2a). However, within-family variation drives overlaps among certain families. Labridae is the most extreme example and presents a clear distinction in intestinal morphology between parrotfishes (Labridae: tribe Scarini) and other wrasses. Conversely, other families with a comparable sample size (e.g., Acanthuridae) have lower within-family variation in intestinal morphology.
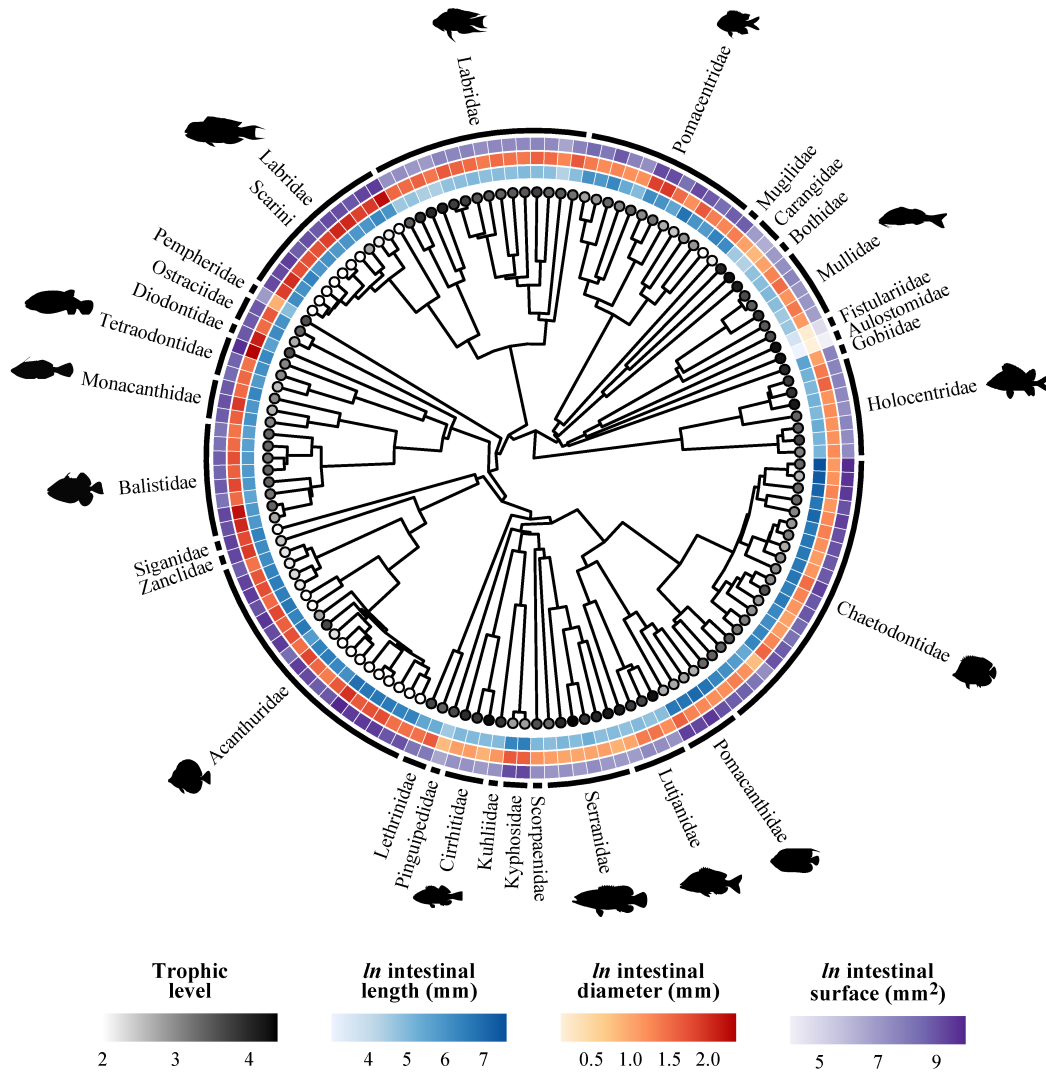
Figure 1.1: Phylogenetic reconstruction of the 139 reef fish species collected in Mo'orea (generated from the Fish Tree of Life, Chang et al. 2019) with each surrounding ring indicating mean fitted intestinal traits at a standardized fish standard length (SL = 15 cm). Intestinal trait predictions were obtained from Bayesian phylogenetic hierarchical linear models. Coloured tip points represent species' trophic level. Each external arc represents a reef fish family, with silhouettes included for the most speciose families (sourced from Schiettekatte et al. 2021).
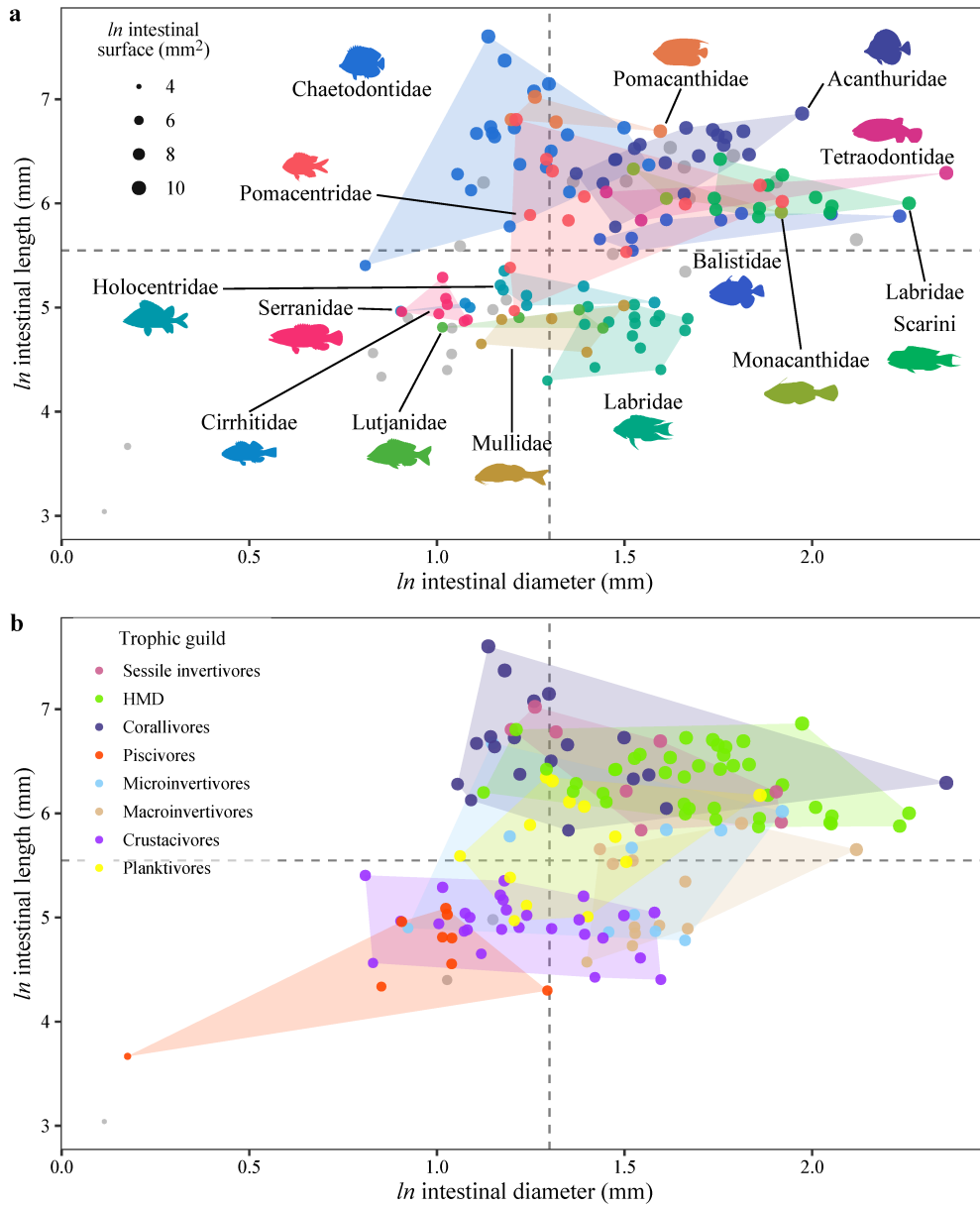
Figure 1.2: Partitioning of intestinal morphology among (**a**) reef fish families and (**b**) trophic guilds (as predicted by Parravicini et al. 2020). Dots (i.e., species) ($n = 142$) are ordered in a morphospace based on intestinal length and diameter and are size-coded to represent variation in intestinal surface area. Intestinal traits are mean fitted values at a standardised fish standard length (SL = 15 cm), estimated through Bayesian phylogenetic hierarchical linear models. Dashed lines represent the estimated average intestinal length and diameter of non-durophagous fishes with a stomach (model intercept at SL = 15 cm). Coloured polygons show the minimum convex hull plotted per (**a**) family and (**b**) trophic guild. Dots are coloured according to (**a**) families represented by at least three species and for which a convex hull could be drawn (for clarity of presentation) and (**b**) trophic guilds. Grey dots depict (**a**) species ($n = 22$) belonging to families represented by less than three species and (**b**) species ($n = 3$) for which Parravicini et al. (2020) did not predict a trophic guild. Fish silhouettes were sourced from Schiettekatte et al. (2021). HMD, herbivores, microvores, and detritivores.

Overlaps are also visible among trophic guilds, despite notable differences in intestinal length (Fig. 1.2b). Herbivores, corallivores, and sessile invertivores have longer intestines than crustacivores and piscivores, while the other trophic guilds have an intermediate intestinal length. Moreover, piscivores generally have a narrower intestine than fishes belonging to other trophic guilds.

1.3.3 Interspecific scaling and relationships with body shape and trophic level

Our model (Eq. (1.2)) explained 92% of the variation in intestinal length and surface area and 85% of the variation in intestinal diameter. Species mean SL consistently had the highest absolute effect size across all intestinal traits (Supplementary Table 1.2) and all traits scaled isometrically across species, with a tendency toward negative allometry for intestinal diameter and surface area (intestinal length: $\beta = 0.97$ [0.82, 1.13]; intestinal diameter: $\beta = 0.93$ [0.83, 1.03]; intestinal surface: $\beta = 1.87$ [1.65, 2.09], mean and 95% CI). After accounting for the other fixed and random effects, all traits decreased with body elongation (intestinal length: $\beta = $ -0.78 [-1.05, -0.52]; intestinal diameter: $\beta = $ -0.42 [-0.56, -0.28]; intestinal surface: $\beta = $ -1.20 [-1.54, -0.85]; Fig. 1.3a,c,e). Additionally, all intestinal traits decreased with trophic level (intestinal length: $\beta = $ -0.38 [-0.53, -0.24]; intestinal diameter: $\beta = $ -0.17 [-0.25, -0.07]; intestinal surface: $\beta = $ -0.55 [-0.81, -0.31]; Fig. 1.3b,d,f), showing a decrease of 59.5% in intestinal length, 32.5% in intestinal diameter and 72.9% in intestinal surface area over the observed trophic levels (from 2.00 to 4.38). The sensitivity analysis confirmed the robustness of the results, even when models were fitted with <50% of the species (Supplementary Tables 1.3-1.4 and Supplementary Fig. 1.7).

1.3.4 Influence of stomach presence and durophagy

The presence of a functional stomach and a durophagous diet did not show any interactive effect on intestinal morphology (Fig. 1.4). However, durophagous fishes had a slightly shorter and wider intestine than non-durophagous fishes, irrespective
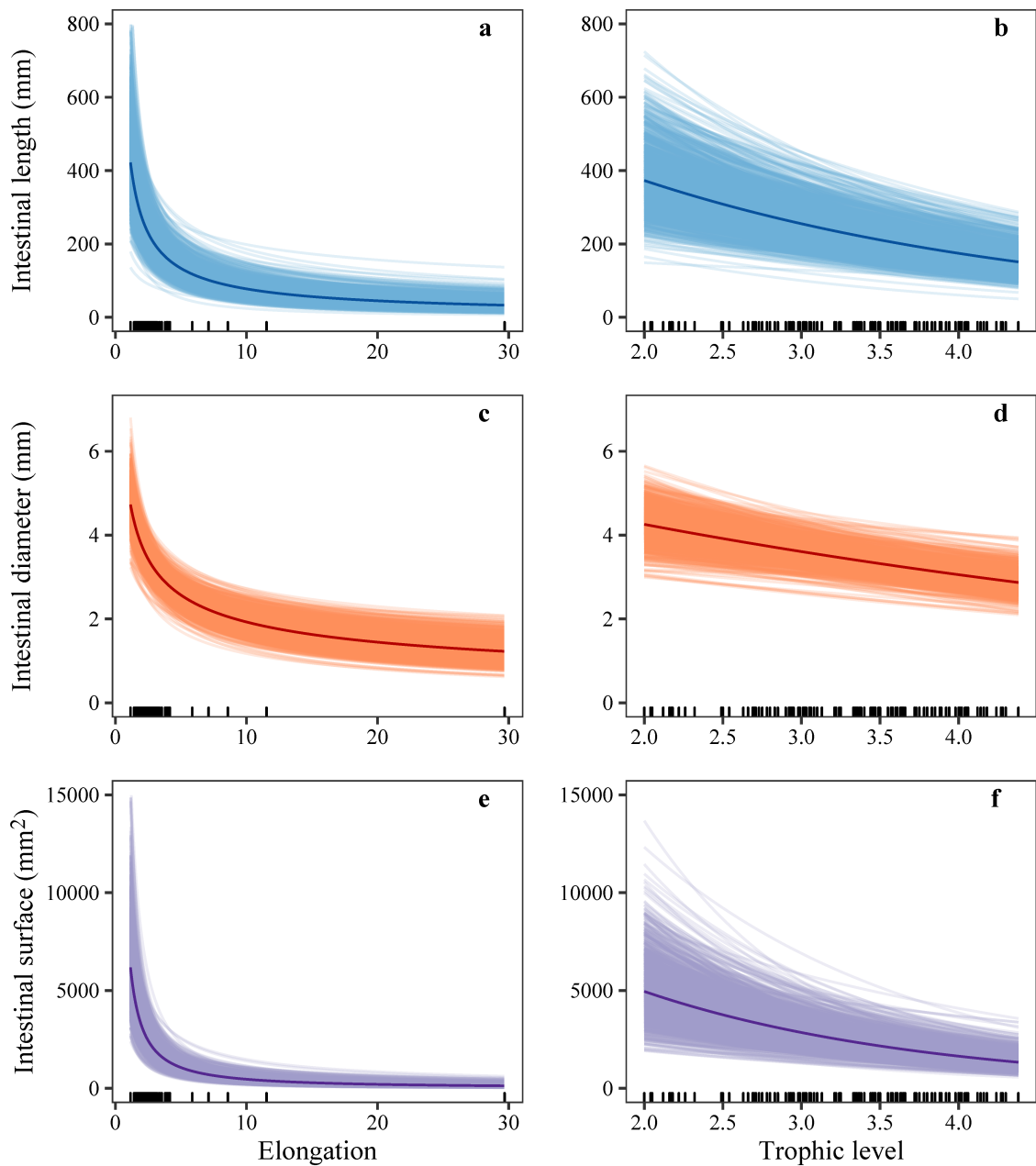
Figure 1.3: Relationship between three intestinal traits and body elongation (**a**, **c**, **e**) and trophic level (**b**, **d**, **f**) for 142 species of coral reef fishes. Thick, darkened lines represent the mean predicted fits of Bayesian phylogenetic hierarchical linear models after controlling for the remaining fixed and random effects. Categorical variables were set to their most common value (stomach = present, durophagy = non-durophagous). Thin lines represent 1,000 draws randomly chosen from the posterior fits and show model fit uncertainty. Model predictions are for natural-log intestinal traits, but are transformed here to show the fitted function on the original scale of the data. Raw data are displayed as marks along the x-axis.
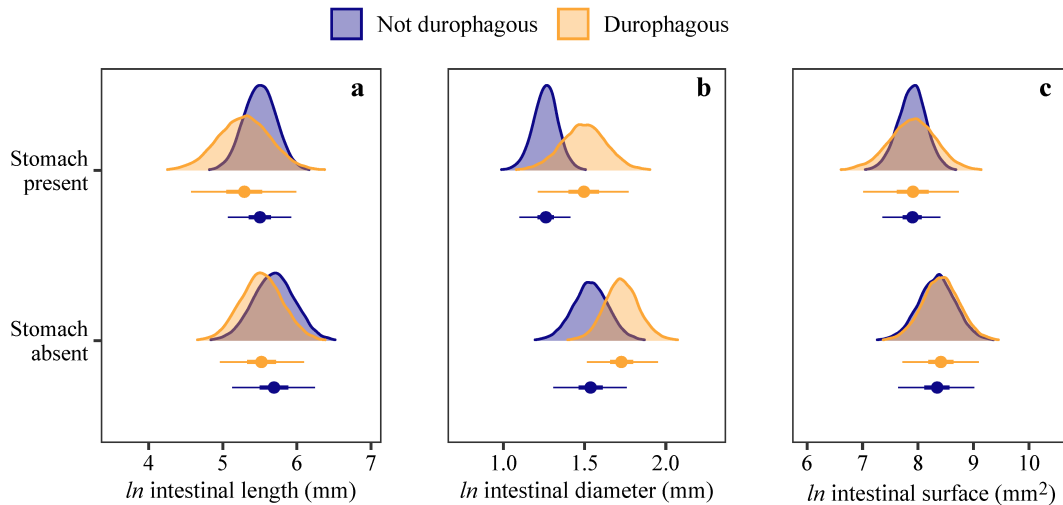
Figure 1.4: Effects of a stomach and durophagous diet on (**a**) intestinal length, (**b**) diameter, and (**c**) surface area for the 142 species of coral reef fishes. Estimates are posterior medians (circles), 50% credible intervals (CIs; thick lines) and 95% CIs (thin lines) from Bayesian phylogenetic hierarchical linear models after controlling for the remaining fixed and random effects. Posterior densities are also displayed (shaded regions).

of stomach presence, which resulted in no difference in intestinal surface area. Conversely, fishes with a stomach had a slightly shorter and narrower intestine than stomachless fishes, irrespective of diet. Thus, stomachless fishes had, on average a larger intestinal surface area. The most noticeable difference was observed between stomachless, durophagous species and fishes with a stomach and a non-durophagous diet, with the former having a larger intestinal diameter. These results remained consistent under our sensitivity analysis (Supplementary Fig. 1.8).

1.3.5 Intraspecific scaling

From the 142 species-specific scaling parameters obtained for each intestinal trait (Supplementary Table 1.5), our selection resulted in 19 reliable estimates for intestinal length, 18 for intestinal diameter, and 20 for intestinal surface area (Fig. 1.5). Considering the 80% CIs, three species (16%) showed allometric scaling of intestinal length, including two negative (*Balistapus undulatus*: $\beta = 0.51$ (0.26, 0.75); *Chromis xanthura*: $\beta = 0.61$ (0.31, 0.91); median and 80% CI) and one positive allometric relationships (*Chaetodon ornatissimus*: $\beta = 1.40$ (1.21, 1.57);
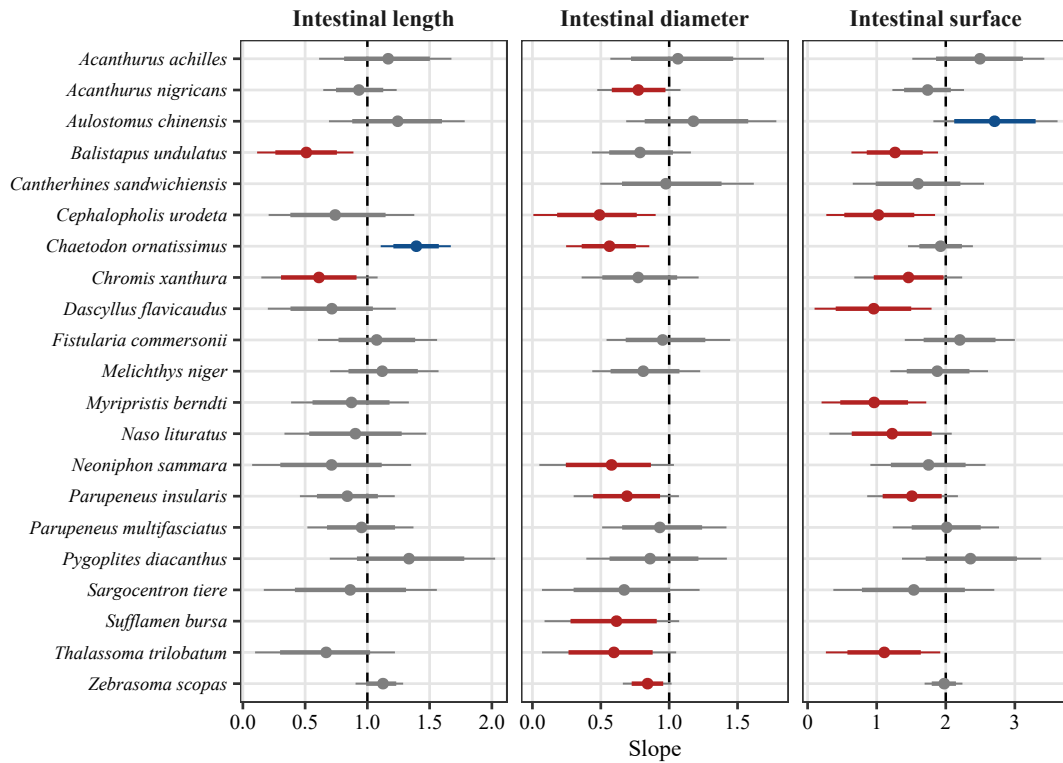
Figure 1.5: Species-specific scaling parameters of three natural-log intestinal traits against natural-log fish standard length for 21 species of coral reef fishes. Estimates are posterior medians (circles), 80% credible intervals (CIs; thick lines) and 95% CIs (thin lines) from Bayesian phylogenetic hierarchical linear models. Vertical dashed lines represent isometric scaling ($\beta = 1$ for intestinal length and diameter; $\beta = 2$ for intestinal surface area). Coloured intervals indicate allometric scaling, indicating that more than 90% (if 80% CIs) or 97.5% (if 95% CIs) of the posterior density was either above (blue; positive allometry) or below (red; negative allometry) the isometric scaling parameter, whereas grey intervals indicate that they overlap the parameter. For each trait, species were selected based on a minimum sample size of ten individuals whose size range covered at least 25% of the reported maximum body size (retrieved from FishBase) and a posterior 95% CI above zero to provide reliable estimates of scaling parameters. This selection resulted in missing estimates for one or two traits in five species.

median and 80% CI). Although no species had positive allometry for intestinal diameter, a negative allometry was found for eight out of 18 species (44%). Lastly, intestinal surface area exhibited allometry in nine species, including one positive scaling (*Aulostomus chinensis*: $\beta = 2.72$ (2.13, 3.32); median and 80% CI). The remaining 11 species did not deviate from an isometric relationship ($\beta = 2$).

1.4 Discussion

We investigated the relationship between reef fish intestinal morphology and phylogeny, body morphology, and diet using a large dataset of 142 species and 1,208 individuals. Our results indicate that, although intestinal traits in coral reef fishes are phylogenetically conserved, they are strongly related to body size, body elongation, and trophic level. Among species, intestinal length, diameter, and surface area are negatively correlated with trophic level and body elongation, and they generally scale isometrically with body size. Similarly, within species they predominantly scale isometrically. Furthermore, our analysis shows that intestinal diameter is related to stomach presence and a durophagous diet.

1.4.1 Phylogenetic conservatism

Reef fish intestinal morphology exhibits a high degree of phylogenetic conservatism. The strong phylogenetic signal observed for intestinal length is consistent with previous studies on fishes of the family Cichlidae and Terapontidae (Davis et al. 2013; Wagner et al. 2009), but our analysis revealed less conservatism for intestinal diameter. Further, we confirm that convergent evolution of long and/or wide intestines occurred several times across different lineages (Davis et al. 2013; Davis and Betancur-R 2017; Wagner et al. 2009). Chaetodontidae, Pomacanthidae, and herbivorous taxa evolved long intestines with large surface area to exploit trophic niches with nutritionally poor food resources. Conversely, Labridae and Tetraodontiformes, which generally lack a true stomach (Fagundes et al. 2016; Ray and Ringø 2014; Wilson and Castro 2010), evolved wide intestines to overcome limitations arising from the lack of food storage and processing inside the stomach. Furthermore, these species have a durophagous diet and well-developed teeth and/or pharyngeal jaws that grind food into smaller fragments, partly replacing the function of the stomach (Gromova and Maktotin 2019; Wainwright et al. 2012). The size of these particles remains, however, too large to be funnelled through a thin intestine and may require a thicker intestinal wall to protect from mechanical

damage (Fagundes et al. 2016). Although we cannot discern whether the large external intestinal diameter in Labridae and Tetraodontiformes is the result of a wider intestinal lumen, thicker intestinal wall, or a combination of the two, it appears that wide intestines have evolved multiple times, along with specialisations of the feeding apparatus (Wainwright et al. 2012), to exploit trophic resources otherwise unattainable.

Additionally, phylogenetic conservatism can be clearly observed within the Labridae. Within this family, parrotfishes (Labridae: tribe Scarini) have a larger intestine than other species. Evolutionary history has mainly led to an increase in the intestinal length and surface area in parrotfishes; however, intestinal diameter is conserved at the family level (see Supplementary Fig. 1.9). The large intestine, together with cranial specialisations (Gobalet 2018), could have played a substantial role in the initial divergence of the Scarini clade (Streelman et al. 2002), allowing them to adapt to an herbivorous diet and diversify rapidly (Siqueira et al. 2020), whereas other wrasses remained carnivores (Cowman et al. 2009; Floeter et al. 2018).

1.4.2 Interspecific scaling and relationships with body shape and trophic level

Among coral reef fishes, intestinal traits scale isometrically with body size after accounting for variation in body shape. Correction for body shape, in addition to allometry, is important because larger fishes have long body plans (Friedman et al. 2019), which in turn have relatively small abdominal cavities (Burns 2021) that may not accommodate large intestines. For instance, the two most distinctively elongated species in our dataset, *Aulostomus chinensis* and *Fistularia commersonii*, both of which are strict piscivores, had the lowest values across all intestinal traits.

Regardless of taxonomic identity, body size, and elongation, trophic level strongly influences intestinal morphology. The negative relationship between intestinal length and trophic level is consistent with previous work on marine and freshwater fishes (Elliott and Bellwood 2003; Kramer and Bryant 1995b; Wagner et al. 2009).

Furthermore, we found that the same negative relationship holds true for other intestinal traits, providing the first quantitative evidence that intestinal diameter, as well as length, varies as a function of trophic level. However, while carnivores and herbivores have the widest intestine and corallivores the narrowest across three reef fish families (Elliott and Bellwood 2003), a clear relationship between intestinal diameter and diet has not yet been established. We observed a significant decrease in diameter with increasing trophic level. Fishes with the highest trophic level (4.38) had a 32.5% narrower intestine than herbivorous fishes. Beyond the larger number of families sampled here, using a continuous variable to delineate reef fish diet (i.e., trophic level) helped uncover this relationship as opposed to the use of categorical trophic groups (Elliott and Bellwood 2003). These results suggest that intestinal diameter is useful to further delineate fish diet partitioning, and intestinal surface area, which incorporates variability in both length and diameter, may be a better descriptor of interspecific differences in intestinal morphology than intestinal length alone.

On average, the predicted intestinal surface area of herbivorous fishes in Mo'orea was four times that of fishes that occupy the highest trophic level. While this difference is determined by the increase in both intestinal length and diameter, the different rate of variation in these traits leads to intestinal elongation with decreasing trophic level. This increases the intestinal surface available for the absorption of nutrients, but it also increases food retention time, which is known to favour the digestion of food with low nutritional quality (Lassuy 1984; Sibly 1981).

1.4.3 Intraspecific scaling

In the present study, we provide estimates of scaling parameters for at least one intestinal trait of 21 reef fish species. Our results show that two thirds of these species exhibit allometric scaling in one or more traits, with several taxa decreasing the relative size of their intestinal diameter or surface area with increasing body size. For the remaining species, our data do not show any significant deviation from isometry. Widespread allometric elongation of the intestine has been observed

in both marine and freshwater fishes (Karachle and Stergiou 2010a; Kramer and Bryant 1995a; Ribble and Smith 1983). In contrast, we found positive allometry in intestinal length only for *C. ornatissimus*, while most species showed isometry. Our results highlight a tendency toward negative allometry in intestinal diameter and surface area. Thus, while the relative length of the intestine may remain constant or increase throughout an individual's lifetime, it generally becomes narrower and decreases in surface area. These results are consistent with the decrease in relative intestinal surface area observed in some herbivorous fishes (Al-Hussaini 1949; Gohar and Latif 1959; Horn 1989; Montgomery 1977) and the negative allometry in intestinal mass and metabolic capacity reported for two species of Cyprinidae (Goolish and Adelman 1988), and are potentially related to decreases in growth with increased size.

1.4.4 Intestinal morphology and function

Our results highlight the tight link between intestinal morphology and the digestive and assimilating functions in reef fishes. Intestinal traits are clear indicators of fish trophic roles and thus suitable for trait-based ecological research (Villéger et al. 2017). While intestinal length is commonly used in fish functional studies (Mouchet et al. 2013; Villéger et al. 2010; Zhao et al. 2019), we show that intestinal diameter provides an important addition to better segregate fish dietary habits and should therefore be considered. The intestine also play an important role in other fish functions, such as the absorption of nutrients (Crossman et al. 2005) and carbonate excretion (Wilson et al. 2002), which are key contributors to nutrient cycling and inorganic carbon cycling. Therefore, the intestinal traits presented herein could be used to explore relationship with these functions in future studies.

In the present study, we mainly focused on interspecific variability in intestinal morphology. However, in Mo'orea, the fishes were collected around the entire island, including a great span of habitats (lagoon and slope; coral-dominated and algae-dominated reefs), and across multiple seasons. While these variables were not explicitly accounted for in our analysis due to limited replication, our models

explained 85% to 92% of the variation in the data, demonstrating that intraspecific variability, independent of body size, was minor compared to interspecific variability in our dataset. Nevertheless, spatial and temporal variation in food availability and/or nutritional quality may lead to intraspecific variability (Olsson et al. 2007; Wagner et al. 2009). Therefore, these factors should be considered in future studies to fully understand the relationship between intestinal morphology and diet and assess the extent of intraspecific variability.

1.5 Conclusion

Our findings show that intestinal traits are highly conserved across reef fish phylogeny. We also demonstrate that via adaptive convergent evolution, intestinal flexibility permitted the occupation of trophic niches characterised by the uptake of food resources with low nutritional quality across diverse phylogenetic groups. Further, trophic level is strongly related to intestinal diameter, as well as length, in coral reef fishes. Species that occupy low trophic levels surmount the low nutritional value of food items by increasing intestinal absorptive surface and maximising nutrient intake. This is achieved with a differential increase in the length and diameter of the intestine, which results in an elongate alimentary tract that prolongs food retention. Thus, for trait-based ecological studies, intestinal length and diameter should be used together. Alternatively, if using a single trait, intestinal surface area may be a better descriptor of inter and intraspecific differences in diet than intestinal length.

Acknowledgements

References

Alfaro, Michael E., Francesco Santini, and Chad D. Brock (2007). "Do reefs drive diversification in marine teleosts? Evidence from the pufferfish and their allies (order tetraodontiformes)". In: *Evolution* 61.9, pp. 2104–2126. DOI: `10.1111/j.1558-5646.2007.00182.x`.

Banavar, Jayanth R. et al. (2014). "Form, function, and evolution of living organisms". In: *Proceedings of the National Academy of Sciences* 111.9, pp. 3332–3337. DOI: `10.1073/pnas.1401336111`.

Battley, Philip F and Theunis Piersma (2005). *Adaptive interplay between feeding ecology and feature of the digestive tract in birds*. Ed. by J Matthias Starck and Tobias Wang. Enfield: Science Publishers Inc., pp. 201–228.

Berumen, M. L., M. S. Pratchett, and B. A. Goodman (2011). "Relative gut lengths of coral reef butterflyfishes (Pisces: Chaetodontidae)". In: *Coral Reefs* 30.4, pp. 1005–1010. DOI: `10.1007/s00338-011-0791-x`.

Boettiger, Carl, D. T. Lang, and P. C. Wainwright (2012). "Rfishbase: Exploring, manipulating and visualizing FishBase data from R". In: *Journal of Fish Biology* 81.6, pp. 2030–2039. DOI: `10.1111/j.1095-8649.2012.03464.x`.

Brewster, Casey L, Jason Ortega, and Steven J Beaupre (2020). "Integrating bioenergetics and conservation biology: thermal sensitivity of digestive performance in Eastern Collared Lizards (Crotaphytus collaris) may affect population persistence". In: *Conservation Physiology* 8.1, pp. 1–9. DOI: `10.1093/conphys/coaa018`.

Bürkner, Paul Christian (2017). "brms: An R package for Bayesian multilevel models using Stan". In: *Journal of Statistical Software* 80.1, pp. 1–28. DOI: `10.18637/jss.v080.i01`.

Burns, Michael D. (2021). "Adaptation to herbivory and detritivory drives the convergent evolution of large abdominal cavities in a diverse freshwater fish radiation (Otophysi: Characiformes)". In: *Evolution* 75.3, pp. 688–705. DOI: `10.1111/evo.14178`.

Cant, John P., Brian W. McBride, and Warren J. Croom (1996). "The Regulation of Intestinal Metabolism and Its Impact on Whole Animal Energetics". In: *Journal of Animal Science* 74.10, pp. 2541–2553. DOI: `10.2527/1996.74102541x`.

Chang, Jonathan et al. (2019). "An r package and online resource for macroevolutionary studies using the ray-finned fish tree of life". In: *Methods in Ecology and Evolution* 10, pp. 1118–1124. DOI: `10.1111/2041-210X.13182`.

Claverie, Thomas and Peter C. Wainwright (2014). "A morphospace for reef fishes: Elongation is the dominant axis of body shape evolution". In: *PLoS ONE* 9.11, e112732. DOI: 10.1371/journal.pone.0112732.

Clements, K. D. and J. H Choat (2018). "Nutritional Ecology Of Parrotfishes (Scarinae, Labridae)". In: *Biology of parrotfishes*. Ed. by Andrew S. Hoey and Roberta M. Bonaldo. 1st ed. CRC Press. Chap. 3, pp. 42–68. DOI: 10.1201/9781315118079-3.

Cleveland, A and L Montgomery (2003). "Gut characteristics and assimilation efficiencies in two species of herbivorous damselfishes (Pomacentridae : Stegastes dorsopunicans and S . planifrons)". In: pp. 35–44. DOI: 10.1007/s00227-002-0916-4.

Cowman, Peter F., David R. Bellwood, and Lynne van Herwerden (2009). "Dating the evolutionary origins of wrasse lineages (Labridae) and the rise of trophic novelty on coral reefs". In: *Molecular Phylogenetics and Evolution* 52.3, pp. 621–631. DOI: 10.1016/j.ympev.2009.05.015.

Crossman, David J., J. Howard Choat, and Kendall D. Clements (2005). "Nutritional ecology of nominally herbivorous fishes on coral reefs". In: *Marine Ecology Progress Series* 296.July, pp. 129–142. DOI: 10.3354/meps296129.

Al-Dabbagh, Khalid Y., Jameel H. Jiad, and Intisar N. Waheed (1987). "The Influence of Diet on the Intestine Length of the White-Cheeked Bulbul". In: *Ornis Scandinavica* 18.2, pp. 150–152. DOI: 10.2307/3676852.

Dala-Corte, Renato Bolson, Fernando Gertum Becker, and Adriano Sanches Melo (2017). "Riparian integrity affects diet and intestinal length of a generalist fish species". In: *Marine and Freshwater Research* 68.7, pp. 1272–1281. DOI: 10.1071/MF16167.

Davis, Aaron M et al. (2013). "Ontogenetic development of intestinal length and relationships to diet in an Australasian fish family (Terapontidae)". In: *BMC Evolutionary Biology* 13, p. 53. DOI: 10.1186/1471-2148-13-53.

Davis, Aaron M. and Ricardo Betancur-R (2017). "Widespread ecomorphological convergence in multiple fish families spanning the marinefreshwater interface". In: *Proceedings of the Royal Society B: Biological Sciences* 284.1854. DOI: 10.1098/rspb.2017.0565.

Dykstra, Cheryl R. and William H. Karasov (1992). "Changes in Gut Structure and Function of House Wrens (Troglodytes aedon) in Response to Increased Energy Demands". In: *Physiological Zoology* 65.2, pp. 422–442. DOI: 10.1086/physzool.65.2.30158261.

Ekdale, Eric G. (2016). "Form and function of the mammalian inner ear". In: *Journal of Anatomy* 228.2, pp. 324–337. DOI: 10.1111/joa.12308.

Elliott, J. P. and D. R. Bellwood (2003). "Alimentary tract morphology and diet in three coral reef fish families". In: *Journal of Fish Biology* 63, pp. 1598–1609. DOI: 10.1046/j.1095-8649.2003.00272.x.

Emery, Alan R (1973). "Comparative ecology and functional osteology of fourteen species of damselfish (Pisces: Pomacentridae) at Alligator Reef, Florida Keys". In: *Bulletin of Marine Science* 23.3, pp. 649–770.

Fagundes, Kainã R.C., Matheus M. Rotundo, and Renata B. Mari (2016). "Morphological and histochemical characterization of the digestive tract of the puffer fish Sphoeroides testudineus (Linnaeus 1758) (Tetraodontiformes:

Tetraodontidae)". In: *Anais da Academia Brasileira de Ciencias* 88.3, pp. 1615–1624. DOI: 10.1590/0001-3765201620150167.

Floeter, Sergio R. et al. (2018). "Phylogenetic perspectives on reef fish functional traits". In: *Biological Reviews* 93.1, pp. 131–151. DOI: 10.1111/brv.12336.

Friedman, Sarah T. et al. (2019). "The influence of size on body shape diversification across Indo-Pacific shore fishes". In: *Evolution* 73.9, pp. 1873–1884. DOI: https://doi.org/10.1111/evo.13755.

Froese, R. and Daniel Pauly, eds. (2000). *FishBase 2000: Concepts, designs and data sources*. Los Banos, Laguna, Philippines: ICLARM, p. 344.

Gelman, Andrew et al. (2019). "Rsquared for Bayesian Regression Models". In: *The American Statistician* 73.3, pp. 307–309. DOI: 10.1080/00031305.2018.1549100.

German, Donovan P et al. (2010). "Evolution of Herbivory in a Carnivorous Clade of Minnows (Teleostei : Cyprinidae): Effects on Gut Size and Digestive Physiology". In: *Physiological and Biochemical Zoology* 83.1, pp. 1–18. DOI: 10.1086/648510.

Gobalet, Kenneth W. (2018). "Cranial Specializations of Parrotfishes, Genus Scarus (Scarinae, Labridae) for Scraping Reef Surfaces". In: *Biology of parrotfishes*. Ed. by Andrew S. Hoey and Roberta M. Bonaldo. 1st ed. CRC Press. Chap. 1, pp. 1–23. DOI: 10.1201/9781315118079-1.

Gohar, H. A. F. and A. F. A. Latif (1959). "Morphological studies on the gut of some scarid and labrid fishes". In: *Publications of the Marine Biology Station, Ghardaga, Red Sea* 10, 145–189.

Goolish, Edward M. and Ira R. Adelman (1988). "Tissue-specific allometry of an aerobic respiratory enzyme in a large and a small species of cyprinid (Teleostei)". In: *Canadian Journal of Zoology* 66.10, pp. 2199–2208. DOI: 10.1139/z88-327.

Griffen, Blaine D. and Hallie Mosblack (2011). "Predicting diet and consumption rate differences between and within species using gut ecomorphology". In: *Journal of Animal Ecology* 80.4, pp. 854–863. DOI: 10.1111/j.1365-2656.2011.01832.x.

Gromova, E. S. and V. V. Maktotin (2019). "Details of Structure and Functioning of the Pharyngeal Jaw Apparatus of Ember Parrotfish Scarus rubroviolaceus (Scaridae)". In: *Journal of Ichthyology* 59.6, pp. 907–927. DOI: 10.1134/S0032945219060031.

Hadfield, J. D. and S. Nakagawa (2010). "General quantitative genetic methods for comparative biology: Phylogenies, taxonomies and multi-trait models for continuous and categorical characters". In: *Journal of Evolutionary Biology* 23.3, pp. 494–508. DOI: 10.1111/j.1420-9101.2009.01915.x.

Herrel, Anthony et al. (2008). "Rapid large-scale evolutionary divergence in morphology and performance associated with exploitation of a different dietary resource". In: *Proceedings of the National Academy of Sciences* 105.12, pp. 4792–4795. DOI: 10.1073/pnas.0711998105.

Hesslein, R.H., K.A. Hallard, and P. Ramlal (1993). "Replacement of Sulfur, Carbon, and Nitrogen in Tissue of Growing Broad Whitefish (Coregonus nasus) in Response to a Change in Diet Traced by $\delta34S$, $\delta13C$, and $\delta15N$". In: *Canadian Journal of Fish and Aquatic Sciences* 50, pp. 2071–2076. DOI: 10.1139/f93-230.

Horn, M. H. (1989). "Biology of marine herbivorous fishes". In: *Oceanography and Marine Biology: An Annual Review*. Vol. 27, pp. 167–272.

Hunt, Andrew et al. (2019). "Phylogeny and herbivory are related to avian cecal size". In: *Scientific Reports* 9.1, pp. 1–9. DOI: 10.1038/s41598-019-40822-0.

Al-Hussaini, A. H. (1947). "The feeding habits and the morphology of the alimentary tract of some teleosts living in the neighbourhood of the Marine Biological Station,

Ghardaga, Red Sea." In: *Publications of the Marine Biology Station, Ghardaga, Red Sea* 5, pp. 1–61.

— (1949). "On the functional morphology of the alimentary tract of some fish in relation to differences in their feeding habits: Anatomy and histology". In: *Quarterly Journal of Microscopical Science* 90.June, pp. 109–139.

Hutchinson, John R et al. (2011). "From Flat Foot to Fat Foot: Structure, of Elephant Sixth Toes". In: *Science* 334.6063, pp. 1699–1703. DOI: 10.1126/science.1211437.

Karachle, Paraskevi K and Konstantinos I Stergiou (2010a). "Gut length for several marine fish : relationships with body length and trophic implications". In: *Marine Biodiversity Records* 3, pp. 1–10. DOI: 10.1017/S1755267210000904.

Kline, Thomas C. and Daniel Pauly (1998). "Cross-Validation of Trophic Level Estimates from a Mass-Balance Model of Prince William Sound Using 15N/14N Data". In: *Fishery Stock Assessment Models*. Ed. by et al. F. Funk, T.J. Quinn II, J. Heifetz. Alaska Sea Grant College Program Report No AK-SG-98-01, University of Alaska, Fairbanks, USA, pp. 693–702.

Koide, Yuki and Yoichi Sakai (2021). "Feeding habits of the white-spotted boxfish Ostracion meleagris reveal a strong preference for colonial ascidians". In: *Ichthyological Research* 68.4, pp. 461–470. DOI: 10.1007/s10228-021-00800-x.

Korn, Horst (1992). "Intestine lengths of Southern African savanna rodents and insectivores: intra and interspecific comparisons". In: *Journal of Zoology* 228.3, pp. 455–460. DOI: 10.1111/j.1469-7998.1992.tb04448.x.

Kramer, Donald L and Michael J Bryant (1995a). "Intestine length in the fishes of a tropical stream: 1. Ontogenetic allometry". In: *Environmental Biology of Fishes* 42, pp. 115–127. DOI: 10.1007/BF00001990.

— (1995b). "Intestine length in the fishes of a tropical stream: 2 . Relationships to diet - the long and short of a convoluted issue". In: *Environmental Biology of Fishes* 42, pp. 129–141. DOI: 10.1007/BF00001991.

Lassuy, Dennis R (1984). "Diet, intestinal morphology, and nitrogen assimilation efficiency in the damselfish, *Stegastes lividus*, in Guam". In: *Environmental Biology of Fishes* 10.3, pp. 183–193. DOI: 10.1007/BF00001125.

Lauder, George V. (1981). "Form and function: structural analysis in evolutionary morphology". In: *Paleobiology* 7.04, pp. 430–442. DOI: 10.1017/s0094837300025495.

Lynch, Michael (1991). "Methods for the analysis of comparative data in evolutionary biology". In: *Evolution* 45, pp. 993–1007. DOI: https://doi.org/10.1111/j.1558-5646.1991.tb04375.x.

Montgomery, W Linn (1977). "Diet and Gut Morphology in Fishes , with Special Reference to the Monkeyface Prickleback , Cebidichthys violaceus (Stichaeidae : Blennioidei)". In: *Copeia* 1977.1, pp. 178–182.

Mouchet, Maud A. et al. (2013). "Invariant scaling relationship between functional dissimilarity and co-occurrence in fish assemblages of the Patos Lagoon estuary (Brazil): Environmental filtering consistently overshadows competitive exclusion". In: *Oikos* 122.2, pp. 247–257. DOI: 10.1111/j.1600-0706.2012.20411.x.

Nakagawa, Shinichi and Eduardo S.A. Santos (2012). "Methodological issues and advances in biological meta-analysis". In: *Evolutionary Ecology* 26.5, pp. 1253–1274. DOI: 10.1007/s10682-012-9555-5.

Naya, Daniel E., William H. Karasov, and Francisco Bozinovic (2007). "Phenotypic plasticity in laboratory mice and rats: a meta-analysis of current ideas on gut size

flexibility". In: *Evolutionary Ecology Research* 9, pp. 1363–1374. DOI: `10.1016/j.cbpa.2007.06.336`.

Naya, Daniel E., Claudio Veloso, and Francisco Bozinovic (2009). "Gut Size Variation Among Bufo spinulosus Populations Along an Altitudinal (and Dietary) Gradient". In: *Annales Zoologici Fennici* 46.1, pp. 16–20. DOI: `10.5735/086.046.0102`.

Naya, Daniel E. et al. (2014). " Digestive morphology of two species of Abrothrix (Rodentia, Cricetidae): comparison of populations from contrasting environments ". In: *Journal of Mammalogy* 95.6, pp. 1222–1229. DOI: `10.1644/13-mamm-a-261`.

O'Grady, Shannon P. et al. (2005). "Correlating diet and digestive tract specialization: examples from the lizard family Liolaemidae". In: *Zoology* 108, pp. 201–210. DOI: `10.1016/j.zool.2005.06.002`.

Olsson, Jens et al. (2007). "Gut length plasticity in perch: into the bowels of resource polymorphisms". In: *Biological Journal of the Linnean Society* 90.3, pp. 517–523. DOI: `10.1111/j.1095-8312.2007.00742.x`.

Pagel, Mark (1999). "Inferring historical patterns of biological evolution". In: *Nature* 401, pp. 877–884. DOI: `10.1038/44766`.

Parravicini, Valeriano et al. (2020). "Delineating reef fish trophic guilds with global gut content data synthesis and phylogeny". In: *PLoS Biology* 18.12, e3000702. DOI: `10.1371/journal.pbio.3000702`.

Piersma, Theunis and Ake Lindström (1997). "Rapid reversible changes in organ size as a component of adaptive behaviour". In: *Trends in Ecology and Evolution* 12.4, pp. 134–138. DOI: `10.1016/S0169-5347(97)01003-3`.

Price, S A et al. (2011). "Coral reefs promote the evolution of morphological diversity and ecological novelty in labrid fishes". In: *Ecology letters* 14.5, pp. 462–9. DOI: `10.1111/j.1461-0248.2011.01607.x`.

Price, Samantha A et al. (2013). "Elevated rates of morphological and functional diversification in reef-dwelling haemulid fishes". In: *Evolution* 67.2, pp. 417–428. DOI: `10.1111/j.1558-5646.2012.01773.x`.

R Core Team (2020). *R: a language and environment for statistical computing*.

Rabosky, Daniel L. et al. (2018). "An inverse latitudinal gradient in speciation rate for marine fishes". In: *Nature* 559.7714, pp. 392–395. DOI: `10.1038/s41586-018-0273-1`.

Ray, Arun Kumar and Einar Ringø (2014). "The Gastrointestinal Tract of Fish". In: *Aquaculture Nutrition* September 2014, pp. 1–13. DOI: `10.1002/9781118897263.ch1`.

Ribble, D O and M H Smith (1983). "Relative intestine length and feeding ecology of freshwater fishes." In: *Growth* 47.3, pp. 292–300.

Ricklefs, R. E. (1996). "Morphometry of the Digestive Tracts of Some Passerine Birds". In: *The Condor* 98.2, pp. 279–292. DOI: `10.2307/1369146`.

Schiettekatte, Nina M. D., Simon J. Brandl, and Jordan M. Casey (2021). *fishualize: Color Palettes Based on Fish Species*. R package version 0.2.2. URL: `https://CRAN.R-project.org/package=fishualize`.

Schindelin, Johannes et al. (2012). "Fiji: an open-source platform for biological-image analysis". In: *Nature methods* 9.7, pp. 676–82. DOI: `10.1038/nmeth.2019`.

Sibly, R. M. (1981). "Strategies of digestion and defecation." In: *Physiological ecology: an evolutionary approach to resource use*. Ed. by C. R. Townsend and P. Calow. Oxford: Blackwell Publishing, pp. 109–139.

Siqueira, Alexandre C. et al. (2020). "Trophic innovations fuel reef fish diversification". In: *Nature Communications* 11, p. 2669. DOI: 10.1038/s41467-020-16498-w.

Sorenson, Laurie et al. (2013). "A multi-locus timetree of surgeonfishes (Acanthuridae, Percomorpha), with revised family taxonomy". In: *Molecular Phylogenetics and Evolution* 68.1, pp. 150–160. DOI: 10.1016/j.ympev.2013.03.014.

Starck, J M and K Beese (2001). "Structural flexibility of the intestine of Burmese python in response to feeding." In: *Journal of Experimental Biology* 204.Pt 2, pp. 325–335.

— (2002). "Structural flexibility of the small intestine and liver of garter snakes in response to feeding and fasting". In: *Journal of Experimental Biology* 205.Pt 10, pp. 1377–1388.

Starck, J. Matthias (2003). "Shaping up: How vertebrates adjust their digestive system to changing environmental conditions". In: *Animal Biology* 53.3, pp. 245–257. DOI: 10.1163/157075603322539444.

Steinberg, Christian E.W. (2018). "Diets and Digestive Tracts Your Food Determines Your Intestine'". In: *Aquatic Animal Nutrition: A Mechanistic Perspective from Individuals to Generations.* Springer International Publishing, pp. 9–59. DOI: 10.1007/978-3-319-91767-2.

Streelman, J. T. et al. (2002). "Evolutionary history of the parrotfishes: Biogeography, ecomorphology, and comparative diversity". In: *Evolution* 56.5, pp. 961–971. DOI: 10.1111/j.0014-3820.2002.tb01408.x.

Villéger, Sébastien et al. (2010). "Contrasting changes in taxonomie vs. functional diversity of tropical fish communities after habitat degradation". In: *Ecological Applications* 20.6, pp. 1512–1522. DOI: 10.1890/09-1310.1.

Villéger, Sébastien et al. (2017). "Functional ecology of fish: current approaches and future challenges". In: *Aquatic Sciences* 79.4, pp. 783–801. DOI: 10.1007/s00027-017-0546-z.

Wagner, Catherine E et al. (2009). "Diet predicts intestine length in Lake Tanganyika's cichlid fishes". In: *Functional Ecology* 23, pp. 1122–1131. DOI: 10.1111/j.1365-2435.2009.01589.x.

Wainwright, Peter C. et al. (2012). "The Evolution of Pharyngognathy: A Phylogenetic and Functional Appraisal of the Pharyngeal Jaw Key Innovation in Labroid Fishes and beyond". In: *Systematic Biology* 61.6, pp. 1001–1027. DOI: 10.1093/sysbio/sys060.

Wainwright, Stephen A. (1988). "Form and Function in Organism". In: *American Zoologist* 28.2, pp. 671–680. DOI: 10.2307/2577560.

Wang, R. Z., L. Addadi, and S. Weiner (1997). "Design strategies of sea urchin teeth : Structure, composition and micromechanical relations to function". In: *Philosophical Transactions of the Royal Society B: Biological Sciences* 352.1352, pp. 469–480. DOI: 10.1098/rstb.1997.0034.

Wang De-Hua et al. (2003). "Digestive tract morphology and food habits in six species of rodents". In: *Folia Zoologica* 52.1, pp. 51–55.

Westneat, Mark W (1995). "Feeding , Function , and Phylogeny : Analysis of Historical Biomechanics in Labrid Fishes Using Comparative Methods". In: *Systematic Biology* 44.3, pp. 361–383. DOI: 10.2307/2413598.

Wilson, J. M. and L. F.C. Castro (2010). *Morphological diversity of the gastrointestinal tract in fishes.* First Edition. Vol. 30. C. Elsevier Inc., pp. 1–55. DOI: 10.1016/S1546-5098(10)03001-3.

Wilson, Rod W., Jonathan M. Wilson, and Martin Grosell (2002). "Intestinal bicarbonate secretion by marine teleost fish-why and how?" In: *Biochimica et Biophysica Acta* 1566, pp. 182–193. DOI: `10.1016/s0005-2736(02)00600-4`.

Yu, Guangchuang et al. (2017). "GGTREE: an R Package for Visualization and Annotation of Phylogenetic Trees With Their Covariates and Other Associated Data". In: *Methods in Ecology and Evolution* 8.1, pp. 28–36. DOI: `10.1111/2041-210X.12628`.

Zaldúa, Natalia and Daniel E. Naya (2014). "Digestive flexibility during fasting in fish: A review". In: *Comparative Biochemistry and Physiology - A Molecular and Integrative Physiology* 169, pp. 7–14. DOI: `10.1016/j.cbpa.2013.12.006`.

Zhao, Yanyang et al. (2019). "Bio-precipitation of calcium and magnesium ions through extracellular and intracellular process induced by bacillus licheniformis SRB2". In: *Minerals* 9.9, pp. 1–23. DOI: `10.3390/min9090526`.

Supplementary Information

Supplementary Methods

Relationship between trophic level and δ^{15}N

To test whether food-item based trophic levels in FishBase are representative of fish diet in Mo'orea we built a dataset of nitrogen stable isotope ratios (δ^{15}N) for 83 of the 142 species present in our dataset of intestinal traits. A total of 700 individuals ($n = 3$ per species minimum) collected from reefs around Mo'orea, in French Polynesia, including 319 in 2016 and 381 in 2018, were examined. All individuals were collected by spearfishing between 10:00 and 15:00 and transferred to the laboratory in a cooler. In the laboratory, each individual was measured and weighed, and a small piece of dorsal muscle was sampled and immediately frozen at -20 °C.

Nitrogen stable isotope data (^{15}N) were determined in all samples that were freeze-dried and ground to fine powder. Measurements were done by continuous-flow isotope-ratio mass spectrometry with a NC2500 elemental analyzer (CE Instruments, Wigan, UK), coupled with a Delta V isotope ratio mass spectrometer (Thermo Scientific, Bremen, Germany) at the Cornell University Stable Isotope Laboratory (COIL). Isotope compositions were expressed in the δ notation as parts per mil (‰) as deviations from atmospheric N$_2$ following the formula:

$$\delta X = [(R_{\text{sample}}/R_{\text{standard}}) - 1] \times 1000, \tag{S1.1}$$

where X is ^{15}N, R is the corresponding ^{15}N/^{14}N ratio. Calibration was done using two in-house standards (CBT and KCRN). The analytical precision of the measurements was 0.24‰ based on analyses of an in-house animal standard (Deer).

To assess the relationship between trophic level and δ^{15}N we fitted a Bayesian phylogenetic hierarchical linear model. We extracted the phylogeny for the 83 species in the dataset from the Fish Tree of Life (Rabosky et al. 2018) using the R package *fishtree* version 0.3.2 (Chang et al. 2019). Using this phylogenetic information, we constructed a phylogenetic relatedness matrix (Hadfield and Nakagawa

2010) and we tested whether body size, trophic level and phylogeny explain the variation in δ^{15}N values using a Bayesian phylogenetic hierarchical linear model. The δ^{15}N value of the ith individual of the jth species is estimated as follows:

$$\delta^{15}N_{ij} = \beta_{0j} + \beta_{1j}\ln(SL)_{ij} + \beta_2 TL_j, \tag{S1.2}$$

with β_{0j} and β_{1j} defined as:

$$\beta_{0j} = \gamma_{00} + u_{0\text{phy}} + u_{0j}, \tag{S1.3}$$

$$\beta_{1j} = \gamma_{10} + u_{1j}, \tag{S1.4}$$

where γ_{00} is the estimated average intercept, $u_{0\text{phy}}$ and u_{0j} represent deviations from the model intercept attributable to species-level variation related and unrelated to the phylogeny, respectively, γ_{10} is the average slope for the natural-log transformed standard length (SL), u_{1j} represents deviations from γ_{10} attributable to species-level variation, and β_2 is the slope for trophic level (TL). All predictors were centred and scaled. We fitted the model with the R package *brms* version 2.14.4 (Bürkner 2017) using a student-t error distribution. We used normally distributed priors with a mean of zero for intercept, fixed and random effects, and ran the model for four chains, each with 4,000 steps and a warm-up of 1,000 steps.

Our model explained 82.2% of the variation in δ^{15}N values across species. Nitrogen isotope ratios were influenced by phylogeny ($H^2 = 0.74$ [0.40, 0.94], mean and 95% credible interval). After controlling for the phylogenetic relationships, δ^{15}N was positively related to body size ($\beta = 0.79$ [0.45, 1.14]) and trophic level ($\beta = 0.97$ [0.42, 1.51]), and the latter explained the highest proportion of variance in δ^{15}N (highest standardised effect; Supplementary Table 1.6). Nitrogen isotope ratios increased linearly with trophic level (one unit increase in δ^{15}N for every one unit increase in trophic level on average), implying a 27.6% increase in δ^{15}N over the observed range of trophic level (from 2.00 to 4.38; Supplementary Fig. 1.10). Although on average δ^{15}N was positively related to body size, this relationship varied greatly among species (Supplementary Table 1.6).

Supplementary Figures

Posterior predictive draws (thin lines) vs observed data (thick line)
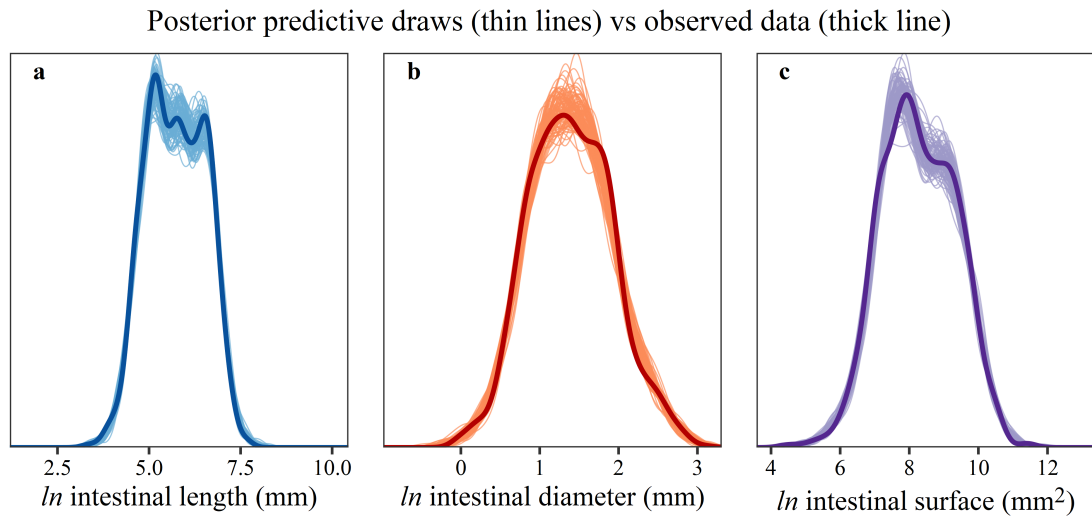
Figure 1.6: Posterior predictive checks based on 100 posterior samples for Bayesian phylogenetic hierarchical linear models of (**a**) intestinal length, (**b**) diameter, and (**c**) surface area of coral reef fishes.
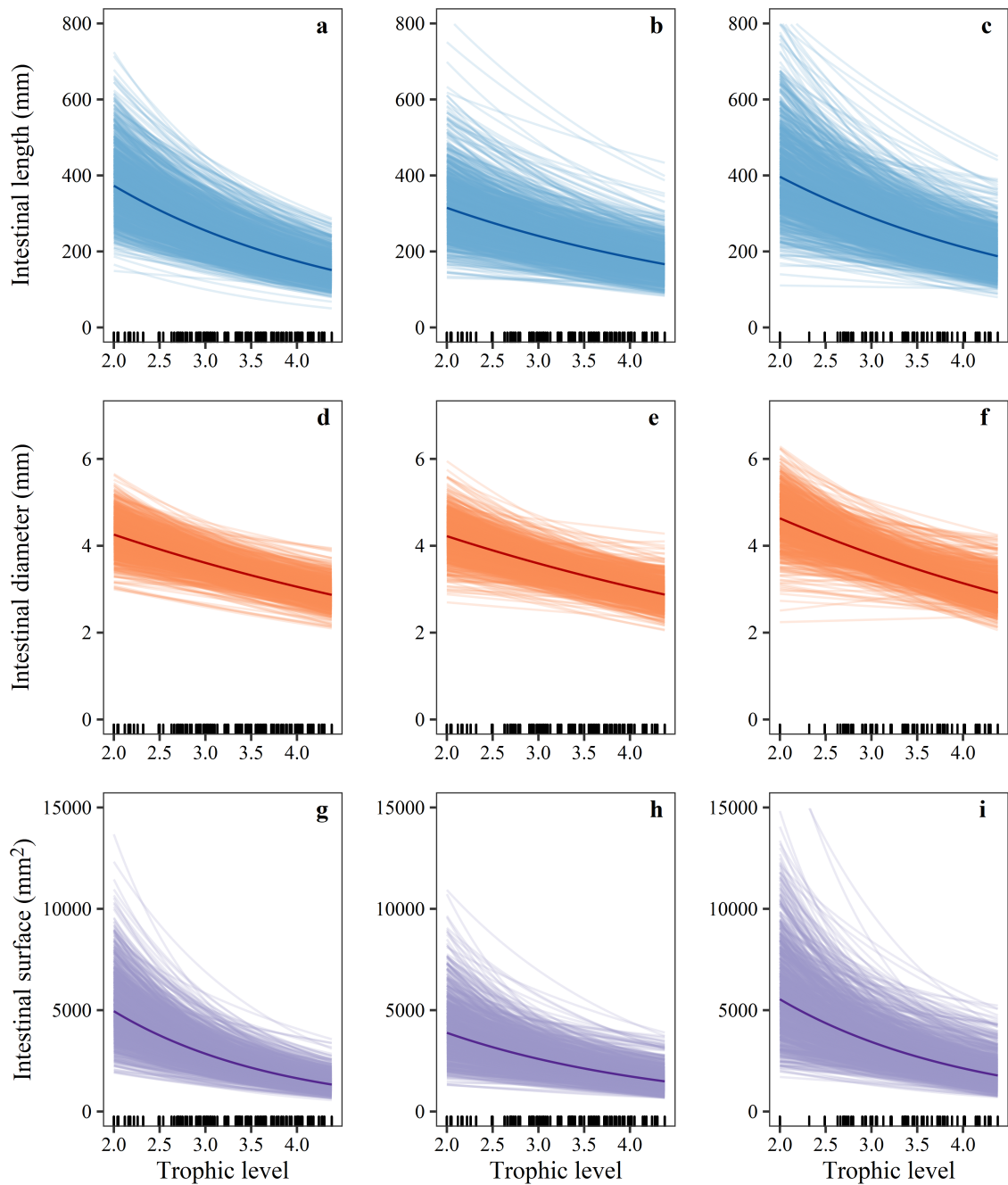
Figure 1.7: Relationship between three intestinal traits and trophic level for: 142 species of coral reef fishes with a minimum sample size of three individuals per species (**a**, **d**, **g**); 122 species of coral reef fishes with a minimum sample size of three individuals per species (**b**, **e**, **h**); and 69 species of coral reef fishes with a minimum sample size of eight individuals per species (**c**, **f**, **i**). Thick, darkened lines represent the mean predicted fits of Bayesian phylogenetic hierarchical linear models after controlling for the remaining fixed and random effects. Categorical variables were set to their most common value (stomach = present, durophagy = non-durophagous). Thin lines represent 1,000 draws randomly chosen from the posterior fits and show model fit uncertainty. Model predictions are for natural-log intestinal traits, but are transformed here to show the fitted function on the original scale of the data. Raw data are displayed as marks along the x-axis.
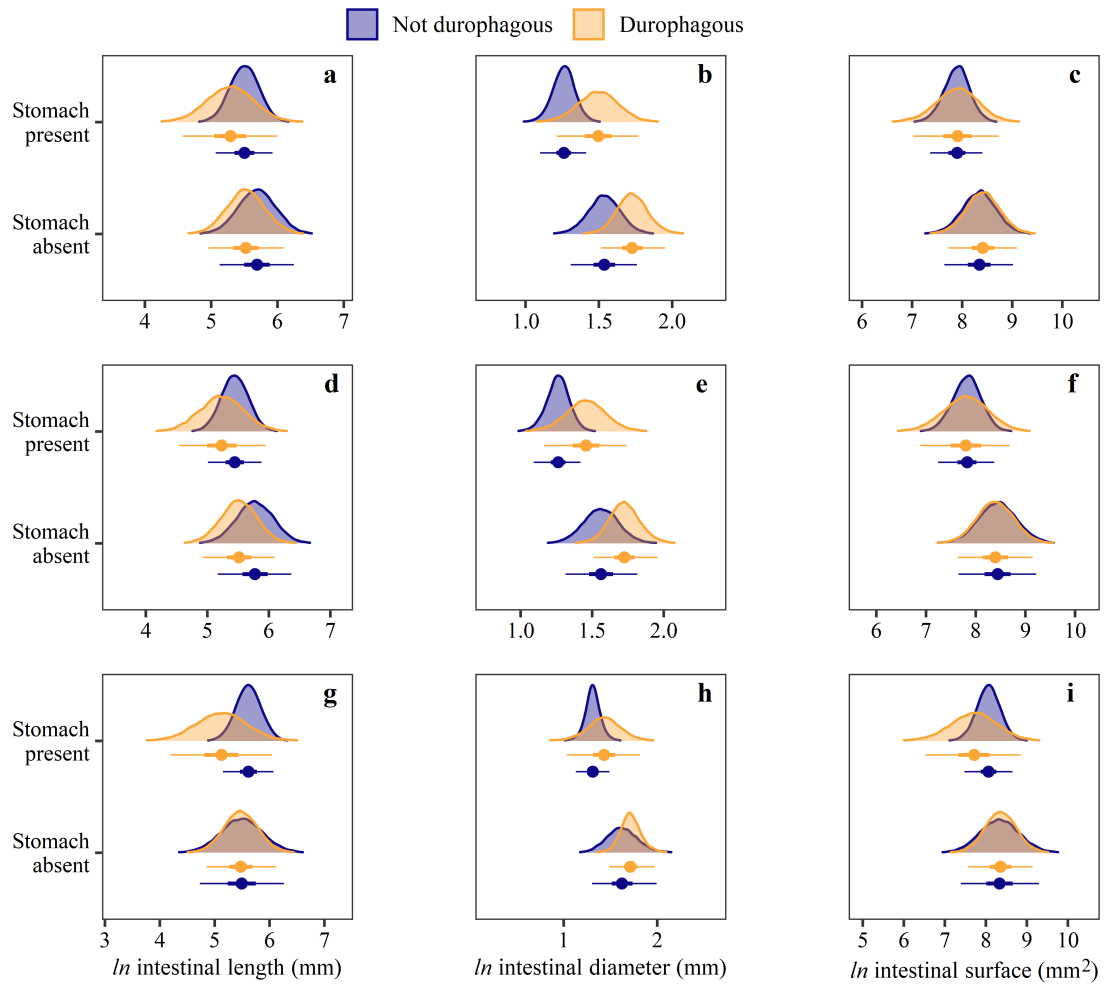
Figure 1.8: Effects of stomach presence and durophagous diet on three intestinal traits for: 142 species of coral reef fishes with a minimum sample size of three individuals per species (**a**, **b**, **c**); 122 species of coral reef fishes with a minimum sample size of three individuals per species (**d**, **e**, **f**); and 69 species of coral reef fishes with a minimum sample size of eight individuals per species (**g**, **h**, **i**). Estimates are posterior medians (circles), 50% credible intervals (CIs; thick lines) and 95% CIs (thin lines) from Bayesian phylogenetic hierarchical linear models after controlling for the remaining fixed and random effects. Posterior densities are also displayed (shaded regions).
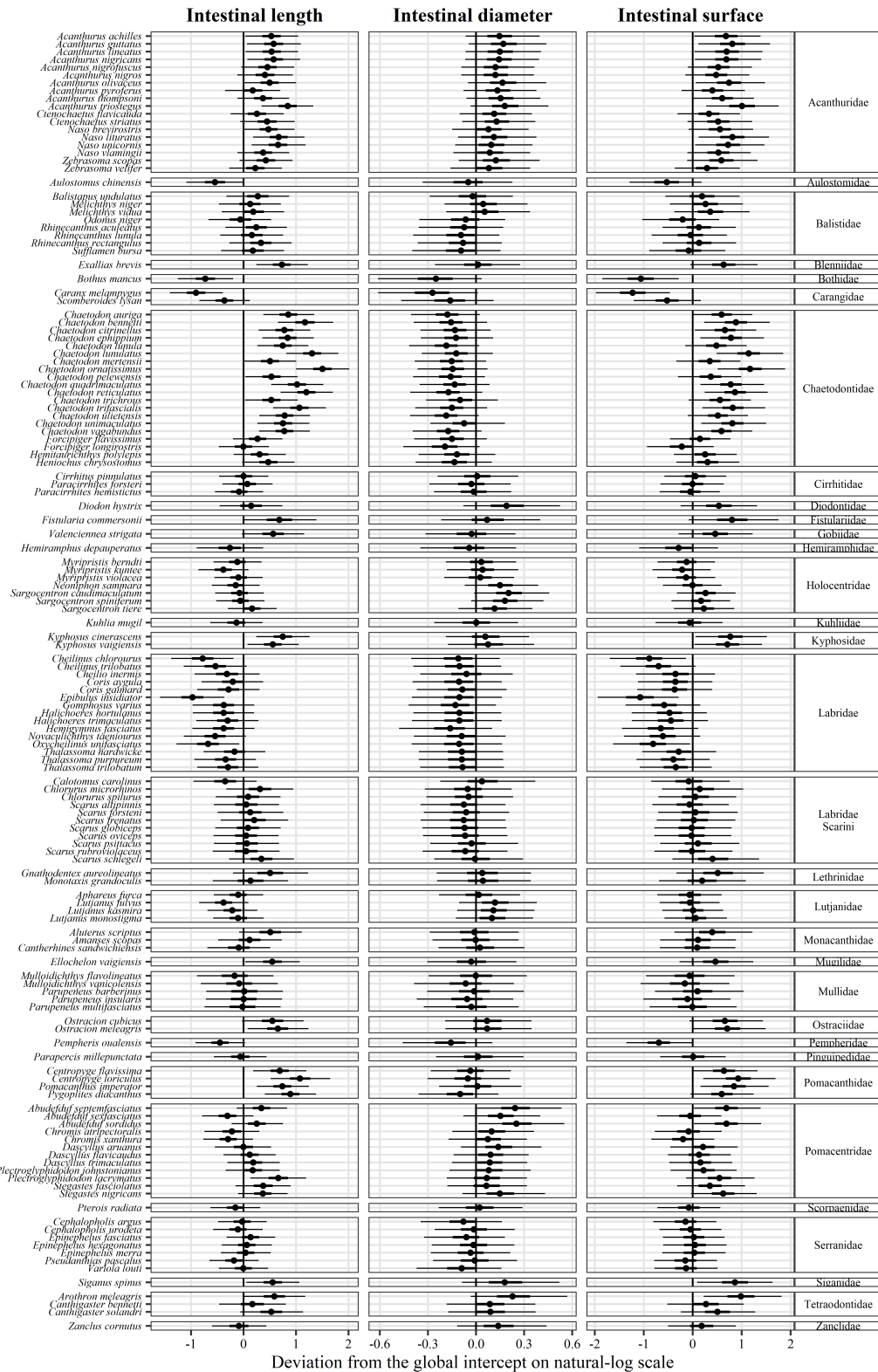
Figure 1.9: Effect of phylogeny on three intestinal traits for 142 species of coral reef fishes. Estimates are posterior medians (circles), 50% credible intervals (CIs; thick lines) and 95% CIs (thin lines) from Bayesian phylogenetic hierarchical linear models, and represent deviations from the global intercept on natural-log scale.
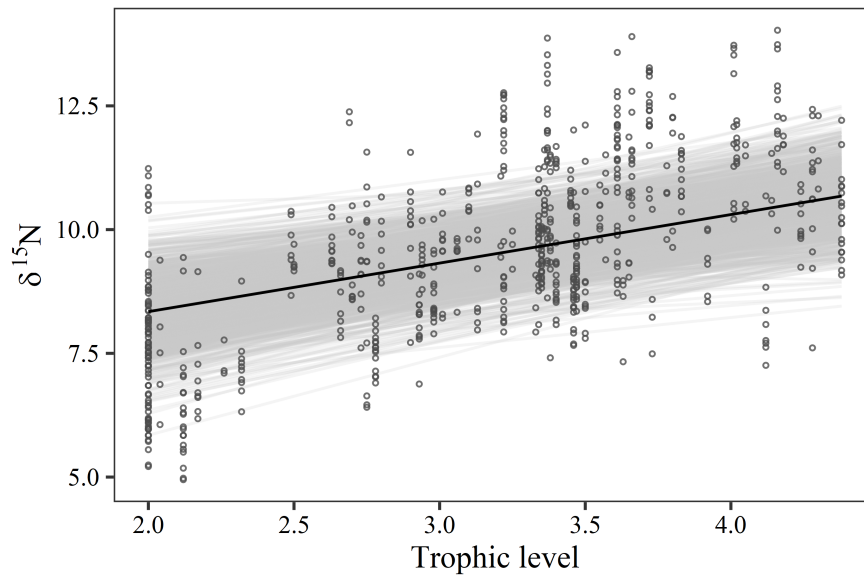
Figure 1.10: Relationship between $\delta^{15}N$ and trophic level for 83 species of coral reef fishes. Thick, darkened line represents the mean predicted fit of a Bayesian phylogenetic hierarchical linear model after controlling for body size and phylogeny. Thin lines represent 1,000 draws randomly chosen from the posterior fits and show model fit uncertainty. Dots represent the raw values.

Supplementary Tables

Table 1.1: Number of individuals per species collected from three different habitats.

Family	Species	Slope	Lagoon	Pass	Total
Acanthuridae	*Acanthurus achilles*	12	0	0	12
Acanthuridae	*Acanthurus guttatus*	8	1	0	9
Acanthuridae	*Acanthurus lineatus*	7	0	2	9
Acanthuridae	*Acanthurus nigricans*	12	1	0	13
Acanthuridae	*Acanthurus nigrofuscus*	2	3	1	6
Acanthuridae	*Acanthurus nigros*	3	0	1	4
Acanthuridae	*Acanthurus olivaceus*	5	0	1	6
Acanthuridae	*Acanthurus pyroferus*	2	2	1	5
Acanthuridae	*Acanthurus thompsoni*	3	0	1	4
Acanthuridae	*Acanthurus triostegus*	5	8	2	15
Acanthuridae	*Ctenochaetus flavicauda*	4	0	2	6
Acanthuridae	*Ctenochaetus striatus*	2	3	0	5
Acanthuridae	*Naso brevirostris*	6	0	0	6
Acanthuridae	*Naso lituratus*	17	0	0	17
Acanthuridae	*Naso unicornis*	1	0	4	5
Acanthuridae	*Naso vlamingii*	3	0	2	5
Acanthuridae	*Zebrasoma scopas*	26	16	0	42
Acanthuridae	*Zebrasoma velifer*	4	0	5	9
Aulostomidae	*Aulostomus chinensis*	3	7	1	11
Balistidae	*Balistapus undulatus*	8	4	0	12
Balistidae	*Melichthys niger*	14	0	0	14
Balistidae	*Melichthys vidua*	10	2	0	12
Balistidae	*Odonus niger*	11	3	0	14
Balistidae	*Rhinecanthus aculeatus*	0	7	2	9
Balistidae	*Rhinecanthus lunula*	2	0	1	3
Balistidae	*Rhinecanthus rectangulus*	6	0	3	9
Balistidae	*Sufflamen bursa*	6	6	0	12
Blenniidae	*Exallias brevis*	3	0	2	5
Bothidae	*Bothus mancus*	0	1	2	3
Carangidae	*Caranx melampygus*	4	0	1	5
Carangidae	*Scomberoides lysan*	2	0	1	3
Chaetodontidae	*Chaetodon auriga*	2	2	5	9
Chaetodontidae	*Chaetodon bennetti*	0	0	3	3
Chaetodontidae	*Chaetodon citrinellus*	3	2	2	7
Chaetodontidae	*Chaetodon ephippium*	3	4	1	8
Chaetodontidae	*Chaetodon lunula*	1	4	4	9
Chaetodontidae	*Chaetodon lunulatus*	0	8	0	8
Chaetodontidae	*Chaetodon mertensii*	0	1	4	5
Chaetodontidae	*Chaetodon ornatissimus*	29	0	0	29
Chaetodontidae	*Chaetodon pelewensis*	6	0	0	6
Chaetodontidae	*Chaetodon quadrimaculatus*	6	0	2	8
Chaetodontidae	*Chaetodon reticulatus*	32	0	0	32
Chaetodontidae	*Chaetodon trichrous*	2	1	3	6
Chaetodontidae	*Chaetodon trifascialis*	2	1	3	6
Chaetodontidae	*Chaetodon ulietensis*	2	1	5	8
Chaetodontidae	*Chaetodon unimaculatus*	5	3	1	9
Chaetodontidae	*Chaetodon vagabundus*	4	9	0	13
Chaetodontidae	*Forcipiger flavissimus*	2	6	0	8

Family	Species	Slope	Lagoon	Pass	Total
Chaetodontidae	*Forcipiger longirostris*	7	0	0	7
Chaetodontidae	*Hemitaurichthys polylepis*	5	0	2	7
Chaetodontidae	*Heniochus chrysostomus*	1	7	0	8
Cirrhitidae	*Cirrhitus pinnulatus*	6	0	4	10
Cirrhitidae	*Paracirrhites forsteri*	6	1	2	9
Cirrhitidae	*Paracirrhites hemistictus*	17	0	1	18
Diodontidae	*Diodon hystrix*	1	2	2	5
Fistulariidae	*Fistularia commersonii*	1	4	5	10
Gobiidae	*Valenciennea strigata*	0	5	1	6
Hemiramphidae	*Hemiramphus depauperatus*	1	2	0	3
Holocentridae	*Myripristis berndti*	1	15	0	16
Holocentridae	*Myripristis kuntee*	0	6	1	7
Holocentridae	*Myripristis violacea*	0	2	7	9
Holocentridae	*Neoniphon sammara*	0	12	0	12
Holocentridae	*Sargocentron caudimaculatum*	0	7	0	7
Holocentridae	*Sargocentron spiniferum*	5	4	1	10
Holocentridae	*Sargocentron tiere*	5	5	1	11
Kuhliidae	*Kuhlia mugil*	2	0	1	3
Kyphosidae	*Kyphosus cinerascens*	0	0	3	3
Kyphosidae	*Kyphosus vaigiensis*	2	0	2	4
Labridae	*Calotomus carolinus*	3	2	4	9
Labridae	*Cheilinus chlorourus*	0	9	0	9
Labridae	*Cheilinus trilobatus*	1	6	0	7
Labridae	*Cheilio inermis*	0	0	4	4
Labridae	*Chlorurus microrhinos*	4	0	0	4
Labridae	*Chlorurus spilurus*	5	1	0	6
Labridae	*Coris aygula*	3	4	2	9
Labridae	*Coris gaimard*	5	0	2	7
Labridae	*Epibulus insidiator*	12	4	0	16
Labridae	*Gomphosus varius*	4	3	0	7
Labridae	*Halichoeres hortulanus*	0	8	1	9
Labridae	*Halichoeres trimaculatus*	0	5	0	5
Labridae	*Hemigymnus fasciatus*	8	0	1	9
Labridae	*Novaculichthys taeniourus*	2	1	3	6
Labridae	*Oxycheilinus unifasciatus*	3	0	1	4
Labridae	*Scarus altipinnis*	6	0	0	6
Labridae	*Scarus forsteni*	8	1	0	9
Labridae	*Scarus frenatus*	2	2	0	4
Labridae	*Scarus globiceps*	1	2	4	7
Labridae	*Scarus oviceps*	6	1	0	7
Labridae	*Scarus psittacus*	0	6	3	9
Labridae	*Scarus rubroviolaceus*	2	0	3	5
Labridae	*Scarus schlegeli*	3	0	4	7
Labridae	*Thalassoma hardwicke*	0	7	0	7
Labridae	*Thalassoma purpureum*	4	1	0	5
Labridae	*Thalassoma trilobatum*	6	1	3	10
Lethrinidae	*Gnathodentex aureolineatus*	1	4	2	7
Lethrinidae	*Monotaxis grandoculis*	4	2	1	7
Lutjanidae	*Aphareus furca*	7	0	2	9
Lutjanidae	*Lutjanus fulvus*	3	6	2	11
Lutjanidae	*Lutjanus kasmira*	6	0	3	9

Table 1.1: *(continued)*

Family	Species	Slope	Lagoon	Pass	Total
Lutjanidae	*Lutjanus monostigma*	2	0	3	5
Monacanthidae	*Aluterus scriptus*	0	0	4	4
Monacanthidae	*Amanses scopas*	8	0	1	9
Monacanthidae	*Cantherhines sandwichiensis*	9	0	1	10
Mugilidae	*Ellochelon vaigiensis*	0	2	2	4
Mullidae	*Mulloidichthys flavolineatus*	0	8	1	9
Mullidae	*Mulloidichthys vanicolensis*	1	1	3	5
Mullidae	*Parupeneus barberinus*	0	3	1	4
Mullidae	*Parupeneus insularis*	7	2	2	11
Mullidae	*Parupeneus multifasciatus*	3	8	0	11
Ostraciidae	*Ostracion cubicus*	0	1	2	3
Ostraciidae	*Ostracion meleagris*	0	5	2	7
Pempheridae	*Pempheris oualensis*	6	0	1	7
Pinguipedidae	*Parapercis millepunctata*	0	7	0	7
Pomacanthidae	*Centropyge flavissima*	4	2	2	8
Pomacanthidae	*Centropyge loriculus*	3	0	0	3
Pomacanthidae	*Pomacanthus imperator*	7	0	0	7
Pomacanthidae	*Pygoplites diacanthus*	3	3	4	10
Pomacentridae	*Abudefduf septemfasciatus*	1	8	2	11
Pomacentridae	*Abudefduf sexfasciatus*	0	8	1	9
Pomacentridae	*Abudefduf sordidus*	2	1	3	6
Pomacentridae	*Chromis atripectoralis*	0	3	2	5
Pomacentridae	*Chromis xanthura*	22	0	2	24
Pomacentridae	*Dascyllus aruanus*	0	3	4	7
Pomacentridae	*Dascyllus flavicaudus*	9	5	0	14
Pomacentridae	*Dascyllus trimaculatus*	1	5	2	8
Pomacentridae	*Plectroglyphidodon johnstonianus*	6	0	0	6
Pomacentridae	*Plectroglyphidodon lacrymatus*	6	0	0	6
Pomacentridae	*Stegastes fasciolatus*	6	0	3	9
Pomacentridae	*Stegastes nigricans*	0	7	3	10
Scorpaenidae	*Pterois radiata*	3	5	1	9
Serranidae	*Cephalopholis argus*	15	1	1	17
Serranidae	*Cephalopholis urodeta*	13	0	1	14
Serranidae	*Epinephelus fasciatus*	5	0	1	6
Serranidae	*Epinephelus hexagonatus*	5	0	2	7
Serranidae	*Epinephelus merra*	0	8	1	9
Serranidae	*Pseudanthias pascalus*	5	0	2	7
Serranidae	*Variola louti*	6	0	1	7
Siganidae	*Siganus spinus*	2	3	0	5
Tetraodontidae	*Arothron meleagris*	4	5	0	9
Tetraodontidae	*Canthigaster bennetti*	0	3	0	3
Tetraodontidae	*Canthigaster solandri*	0	5	1	6
Zanclidae	*Zanclus cornutus*	8	3	0	11

Table 1.2: Posterior mean and 95% credible interval for each parameter of Bayesian phylogenetic hierarchical linear models of intestinal length, diameter, and surface area for 142 species of coral reef fishes with a minimum sample size of three individuals per species. α = model intercept; $\beta_{SL-inter}$ = scaled species mean standard length slope; β_{TL} = scaled trophic level slope; $\beta_{SL-intra}$ = scaled species-mean-centred standard length slope; β_{EL} = scaled elongation slope; β_{ST} = stomach slope; β_{DU} = durophagy slope; $\beta_{ST:DU}$ = stomach X durophagy slope; σ_{phy} = random intercept standard deviation, phylogenetic relationship; σ_{sp} = random intercept standard deviation, species; $\sigma_{\beta sp}$ = random slope standard deviation, species; σ_{ϵ} = residual standard deviation; ν = degrees of freedom of student-t distribution.

	Length			Diameter			Surface		
parameter	mean	2.5%	97.5%	mean	2.5%	97.5%	mean	2.5%	97.5%
α	5.69	5.13	6.25	1.54	1.31	1.76	8.34	7.64	9.01
$\beta_{SL-inter}$	0.42	0.35	0.49	0.40	0.36	0.45	0.81	0.71	0.90
β_{TL}	-0.26	-0.36	-0.16	-0.11	-0.17	-0.05	-0.38	-0.55	-0.21
$\beta_{SL-intra}$	0.13	0.11	0.15	0.11	0.10	0.13	0.24	0.21	0.27
β_{EL}	-0.32	-0.43	-0.21	-0.17	-0.23	-0.11	-0.49	-0.63	-0.35
β_{ST}	-0.19	-0.68	0.30	-0.28	-0.49	-0.07	-0.45	-1.07	0.17
β_{DU}	-0.17	-0.57	0.23	0.19	-0.01	0.40	0.07	-0.43	0.59
$\beta_{ST:DU}$	-0.05	-0.81	0.70	0.04	-0.29	0.37	-0.06	-0.99	0.84
σ_{phy}	0.54	0.44	0.64	0.18	0.10	0.27	0.64	0.42	0.83
σ_{sp}	0.07	0.00	0.16	0.15	0.11	0.19	0.19	0.02	0.33
$\sigma_{\beta sp}$	0.06	0.04	0.08	0.04	0.02	0.07	0.10	0.07	0.13
σ	0.16	0.14	0.17	0.19	0.18	0.21	0.28	0.26	0.30
ν	4.52	3.34	6.25	15.96	7.27	37.44	12.51	6.63	26.09

Table 1.3: Posterior mean and 95% credible interval for each parameter of Bayesian phylogenetic hierarchical linear models of intestinal length, diameter, and surface area for 122 species of coral reef fishes with a minimum sample size of five individuals per species. α = model intercept; $\beta_{SL-inter}$ = scaled species mean standard length slope; β_{TL} = scaled trophic level slope; $\beta_{SL-intra}$ = scaled species-mean-centred standard length slope; β_{EL} = scaled elongation slope; β_{ST} = stomach slope; β_{DU} = durophagy slope; $\beta_{ST:DU}$ = stomach X durophagy slope; σ_{phy} = random intercept standard deviation, phylogenetic relationship; σ_{sp} = random intercept standard deviation, species; $\sigma_{\beta sp}$ = random slope standard deviation, species; σ_{ϵ} = residual standard deviation; ν = degrees of freedom of student-t distribution.

parameter	Length			Diameter			Surface		
	mean	2.5%	97.5%	mean	2.5%	97.5%	mean	2.5%	97.5%
α	5.77	5.17	6.37	1.56	1.31	1.81	8.44	7.65	9.22
$\beta_{SL-inter}$	0.40	0.32	0.47	0.40	0.34	0.45	0.77	0.67	0.88
β_{TL}	-0.18	-0.30	-0.08	-0.11	-0.18	-0.03	-0.27	-0.49	-0.09
$\beta_{SL-intra}$	0.13	0.12	0.15	0.11	0.10	0.13	0.25	0.22	0.28
β_{EL}	-0.33	-0.45	-0.21	-0.17	-0.24	-0.11	-0.50	-0.67	-0.34
β_{ST}	-0.33	-0.87	0.22	-0.30	-0.55	-0.06	-0.62	-1.36	0.11
β_{DU}	-0.26	-0.68	0.17	0.16	-0.06	0.39	-0.04	-0.61	0.52
$\beta_{ST:DU}$	0.05	-0.72	0.82	0.03	-0.32	0.38	0.02	-0.97	1.03
σ_{phy}	0.54	0.46	0.63	0.18	0.09	0.29	0.68	0.46	0.86
σ_{sp}	0.05	0.00	0.13	0.16	0.11	0.20	0.14	0.01	0.31
$\sigma_{\beta sp}$	0.05	0.04	0.07	0.05	0.02	0.07	0.10	0.06	0.13
σ	0.16	0.14	0.17	0.19	0.18	0.21	0.28	0.26	0.30
ν	4.54	3.35	6.21	15.58	7.18	36.07	12.15	6.39	25.13

Table 1.4: Posterior mean and 95% credible interval for each parameter of Bayesian phylogenetic hierarchical linear models of intestinal length, diameter, and surface area for 69 species of coral reef fishes with a minimum sample size of eight individuals per species. α = model intercept; $\beta_{SL-inter}$ = scaled species mean standard length slope; β_{TL} = scaled trophic level slope; $\beta_{SL-intra}$ = scaled species-mean-centred standard length slope; β_{EL} = scaled elongation slope; β_{ST} = stomach slope; β_{DU} = durophagy slope; $\beta_{ST:DU}$ = stomach X durophagy slope; σ_{phy} = random intercept standard deviation, phylogenetic relationship; σ_{sp} = random intercept standard deviation, species; $\sigma_{\beta sp}$ = random slope standard deviation, species; σ_{ϵ} = residual standard deviation; ν = degrees of freedom of student-t distribution.

parameter	Length			Diameter			Surface		
	mean	2.5%	97.5%	mean	2.5%	97.5%	mean	2.5%	97.5%
α	5.49	4.73	6.26	1.63	1.30	1.99	8.34	7.39	9.29
$\beta_{SL-inter}$	0.30	0.18	0.42	0.36	0.27	0.45	0.64	0.47	0.81
β_{TL}	-0.22	-0.37	-0.09	-0.14	-0.22	-0.03	-0.33	-0.58	-0.11
$\beta_{SL-intra}$	0.14	0.11	0.16	0.11	0.09	0.13	0.25	0.21	0.28
β_{EL}	-0.35	-0.52	-0.19	-0.18	-0.28	-0.08	-0.53	-0.77	-0.31
β_{ST}	0.12	-0.64	0.89	-0.32	-0.69	0.02	-0.27	-1.23	0.67
β_{DU}	-0.02	-0.57	0.54	0.09	-0.23	0.39	0.02	-0.70	0.75
$\beta_{ST:DU}$	-0.48	-1.54	0.61	0.03	-0.46	0.53	-0.38	-1.72	0.99
σ_{phy}	0.53	0.42	0.66	0.17	0.03	0.35	0.66	0.40	0.86
σ_{sp}	0.06	0.00	0.17	0.16	0.07	0.23	0.14	0.01	0.33
$\sigma_{\beta sp}$	0.06	0.04	0.09	0.05	0.02	0.08	0.10	0.06	0.14
σ	0.16	0.15	0.18	0.18	0.17	0.20	0.28	0.25	0.30
ν	5.34	3.61	8.15	13.21	5.86	31.94	14.43	6.23	35.68

Table 1.5: Species-specific scaling parameters of three natural-log intestinal traits (intestinal length, diameter, and surface area) against natural-log fish standard length for 142 species of coral reef fishes. Estimates are posterior medians and 95% credible intervals (CIs) from Bayesian phylogenetic hierarchical linear models. Values in bold were selected based on a minimum number of ten sampled individuals, covering a length range of at least a quarter of the reported maximum length (retrieved from FishBase), and a posterior 95% CI above zero to provide reliable estimates of scaling parameters within the observed size range (see Fig. 5 in the main manuscript). The remaining estimates cannot be considered reliable. n = number of sampled individuals; TL = total length.

Family	Species	Length slope	Diameter slope	Surface slope	n	TL range (mm)
Acanthuridae	*Acanthurus achilles*	**1.17 (0.61, 1.68)**	**1.06 (0.57, 1.69)**	**2.50 (1.52, 3.43)**	12	122-222
Acanthuridae	*Acanthurus guttatus*	0.83 (0.17, 1.52)	0.67 (0.08, 1.20)	1.46 (0.34, 2.54)	9	161-198
Acanthuridae	*Acanthurus lineatus*	0.68 (0.11, 1.24)	0.69 (0.15, 1.18)	1.34 (0.38, 2.29)	9	160-252
Acanthuridae	*Acanthurus nigricans*	**0.93 (0.65, 1.24)**	**0.77 (0.47, 1.08)**	**1.74 (1.23, 2.26)**	13	82-184
Acanthuridae	*Acanthurus nigrofuscus*	0.71 (0.15, 1.28)	0.70 (0.21, 1.19)	1.39 (0.45, 2.33)	6	109-176
Acanthuridae	*Acanthurus nigros*	0.75 (0.03, 1.45)	0.59 (-0.02, 1.10)	1.14 (-0.01, 2.22)	4	119-156
Acanthuridae	*Acanthurus olivaceus*	0.80 (0.07, 1.54)	0.71 (0.11, 1.29)	1.49 (0.25, 2.70)	6	220-271
Acanthuridae	*Acanthurus pyroferus*	0.60 (-0.22, 1.33)	0.73 (0.13, 1.35)	1.30 (0.03, 2.53)	5	130-155
Acanthuridae	*Acanthurus thompsoni*	0.73 (-0.03, 1.46)	0.69 (0.08, 1.27)	1.32 (0.02, 2.55)	4	192-209
Acanthuridae	*Acanthurus triostegus*	0.76 (0.09, 1.43)	0.70 (0.13, 1.25)	1.47 (0.34, 2.59)	15	140-166
Acanthuridae	*Ctenochaetus flavicauda*	0.75 (0.02, 1.46)	0.67 (0.05, 1.23)	1.34 (0.12, 2.53)	6	108-139
Acanthuridae	*Ctenochaetus striatus*	0.91 (0.31, 1.53)	0.54 (-0.07, 1.02)	1.32 (0.31, 2.32)	5	120-215
Acanthuridae	*Naso brevirostris*	0.94 (0.38, 1.49)	0.74 (0.25, 1.24)	1.71 (0.77, 2.63)	6	224-343
Acanthuridae	*Naso lituratus*	**0.90 (0.33, 1.47)**	0.53 (-0.02, 0.98)	**1.22 (0.32, 2.09)**	17	181-356
Acanthuridae	*Naso unicornis*	1.07 (0.53, 1.65)	0.93 (0.48, 1.51)	2.16 (1.25, 3.14)	5	341-670
Acanthuridae	*Naso vlamingii*	0.46 (-0.04, 0.97)	0.54 (0.00, 0.97)	0.85 (-0.01, 1.69)	5	276-549
Acanthuridae	*Zebrasoma scopas*	**1.13 (0.91, 1.29)**	**0.84 (0.66, 1.02)**	**1.98 (1.69, 2.24)**	42	29-177
Acanthuridae	*Zebrasoma velifer*	0.89 (0.26, 1.54)	0.58 (-0.07, 1.08)	1.31 (0.23, 2.37)	9	196-259
Aulostomidae	*Aulostomus chinensis*	**1.24 (0.69, 1.78)**	**1.18 (0.69, 1.78)**	**2.71 (1.82, 3.62)**	11	365-623
Balistidae	*Balistapus undulatus*	**0.51 (0.11, 0.89)**	**0.79 (0.44, 1.16)**	**1.27 (0.63, 1.89)**	12	125-267
Balistidae	*Melichthys niger*	**1.12 (0.70, 1.57)**	**0.81 (0.44, 1.23)**	**1.88 (1.20, 2.61)**	14	125-258
Balistidae	*Melichthys vidua*	0.71 (0.08, 1.32)	0.79 (0.31, 1.34)	1.47 (0.52, 2.44)	12	176-225
Balistidae	*Odonus niger*	0.47 (-0.13, 1.04)	0.59 (0.06, 1.06)	0.94 (-0.04, 1.87)	14	158-277
Balistidae	*Rhinecanthus aculeatus*	0.46 (-0.15, 1.05)	0.71 (0.22, 1.20)	1.12 (0.20, 2.01)	9	145-222
Balistidae	*Rhinecanthus lunula*	0.79 (0.02, 1.54)	0.72 (0.12, 1.32)	1.51 (0.26, 2.78)	3	251-258
Balistidae	*Rhinecanthus rectangulus*	0.55 (0.04, 1.06)	0.71 (0.28, 1.15)	1.21 (0.42, 2.01)	9	117-195
Balistidae	*Sufflamen bursa*	0.53 (-0.05, 1.11)	**0.61 (0.09, 1.07)**	0.93 (-0.03, 1.85)	12	118-182
Blenniidae	*Exallias brevis*	0.95 (0.25, 1.69)	0.77 (0.21, 1.40)	1.81 (0.62, 3.05)	5	99-120
Bothidae	*Bothus mancus*	0.77 (0.02, 1.49)	0.68 (0.04, 1.26)	1.39 (0.12, 2.61)	3	366-405
Carangidae	*Caranx melampygus*	0.66 (0.11, 1.23)	0.65 (0.13, 1.13)	1.25 (0.33, 2.17)	5	349-545
Carangidae	*Scomberoides lysan*	0.78 (0.07, 1.47)	0.57 (-0.15, 1.11)	1.11 (-0.18, 2.31)	3	356-409
Chaetodontidae	*Chaetodon auriga*	0.70 (-0.10, 1.44)	0.62 (-0.01, 1.18)	1.21 (-0.10, 2.43)	9	145-205

Family	Species	Length slope	Diameter slope	Surface slope	n	TL range (mm)
Chaetodontidae	*Chaetodon bennetti*	0.77 (-0.01, 1.53)	0.71 (0.12, 1.31)	1.45 (0.15, 2.74)	3	151-168
Chaetodontidae	*Chaetodon citrinellus*	0.77 (0.02, 1.47)	0.77 (0.21, 1.39)	1.52 (0.32, 2.70)	7	96-113
Chaetodontidae	*Chaetodon ephippium*	0.91 (0.21, 1.62)	0.62 (-0.03, 1.15)	1.35 (0.11, 2.54)	8	157-194
Chaetodontidae	*Chaetodon lunula*	0.98 (0.40, 1.55)	0.57 (-0.02, 1.03)	1.24 (0.25, 2.19)	9	130-175
Chaetodontidae	*Chaetodon lunulatus*	1.14 (0.39, 1.89)	0.60 (0.08, 1.06)	1.84 (0.88, 2.79)	8	85-135
Chaetodontidae	*Chaetodon mertensii*	0.56 (-0.21, 1.28)	0.68 (0.08, 1.24)	1.08 (-0.23, 2.26)	5	103-129
Chaetodontidae	*Chaetodon ornatissimus*	**1.39 (1.11, 1.67)**	**0.56 (0.25, 0.85)**	**1.92 (1.45, 2.39)**	29	70-149
Chaetodontidae	*Chaetodon pelewensis*	0.81 (0.12, 1.49)	0.76 (0.19, 1.38)	1.61 (0.42, 2.82)	6	75-92
Chaetodontidae	*Chaetodon quadrimaculatus*	0.76 (0.08, 1.43)	0.68 (0.11, 1.21)	1.40 (0.32, 2.45)	8	97-129
Chaetodontidae	*Chaetodon reticulatus*	1.04 (0.60, 1.49)	0.79 (0.37, 1.24)	1.87 (1.14, 2.62)	32	86-130
Chaetodontidae	*Chaetodon trichrous*	0.95 (0.25, 1.69)	0.74 (0.16, 1.34)	1.72 (0.54, 2.94)	6	102-120
Chaetodontidae	*Chaetodon trifascialis*	0.97 (0.21, 1.77)	0.77 (0.20, 1.39)	1.91 (0.72, 3.17)	6	111-147
Chaetodontidae	*Chaetodon ulietensis*	0.68 (-0.08, 1.39)	0.67 (0.05, 1.22)	1.27 (0.02, 2.44)	8	134-158
Chaetodontidae	*Chaetodon unimaculatus*	0.42 (-0.22, 1.01)	0.58 (0.02, 1.06)	0.88 (-0.19, 1.86)	9	18-143
Chaetodontidae	*Chaetodon vagabundus*	0.53 (-0.25, 1.23)	0.69 (0.11, 1.25)	1.11 (-0.13, 2.21)	13	125-151
Chaetodontidae	*Forcipiger flavissimus*	0.80 (0.06, 1.50)	0.73 (0.14, 1.33)	1.52 (0.32, 2.70)	8	142-176
Chaetodontidae	*Forcipiger longirostris*	0.79 (0.08, 1.49)	0.74 (0.17, 1.33)	1.57 (0.38, 2.74)	7	170-222
Chaetodontidae	*Hemitaurichthys polylepis*	1.15 (0.56, 1.76)	0.88 (0.40, 1.50)	2.24 (1.23, 3.30)	7	97-140
Chaetodontidae	*Heniochus chrysostomus*	1.24 (0.53, 2.05)	0.70 (0.13, 1.25)	2.08 (1.00, 3.26)	8	110-142
Cirrhitidae	*Cirrhitus pinnulatus*	0.93 (0.39, 1.44)	0.72 (0.23, 1.20)	1.66 (0.74, 2.58)	10	126-190
Cirrhitidae	*Paracirrhites forsteri*	0.64 (0.06, 1.25)	0.67 (0.15, 1.16)	1.24 (0.27, 2.21)	9	124-183
Cirrhitidae	*Paracirrhites hemistictus*	0.86 (0.30, 1.43)	0.63 (0.09, 1.12)	1.45 (0.48, 2.40)	18	162-221
Diodontidae	*Diodon hystrix*	0.74 (0.06, 1.39)	0.81 (0.29, 1.44)	1.69 (0.59, 2.82)	5	300-404
Fistulariidae	*Fistularia commersonii*	**1.07 (0.60, 1.56)**	**0.95 (0.54, 1.45)**	**2.20 (1.41, 3.00)**	10	558-985
Gobiidae	*Valenciennea strigata*	1.14 (0.48, 1.81)	0.61 (0.04, 1.09)	1.67 (0.67, 2.66)	6	120-167
Hemiramphidae	*Hemiramphus depauperatus*	0.87 (0.11, 1.64)	0.70 (0.07, 1.29)	1.55 (0.23, 2.82)	3	230-271
Holocentridae	*Myripristis berndti*	**0.87 (0.39, 1.33)**	0.40 (-0.07, 0.79)	**0.96 (0.20, 1.72)**	16	120-260
Holocentridae	*Myripristis kuntee*	1.00 (0.35, 1.67)	0.49 (-0.20, 0.99)	1.10 (-0.01, 2.14)	7	139-178
Holocentridae	*Myripristis violacea*	0.99 (0.29, 1.71)	0.79 (0.25, 1.39)	1.85 (0.75, 3.01)	9	170-213
Holocentridae	*Neoniphon sammara*	**0.71 (0.07, 1.35)**	**0.58 (0.05, 1.03)**	**1.75 (0.91, 2.58)**	12	141-222
Holocentridae	*Sargocentron caudimaculatum*	0.95 (0.34, 1.56)	0.82 (0.32, 1.42)	1.93 (0.89, 3.01)	7	142-192
Holocentridae	*Sargocentron spiniferum*	0.91 (0.28, 1.55)	0.89 (0.39, 1.53)	1.94 (0.92, 3.00)	10	212-285
Holocentridae	*Sargocentron tiere*	**0.86 (0.17, 1.56)**	**0.67 (0.07, 1.22)**	**1.54 (0.37, 2.70)**	11	190-312
Kuhliidae	*Kuhlia mugil*	0.90 (0.15, 1.68)	0.70 (0.08, 1.31)	1.60 (0.36, 2.86)	3	251-282
Kyphosidae	*Kyphosus cinerascens*	0.84 (0.08, 1.60)	0.73 (0.13, 1.35)	1.59 (0.36, 2.87)	3	365-395

Table 1.5: *(continued)*

Family	Species	Length slope	Diameter slope	Surface slope	n	TL range (mm)
Kyphosidae	*Kyphosus vaigiensis*	0.83 (0.26, 1.39)	0.71 (0.20, 1.24)	1.54 (0.58, 2.51)	4	266-425
Labridae	*Calotomus carolinus*	0.67 (0.16, 1.17)	0.52 (-0.02, 0.95)	1.04 (0.17, 1.89)	9	261-410
Labridae	*Cheilinus chlorourus*	0.51 (-0.08, 1.08)	0.69 (0.18, 1.19)	1.15 (0.19, 2.09)	9	150-241
Labridae	*Cheilinus trilobatus*	1.18 (0.65, 1.70)	1.00 (0.54, 1.59)	2.39 (1.48, 3.29)	7	131-247
Labridae	*Cheilio inermis*	0.89 (0.17, 1.62)	0.81 (0.26, 1.47)	1.85 (0.65, 3.15)	4	322-391
Labridae	*Chlorurus microrhinos*	0.80 (0.06, 1.53)	0.69 (0.07, 1.28)	1.45 (0.20, 2.68)	4	360-390
Labridae	*Chlorurus spilurus*	0.58 (-0.12, 1.23)	0.90 (0.40, 1.56)	1.61 (0.51, 2.71)	6	187-475
Labridae	*Coris aygula*	1.00 (0.59, 1.40)	0.62 (0.22, 0.99)	1.59 (0.93, 2.23)	9	197-435
Labridae	*Coris gaimard*	1.01 (0.44, 1.52)	0.76 (0.31, 1.22)	1.76 (0.94, 2.58)	7	149-287
Labridae	*Epibulus insidiator*	0.56 (-0.08, 1.18)	0.66 (0.18, 1.11)	1.20 (0.36, 2.04)	16	170-300
Labridae	*Gomphosus varius*	0.93 (0.36, 1.50)	0.56 (-0.03, 1.05)	1.31 (0.33, 2.26)	7	183-280
Labridae	*Halichoeres hortulanus*	0.91 (0.40, 1.42)	0.91 (0.46, 1.48)	2.02 (1.14, 2.94)	9	164-261
Labridae	*Halichoeres trimaculatus*	0.78 (0.17, 1.39)	0.82 (0.31, 1.42)	1.75 (0.68, 2.84)	5	117-166
Labridae	*Hemigymnus fasciatus*	0.90 (0.39, 1.39)	0.70 (0.22, 1.17)	1.55 (0.73, 2.38)	9	145-229
Labridae	*Novaculichthys taeniourus*	0.72 (0.10, 1.32)	0.65 (0.08, 1.16)	1.28 (0.24, 2.30)	6	235-299
Labridae	*Oxycheilinus unifasciatus*	0.66 (-0.02, 1.33)	0.78 (0.25, 1.37)	1.53 (0.44, 2.63)	4	190-250
Labridae	*Scarus altipinnis*	0.70 (0.06, 1.34)	0.68 (0.11, 1.22)	1.36 (0.22, 2.45)	6	297-399
Labridae	*Scarus forsteni*	0.74 (0.16, 1.32)	0.66 (0.13, 1.13)	1.39 (0.40, 2.36)	9	235-382
Labridae	*Scarus frenatus*	0.05 (-0.53, 0.73)	0.66 (0.22, 1.07)	0.51 (-0.28, 1.29)	4	222-390
Labridae	*Scarus globiceps*	0.60 (-0.14, 1.27)	0.71 (0.19, 1.22)	0.87 (-0.16, 1.88)	7	196-261
Labridae	*Scarus oviceps*	0.85 (0.26, 1.43)	0.66 (0.12, 1.15)	1.47 (0.49, 2.44)	7	215-298
Labridae	*Scarus psittacus*	0.62 (0.04, 1.23)	0.46 (-0.10, 0.90)	1.10 (0.16, 2.00)	9	187-315
Labridae	*Scarus rubroviolaceus*	0.87 (0.20, 1.56)	0.96 (0.45, 1.64)	1.94 (0.82, 3.19)	5	255-454
Labridae	*Scarus schlegeli*	0.98 (0.40, 1.55)	0.83 (0.35, 1.39)	1.97 (1.02, 2.95)	7	193-301
Labridae	*Thalassoma hardwicke*	0.81 (0.29, 1.35)	0.65 (0.12, 1.11)	1.41 (0.49, 2.31)	7	119-202
Labridae	*Thalassoma purpureum*	0.91 (0.23, 1.58)	0.56 (-0.11, 1.08)	1.21 (0.05, 2.32)	5	230-287
Labridae	*Thalassoma trilobatum*	**0.67 (0.10, 1.22)**	**0.60 (0.07, 1.05)**	**1.11 (0.26, 1.92)**	10	166-284
Lethrinidae	*Gnathodentex aureolineatus*	0.77 (0.06, 1.46)	0.58 (-0.11, 1.11)	1.15 (-0.13, 2.33)	7	214-311
Lethrinidae	*Monotaxis grandoculis*	0.94 (0.31, 1.65)	0.55 (0.12, 0.92)	1.79 (0.92, 2.60)	7	158-365
Lutjanidae	*Aphareus furca*	0.84 (0.32, 1.36)	0.90 (0.46, 1.44)	1.81 (0.96, 2.67)	9	239-366
Lutjanidae	*Lutjanus fulvus*	1.31 (0.80, 1.80)	0.81 (0.39, 1.29)	2.19 (1.38, 3.02)	11	173-265
Lutjanidae	*Lutjanus kasmira*	0.89 (0.19, 1.60)	0.69 (0.09, 1.24)	1.54 (0.38, 2.68)	9	209-265
Lutjanidae	*Lutjanus monostigma*	0.88 (0.34, 1.39)	0.82 (0.35, 1.34)	1.77 (0.80, 2.69)	5	263-572
Monacanthidae	*Aluterus scriptus*	0.68 (0.17, 1.18)	0.81 (0.35, 1.31)	1.60 (0.74, 2.46)	4	328-616
Monacanthidae	*Amanses scopas*	0.47 (-0.08, 1.04)	0.67 (0.16, 1.14)	1.08 (0.18, 1.95)	9	104-168
Monacanthidae	*Cantherhines sandwichiensis*	0.45 (-0.21, 1.11)	**0.98 (0.50, 1.62)**	**1.60 (0.65, 2.55)**	10	115-172
Mugilidae	*Ellochelon vaigiensis*	0.72 (-0.02, 1.44)	0.67 (0.04, 1.24)	1.32 (0.06, 2.52)	4	340-398
Mullidae	*Mulloidichthys flavolineatus*	1.16 (0.63, 1.70)	0.69 (0.20, 1.18)	1.81 (0.93, 2.73)	9	194-319
Mullidae	*Mulloidichthys vanicolensis*	1.07 (0.49, 1.62)	0.92 (0.44, 1.51)	2.17 (1.19, 3.14)	5	187-297
Mullidae	*Parupeneus barberinus*	0.76 (0.35, 1.19)	0.81 (0.41, 1.22)	1.62 (0.93, 2.32)	4	200-440
Mullidae	*Parupeneus insularis*	**0.84 (0.46, 1.22)**	**0.69 (0.30, 1.07)**	**1.51 (0.86, 2.18)**	11	161-365

Family	Species	Length slope	Diameter slope	Surface slope	n	TL range (mm)
Mullidae	*Parupeneus multifasciatus*	**0.95 (0.52, 1.37)**	**0.93 (0.51, 1.42)**	**2.01 (1.23, 2.77)**	11	139-298
Ostraciidae	*Ostracion cubicus*	0.98 (0.25, 1.74)	0.67 (0.04, 1.23)	1.61 (0.41, 2.82)	3	244-298
Ostraciidae	*Ostracion meleagris*	0.59 (-0.01, 1.22)	0.66 (0.12, 1.15)	1.17 (0.22, 2.15)	7	90-121
Pempheridae	*Pempheris oualensis*	0.65 (-0.09, 1.34)	0.73 (0.15, 1.32)	1.37 (0.16, 2.53)	7	192-216
Pinguipedidae	*Parapercis millepunctata*	0.96 (0.31, 1.63)	0.80 (0.27, 1.42)	1.87 (0.76, 3.02)	7	114-145
Pomacanthidae	*Centropyge flavissima*	1.21 (0.76, 1.66)	0.76 (0.36, 1.19)	2.03 (1.31, 2.75)	8	55-101
Pomacanthidae	*Centropyge loriculus*	1.01 (0.28, 1.77)	0.80 (0.24, 1.44)	1.94 (0.80, 3.18)	3	50-64
Pomacanthidae	*Pomacanthus imperator*	0.93 (0.30, 1.54)	0.94 (0.47, 1.56)	1.99 (0.97, 3.02)	7	197-281
Pomacanthidae	*Pygoplites diacanthus*	**1.33 (0.70, 2.03)**	**0.86 (0.39, 1.42)**	**2.36 (1.37, 3.38)**	10	103-221
Pomacentridae	*Abudefduf septemfasciatus*	0.87 (0.18, 1.56)	0.73 (0.16, 1.29)	1.58 (0.46, 2.73)	11	161-194
Pomacentridae	*Abudefduf sexfasciatus*	0.93 (0.31, 1.57)	0.88 (0.38, 1.53)	2.07 (1.03, 3.19)	9	129-168
Pomacentridae	*Abudefduf sordidus*	0.69 (0.04, 1.32)	0.56 (-0.05, 1.04)	1.15 (0.09, 2.13)	6	147-228
Pomacentridae	*Chromis atripectoralis*	0.94 (0.24, 1.66)	0.72 (0.13, 1.30)	1.66 (0.52, 2.83)	5	54-68
Pomacentridae	*Chromis xanthura*	**0.61 (0.15, 1.08)**	**0.77 (0.36, 1.22)**	**1.46 (0.68, 2.24)**	24	111-158
Pomacentridae	*Dascyllus aruanus*	1.40 (0.92, 1.88)	0.71 (0.30, 1.11)	2.17 (1.46, 2.90)	7	29-54
Pomacentridae	*Dascyllus flavicaudus*	0.71 (0.20, 1.23)	0.50 (-0.03, 0.92)	0.96 (0.10, 1.79)	14	75-110
Pomacentridae	*Dascyllus trimaculatus*	0.74 (-0.03, 1.47)	0.65 (0.01, 1.22)	1.27 (0.00, 2.46)	8	120-135
Pomacentridae	*Plectroglyphidodon johnstonianus*	0.86 (0.14, 1.59)	0.79 (0.23, 1.42)	1.74 (0.58, 2.95)	6	59-76
Pomacentridae	*Plectroglyphidodon lacrymatus*	1.19 (0.60, 1.80)	0.71 (0.22, 1.20)	1.98 (1.07, 2.94)	6	50-91
Pomacentridae	*Stegastes fasciolatus*	0.78 (0.06, 1.47)	0.57 (-0.09, 1.11)	1.19 (-0.05, 2.33)	9	79-96
Pomacentridae	*Stegastes nigricans*	0.76 (0.01, 1.48)	0.76 (0.16, 1.38)	1.59 (0.35, 2.84)	10	120-141
Scorpaenidae	*Pterois radiata*	0.62 (0.14, 1.10)	0.62 (0.20, 1.01)	1.14 (0.41, 1.85)	9	117-197
Serranidae	*Cephalopholis argus*	0.85 (0.35, 1.33)	0.75 (0.32, 1.21)	1.60 (0.80, 2.39)	17	180-310
Serranidae	*Cephalopholis urodeta*	**0.74 (0.21, 1.38)**	**0.49 (0.01, 0.90)**	**1.03 (0.27, 1.85)**	14	105-191
Serranidae	*Epinephelus fasciatus*	0.62 (-0.03, 1.24)	0.65 (0.10, 1.16)	1.19 (0.16, 2.20)	6	190-288
Serranidae	*Epinephelus hexagonatus*	0.97 (0.36, 1.58)	0.76 (0.24, 1.32)	1.88 (0.86, 2.91)	7	152-225
Serranidae	*Epinephelus merra*	0.85 (0.25, 1.44)	0.88 (0.39, 1.49)	1.89 (0.89, 2.94)	9	165-230
Serranidae	*Pseudanthias pascalus*	0.67 (0.13, 1.22)	0.80 (0.30, 1.34)	1.56 (0.61, 2.48)	7	89-152
Serranidae	*Variola louti*	0.76 (0.24, 1.33)	0.61 (0.06, 1.08)	1.26 (0.34, 2.20)	7	304-420
Siganidae	*Siganus spinus*	0.67 (0.05, 1.26)	0.80 (0.28, 1.38)	1.56 (0.52, 2.59)	5	192-223
Tetraodontidae	*Arothron meleagris*	0.63 (0.16, 1.15)	0.88 (0.47, 1.35)	1.60 (0.89, 2.34)	9	141-269
Tetraodontidae	*Canthigaster bennetti*	0.72 (-0.08, 1.47)	0.75 (0.16, 1.37)	1.41 (0.16, 2.62)	3	79-94
Tetraodontidae	*Canthigaster solandri*	0.66 (-0.02, 1.32)	0.72 (0.16, 1.27)	1.33 (0.24, 2.40)	6	70-97
Zanclidae	*Zanclus cornutus*	0.77 (0.13, 1.41)	0.77 (0.24, 1.36)	1.61 (0.52, 2.70)	11	131-171

Table 1.6: Posterior mean and 95% credible interval for each parameter of a Bayesian phylogenetic hierarchical linear model of δ^{15}N for 83 species of coral reef fishes. $\alpha =$ model intercept; $\beta_{SL} =$ scaled log standard length slope; $\beta_{TL} =$ scaled trophic level slope; $\sigma_{phy} =$ random intercept standard deviation, phylogenetic relationship; $\sigma_{sp} =$ random intercept standard deviation, species; $\sigma_{\beta sp} =$ random slope standard deviation, species; $\sigma_{\epsilon} =$ residual standard deviation; $\nu =$ degrees of freedom of student-t distribution.

parameter	mean	2.5%	97.5%
α	9.51	8.44	10.53
β_{SL}	0.40	0.22	0.57
β_{TL}	0.66	0.29	1.03
σ_{phy}	1.33	0.79	1.90
σ_{sp}	0.53	0.06	0.91
$\sigma_{\beta sp}$	0.47	0.31	0.66
σ	0.47	0.41	0.53
ν	2.81	2.11	3.76

2

Temperature, species identity and morphological traits predict carbonate excretion and mineralogy in tropical reef fishes

Mattia Ghilardi[1,2]*, Michael A. Salter[3], Valeriano Parravicini[4,5], Sebastian C. A. Ferse[1,2], Tim Rixen[1], Christian Wild[2], Matthias Birkicht[1], Chris T. Perry[6], Alex Berry[3], Rod W. Wilson[3], David Mouillot[7,5], Sonia Bejarano[1]

1. Leibniz Centre for Tropical Marine Research (ZMT), FahrenheitstraSSe 6, 28359 Bremen, Germany

2. Department of Marine Ecology, Faculty of Biology and Chemistry, University of Bremen, Leobener StraSSe UFT, 28359 Bremen, Germany

3. Biosciences, University of Exeter, Exeter EX4 4QD, UK

4. PSL Université Paris: EPHE-UPVD-CNRS, USR3278 CRIOBE, University of Perpignan, 66860 Perpignan, France

5. Institut Universitaire de France, Paris, France

6. Geography, University of Exeter, Exeter EX4 4RJ, UK

7. MARBEC, Univ Montpellier, CNRS, Ifremer, IRD, 34095 Montpellier, France

*Correspondence:** M. Ghilardi (`mattia.ghilardi91@gmail.com`)

Abstract

Anthropogenic pressures are restructuring coral reefs globally. Sound predictions of the expected changes in key reef functions require adequate knowledge of their drivers. Here we investigate the determinants of a poorly-studied yet relevant biogeochemical function sustained by marine bony fishes: the excretion of intestinal carbonates. Compiling carbonate excretion rates and mineralogical composition from 382 individual coral reef fishes (85 species and 35 families), we identify the environmental factors and fish traits that predict them. We find that body mass and relative intestinal length (RIL) are the strongest predictors of carbonate excretion. Larger fishes and those with longer intestines excrete disproportionately less carbonate per unit mass than smaller fishes and those with shorter intestines. The mineralogical composition of excreted carbonates is highly conserved within families, but also controlled by RIL and temperature. These results fundamentally advance our understanding of the role of fishes in inorganic carbon cycling and how this contribution will change as community composition shifts under increasing anthropogenic pressures.

2.1 Introduction

Ecosystems globally are rapidly restructuring into novel configurations in response to anthropogenic pressures (Keith et al. 2022; Stuart-Smith et al. 2022). These profound changes have wide-reaching implications for ecosystem functioning, climate warming mitigation, the provision of ecosystem services, and human wellbeing (Eddy et al. 2021; Hicks et al. 2021; Mariani et al. 2020; Williams and Graham 2019; Woodhead et al. 2019). To better understand, anticipate, and address the impact of these changes on ecosystems, a detailed understanding of key ecosystem functions and their drivers is critical.

In addition to being ecologically, nutritionally, and economically important, fishes are major contributors to biogeochemical cycles in the global ocean (Allgeier et al. 2014; Bianchi et al. 2021; Le Mézo et al. 2022; Martin et al. 2021; Saba et al.

2021; Wilson et al. 2009). Beyond contributing to nutrient cycling (Allgeier et al. 2014; Allgeier et al. 2021; Le Mézo et al. 2022; Schiettekatte et al. 2020; Shantz et al. 2015), marine bony fishes (Teleostei) significantly influence the biological carbon pump (Saba et al. 2021) and the cycling of inorganic carbon through the excretion of fine-grained carbonates as a by-product of osmoregulation (Walsh et al. 1991; Wilson et al. 2002; Wilson et al. 2009). Fish precipitate ingested calcium and magnesium ions as carbonate crystals within their alkaline and bicarbonate-rich intestinal fluid and excrete them at high rates either within mucus-coated pellets or in faeces (Shehadeh and Gordon 1969; Walsh et al. 1991; Wilson et al. 1996; Wilson et al. 2002). This process reduces the osmotic pressure in the intestinal fluid, thus facilitating water absorption into the blood (Grosell et al. 2009; Wilson et al. 2002). It also plays an important role in the fish's calcium homeostasis (Whittamore 2012), protecting them against renal stone formation by preventing intestinal calcium being absorbed into the blood (Wilson and Grosell 2003). Fish carbonate excretion is estimated to potentially represent ~15% (8.9 Tmol year^{-1}) of the global carbonate production in surface oceans, with less conservative estimates as high as 45% (Wilson et al. 2009).

The rate of carbonate excretion by fish is assumed to be proportional to metabolic rate since it is directly related to drinking rate and thus to the amount of calcium and magnesium ingested through seawater, which determines carbonate excretion rate (Genz et al. 2008; Takei and Tsukada 2001; Wilson et al. 2002). Although this assumption remains untested, fish contribution to global oceanic carbonate production has been estimated by combining metabolic theory (Brown et al. 2004) with observations of carbonate excretion rates for two benthic species (Wilson et al. 2009). Consistent with metabolic theory, carbonate excretion rate was later found to decrease disproportionately (i.e., to scale hypoallometrically) with body mass across reef fishes (Perry et al. 2011; Salter et al. 2018), and to be positively related to water temperature in the sheepshead minnow (*Cyprinodon variegatus*, Wilson et al. 2009) and Gulf toadfish (*Opsanus beta*, Heuer et al. 2016). Although these results suggest a direct link between carbonate excretion rate and

metabolic rate, a rigorous investigation is needed to confirm the consistency of this relationship because of its potential key influence on large-scale carbonate production. Furthermore, several other environmental factors (e.g. salinity, CO_2) and fish traits (e.g. activity, diet, intestinal length) are known or expected to influence carbonate excretion directly or indirectly (Genz et al. 2008; Grosell 2019; Saba et al. 2021; Schauer et al. 2018). However, a comprehensive analysis of the factors determining interspecific differences in fish carbonate excretion rate is lacking, but needed to refine assessments of large-scale carbonate production. Such analysis will be crucial to scale carbonate excretion up from the individual to the community level, thereby increasing our understanding of the contribution of fishes to global carbon cycling in the ocean.

Fish excrete carbonate at high rates (i.e., at least up to 105 g m^{-2} yr^{-1} on coral reefs, Salter et al. 2018). The global significance of this process lies in the typically high Mg/Ca ratios and low degrees of crystallinity in the excreted carbonates compared with most other biogenic marine carbonates (Foran et al. 2013; Perry et al. 2011; Salter et al. 2012; Salter et al. 2018; Walsh et al. 1991; Wilson et al. 2009), which implies relatively high solubility (Woosley et al. 2012). Therefore, fish carbonates are hypothesised to be an important source of upper ocean carbonate dissolution, which is predicted to occur based on observed alkalinity–depth profiles, but for which sources remain enigmatic (Sulpis et al. 2021; Wilson et al. 2009). Mesopelagic fish, the largest biomass of fish (and vertebrates) on the planet, may for instance drive an upward alkalinity pump by producing carbonates at depth and excreting them at the peak of their vertical feeding migrations, where they dissolve rapidly releasing new alkalinity to the surface ocean (Roberts et al. 2017). However, fish are known to produce a wide variety of carbonate polymorphs, including low- and high-magnesium calcite (LMC and HMC, respectively), aragonite, monohydrocalcite (MHC), and amorphous calcium magnesium carbonate (ACMC)(Foran et al. 2013; Perry et al. 2011; Salter et al. 2012; Salter et al. 2017; Salter et al. 2018; Salter et al. 2019), with respective solubilities spanning several orders of magnitude if existing solubility data from mostly non-fish sources are applied (Breevi and Nielsen

1989; Fukushi et al. 2011; Plummer and Busenberg 1982; Woosley et al. 2012). The mineralogical composition of excreted carbonates has been characterised for a wide range of tropical, subtropical, and temperate fishes, showing a high degree of consistency within families, with a few exceptions (Salter et al. 2012; Salter et al. 2017; Salter et al. 2018; Salter et al. 2019). This strong taxonomic conservatism allowed for the first estimates of polymorph-specific production rates by combining individual carbonate excretion rates with family-average carbonate composition (Salter et al. 2017; Salter et al. 2018). Important regional differences in the preservation potential of fish carbonates, driven by variation in fish community composition, were highlighted (Salter et al. 2018). However, despite the apparent family-level consistency, further determinants of the mineralogical composition of fish carbonates have yet to be investigated. Identifying the factors that govern fish carbonate mineralogy and incorporating carbonate composition within production models is essential for assessing (1) the current contribution of fishes to both open ocean and shallow marine carbonate budgets and (2) the impacts of ongoing fishing- and climate-induced changes in fish community composition on ecosystem functioning.

Here, we aimed to identify the environmental factors and fish traits that best explain variation in the excretion rates and mineralogical composition of excreted carbonates. We focus on tropical and subtropical reef fishes as they represent most of marine vertebrate biodiversity within a small fraction of the ocean (Kulbicki et al. 2013). We assembled the largest database available to date, including carbonate excretion rates from 382 individuals across 85 fish species and 35 families, spanning a wide range in body mass (<1 g to >10 kg) and trophic level (2.0-4.5). Data were collected in three tropical and subtropical regions (180 individuals from 29 species in Australia, 90 individuals from 10 species in the Bahamas, and 112 individuals from 46 species in Palau) within three marine biogeographic realms (Spalding et al. 2007). Retaining only families with at least three independent observations (352 individuals from 71 species and 21 families), we tested whether fish traits (body mass, caudal fin aspect ratio—AR [a proxy for general activity level; Pauly

(1989)], relative intestinal length—RIL [intestinal length relative to body standard length]), environmental variables (temperature, salinity), and taxonomic identity (i.e., family) are significant predictors of carbonate excretion rate. Then, we assessed whether the predictors identified in the previous step (i.e., all excluding salinity and total sampling period) can accurately predict the excretion rate of five major carbonate polymorphs produced by fishes (i.e., LMC, HMC, aragonite, MHC, ACMC), and whether temperature, RIL, and taxonomic identity influence carbonate mineralogy. We confirm that carbonate excretion rate scales proportionally with metabolic rate through the effect of body mass, temperature, and AR, and show that, per unit mass, it decreases disproportionately with body mass and RIL. This implies major changes in community-level carbonate production with ongoing human- and climate-induced shifts in fish size and trophic structure on global reefs (Eddy et al. 2021; Parravicini et al. 2021). One step further, we show that carbonate mineralogy is highly taxonomically conserved but also controlled by RIL and water temperature, providing a fundamental advance in quantifying fish contribution to carbonate budgets.

2.2 Methods

Animal collection and holding for this project was conducted under Marine Research Permit RE-19-28 issued by the Ministry of Natural Resources, Environment, and Tourism of the Republic of Palau (10.03.2019), Marine Research/Collection Permit and Agreement 62 issued by the Koror State Government (08.10.2019), Queensland Government GBRMPA Marine Parks Permit G14/36689.1, Queensland Government DNPRSR Marine Parks Permits QS2014/MAN247 and QS2014/MAN247a, Queensland Government General Fisheries Permit 168991, Queensland Government DAFF Animal Ethics approval CA2013/11/733, approval by The Bahamas Department of Marine Resources, approval by the Animal Care Officer of both the University of Bremen and the Leibniz Centre for Tropical Marine Research (ZMT), and in accordance with UK and Germany animal care guidelines.

2.2.1   Sample collection

We collected fish carbonate samples at four study locations across three tropical and subtropical regions: Eleuthera ($24°50'N$, $76°20'W$), The Bahamas, between 2009 and 2011 (Perry et al. 2011; Salter et al. 2017); Heron Reef ($23°27'S$, $151°55'E$) and Moreton Bay ($27°29'S$, $153°24'E$) in Queensland, Australia, in 2014 and 2015 (Salter et al. 2018); and Koror ($7°20'N$, $134°28'E$), Palau, during November and December 2019. At each location fish were collected using barrier nets, dip nets, clove oil or hook and line, and immediately transferred to aquaria facilities at the Cape Eleuthera Institute, Heron Island and Moreton Bay Research Stations, and the Palau International Coral Reef Center. Fish were held in a range of tanks (60, 400, or 1400 L in the Bahamas, 10, 60, 100, 120, or 400 L in Heron Island and Moreton Bay, and 8, 80, 280, or 400 L in Palau) of suitable dimensions for different fish sizes (<1 g to 11 kg), either individually or, for particularly social species, in small groups of similar sized individuals of the same species. All tanks were supplied with flow-through locally-drawn filtered (1-5μm) natural seawater, except in Moreton Bay where we used locally-drawn filtered natural seawater in a recirculation system, and maintained at ambient conditions. Food was withheld throughout the sampling period (typically three days but sometimes shorter or longer) and for at least 48 h prior to ensure that sample material comprised only carbonate precipitated within the intestine from imbibed seawater calcium, rather than from dietary sources. Additionally, each tank was fitted with false mesh bottom to prevent further disturbance on excreted carbonate pellets or potential ingestion by fish. Carbonate pellets were collected from the bottom of the tanks using a siphon or disposable Pasteur pipette at 24 h intervals in The Bahamas and Australia (except a few non-scarine Labridae that were sampled at 4 h intervals— see Salter et al. (2018)), and at 8 h intervals in Palau. Samples were rinsed three times with deionised water (centrifuging each time for 3 min at 2655 x g) to remove saltwater and excess salts and soaked in sodium hypochlorite (commercial bleach; <4% available chlorine) for 6-12 h to disaggregate organic material (Gaffey and Bronnimann 1993). All traces of bleach were removed with further rinses with

deionised water before drying the samples for 24 h at 50 °C. Full details of carbonate collection in The Bahamas and Australia are described in Perry et al. (2011), Salter et al. (2017), and Salter et al. (2018).

2.2.2 Sample analysis

Carbonate composition

Samples where characterised for their morphological and mineralogical composition using scanning electron microscopy (SEM), energy-dispersive X-ray spectroscopy (EDX), and Fourier transform infrared spectroscopy (FTIR). Detailed procedures for samples collected in The Bahamas and Australia are described in Salter et al. (2017) and Salter et al. (2018). The same methodology was applied to samples collected in Palau. Morphological and chemical composition were analysed using a Tescan Vega 3 XMU SEM with integrated Oxford Instruments X-MAX EDX detector. Dry samples were mounted on adhesive carbon tape and covered with a 20 nm conductive coating (Au). Morphological observations were made on at least five pellets per sample and electron microscope images were acquired at accelerating voltages between 5 and 15 kEV and working distances of 7–12 mm using either secondary electron or backscatter detectors. A minimum of 30 EDX scans were performed on each sample, incorporating all present particle morphotypes, using an accelerating voltage of 20 kEV, a working distance of 15 mm, and acquisition time of >40 s. Scans were only performed on particles surrounded by others of similar morphology, or on particles of sufficient size to ensure that data were representative of a particular morphology.

Mineralogical composition was assessed using Attenuated Total Reflection FTIR (ATR-FTIR). Spectra were obtained by the co-addition of 32 repeated scans performed at a resolution of 2 cm^{-1} using a Nicolet 380 FTIR spectometer coupled with a Thermo Scientific SMART iTR ATR sampler equipped with a diamond reflecting cell. To ensure spectra were representative, analyses were performed on at least three sub-samples (each comprising 2–3 pellets) per species. Spectra

were then compared against an extensive spectral database for the identification of carbonate phases (see Salter et al. (2017)).

Finally, each particle morphotype produced by a species was assigned to a carbonate polymorph based on compositional and mineralogical data. The relative abundances of different particle morphotypes were then estimated visually for every sample observed using SEM. These were converted into relative abundances of carbonate polymorphs, which were then averaged for each species.

Carbonate excretion rates

The amount of carbonate excreted by fish in The Bahamas and Australia was quantified using a double-titration approach (Perry et al. 2011; Salter et al. 2018; Wilson et al. 2002). Samples were homogenised in 20 ml of distilled water, titrated with HCl to below pH 4.0 and titrated back to the starting pH with NaOH, while continuously aerating with CO_2-free air to remove all HCO_3^- and CO_3^{2-} as gaseous CO_2. Concentrations of 0.001–0.1 N were used for both HCl and NaOH as appropriate for sample size. Titrations were performed using a Metrohm Titrando autotitrator and Methrohm Aquatrode pH electrode (Australian samples), or manually with combination pH electrodes (Radiometer PHC 2401) and handheld pH meters (Hanna HI 8314 and Russell RL 200), with acid and base delivery via 2-mL micrometer syringes (Gilmont Instruments, Barrington, USA) with a precision of ± 1 μL (Bahamian samples). The amount of HCl used minus the amount of NaOH required to return to the starting pH corresponds to the amount of bicarbonate equivalents (i.e., $HCO_3^- + 2CO_3^{2-}$) in the sample. Therefore, the molar amount of $(Ca,Mg)CO_3$ in the sample was calculated as:

$$n[(Ca,Mg)CO_3] = 0.5 \cdot n(HCO_3^-) = 0.5 \cdot (n(HCl) - n(NaOH)), \qquad (2.1)$$

assuming that each carbonate molecule yields two bicarbonate equivalents.

Due to laboratory constraints, a slightly different approach was applied to the samples collected in Palau. Specifically, carbonate alkalinity was determined by single end point titration using the mixed indicator Bromocresol Green-Methyl Red

(Cooper 1941). Samples were suspended in 5 ml of distilled water and sonicated, then 50 μl of mixed indicator was added to the solution which turned blue (pH>5). Each sample was titrated with 0.01-0.5 N HCl (with continuous aeration with CO_2-free air) until the end point (grey-lavender; pH~4.80) was reached and stable for at least 10 min. If the sample was overtitrated (pink), 0.01-0.1 N NaOH was added to titrate back to the end point and the amount of base used was subtracted from the amount of acid. Acid and base were added using an electronic multi-dispenser pipette (Eppendorf Repeater ®E3X, Eppendorf, Hamburg, Germany) with a precision of ± 1 μL. Additionally, the pH of several samples was monitored using a pH microelectrode (Mettler Toledo InLab Micro) to ascertain the correct-ness of the colorimetric end point. The amount of carbonate in the sample was then calculate using Eq. (2.1). The method was validated using certified reference material (Alkalinity Standard Solution, 25,000 mg/L as $CaCO_3$, HACH) and the accuracy in the determination of solid samples was verified using certified $CaCO_3$ powder (Suprapur, $\geq 99.95\%$ purity, Merck) samples (60 to 500 μg) and resulted in 96.53% $\pm$ 1.94% accuracy (mean $\pm$ SE; $n = 8$).

To compare values obtained with the two titration methods we further analysed 12 samples collected at Lizard Island, Australia, in February 2016. Samples were collected at 24h intervals from one individual of *Lethrinus atkinsoni* (f. Lethrinidae, body mass: 245 g), a group of five *Lutjanus fulvus* (f. Lutjanidae, mean body mass: 21 g), and an individual of *Cephalopholis cyanostigma* (f. Serranidae, body mass: 295 g), following the procedures described above. During sample collection water temperature ranged from 29.1 °C during the night to 32.6 °C during the day, with an average of ~31 °C, mean salinity was 35.4, and pH_{NBS} ranged from 8.13 to 8.21. To compare the amount of carbonate measured by the two methods we added carbonate samples to 20 ml ultrapure water and disaggregated crystals via sonication. We then used a Metrohm Titrando autotitrator and Metrohm Aquatrode pH electrode to measure initial pH of the suspension of carbonates, then titrated each sample of carbonate in two stages. Firstly they were titrated down to pH 4.80 using 0.1 N HCl, adding 20 μl increments of acid until this was

sufficient to keep pH below 4.80 for 10 minutes whilst bubbling with CO_2-free air. This first stage was comparable to the single end point titration used for samples collected in Palau. Secondly, whilst continuing to bubble with CO_2-free air, further acid was added to the sample until it reached pH 3.89 and was stable for 1 minute. Then 0.1 N NaOH was added to the samples to return them to the initial pH. For all samples the first end point titration (to pH 4.80) yielded slightly higher values for carbonate content than the second double titration. The ratio between the two methods (single end point/double titration) was 1.08 ± 0.01 (mean $\pm$ SE; range: 1.04-1.14; Supplementary Table 2.2). As we found a small but consistent difference between the two methods, all following analyses were initially performed on the actual data obtained with the double titration for samples from Australia and The Bahamas, and the single end point titration for samples from Palau. Then, to assess the robustness of the results, we repeated the analyses after applying a correction factor of 1.08 to the excretion rates of Palauan fishes (that used the single end point titration method). All results were consistent and robust to the measured difference between the titration methods (Supplementary Figs. 2.13 and 2.14).

Finally, measurements of multiple samples from each individual collected over periods of 18-169 h (median: 64 h) were combined to produce an average individual excretion rate in μmol h^{-1}. For fish held in groups, carbonate excretion rates per individual (of average biomass) were obtained by averaging the total excretion rate of the group across the sampling period and dividing it by the number of individuals in the tank. Excretion rates obtained from fish groups thus evened the intraspecific variability within tanks, and are therefore more robust than those directly obtained from fish held individually. This aspect was considered in our models by fitting weighted regressions (see the Statistical modelling section). In total, we measured the carbonate excretion rates of 382 individual fishes arranged in 192 groups (i.e., independent observations), representing 85 species from 35 families across three tropical regions (180 individuals from 29 species in Australia, 90 individuals from 10 species in the Bahamas, and 112 individuals from 46 species in Palau; Supplementary Table 2.1).

We assume that during the sampling of carbonates fishes were close to their resting metabolic rate and that their carbonate excretion rates are representative of fish at rest. Although the ratio of tank volume to fish volume in our study (median ~660; inter-quartile range ~180-1700) typically greatly exceeds the guideline ideal range for measuring resting metabolic rate (20-50) (Svendsen et al. 2016), fishes were fasted prior to and throughout sampling, and in most instances their movement was somewhat constrained by tank volume. Fasting reduces metabolic rate in all animals, including fish, as they do not undergo energy-intensive digestive processes and use energy reserves to support vital processes, triggering metabolic changes in many tissues and reducing activity levels (Gingerich et al. 2010; Van Dijk et al. 2002). Additionally, other than the carbonate syphoning (<2 min), no stressors were present. Fishes were not engaged in foraging activity, they experienced no predator-prey interactions, many were held individually so did not engage in social interactions, and social species were held in groups to minimise stress. Therefore, although spontaneous activity likely occurred, fishes were placid throughout the sampling period and the constrained space, minimal disturbance, and fasting suggest that they had very low activity levels.

2.2.3   Selection of families

To assess the main determinants of variability in fish carbonate excretion and composition we considered only families with at least three independent observations (i.e., three individuals or groups of fish). This removed 14 families characterised by only one or two observations, thus reducing our dataset to 175 independent observations from 352 individuals representing 21 families. In our analyses, we considered parrotfishes (f. Labridae: tribe Scarini) separatately from other labrids following Salter et al. (2018), as preliminary data showed that they produce distinct carbonate products, possibly due to their distinct trophic ecology and unique gut chemistry (Smith and Paulson 1975).

2.2.4   Explanatory variables

Fish carbonate production is the result of both extrinsic environmental conditions and intrinsic species traits. To analyse the major factors determining carbonate excretion rate and composition we considered a suite of potential variables, while accounting for taxonomic relationships. Some are known to influence fish carbonate excretion rates, such as salinity, body mass, and temperature (Genz et al. 2008; Mekuchi et al. 2010; Perry et al. 2011; Wilson et al. 2009). Others, such as CO_2 and AR, are likely to indirectly affect carbonate excretion by influencing acid–base regulation (Grosell 2019) and activity level (Killen et al. 2016), respectively. We did not have data for seawater pCO$_2$ during the sampling period, however, due to good aeration of tanks, we assumed that it was close to atmospheric equilibrium (~400 μatm) at all locations, and thus would not have been a relevant factor in our analysis.

Furthermore, diet is expected to strongly influence carbonate excretion rate and composition, as fish obtain large amounts of calcium and magnesium from their food, which are then likely largely precipitated and excreted as carbonates (Wilson and Grosell 2003). However, our data have been collected on fasting fishes, thus we cannot account for the direct effect of diet on carbonate excretion and composition in our analyses. Nevertheless, we accounted for the indirect effect of diet (i.e. the adaptation of the gut morphology to the typical diets each species has evolved to consume) by including RIL as an additional potential variable in our analyses. Indeed, RIL is strictly related to diet in reef fishes (Ghilardi et al. 2021b). As we did not have direct measurements of intestinal length of fishes used to collect carbonate samples, we predicted species-level RIL using a Bayesian phylogenetic model trained with the largest available dataset of intestinal length of reef fishes (Ghilardi et al. 2021a) (see Supplementary Methods).

2.2.5 Statistical modelling

Predictors of total carbonate excretion

Before modelling carbonate excretion rates, we used bivariate correlations to identify potential multicollinearity among all explanatory variables, including two covariates related to our methodologies (total sampling period and titration method). The titration method was strongly correlated with all environmental variables as one protocol was applied to all samples from Palau and the other to all samples from Australia and The Bahamas. Titration method was therefore initially excluded from our models. Conversely, salinity was relatively strongly correlated with RIL (r = -0.60) in our dataset. Therefore, these variables were alternatively included in our models (i.e., the same models were fitted twice including either RIL or salinity as a covariate).

We fitted a series of Bayesian regression models to predict carbonate excretion rates based on the selected traits and environmental variables. Let y_{ijk} be the carbonate excretion rate of the ith individual of the jth species, belonging to the kth family. We assumed that each observation of the response variable (y_{ijk}) was t-distributed:

$$
\begin{aligned}
y_{ijk} &\sim \mathrm{t}(\nu, \mu_{ijk}, \sigma) \\
\sigma &\sim \mathrm{t}(3, 0, 2.5) \\
\nu &\sim \Gamma(2, 0.1)
\end{aligned}
\tag{2.2}
$$

with degrees of freedom ν, scale σ, and observation specific locations μ_{ijk} defined as

$$
\begin{aligned}
\ln(\mu_{ijk}) &= \beta_{0k} + \beta_x x \\
\beta_{0k} &= \gamma_0 + u_k \\
u_k &\sim \mathrm{N}(0, \tau_{u_k}) \\
\gamma_0, \beta_x, \tau_{u_k} &\sim \mathrm{N}(0, 5)
\end{aligned}
\tag{2.3}
$$

where γ_0 is the average model intercept, u_k is the random variation in γ_0 based on taxonomic family, and β_x is a vector of regression coefficients of the fixed effects x.

We fitted a series of 36 linear and multilevel models starting from an intercept-only model and increasing in complexity. All models were fitted by weighting

the response variable based on whether fish were kept individually or in groups. Although some fish were kept in relatively large groups (up to 13 individuals), most were kept individually (61% of tanks). Therefore, to avoid overweighting observations from groups larger than two individuals, we gave a weight of two to all observations derived from fish kept in groups of two or more individuals. We built linear models by first including body mass which was the known major predictor. We then added either RIL or salinity, which in our exploratory data analysis showed the strongest correlation with the response after accounting for body mass. Lastly we included temperature, AR, and total sampling period, either alone or in combination. This procedure resulted in 18 linear models which were then refitted including taxonomic family as a group-level effect. Model selection was performed through leave-one-out cross-validation (LOO-CV) (Supplementary Table 2.3). All multilevel models had a better fit than the corresponding linear models highlighting the importance of including the fish family as a group-level effect. Similarly, all models including RIL performed better than the same models where RIL was replaced by salinity. The selected model included the following set of covariates:

$$\beta_x x = \beta_1 \ln(\mathrm{M})_{ijk} + \beta_2 \ln(\mathrm{RIL})_{jk} + \beta_3 \sqrt{\mathrm{AR}_{jk}} + \beta_4 \mathrm{T}_{ijk} \qquad (2.4)$$

where M is the body mass (in kg), RIL and AR are the species-level relative intestinal length and caudal fin aspect ratio (the latter obtained from FishBase, Froese and Pauly 2021), respectively, and T is the average water temperature (in °C) during the sampling period.

To investigate whether there was some unexplained variance in the response that could be attributed to the excluded explanatory variables, we tested for correlations between model residuals and average salinity during the sampling period, titration method, and total sampling period. No residual correlation was observed. However, residual variance was related to the titration method used to quantify carbonate excretion rate (Levene's test, $F_{1,173} = 22.82$, $p < 0.001$), with a larger residual variance in samples analysed through single end point titration. Therefore, to

account for this, we refitted the selected model as a distributional regression where we allowed the scale parameter σ of the t-distribution to vary with respect to the titration method used:

$$\ln(\sigma_{ijk}) = \gamma_\sigma + \beta_\sigma \text{method}_{ijk}$$
$$\gamma_\sigma \sim \text{t}(3, 0, 2.5) \tag{2.5}$$
$$\beta_\sigma \sim \text{N}(0, 5)$$

where γ_σ is the intercept and β_σ is the regression coefficient for the titration method. Thus, $\sigma = exp(\gamma_\sigma)$ for observations obtained through the reference method (i.e., double titration), while $\sigma = exp(\gamma_\sigma + \beta_\sigma)$ for observations obtained through single end point titration.

Model comparison through LOO-CV showed that modelling σ as a function of the titration method improved model fit (Supplementary Table 2.4). Moreover, the distributional model showed that the parameter σ was actually different between methods (mean and 95% CI: 0.39 [0.31, 0.47] and 0.80[0.63, 0.98], for double and single end point titration, respectively). This model was therefore selected to draw conclusions on the relationship between carbonate excretion rate and the explanatory variables.

Predictors of carbonate composition

Five major carbonate polymorphs are produced by fish: LMC, aragonite, HMC, MHC, and ACMC, in order of increasing expected solubility. To investigate the factors determining the excretion of the different carbonate minerals by fish we modelled the excretion rates of individual polymorphs. This approach has two major strengths: (1) it facilitates investigation of both what drives the probability of a polymorph being excreted, and the predictors of the polymorph-specific excretion rates, and (2) it allows direct predictions of polymorph-specific excretion rates.

To obtain the excretion rate of individual polymorphs, the carbonate excretion rate of each fish was multiplied by the species-level relative carbonate composition. Then, we modelled these excretion rates using a Bayesian multivariate hurdle-lognormal model. We used a multivariate model (i.e., a model with multiple

response variables) because it accounts for the correlation among polymorphs within taxonomic group, while allowing the use of different sets of predictors for each response. As all response variables contained zeros (14% to 83% of the observations), we opted for a hurdle-lognormal model, which is a two-part model that combines a logistic regression for the probability that the outcome is zero or not, with a lognormal model for the non-zero responses:

$$\Pr(y \mid \theta, \mu, \sigma) = \begin{cases} \theta & \text{if y} = 0, \text{ and} \\ (1 - \theta)\frac{\log \mathrm{N}(y|\mu,\sigma)}{1-\log \mathrm{N}_{\mathrm{CDF}}(0|\mu,\sigma)} & \text{if y} > 0, \end{cases} \tag{2.6}$$

where θ is the probability of zero outcome (i.e., no excretion), $(1 - \theta)$ is the probability of positive outcome (i.e., excretion), and $logN_{CDF}$ is the cumulative distribution function for the lognormal distribution of the non-hurdle part.

The hurdle probability of each carbonate polymorph (θ_{ijk}^m), i.e. the probability that the ith individual of the jth species, belonging to the kth family, did not excrete the mth polymorph, was estimated using a multilevel logistic regression as:

$$\begin{aligned} \mathrm{logit}(\theta_{ijk}^m) &= \beta_{0k}^m + \beta_1^m \ln(\mathrm{RIL})_{jk} + \beta_2^m \mathrm{T}_{ijk} \\ \beta_{0k}^m &= \gamma_0^m + v_k^m \\ \gamma_0^m &\sim \mathrm{logistic}(0, 1) \\ \beta_{1:2}^m &\sim \mathrm{N}(0, 5) \end{aligned} \tag{2.7}$$

where γ_0^m is the average intercept for the mth polymorph, v_k^m is the random variation in γ_0^m based on taxonomic family, and $\beta_{1:2}^m$ are the regression coefficients of RIL and T, respectively. While, for each response, we modelled the mean of the lognormal distribution (μ_{ijk}^m) according to Eqs. (2.3) and (2.4) and the standard deviation (σ_{ijk}^m) according to Eq. (2.5). Body mass and AR were only included as predictors of the excretion rates, but not as predictors of the probability of excretion of different carbonate polymorphs because no mechanistic link is described or expected for these variables. Conversely, we used fish family, temperature, and RIL to predict the probability of excretion of the polymorphs because fish carbonate mineralogy is generally consistent within families (Salter et al. 2018; Salter et al. 2019), a potential thermal effect has been suggested (Salter et al. 2019), and fish with long

intestines have long gut residence times (Lassuy 1984; Benavides et al. 1994) likely affecting the precipitation of different polymorphs.

To account for both the between-family variance (τ^2) and covariance (ρ) we modelled the group-level effects as correlated. Therefore, we assumed the family-specific intercepts of both the hurdle (v_k^m) and non-hurdle part (u_k^m) of the model to follow a multivariate normal distribution with zero means and covariance matrix $\sum$ with *2m(2m+1)/2* components:

$$
\begin{bmatrix} u_k^1 \\ u_k^2 \\ \vdots \\ u_k^m \\ v_k^1 \\ v_k^2 \\ \vdots \\ v_k^m \end{bmatrix} \sim \mathrm{N} \left(\mu = \begin{bmatrix} 0 \\ 0 \\ \vdots \\ 0 \\ 0 \\ 0 \\ \vdots \\ 0 \end{bmatrix}, \sum \right) \tag{2.8}
$$

$$
\sum = \begin{bmatrix}
\tau_{u_k^1}^2 & \rho\tau_{u_k^1}\tau_{u_k^2} & \cdots & \rho\tau_{u_k^1}\tau_{u_k^m} & \rho\tau_{u_k^1}\tau_{v_k^1} & \rho\tau_{u_k^1}\tau_{v_k^2} & \cdots & \rho\tau_{u_k^1}\tau_{v_k^m} \\
\rho\tau_{u_k^2}\tau_{u_k^1} & \tau_{u_k^2}^2 & \cdots & \rho\tau_{u_k^2}\tau_{u_k^m} & \rho\tau_{u_k^2}\tau_{v_k^1} & \rho\tau_{u_k^2}\tau_{v_k^2} & \cdots & \rho\tau_{u_k^2}\tau_{v_k^m} \\
\vdots & \vdots & \ddots & \vdots & \vdots & \vdots & \ddots & \vdots \\
\rho\tau_{u_k^m}\tau_{u_k^1} & \rho\tau_{u_k^m}\tau_{u_k^2} & \cdots & \tau_{u_k^m}^2 & \rho\tau_{u_k^m}\tau_{v_k^1} & \rho\tau_{u_k^m}\tau_{v_k^2} & \cdots & \rho\tau_{u_k^m}\tau_{v_k^m} \\
\rho\tau_{v_k^1}\tau_{u_k^1} & \rho\tau_{v_k^1}\tau_{u_k^2} & \cdots & \rho\tau_{v_k^1}\tau_{u_k^m} & \tau_{v_k^1}^2 & \rho\tau_{v_k^1}\tau_{v_k^2} & \cdots & \rho\tau_{v_k^1}\tau_{v_k^m} \\
\rho\tau_{v_k^2}\tau_{u_k^1} & \rho\tau_{v_k^2}\tau_{u_k^2} & \cdots & \rho\tau_{v_k^2}\tau_{u_k^m} & \rho\tau_{v_k^2}\tau_{v_k^1} & \tau_{v_k^2}^2 & \cdots & \rho\tau_{v_k^2}\tau_{v_k^m} \\
\vdots & \vdots & \ddots & \vdots & \vdots & \vdots & \ddots & \vdots \\
\rho\tau_{v_k^m}\tau_{u_k^1} & \rho\tau_{v_k^m}\tau_{u_k^2} & \cdots & \rho\tau_{v_k^m}\tau_{u_k^m} & \rho\tau_{v_k^m}\tau_{v_k^1} & \rho\tau_{v_k^m}\tau_{v_k^2} & \cdots & \tau_{v_k^m}^2
\end{bmatrix} \tag{2.9}
$$

with

$$
\tau_{u_k^m} \sim \mathrm{N}(0,5)
$$
$$
\tau_{v_k^m} \sim \mathrm{N}(0,5) \tag{2.10}
$$
$$
\rho \sim \mathrm{LKJCorr}(1)
$$

Finally, we fitted a second model specifying a different formula for the mean of the lognormal distribution of each polymorph (μ_{ijk}^m). This was achieved by removing the fixed effects with relatively large errors (i.e., those with an estimated error greater than the mean estimate). Specifically, we removed the effects of RIL, AR, and temperature on LMC and the effect of temperature on MHC. Model

comparison through LOO-CV showed no difference in model fit between the two models, therefore, we selected the more parsimonious model to create figures and interpret results.

All analyses were performed with the software program R (version 4.1.3, R Core Team 2021) and all models were fitted with the R package *brms* (version 2.15.0, Bürkner 2017). Linear and multilevel models were run for four chains, each with 4,000 iterations and a warm-up of 1,000 iterations, whereas hurdle models were run for three chains, each with 4,000 iterations and a warm-up of 2,000 iterations. All models were examined for evidence of convergence using trace plots and Gelman–Rubin statistics and we used posterior predictive distributions to check for models' fit.

2.3   Results

2.3.1   Predictors of total carbonate excretion

A Bayesian multilevel distributional regression model exploring the relationship between total carbonate excretion rate and body mass, AR, RIL, temperature, and family explained 85.5% (95% credible interval (CI): 83.7%, 86.8%) of the variation in the response and showed a strong relationship between observed and predicted excretion rate (Supplementary Fig. 2.7), with 96% of the observed values falling within the 95% CIs of the predictions.

Fish body mass was the strongest predictor of carbonate excretion rate. RIL had a stronger influence on carbonate excretion rates compared to temperature and AR, which had the weakest effects (Fig. 2.1a). Further, taxonomic identity explained a minor proportion of variance in the dataset (~5%), with a few families (Labridae excluding Scarini, Lutjanidae, Pomacentridae, and Terapontidae) clearly deviating from the average estimate (Fig. 2.1b).

There was a positive relationship between excretion rate and all three factors related to metabolic rate: body mass, temperature, and AR (Figs. 2.1a and 2.2a-c). Small fishes excreted more carbonate per unit mass than large ones, as indicated
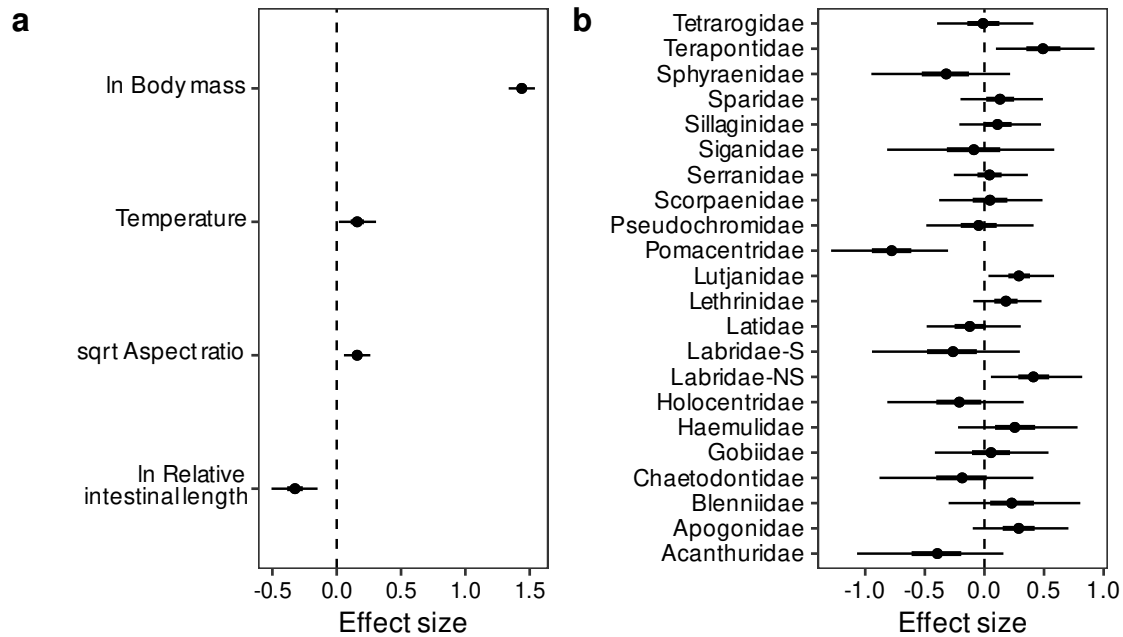
Figure 2.1: Predictors of reef fish carbonate excretion rate. **a** Effects of fish traits and temperature on carbonate excretion rate. **b** Family-specific effects on carbonate excretion rate. Estimates are medians (circles), 50% credible intervals (CIs; thick lines; some are too narrow to be seen) and 95% CIs (thin lines) derived from 12,000 posterior draws of a Bayesian multilevel distributional regression model. All predictors were standardised (mean-centred and scaled by one standard deviation) prior to fitting the model to allow for the comparison of effect sizes (non-standardised effects are reported in the text). Labridae-S scarine Labridae, Labridae-NS non-scarine Labridae. Data underlying the figures are available in the Zenodo repository (`https://doi.org/10.5281/zenodo.7530455`) (Ghilardi et al. 2023a).

by the hypoallometric relationship between excretion rate and body mass (both natural-log transformed; mean and 95% CI: $\beta = 0.78$ [0.72, 0.83]) (Fig. 2.2a). On average, excretion rates increased 48% across the observed range of temperature (23.0-30.2 °C) (mean and 95% CI: $\beta = 0.05$ [0.01, 0.10]) (Fig. 2.2b) and 100% across the observed range of AR (0.76-3.30) (square-root transformed; mean and 95% CI: $\beta = 0.71$ [0.25, 1.17]) (Fig. 2.2c). Moreover, the average temperature coefficient (Q_{10}; i.e., the relative change in carbonate excretion rate for every 10 °C rise in temperature) across the observed temperature range was 1.74 (95% CI: 1.06, 2.73). Carbonate excretion rate was negatively related to RIL (natural-log transformed) (Fig. 2.1a). This relationship was described by a power function with an exponent of -0.59 (95% CI: -0.92, -0.27), which translates into an average 82%
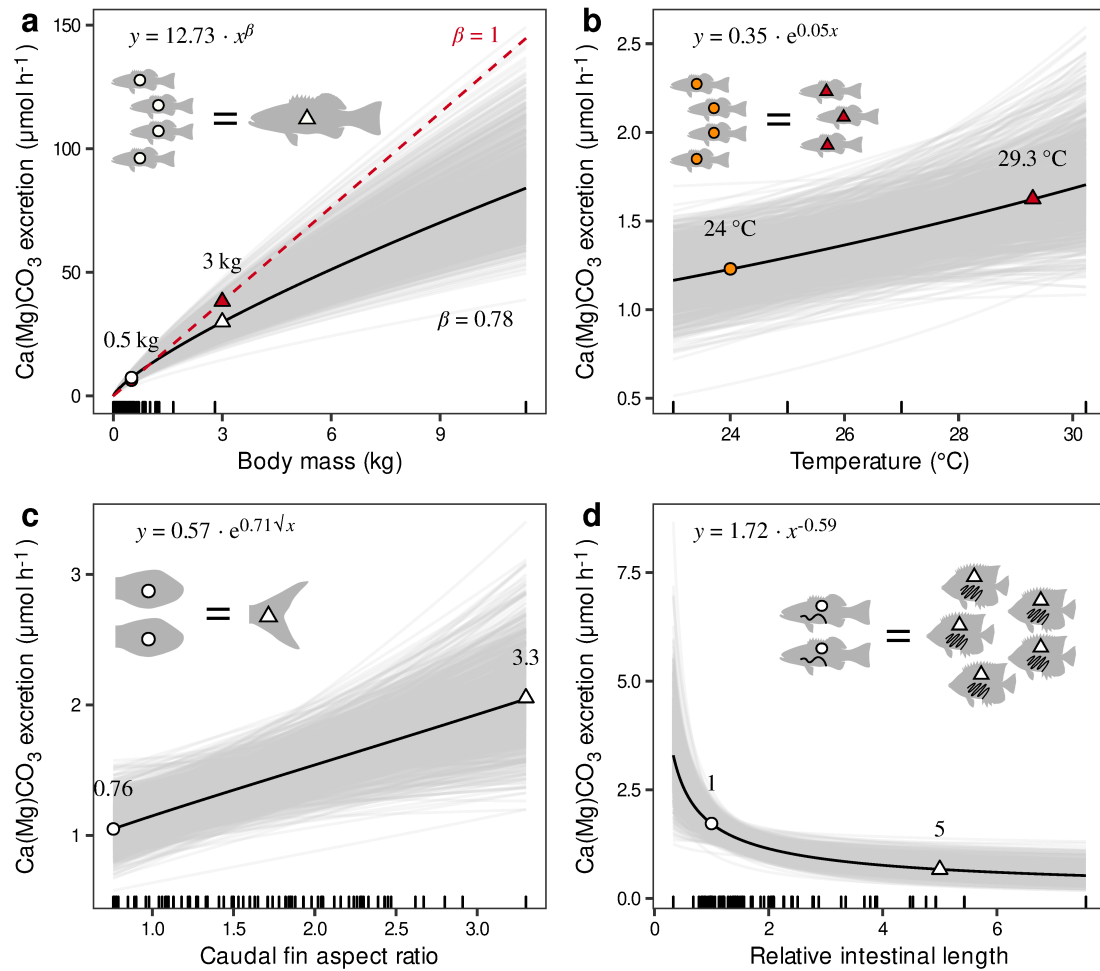
Figure 2.2: Relationships between reef fish carbonate excretion rates, fish traits, and temperature. Marginal effect of (**a**) body mass, (**b**) water temperature, (**c**) caudal fin aspect ratio (AR), and (**d**) relative intestinal length (RIL) after controlling for the remaining fixed and group-level effects of a Bayesian multilevel distributional regression model by standardising the other predictors at their mean values. Thick, black lines represent the mean predicted fits, whereas thin, grey lines represent 1,000 draws randomly chosen from the posterior fits and show model fit uncertainty. Model predictions are for natural-log transformed excretion rates, but here show the fitted functions on the original scale of the data. Raw data are displayed as marks along the x-axis. In (**a**), the red dashed line represents isometric scaling ($\beta = 1$). In each panel, silhouettes show the number of fish required to excrete the same amount of carbonate at two levels of the predictor variable, which are also shown as matching symbols on the mean predicted fits. All silhouettes were drawn by MG and based on photographs taken by J.E. Randall and sourced from FishBase (Froese and Pauly 2021). Data underlying the figures are available in the Zenodo repository (`https://doi.org/10.5281/zenodo.7530455`) (Ghilardi et al. 2023a).

decrease in excretion rate across the observed RIL range (0.33-7.56) (Fig. 2.2d).

2.3.2 Predictors of carbonate composition

The identified predictors of carbonate excretion rate (i.e., body mass, AR, RIL, temperature, and family) were used to predict the excretion rate of five major carbonate polymorphs produced by fishes (i.e., LMC, HMC, aragonite, MHC, ACMC) using a Bayesian multivariate hurdle-lognormal model. The hurdle model allowed us to account for the large zero-inflation in the responses (14-83% of zeros) by modelling the probability of excretion of each polymorph as a function of RIL, temperature, and taxonomic identity, i.e., the variables known or expected to inuence the mineralogical composition of excreted carbonates (Salter et al. 2018; Salter et al. 2019) (see the Statistical modelling section). The model predicted the correct proportion of zeros for all carbonate polymorphs (Supplementary Fig. 2.8) and showed a high predictive performance for positive observations, with a strong relationship between observed and predicted excretion rate for each polymorph (Supplementary Fig. 2.9). Further, over 96% of the observed values of each polymorph fell within the 90% CIs of the predictions (64-93% when considering the 50% CIs).

Fish body mass was consistently the strongest predictor of excretion rate for all carbonate polymorphs (Fig. 2.3a). The excretion rate of HMC scaled hypoallometrically with body mass (mean and 95% CI: $\beta = 0.74$ [0.68, 0.80]), whereas the excretion rate of MHC scaled hyperallometrically (mean and 95% CI: $\beta = 1.40$ [1.04, 1.78]), and that of other polymorphs did not differ from isometry as the wide uncertainty around the estimate overlapped with 1 (mean and 95% CI: $\beta = 0.89$ [0.56, 1.19], $\beta = 1.14$ [0.84, 1.39], $\beta = 0.89$ [0.64, 1.14], for LMC, aragonite, and ACMC, respectively). A positive effect of temperature and AR on excretion rate was consistent among polymorphs. Conversely, RIL negatively affected the excretion rate of ACMC and HMC (in agreement with the effect on total carbonate excretion rate), but had the opposite effect on the excretion rate of MHC and aragonite.
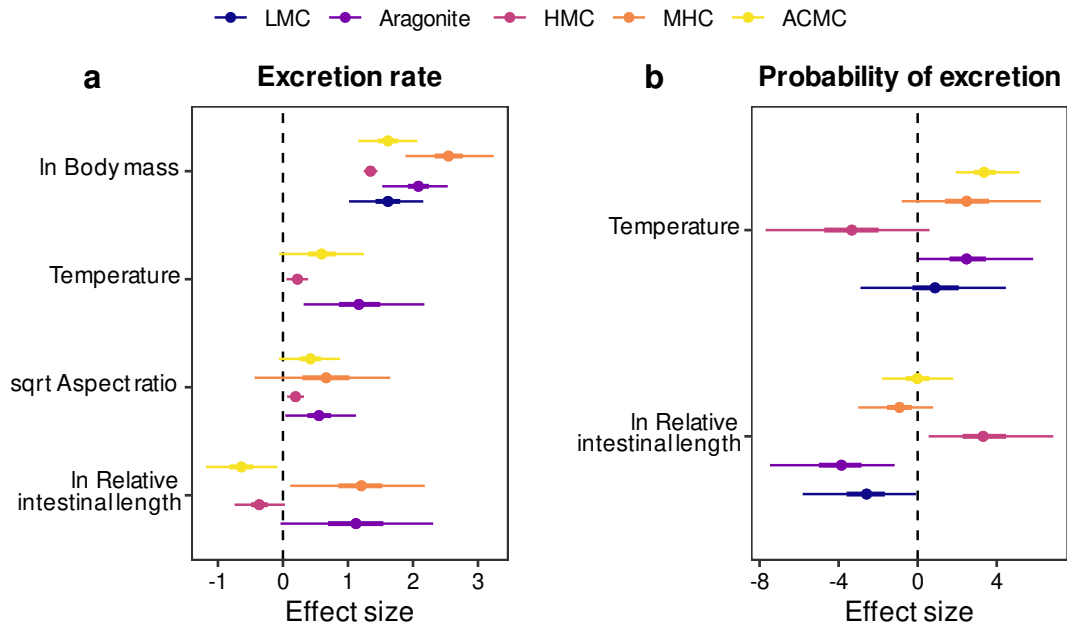
Figure 2.3: Predictors of reef fish carbonate composition. a Effects of fish traits and temperature on the excretion rate of five different carbonate polymorphs. **b** Effects of species relative intestinal length (RIL) and water temperature on the probability of excreting five different carbonate polymorphs. Estimates are medians (circles), 50% credible intervals (CIs; thick lines; some are too narrow to be seen) and 95% CIs (thin lines) derived from 6,000 posterior draws of a Bayesian multivariate hurdle-lognormal model. All predictors were standardised (mean-centred and scaled by one standard deviation) prior to fitting the model to allow for the comparison of effect sizes. Missing estimates correspond to effects excluded from the final model (see the Statistical modelling section). LMC Low-magnesium calcite, HMC High-magnesium calcite, MHC Monohydrocalcite, ACMC Amorphous calcium magnesium carbonate. Data underlying the figures are available in the Zenodo repository (`https://doi.org/10.5281/zenodo.7530455`) (Ghilardi et al. 2023a).

Temperature and RIL had relevant effects on the probability of excreting certain carbonate polymorphs (Fig. 2.3b). Temperature, for instance, positively influenced the probability of excreting ACMC, and to a lesser extent MHC and aragonite, and negatively affected the likelihood of fish excreting HMC. RIL was positively associated with the probability of excreting HMC and negatively associated with the likelihood of excreting aragonite and LMC.

For both aragonite and HMC, RIL had a contrasting effect on the excretion rate and probability of excretion (i.e., on the two parts of the hurdle model), with opposite patterns. Fish with longer intestines were less likely to excrete aragonite

but excreted it at a higher rate than fish with shorter intestines. Conversely, fish with longer intestines were more likely to excrete HMC but excreted it at a lower rate compared to fish with shorter intestines. These contrasting effects resulted in right-skewed unimodal relationships between the excretion rate of the two polymorphs and RIL (Fig. 2.4), with the highest average excretion rates for aragonite and HMC in fish with RIL of about 1 and 1.4, respectively.

Although RIL and temperature increased the probability of excreting HMC and ACMC, respectively, carbonate composition was strongly conserved at the family level (Supplementary Figs. 2.10, 2.11). Indeed, most families showed large effect sizes on the probability of excreting certain polymorphs (Supplementary Fig. 2.10a). Nevertheless, a few families showed smaller effect sizes (e.g., Acanthuridae, Gobiidae) indicating higher intra-familial variability in carbonate composition. A weaker effect of family was observed on the excretion rates of a given polymorph (Supplementary Fig. 2.10b).

Furthermore, the multivariate model allowed us to estimate the correlations among the probabilities of excretion of different polymorphs after accounting for the effects of RIL and temperature (i.e., the group-level effect correlation). Specifically, we estimated correlations among polymorphs at the family level (Fig. 2.5). We found that families that were most likely to excrete HMC were less likely to excrete MHC, aragonite, or LMC. Conversely, the probabilities of excreting aragonite, LMC, and MHC were all positively correlated, highlighting that these polymorphs are generally co-produced by fishes. ACMC may be excreted alongside all other polymorphs, although the probability was highest when LMC was also excreted.

2.4 Discussion

Accurately assessing the role of fishes in the carbon cycle of the ocean requires a comprehensive understanding of the drivers of fish carbonate excretion rate and composition. Initial models of carbonate production in marine fishes primarily assumed a direct link to metabolic rate (Wilson et al. 2009). We demonstrate
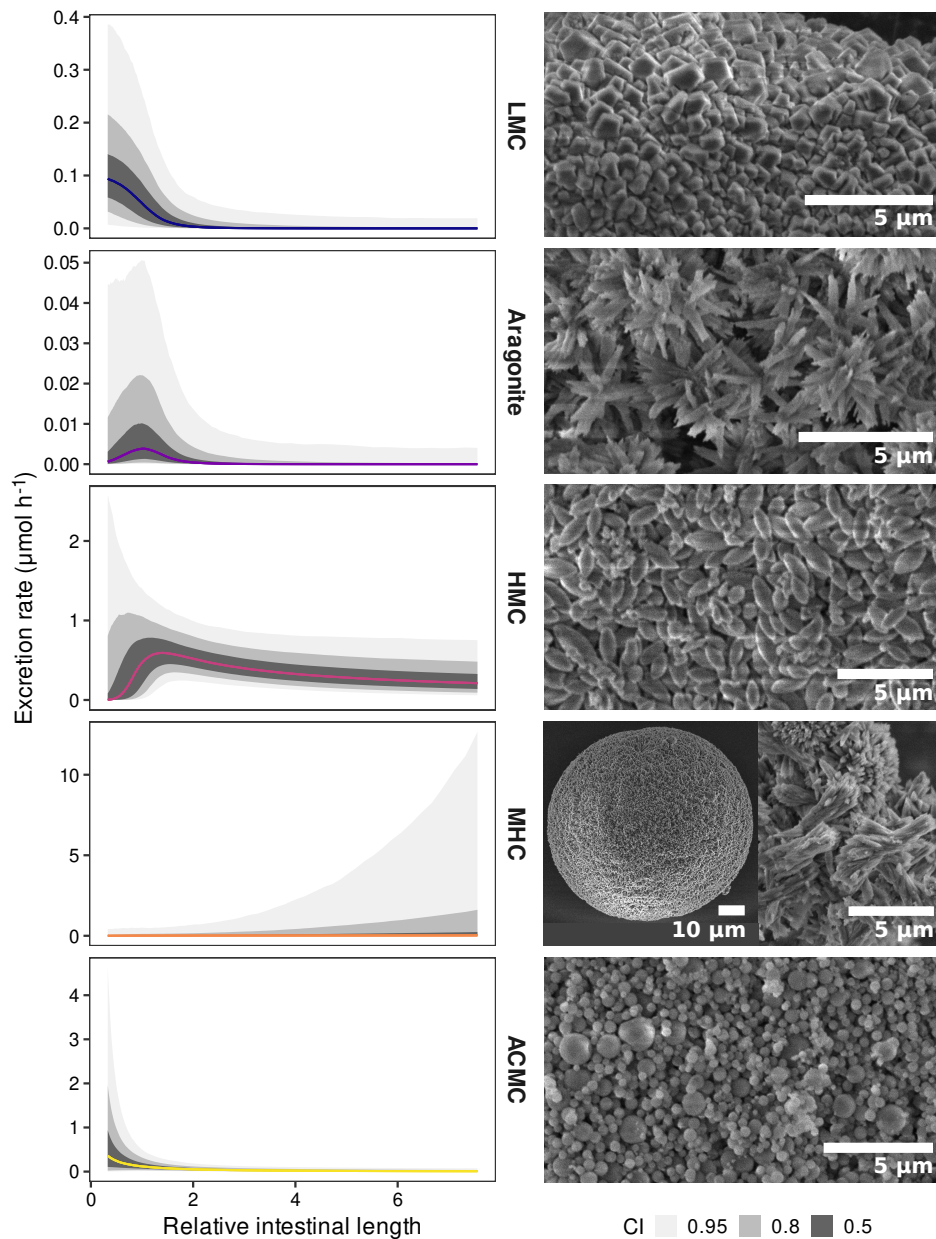
Figure 2.4: Relative intestinal length affects reef fish carbonate composition.
Marginal effect of species relative intestinal length (RIL) on the excretion rate of five
different carbonate polymorphs after controlling for the remaining fixed and group-level
effects of a Bayesian multivariate hurdle-lognormal model by standardising the other
predictors at their mean values. Coloured lines represent the median predicted fits and
the ribbons show the 50%, 80%, and 95% credible intervals (CI) around the estimate.
Note the different scales on the y-axis. Scanning electron microscope images showing
representative crystalline morphologies for each carbonate polymorphs are displayed on
the right of each plot. LMC Low-magnesium calcite, HMC High-magnesium calcite, MHC
Monohydrocalcite, ACMC Amorphous calcium magnesium carbonate. Data underlying
the figures are available in the Zenodo repository (`https://doi.org/10.5281/zenodo`
`.7530455`) (Ghilardi et al. 2023a).

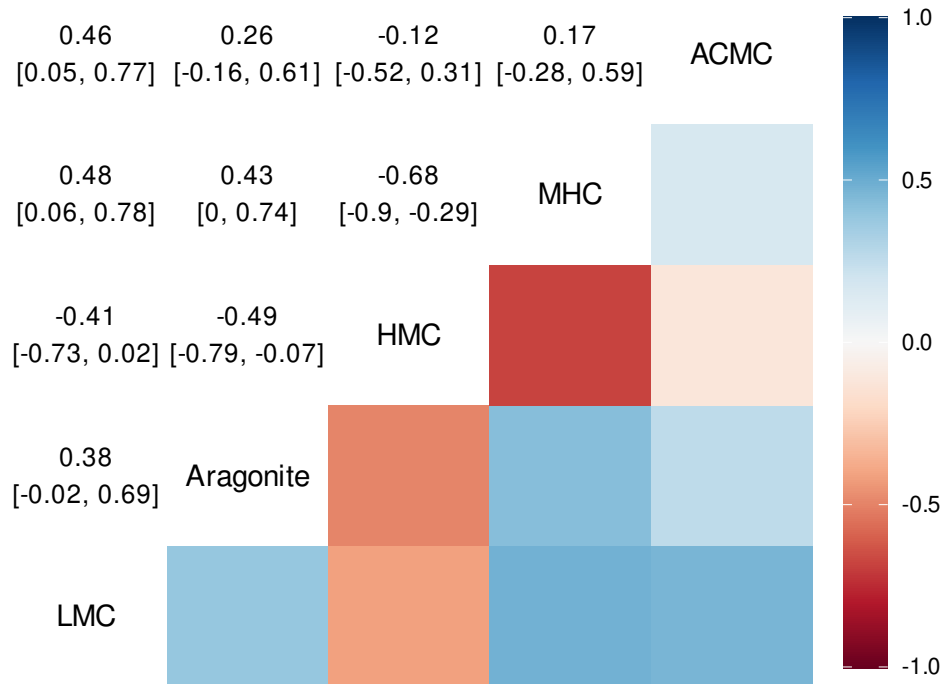**Figure 2.5: Family-level correlations among the probabilities of excretion of five carbonate polymorphs by reef fishes.** Estimates are posterior medians and 95% credible intervals of correlation coefficients derived from 6,000 posterior draws of a Bayesian multivariate hurdle-lognormal model after controlling for temperature and relative intestinal length (Equation (2.9)). LMC Low-magnesium calcite, HMC High-magnesium calcite, MHC Monohydrocalcite, ACMC Amorphous calcium magnesium carbonate. Data underlying the figures are available in the Zenodo repository (`https://doi.org/10.5281/zenodo.7530455`) (Ghilardi et al. 2023a).

the relationships between fish carbonate excretion rate and three key drivers of metabolic rate (i.e., body mass, temperature, and AR), which show that the metabolism-carbonate excretion rate link is consistent across 71 reef fish species from 21 families. Furthermore, we show that this link is also mediated by RIL. These insights have important implications for quantifying community-level estimates of carbonate excretion rates and the indirect impacts of anthropogenic factors (mainly fishing and warming) on the contribution of fishes to the marine carbon cycle. Additionally, we provide evidence that carbonate excretion rate is related to body mass, temperature, and AR, and thus likely to fish metabolism, regardless of the carbonate polymorph excreted. However, intriguingly, polymorph-specific excretion rates differ in their relationship with RIL. Finally, we show that

the mineralogical composition of fish carbonates is highly conserved within families and to a lesser extent controlled by RIL and temperature. These findings allow refined estimates of carbonate excretion and composition at the regional and global scales to be generated. These estimates can be integrated into ocean carbonate and sediment production budgets and used in management and decision-making processes oriented towards the conservation of ecosystem functions (Cinner et al. 2020).

Our multi-species analysis reveals that carbonate excretion rate scales hypoallometrically with body mass, as does metabolic rate. The estimated average scaling exponent of 0.78 is in agreement with the value of 0.80 found for resting metabolic rate across fishes (Clarke and Johnston 1999) and ectotherms (Gillooly et al. 2017). This suggests that carbonate excretion is directly proportional to metabolic rate through the effect of body mass. Furthermore, due to the scaling exponent < 1, size-selective fishing and warming (Robinson et al. 2017; Tu et al. 2018) will increase carbonate excretion rate per unit biomass by reducing fish size, thus averting immediate functional collapse as biomass is depleted (Jennings and Wilson 2009; Morais et al. 2020b) and large fish are extirpated (Mellin et al. 2016a).

The observed positive relationships of carbonate excretion rate with temperature and AR also support a direct link of carbonate excretion with metabolism. We found a Q_{10} of 1.74, which is lower than previously-observed species-specific values (Heuer et al. 2016; Wilson et al. 2009). This is consistent with observations for fish resting metabolic rate, where species-specific Q_{10} values are highly variable and >2 on average (Clarke and Johnston 1999), while observed values across species are typically <2 (Clarke and Johnston 1999; Killen et al. 2010; Killen et al. 2016). Clarke and Johnston (1999) found a Q_{10} of 1.83, calculated over a 0-30 °C temperature range and across 69 fish species. Recalculated over the range of temperature observed in our study, that value is adjusted to 1.75, very close to our estimated value. This suggests that resting metabolic rate would increase by 50% over the same temperature range in which carbonate excretion rate is predicted to increase by 48%. Similarly, the relationship between carbonate excretion and AR is in agreement with results linking this morphological trait to metabolic rate

(Killen et al. 2016). Indeed, if we were to extrapolate carbonate excretion rate across the broader range of AR analysed by Killen et al. (2016) (i.e. 0.66-7.2), which includes pelagic fishes, we would obtain a 314% increase in excretion, which is roughly equivalent to the estimated 3.4-fold difference in resting metabolic rate. While other morphological traits are related to metabolic rate (e.g., gill surface area and muscle protein content, Killen et al. 2016; Bigman et al. 2021), they are also directly related to AR and linked to fish lifestyle (Killen et al. 2016). Therefore, although we did not directly incorporate these traits in our models, they are accounted for by including AR.

Altogether, these results support the prior assumption that carbonate excretion rate is directly proportional to metabolic rate and therefore support previous global estimates (Wilson et al. 2009). Our findings also suggest that the observed relationships could be extended outside the range of body mass and AR considered here, including large and pelagic fishes for which data collection is constrained by space availability in most research stations. However, we show that RIL has also a strong negative effect on carbonate excretion rate, thus affecting its direct link with metabolic rate. Consequently, the model used by Wilson et al. (2009) appears to generally overestimate carbonate excretion rate for fishes with a RIL >1 (Fig. 2.6). Their model was indeed parameterised using data from two benthic, predatory fishes with RIL typically <1 (Braber and de Groot 1973; Mitparian et al. 2021), which produced estimates comparable to those of our model for similar fishes (e.g., AR = 1.5 and RIL = 0.5), regardless of temperature (Fig. 2.6 and Supplementary Fig. 2.12). Furthermore, a constant (i.e., ρ) was added to the earlier model to account for the higher resting metabolic rate of most fishes living in the water column and thus provide more realistic estimates (Wilson et al. 2009). According to our model, this correction is comparable to a seven-fold difference in AR (e.g., from 0.5 to 3.5), and leads to overestimates of the excretion rate for the large majority of fish species (Fig. 2.6). Therefore, carbonate production by marine fishes (at least at rest) may be lower than previously estimated. Furthermore, as RIL is negatively related to trophic level (Ghilardi et al. 2021b; Karachle and
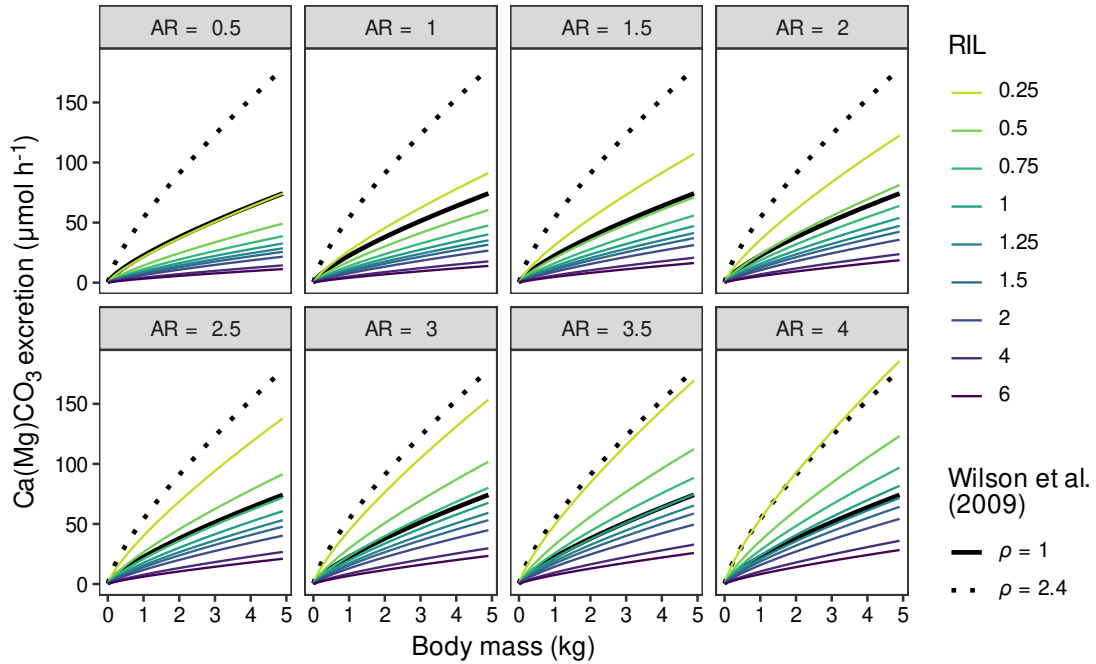
Figure 2.6: Comparison between the estimates of our model and those of the model used by Wilson et al. (2009). Estimates of our model are average predictions (and thus do not account for the effect of family) at different levels of caudal fin aspect ratio (AR) and relative intestinal length (RIL). Estimates of "Wilson's model" are presented at two levels of the constant ρ ($\rho = 1$ corresponds to benthic, sedentary fishes, whereas $\rho = 2.4$ is the value used to adjust model estimates for pelagic fishes with faster resting metabolic rates), while the constant α was set to 1 to be comparable to our estimates (see Wilson et al. 2009, for further details). All estimates are presented for a fixed temperature of 25 °C as results are unchanged at different temperatures (see Supplementary Fig. 2.12). Data underlying the figures are available in the Zenodo repository (`https://doi.org/10.5281/zenodo.7530455`) (Ghilardi et al. 2023a).

Stergiou 2010b), the negative power relationship between excretion rate and RIL suggests that fishing and climate-induced regime shifts may reduce fish carbonate excretion by decreasing the mean trophic level of fish communities, thus potentially counteracting the buffering effect triggered by size-selective fishing. The effect of RIL on the individual carbonate polymorphs also suggests that these impacts may lead to shifts in community-level carbonate composition.

The negative relationship between carbonate excretion rate and RIL is counterintuitive from a metabolic point of view. With the intestine being an energetically expensive organ (Cant et al. 1996), metabolic and carbonate excretion rates should increase with increasing RIL. However, the energetic investment in the intestine

may be balanced by the size of other expensive organs (Tsuboi et al. 2015). Factors unrelated to metabolism may thus explain this result. In our dataset, RIL was negatively related to salinity (r = -0.60), suggesting that part of the RIL effect may be confounded with the positive salinity effect on carbonate excretion (Genz et al. 2008; Mekuchi et al. 2010; Schauer et al. 2018). However, the salinity range in our study (33.8–36.6) is an order of magnitude lower than the range driving a ~2.5 fold change in carbonate excretion rate in the Gulf toadfish (Schauer et al. 2018). Therefore, salinity should explain minimal, if any, variability in our carbonate excretion rates.

Fishes with long intestines have a large intestinal surface area (Ghilardi et al. 2021b) and long gut residence time (Benavides et al. 1994; Lassuy 1984), which may enhance water absorption efficiency. These fishes would presumably require correspondingly lower drinking rates and excrete lower amounts of carbonate. Water absorption efficiency has been measured in fishes with relatively short intestines (Fletcher 1978; Genz et al. 2008; Hickman 1968; Shehadeh and Gordon 1969; Sleet and Weber 1982; Smith 1930; Whittamore et al. 2010; Wilson et al. 1996; Wilson et al. 2002). To the best of our knowledge, no values of water absorption efficiency are currently available for fishes with RIL >2. Nevertheless, the known range of water absorption efficiency (38.5-85%, Whittamore 2012) suggests that fishes with the lowest absorption efficiency must drink more than twice as much seawater as fishes with the highest absorption efficiency, with a direct effect on carbonate excretion. We also hypothesise that long gut residence times directly reduce carbonate excretion rates, while potentially leading to accumulation of carbonate and irregular or delayed release of larger pellets, as previously reported for three temperate species (Salter et al. 2019). Thus, we cannot discard that some of the excretion rates measured here could be affected by the relatively short sampling period considered (median: 64 h; range: 18-169 h). Simultaneous measurements of RIL, water absorption efficiency, and gut residence times are needed to better understand the mechanistic link underlying the observed relationships.

Residence time may also prove a viable explanation of the observed effect of RIL on carbonate composition. In this context, a longer residence time may allow unstable ACMC to transform into more stable polymorphs, such as aragonite and calcite, or into metastable MHC, which may then undergo further transformation (Blue et al. 2017; Rodriguez-Blanco et al. 2014; Zhang et al. 2012). We show that ACMC excretion rate is highest in fishes with very short intestines, while aragonite and HMC excretion rates are highest in fishes with intermediate RIL, and MHC is mostly excreted by fishes with long intestines. These results are consistent with previous observations that synthetic ACMC requires much longer time to transform into MHC than into aragonite and calcite (Blue et al. 2017). Available compositional data from this and previous studies (Salter et al. 2017; Salter et al. 2018) for fish families not included in the analysis (due to low sample size) also confirm the observed patterns, with ACMC being the major polymorph produced by families with short intestines (e.g., Muraenidae) and MHC by families with long intestines (e.g., Zanclidae). Such mechanisms deserve further investigation and an analysis of carbonate development through the length of the intestine of species producing different polymorphs would permit testing of this hypothesis.

Nevertheless, RIL is highly phylogenetically conserved (Ghilardi et al. 2021b; Wagner et al. 2009), leading to strong conservatism in carbonate composition at the family level. Our findings reiterate recent observations that the mineralogical composition of fish carbonates is broadly consistent within families across regions (Salter et al. 2018) and over large thermal gradients (Salter et al. 2019). The family Labridae (excluding Scarini), however, has been highlighted as an exception to this general pattern in that it produced mainly ACMC with minor calcite in warm conditions (25-27 °C), but the opposite occurred at 10 °C (Salter et al. 2019). A potential thermal control on the excretion of ACMC over calcite widely applicable across families has been recognised (Salter et al. 2019). Our results provide evidence in support of this control given that we find a strong positive association between temperature and the probability of fishes excreting ACMC across families. Regardless of the underlying mechanism (increased gut residence

times at lower temperature have been suggested, Knight et al. 2021; Salter et al. 2019), carbonates excreted by fish in warmer temperatures would contain more ACMC and less HMC (Supplementary Fig. 2.13), suggesting higher solubility and a reduced export of carbonate particles into the deep sea (Saba et al. 2021; Sulpis et al. 2021). The associated reduced removal of alkalinity from surface waters weakens ocean acidification and favours the CO_2 uptake of the ocean. However, higher carbonate dissolution also lowers the CO_2 uptake by the biological carbon pump. This pump increases the CO_2 uptake of the ocean via the fixation of CO_2 into biomass (photosynthesis) and its export from the oceanic surface towards the deep sea, which is accelerated by carbonate minerals by increasing the density of sinking particles (Klaas and Archer 2002; Rixen et al. 2019). Hence, our findings have strong implications for understanding the role of fish carbonates in the marine carbon cycle and sequestration.

Our models provide substantial improvements to previous carbonate production models based on the parsimonious relationship with body mass and temperature (Perry et al. 2011; Salter et al. 2017; Salter et al. 2018; Wilson et al. 2009) and allow us to produce species-level estimates under given thermal conditions. A major improvement lies in the ability to directly predict species-level excretion rates for individual carbonate polymorphs. These advances come, however, with limitations that have to be considered for any future application of our results and models. While variation in carbonate excretion rates among families is relatively small, carbonate composition is strongly conserved at the family level, hampering extrapolation to unsampled families. As the taxonomic scope of the existing carbonate database remains limited (35 reef-associated fish families out of 158, Froese and Pauly 2021, with 14 having <3 observations), a targeted data collection campaign (preferably including small pelagic fishes) is needed to increase the proportion of fish biomass for which carbonate excretion rate can be predicted. Nevertheless, our models allow us to predict carbonate excretion rate and composition for several of the most abundant and biomass-rich fish families on coral reefs. Furthermore, the models were trained with data collected in shallow tropical and subtropical reefs,

thereby limiting the potential geographic scope of their application. Additional data are needed to broaden the applicability of our results to marginal, non-reef, high-latitude, and pelagic environments. Progress has been made in expanding existing compositional data to temperate regions (Salter et al. 2019). If associated production data becomes available, a potential extension of our models to temperate regions is possible.

It should also be noted that our models predict carbonate excretion rates for fishes that are most likely close to their resting metabolic rate, as data were collected from fasting fishes held individually (or in small monospecific groups) in relatively small tanks. However, as we found that carbonate excretion rate is likely directly related to metabolic rate, excretion rates of free-living fishes should scale proportionally to their metabolic rate. Previous studies have applied a common scaling factor to all species to overcome this issue (Jennings and Wilson 2009; Perry et al. 2011; Salter et al. 2017; Salter et al. 2018; Wilson et al. 2009). This value was derived from a study which estimated the factorial activity scope (i.e., the ratio of field metabolic rate to resting metabolic rate, White and Kearney 2014) for the Atlantic cod (Kerr 1982). It is thus unlikely that this estimate is representative of all species, particularly for tropical reef fishes. Current knowledge on the factorial activity scope of reef fishes is limited and this parameter is likely highly variable among taxa and across body size (Schiettekatte et al. 2022b; White and Kearney 2014). The use of a single value as scaling factor may thus potentially introduce large errors in the estimated carbonate excretion rates. Instead, we suggest that future studies provide estimates of carbonate excretion rate for fishes at rest and discuss this limitation.

Improvements in the measurement of field metabolic rates in fishes (Chung et al. 2019; Schiettekatte et al. 2022b) may soon allow updates to our models to predict carbonate excretion rates for fishes in their natural habitat. To do so, we must, however, consider the role of fish diet in carbonate production. Fish diet is often rich in calcium, leading to high luminal calcium concentration with a direct effect on carbonate precipitation (Mekuchi et al. 2010; Wilson and Grosell 2003). It

would therefore seem reasonable to expect carbonate excretion rates several times higher in feeding compared to fasting fishes. It is thus likely that calcium (and in minor measure magnesium) obtained from food accounts for a large proportion of the carbonate excreted in wild feeding fishes. Diet may also alter intestinal fluid composition, and thus the precipitated carbonate polymorphs. However, existing data show no difference in the composition of carbonates excreted by fishes when feeding or fasting (Salter et al. 2017). The calculation of calcium ingestion rates and subsequent carbonate precipitation given food ingestion rates (Schiettekatte et al. 2020) and food calcium content may be a feasible way to greatly improve carbonate production models.

Acknowledgements

References

Allgeier, Jacob E. et al. (2014). "Consistent nutrient storage and supply mediated by diverse fish communities in coral reef ecosystems". In: *Global Change Biology* 20.8, pp. 2459–2472. DOI: `10.1111/gcb.12566`.

Allgeier, Jacob E. et al. (2021). "Phylogenetic conservatism drives nutrient dynamics of coral reef fishes". In: *Nature Communications* 12, p. 5432. DOI: 10.1038/s41467-021-25528-0.

Benavides, A. G., J M Cancino, and F P Ojeda (1994). "Ontogenetic changes in gut dimensions and macroalgal digestibility in the marine herbivorous fish, *Aplodactylus punctatus*". In: *Functional Ecology* 8, pp. 46–51.

Bianchi, Daniele et al. (2021). "Estimating global biomass and biogeochemical cycling of marine fish with and without fishing". In: *Science Advances* 7, eabd7554. DOI: 10.1126/sciadv.abd7554.

Bigman, Jennifer S. et al. (2021). "Respiratory capacity is twice as important as temperature in explaining patterns of metabolic rate across the vertebrate tree of life". In: *Science Advances* 7, eabe5163. DOI: 10.1126/sciadv.abe5163.

Blue, C. R. et al. (2017). "Chemical and physical controls on the transformation of amorphous calcium carbonate into crystalline CaCO3 polymorphs". In: *Geochimica et Cosmochimica Acta* 196, pp. 179–196. DOI: 10.1016/j.gca.2016.09.004.

Boettiger, Carl, D. T. Lang, and P. C. Wainwright (2012). "Rfishbase: Exploring, manipulating and visualizing FishBase data from R". In: *Journal of Fish Biology* 81.6, pp. 2030–2039. DOI: 10.1111/j.1095-8649.2012.03464.x.

Braber, L. and S. J. de Groot (1973). "On the morphology of the alimentary tract of flatfishes (Pleuronectiformes)". In: *Journal of Fish Biology* 5.2, pp. 147–153. DOI: 10.1111/j.1095-8649.1973.tb04443.x.

Breevi, Ljerka and Arne Erik Nielsen (1989). "Solubility of amorphous calcium carbonate". In: *Journal of Crystal Growth* 98, pp. 504–510.

Brown, J. H. et al. (2004). "Toward a metabolic theory of ecology". In: *Ecology* 85.7, pp. 1771–1789. DOI: 10.1007/978-3-030-84771-5_8.

Bürkner, Paul Christian (2017). "brms: An R package for Bayesian multilevel models using Stan". In: *Journal of Statistical Software* 80.1, pp. 1–28. DOI: 10.18637/jss.v080.i01.

Cant, John P., Brian W. McBride, and Warren J. Croom (1996). "The Regulation of Intestinal Metabolism and Its Impact on Whole Animal Energetics". In: *Journal of Animal Science* 74.10, pp. 2541–2553. DOI: 10.2527/1996.74102541x.

Chang, Jonathan et al. (2019). "An r package and online resource for macroevolutionary studies using the ray-finned fish tree of life". In: *Methods in Ecology and Evolution* 10, pp. 1118–1124. DOI: 10.1111/2041-210X.13182.

Chung, Ming Tsung et al. (2019). "Field metabolic rates of teleost fishes are recorded in otolith carbonate". In: *Communications Biology* 2, p. 24. DOI: 10.1038/s42003-018-0266-5.

Cinner, Joshua E. et al. (2020). "Meeting fisheries, ecosystem function, and biodiversity goals in a human-dominated world". In: *Science* 368.6488, pp. 307–311. DOI: 10.1126/science.aax9412.

Clarke, Andrew and Nadine M. Johnston (1999). "Scaling of metabolic rate with body mass and temperature in teleost fish". In: *Journal of Animal Ecology* 68.5, pp. 893–905. DOI: 10.1046/j.1365-2656.1999.00337.x.

Cooper, Stancil S. (1941). "The mixed indicator Bromocresol Green-Methyl Red for carbonates in water". In: *Industrial and Engineering Chemistry - Analytical Edition* 13.7, pp. 466–470. DOI: 10.1021/i560095a011.

Eddy, Tyler D. et al. (2021). "Global decline in capacity of coral reefs to provide ecosystem services". In: *One Earth* 4.9, pp. 1278–1285. DOI: 10.1016/j.oneear.2021.08.016.

Fletcher, C. R. (1978). "Osmotic and ionic regulation in the cod (*Gadus callarias* L.) - I. Water Balance". In: *Journal of Comparative Physiology* 124, pp. 149–155. DOI: 10.1007/BF00689176.

Foran, Elizabeth, Steve Weiner, and Maoz Fine (2013). "Biogenic fish-gut calcium carbonate is a stable amorphous phase in the gilt-head seabream, sparus aurata". In: *Scientific Reports* 3, p. 1700. DOI: 10.1038/srep01700.

Froese, Rainer and Daniel Pauly (2021). *FishBase*. version (04/2021). URL: www.fishbase.org.

Fukushi, Keisuke et al. (2011). "Monohydrocalcite: A promising remediation material for hazardous anions". In: *Science and Technology of Advanced Materials* 12.6, p. 064702. DOI: 10.1088/1468-6996/12/6/064702.

Gaffey, S. J. and C. E. Bronnimann (1993). "Effects of bleaching on organic and mineral phases in biogenic carbonates". In: *Journal of Sedimentary Petrology* 63.4, pp. 752–754. DOI: 10.1306/d4267be0-2b26-11d7-8648000102c1865d.

Genz, J., J. R. Taylor, and M. Grosell (2008). "Effects of salinity on intestinal bicarbonate secretion and compensatory regulation of acid-base balance in *Opsanus beta*". In: *Journal of Experimental Biology* 211.14, pp. 2327–2335. DOI: 10.1242/jeb.016832.

Ghilardi, Mattia et al. (2021a). *Data and code of accepted version of manuscript: Phylogeny, body morphology, and trophic level shape intestinal traits in coral reef fishes (Ecology and Evolution)*. DOI: 10.5281/zenodo.5172790.

— (2021b). "Phylogeny, body morphology, and trophic level shape intestinal traits in coral reef fishes". In: *Ecology and Evolution* 11.19, pp. 13218–13231. DOI: 10.1002/ece3.8045.

Ghilardi, Mattia et al. (2023a). *Source Data for: Temperature, species identity and morphological traits predict carbonate excretion and mineralogy in tropical reef shes.* DOI: 10.5281/zenodo.7530455.

Gillooly, James F., Juan Pablo Gomez, and Evgeny V. Mavrodiev (2017). "A broad-scale comparison of aerobic activity levels in vertebrates: Endotherms versus ectotherms". In: *Proceedings of the Royal Society B: Biological Sciences* 284, p. 20162328. DOI: 10.1098/rspb.2016.2328.

Gingerich, Andrew J., David P. Philipp, and Cory D. Suski (2010). "Effects of nutritional status on metabolic rate, exercise and recovery in a freshwater fish." In: *Journal of comparative physiology. B, Biochemical, systemic, and environmental physiology* 180.3, pp. 371–384. DOI: 10.1007/s00360-009-0419-4.

Grosell, Martin (2019). "CO2 and calcification processes in fish". In: *Fish Physiology*. Ed. by Martin Grosell et al. 1st ed. Vol. 37. Elsevier Inc., pp. 133–159. DOI: 10.1016/bs.fp.2019.07.002.

Grosell, Martin et al. (2009). "The involvement of H+-ATPase and carbonic anhydrase in intestinal HCO3- secretion in seawater-acclimated rainbow trout". In: *Journal of Experimental Biology* 212.12, pp. 1940–1948. DOI: 10.1242/jeb.026856.

Hadfield, J. D. and S. Nakagawa (2010). "General quantitative genetic methods for comparative biology: Phylogenies, taxonomies and multi-trait models for continuous and categorical characters". In: *Journal of Evolutionary Biology* 23.3, pp. 494–508. DOI: 10.1111/j.1420-9101.2009.01915.x.

Heuer, Rachael M. et al. (2016). "Changes to intestinal transport physiology and carbonate production at various CO2 levels in a marine teleost, the Gulf Toadfish (*Opsanus beta*)". In: *Physiological and Biochemical Zoology* 89.5, pp. 402–416. DOI: 10.1086/688235.

Hickman, C. P. (1968). "Ingestion, intestinal absorption, and elimination of seawater and salts in the southern flounder, *Paralichthys lethostigma*." In: *Canadian journal of zoology* 46.3, pp. 457–466. DOI: 10.1139/z68-063.

Hicks, Christina C. et al. (2021). "Secure local aquatic food systems in the face of declining coral reefs". In: *One Earth* 4.9, pp. 1214–1216. DOI: 10.1016/j.oneear.2021.08.023.

Jennings, Simon and Rod W. Wilson (2009). "Fishing impacts on the marine inorganic carbon cycle". In: *Journal of Applied Ecology* 46.5, pp. 976–982. DOI: 10.1111/j.1365-2664.2009.01682.x.

Karachle, Paraskevi K and Konstantinos I Stergiou (2010b). "Intestine morphometrics of fishes: a compilation and analysis of bibliographic data". In: *Acta Ichthyologica et Piscatoria* 40.1, pp. 45–54. DOI: 10.3750/AIP2010.40.1.06.

Keith, David A. et al. (2022). "A function-based typology for Earth's ecosystems". In: *Nature* 610, pp. 513–518. DOI: 10.1038/s41586-022-05318-4.

Kembel, Steven W. et al. (2010). "Picante: R tools for integrating phylogenies and ecology". In: *Bioinformatics* 26.11, pp. 1463–1464. DOI: 10.1093/bioinformatics/btq166.

Kerr, S. R. (1982). "Estimating the energy budgets of actively predatory fishes". In: *Canadian Journal of Fisheries and Aquatic Sciences* 39.3, pp. 371–379.

Killen, Shaun S., David Atkinson, and Douglas S. Glazier (2010). "The intraspecific scaling of metabolic rate with body mass in fishes depends on lifestyle and temperature". In: *Ecology Letters* 13.2, pp. 184–193. DOI: 10.1111/j.1461-0248.2009.01415.x.

Killen, Shaun S. et al. (2016). "Ecological influences and morphological correlates of resting and maximal metabolic rates across teleost fish species". In: *American Naturalist* 187.5, pp. 592–606. DOI: 10.1086/685893.

Klaas, Christine and David E. Archer (2002). "Association of sinking organic matter with various types of mineral ballast in the deep sea: Implications for the rain ratio". In: *Global Biogeochemical Cycles* 16.4, p. 1116. DOI: 10.1029/2001gb001765.

Knight, Nicole S., Frédéric Guichard, and Andrew H. Altieri (2021). "A global meta-analysis of temperature effects on marine fishes' digestion across trophic groups". In: *Global Ecology and Biogeography* 30.4, pp. 795–810. DOI: 10.1111/geb.13262.

Kulbicki, Michel et al. (2013). "Global biogeography of reef fishes: A hierarchical quantitative delineation of regions". In: *PLoS ONE* 8.12, e81847. DOI: 10.1371/journal.pone.0081847.

Lassuy, Dennis R (1984). "Diet, intestinal morphology, and nitrogen assimilation efficiency in the damselfish, *Stegastes lividus*, in Guam". In: *Environmental Biology of Fishes* 10.3, pp. 183–193. DOI: 10.1007/BF00001125.

Le Mézo, Priscilla et al. (2022). "Global nutrient cycling by commercially targeted marine fish". In: *Biogeosciences* 19, pp. 2537–2555. DOI: /10.5194/bg-19-2537-2022.

Mariani, Gaël et al. (2020). "Let more big fish sink: Fisheries prevent blue carbon sequestration-half in unprofitable areas". In: *Science Advances* 6.44, pp. 1–9. DOI: `10.1126/sciadv.abb4848`.

Martin, Angela Helen et al. (2021). "Integral functions of marine vertebrates in the ocean carbon cycle and climate change mitigation". In: *One Earth* 4.5, pp. 680–693. DOI: `10.1016/j.oneear.2021.04.019`.

Mekuchi, Miyuki, Tamao Hatta, and Toyoji Kaneko (2010). "Mg-calcite, a carbonate mineral, constitutes Ca precipitates produced as a byproduct of osmoregulation in the intestine of seawater-acclimated Japanese eel *Anguilla japonica*". In: *Fisheries Science* 76.2, pp. 199–205. DOI: `10.1007/s12562-009-0199-5`.

Mellin, Camille et al. (2016a). "Humans and seasonal climate variability threaten large-bodied coral reef fish with small ranges". In: *Nature Communications* 7, p. 10491. DOI: `10.1038/ncomms10491`.

Mitparian, Tappadit et al. (2021). "Comprehensive morpho-histological observation of digestive system and gut content of wild-grunting toadfish, *Allenbatrachus grunniens* (Linnaeus, 1758)". In: *Maejo International Journal of Science and Technology* 15.3, pp. 222–241.

Morais, Renato A., Sean R. Connolly, and David R. Bellwood (2020b). "Human exploitation shapes productivitybiomass relationships on coral reefs". In: *Global Change Biology* 26.3, pp. 1295–1305. DOI: `10.1111/gcb.14941`.

Parravicini, V. et al. (2021). "Coral reef fishes reveal strong divergence in the prevalence of traits along the global diversity gradient". In: *Proceedings of the Royal Society B: Biological Sciences* 288, p. 20211712. DOI: `10.1098/rspb.2021.1712`.

Parravicini, Valeriano et al. (2020). "Delineating reef fish trophic guilds with global gut content data synthesis and phylogeny". In: *PLoS Biology* 18.12, e3000702. DOI: `10.1371/journal.pbio.3000702`.

Pauly, Daniel (1989). "Food consumption by tropical and temperate fish populations: some generalizations". In: *Journal of Fish Biology* 35, pp. 11–20. DOI: `10.1111/j.1095-8649.1989.tb03041.x`.

Perry, Chris T. et al. (2011). "Fish as major carbonate mud producers and missing components of the tropical carbonate factory". In: *Proceedings of the National Academy of Sciences* 108.10, pp. 3865–3869. DOI: `10.1073/pnas.1015895108`.

Plummer, L. Niel and Eurybiades Busenberg (1982). "The solubilities of calcite, aragonite and vaterite in CO2-H2O solutions between 0 and 90řC, and an evaluation of the aqueous model for the system CaCO3-CO2-H2O". In: *Geochimica et Cosmochimica Acta* 46.6, pp. 1011–1040. DOI: `10.1016/0016-7037(82)90056-4`.

R Core Team (2021). *R: a language and environment for statistical computing.*

Rabosky, Daniel L. et al. (2018). "An inverse latitudinal gradient in speciation rate for marine fishes". In: *Nature* 559.7714, pp. 392–395. DOI: `10.1038/s41586-018-0273-1`.

Rixen, Tim et al. (2019). "The ballast effect of lithogenic matter and its influences on the carbon fluxes in the Indian Ocean". In: *Biogeosciences* 16.2, pp. 485–503. DOI: `10.5194/bg-16-485-2019`.

Roberts, Callum M. et al. (2017). "Marine reserves can mitigate and promote adaptation to climate change". In: *Proceedings of the National Academy of Sciences* 114.24, pp. 6167–6175. DOI: `10.1073/pnas.1701262114`.

Robinson, James P.W. et al. (2017). "Fishing degrades size structure of coral reef fish communities". In: *Global Change Biology* 23.3, pp. 1009–1022. DOI: 10.1111/gcb.13482.

Rodriguez-Blanco, Juan Diego et al. (2014). "The role of Mg in the crystallization of monohydrocalcite". In: *Geochimica et Cosmochimica Acta* 127, pp. 204–220. DOI: 10.1016/j.gca.2013.11.034.

Saba, Grace K. et al. (2021). "Toward a better understanding of fish-based contribution to ocean carbon flux". In: *Limnology and Oceanography* 66.5, pp. 1639–1664. DOI: 10.1002/lno.11709.

Salter, Michael A., Chris T. Perry, and Abigail M. Smith (2019). "Calcium carbonate production by fish in temperate marine environments". In: *Limnology and Oceanography* 64.6, pp. 2755–2770. DOI: 10.1002/lno.11339.

Salter, Michael A., Christopher T. Perry, and Rod W. Wilson (2012). "Production of mud-grade carbonates by marine fish: Crystalline products and their sedimentary significance". In: *Sedimentology* 59.7, pp. 2172–2198. DOI: 10.1111/j.1365-3091.2012.01339.x.

Salter, Michael A. et al. (2017). "Phase heterogeneity in carbonate production by marine fish influences their roles in sediment generation and the inorganic carbon cycle". In: *Scientific Reports* 7.1, pp. 1–15. DOI: 10.1038/s41598-017-00787-4.

Salter, Michael A. et al. (2018). "Reef fish carbonate production assessments highlight regional variation in sedimentary significance". In: *Geology* 46.8, pp. 699–702. DOI: 10.1130/G45286.1.

Schauer, Kevin L. et al. (2018). "Interrogation of the Gulf toadfish intestinal proteome response to hypersalinity exposure provides insights into osmoregulatory mechanisms and regulation of carbonate mineral precipitation". In: *Comparative Biochemistry and Physiology - Part D: Genomics and Proteomics* 27.June, pp. 66–76. DOI: 10.1016/j.cbd.2018.06.004.

Schiettekatte, Nina M D et al. (2022b). "Combining stereo-video monitoring and physiological trials to estimate reef fish metabolic demands in the wild". In: *Ecology and Evolution* 12.7, e9084. DOI: 10.1002/ece3.9084.

Schiettekatte, Nina M.D. et al. (2020). "Nutrient limitation, bioenergetics and stoichiometry: A new model to predict elemental fluxes mediated by fishes". In: *Functional Ecology* 34.9, pp. 1857–1869. DOI: 10.1111/1365-2435.13618.

Shantz, Andrew A. et al. (2015). "Fish-derived nutrient hotspots shape coral reef benthic communities". In: *Ecological Applications* 25.8, pp. 2142–2152. DOI: 10.1890/14-2209.1.

Shehadeh, Ziad H. and Malcolm S. Gordon (1969). "The role of the intestine in salinity adaptation of the rainbow trout, *Salmo gairdneri*". In: *Comparative Biochemistry And Physiology* 30.3, pp. 397–418. DOI: 10.1016/0010-406X(69)92011-8.

Sleet, R. B. and L. J. Weber (1982). "The rate and manner of seawater ingestion by a marine teleost and corresponding seawater modification by the gut". In: *Comparative Biochemistry and Physiology – Part A: Physiology* 72.3, pp. 469–475. DOI: 10.1016/0300-9629(82)90110-4.

Smith, Homer W. (1930). "The absorption and excretion of water and salts by marine teleosts". In: *American Journal of Physiology* 93, pp. 480–505.

Smith, R. L. and A. C. Paulson (1975). "Carbonic anhydrase in some coral reef fishes: Adaptation to carbonate ingestion?" In: *Comparative Biochemistry and Physiology – Part A: Physiology* 50.1, pp. 131–134. DOI: 10.1016/S0010-406X(75)80214-3.

Spalding, Mark D. et al. (2007). "Marine ecoregions of the world: A bioregionalization of coastal and shelf areas". In: *BioScience* 57.7, pp. 573–583. DOI: 10.1641/B570707.

Stuart-Smith, Rick D. et al. (2022). "Tracking widespread climate-driven change on temperate and tropical reefs". In: *Current Biology* 32.19, 4128–4138.e3. DOI: 10.1016/j.cub.2022.07.067.

Sulpis, Olivier et al. (2021). "Calcium carbonate dissolution patterns in the ocean". In: *Nature Geoscience* 14.6, pp. 423–428. DOI: 10.1038/s41561-021-00743-y.

Svendsen, M. B.S., P. G. Bushnell, and J. F. Steffensen (2016). "Design and setup of intermittent-flow respirometry system for aquatic organisms". In: *Journal of Fish Biology* 88.1, pp. 26–50. DOI: 10.1111/jfb.12797.

Takei, Yoshio and Takehiro Tsukada (2001). "Ambient temperature regulates drinking and arterial pressure in eels". In: *Zoological Science* 18.7, pp. 963–967. DOI: 10.2108/zsj.18.963.

Tsuboi, Masahito et al. (2015). "Comparative support for the expensive tissue hypothesis: Big brains are correlated with smaller gut and greater parental investment in Lake Tanganyika cichlids". In: *Evolution* 69.1, pp. 190–200. DOI: 10.1111/evo.12556.

Tu, Chen Yi, Kuan Ting Chen, and Chih Hao Hsieh (2018). "Fishing and temperature effects on the size structure of exploited fish stocks". In: *Scientific Reports* 8.1, pp. 1–10. DOI: 10.1038/s41598-018-25403-x.

Van Dijk, P. L.M., G. Staaks, and I. Hardewig (2002). "The effect of fasting and refeeding on temperature preference, activity and growth of roach, *Rutilus rutilus*". In: *Oecologia* 130.4, pp. 496–504. DOI: 10.1007/s00442-001-0830-3.

Wagner, Catherine E et al. (2009). "Diet predicts intestine length in Lake Tanganyika's cichlid fishes". In: *Functional Ecology* 23, pp. 1122–1131. DOI: 10.1111/j.1365-2435.2009.01589.x.

Walsh, Patrick J. et al. (1991). "Carbonate deposits in marine fish intestines: A new source of biomineralization". In: *Limnology and Oceanography* 36.6, pp. 1227–1232. DOI: 10.4319/lo.1991.36.6.1227.

White, Craig R. and Michael R. Kearney (2014). "Metabolic scaling in animals: Methods, empirical results, and theoretical explanations". In: *Comprehensive Physiology* 4.1, pp. 231–256. DOI: 10.1002/cphy.c110049.

Whittamore, Jonathan M. (2012). "Osmoregulation and epithelial water transport: Lessons from the intestine of marine teleost fish". In: *Journal of Comparative Physiology B: Biochemical, Systemic, and Environmental Physiology* 182.1, pp. 1–39. DOI: 10.1007/s00360-011-0601-3.

Whittamore, Jonathan M., Christopher A. Cooper, and Rod W. Wilson (2010). "HCO3-secretion and CaCO3 precipitation play major roles in intestinal water absorption in marine teleost fish in vivo". In: *American Journal of Physiology - Regulatory Integrative and Comparative Physiology* 298.4, pp. 877–886. DOI: 10.1152/ajpregu.00545.2009.

Williams, Gareth J. and Nicholas A.J. Graham (2019). "Rethinking coral reef functional futures". In: *Functional Ecology* 33.6, pp. 942–947. DOI: 10.1111/1365-2435.13374.

Wilson, Rod W. and Martin Grosell (2003). "Intestinal bicarbonate secretion in marine teleost fish - Source of bicarbonate, pH sensitivity, and consequences for whole animal acid-base and calcium homeostasis". In: *Biochimica et Biophysica Acta - Biomembranes* 1618.2, pp. 163–174. DOI: 10.1016/j.bbamem.2003.09.014.

Wilson, Rod W., Jonathan M. Wilson, and Martin Grosell (2002). "Intestinal bicarbonate secretion by marine teleost fish-why and how?" In: *Biochimica et Biophysica Acta* 1566, pp. 182–193. DOI: `10.1016/s0005-2736(02)00600-4`.

Wilson, Rod W. et al. (1996). "Intestinal base excretion in the seawater-adapted rainbow trout: a role in acid-base balance?" In: *The Journal of experimental biology* 199.Pt 10, pp. 2331–43. DOI: `10.1242/jeb.199.10.2331`.

Wilson, Rod W. et al. (2009). "Contribution of fish to the marine inorganic carbon cycle". In: *Science* 323.January, pp. 359–362. DOI: `10.1126/science.1157972`.

Woodhead, Anna J. et al. (2019). "Coral reef ecosystem services in the Anthropocene". In: *Functional Ecology* 33.6, pp. 1023–1034. DOI: `10.1111/1365-2435.13331`.

Woosley, Ryan J., Frank J. Millero, and Martin Grosell (2012). "The solubility of fish-produced high magnesium calcite in seawater". In: *Journal of Geophysical Research: Oceans* 117.4, pp. 1–5. DOI: `10.1029/2011JC007599`.

Zhang, Zhuona et al. (2012). "Transformation of amorphous calcium carbonate into aragonite". In: *Journal of Crystal Growth* 343.1, pp. 62–67. DOI: `10.1016/j.jcrysgro.2012.01.025`.

Supplementary information

Supplementary Methods

Predicting relative intestinal length

Using the largest available dataset of intestinal length of reef fishes (Ghilardi et al. 2021a), we fitted a Bayesian phylogenetic multilevel linear model to predict fish intestinal length according to individual standard length (SL) and species-level trophic level (TL) and body elongation (EL), both obtained from FishBase (Froese and Pauly 2021) using the R package *rfishbase* (Boettiger et al. 2012). We extracted the phylogeny from the Fish Tree of Life (Rabosky et al. 2018) using the R package *fishtree* (Chang et al. 2019) and converted into a phylogenetic relatedness matrix (Hadfield and Nakagawa 2010). We modelled the intestinal length of the ith individual in the jth species (y_{ij}) following a Student-t distribution:

$$y_{ij} \sim \mathrm{t}(\nu, \mu_{ij}, \sigma)$$
$$\sigma \sim \mathrm{t}(3, 0, 2.5) \tag{S2.1}$$
$$\nu \sim \Gamma(2, 0.1)$$

with degrees of freedom ν, scale σ, and observation specific locations μ_{ij} defined as

$$\ln(\mu_{ij}) = \beta_{0j} + \beta_1 \ln(\mathrm{SL})_{ij} + \beta_2 (\mathrm{TL})_j + \beta_3 \ln(\mathrm{EL})_j$$
$$\beta_{0j} = \gamma_0 + \gamma_{0\mathrm{phy}}$$
$$\gamma_{0\mathrm{phy}} \sim \mathrm{N}(0, \tau) \tag{S2.2}$$
$$\gamma_0 \sim \mathrm{N}(0, 10)$$
$$\beta_{1:3}, \tau \sim \mathrm{N}(0, 5)$$

where γ_0 is the average model intercept, $\gamma_{0\mathrm{phy}}$ is the random variation in γ_0 based on phylogenetic relatedness, and $\beta_{1:3}$ are the regression coefficients of the fixed effects. We ran the model for 4 chains, each with 4,000 iterations and a warm-up of 1,000 iterations using the R package *brms* Bürkner (2017).

Then, we performed a cross-validation to validate the extrapolation of intestinal length to unobserved species (i.e., species not used to train the model). No direct method to make predictions for unobserved taxa from a phylogenetic linear model

(while accounting for phylogenetic relatedness) exists yet. Thus, in order to predict intestinal length for these species we followed a recent approach used to predict fish trophic guilds from a multinomial phylogenetic model (Parravicini et al. 2020). We extracted posterior draws of the phylogenetic effect ($\gamma_{0\text{phy}}$) of all species in the model and used them to estimate the phylogenetic effect of unobserved species using ancestral state reconstruction with the function *phyEstimate()* in the R package *picante* (Kembel et al. 2010). This estimation was repeated 2,000 times, each time using a different draw and randomly sampling one of 100 synthetic stochastically resolved phylogenies retrieved from the Fish Tree of Life, where species without genetic information are placed using stochastic polytomy resolution (Rabosky et al. 2018). Then, we computed the intestinal length by combining, for each draw, the model intercept and slopes of the fixed effects with the predicted phylogenetic effect according to Equation (S2.2). For the cross-validation we used the whole training dataset (including 1,208 individuals representing 142 species and 31 families) and repeated the extrapolation approach 142 times, each time leaving out 1 species (thus simulating an unobserved species) and predicting the intestinal length for all individuals of that species. Finally, the average predictions were compared to the measured intestinal length to assess model accuracy. We observed a strong relationship between observed and predicted intestinal length ($R^2 = 0.81$ for a regression of slope 1 and intercept -0.16; Supplementary Fig. 2.16).

Therefore, using this model and the extrapolation procedure described above we predicted the intestinal length of all species in the carbonate dataset. Predictions were performed at the species level (not at the individual level) using a common SL for all species. The relative intestinal length (RIL) was then computed by dividing the average prediction of each species by the SL used. This procedure was necessary in order to use both RIL and body mass as potential predictors of carbonate excretion and composition, since intestinal length and body mass are strongly correlated. Since our model (Equation (S2.2)) does not include species-level variation on the coefficient of SL, the predicted RIL is not influenced by the SL used in the computation.

For one individual, which was identified at the genus level (*Haemulon* sp.), we predicted a genus-average RIL. First, we retrieved the genus-average TL and EL from FishBase (Froese and Pauly 2021). These were then used to predict, at a fixed SL, the intestinal length of all species in the genus having genetic information in the Fish Tree of Life. Thus, each of the 2,000 posterior draws was averaged across species to obtain a full posterior distribution for the intestinal length of our unidentified species. Finally, the mean RIL was computed. This procedure was first validated using 200 randomly chosen observations of the training dataset. For each observation the species name was modified to simulate individuals identified at the genus level (the sample included 51 different genera). The intestinal lengths were then predicted and compared to the observed measurements, showing a strong relationship ($R^2 = 0.84$ for a regression of slope 1.1 and intercept -0.44; Supplementary Fig. 2.17).

Supplementary Figures
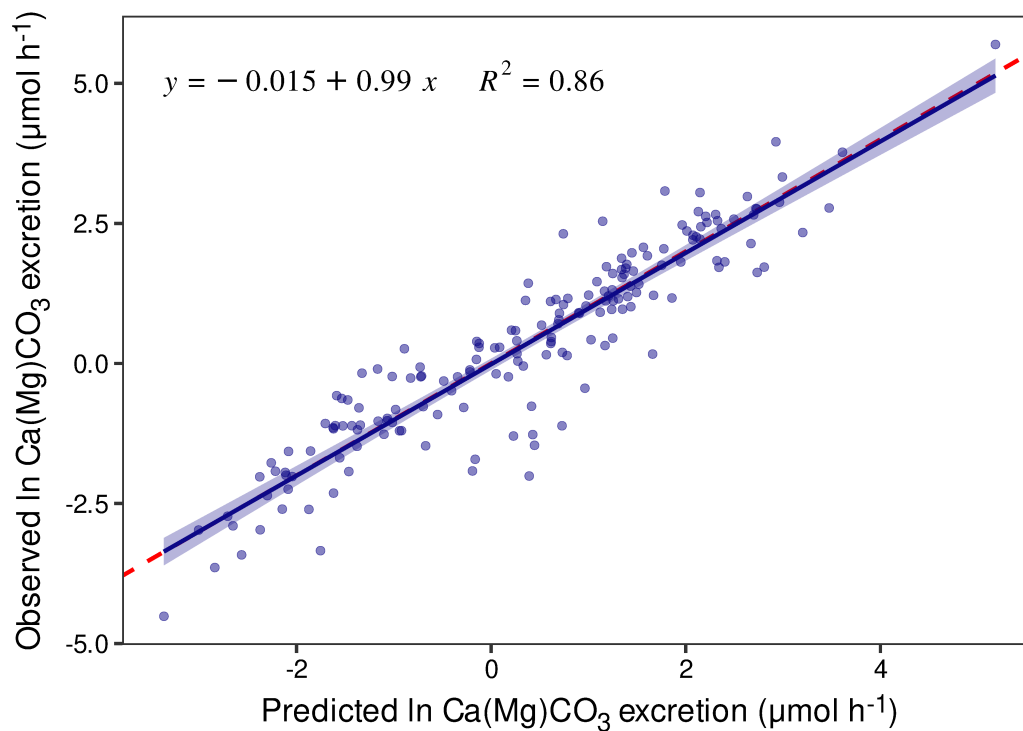
Figure 2.7: Observed vs predicted total carbonate excretion rates. The solid line and ribbon show the mean estimate and 95% confidence interval, respectively, of a linear regression, whose equation and goodness of fit (R^2) are shown in the upper left of the panel. Dots represent raw data ($n = 175$). The dashed, red line represents the identity line (y = x).
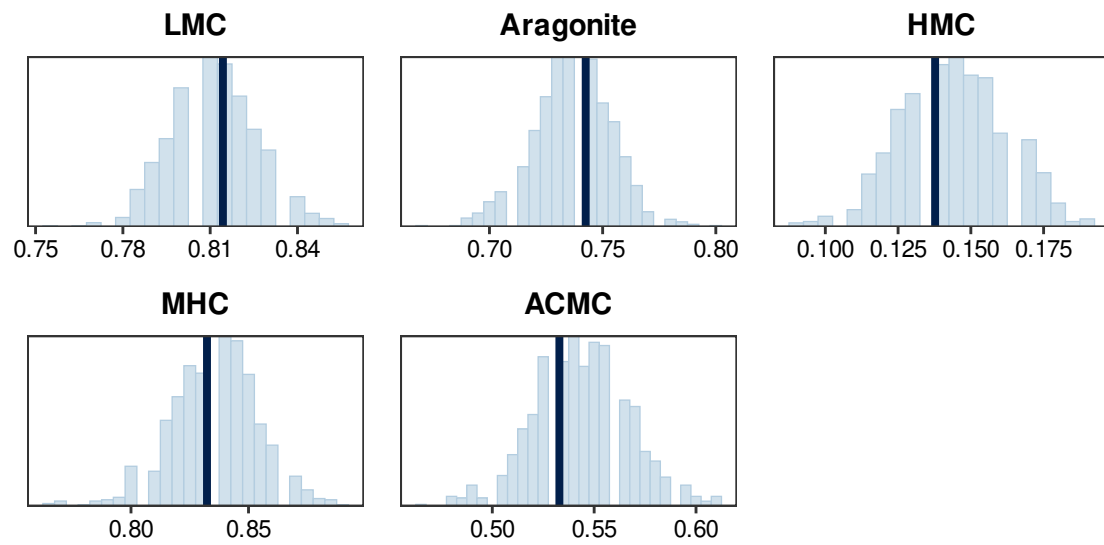
Figure 2.8: Posterior predictive check of the proportion of zeros in the excretion rate of five carbonate polymorphs produced by reef fishes. Histograms represent the distribution of the proportion of zeroes in 1000 random draws of a Bayesian multivariate hurdle-lognormal model. Black lines depict the observed proportion of zeroes in the data. LMC, low-magnesium calcite; HMC, high-magnesium calcite; MHC, monohydrocalcite; ACMC, amorphous calcium magnesium carbonate.
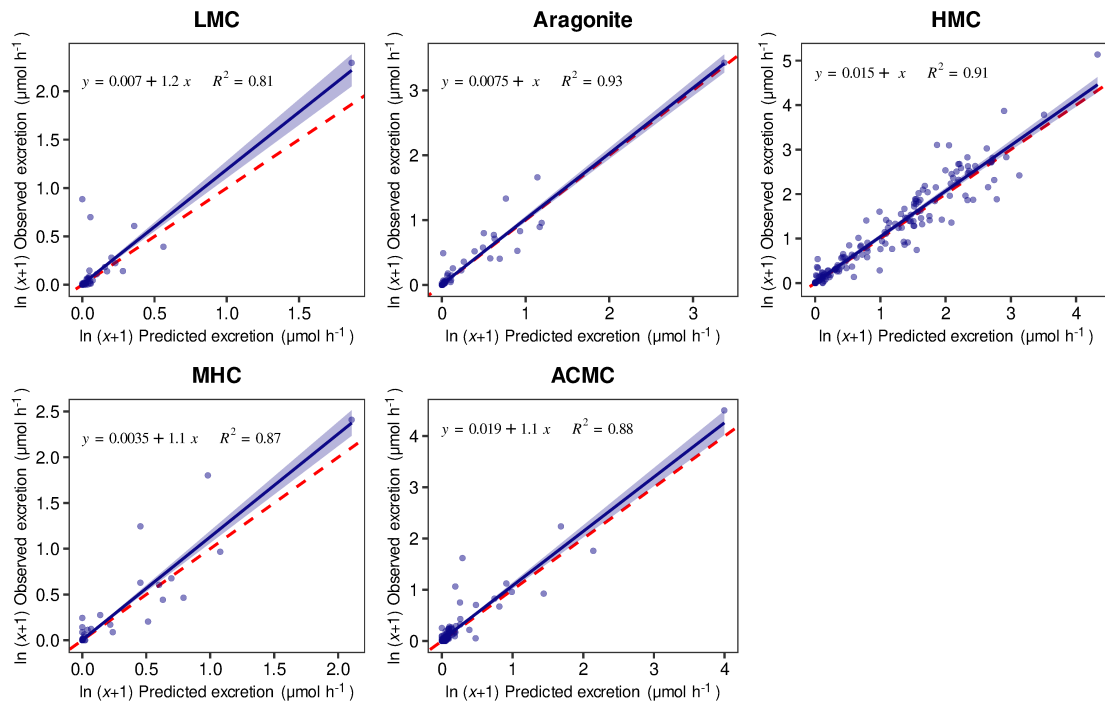
Figure 2.9: Observed vs predicted excretion rates for five carbonate polymorphs produced by reef fishes. Solid lines and ribbons show the mean estimates and 95% confidence intervals, respectively, of linear regressions, whose equations and goodness of fit (R^2) are shown in the upper left of the panels. Dots represent raw data ($n = 175$). Dashed, red lines represent the identity lines (y = x). LMC, low-magnesium calcite; HMC, high-magnesium calcite; MHC, monohydrocalcite; ACMC, amorphous calcium magnesium carbonate.
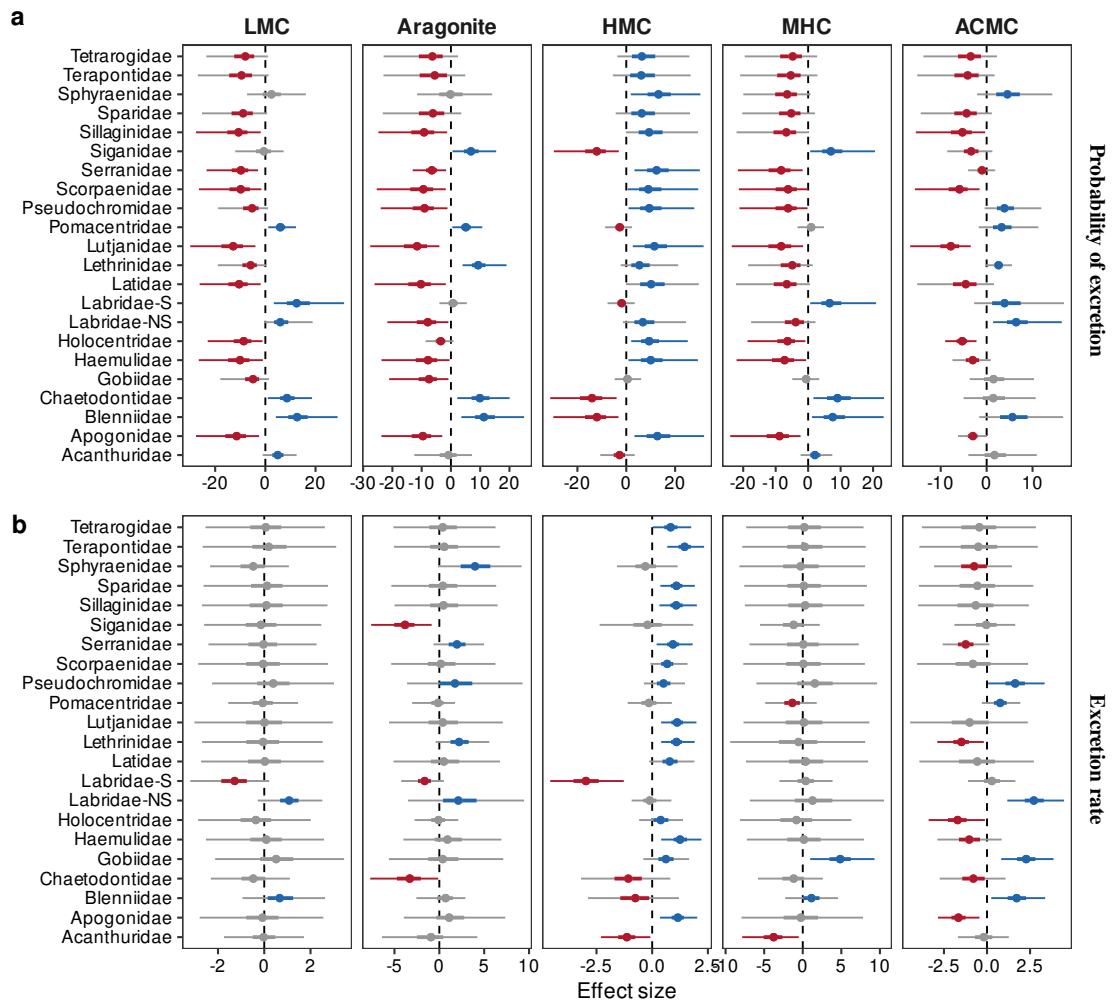
Figure 2.10: (**a**) Family-specific effects on the probability of fish excreting each of five different carbonate polymorphs. (**b**) Family-specific effects on the excretion rate of five different carbonate polymorphs. Estimates are medians (circles), 50% credible intervals (CIs; thick lines) and 95% CIs (thin lines) derived from 6,000 posterior draws of a Bayesian multivariate hurdle-lognormal model. Coloured intervals indicate positive (blue) or negative (red) effects, indicating that more than 75% (if 50% CIs) or 97.5% (if 95% CIs) of the posterior density was either above or below the average model estimate, whereas grey intervals indicate that they overlap the average estimate. LMC, low-magnesium calcite; HMC, high-magnesium calcite; MHC, monohydrocalcite; ACMC, amorphous calcium magnesium carbonate; Labridae-S, scarine Labridae; Labridae-NS, non-scarine Labridae.
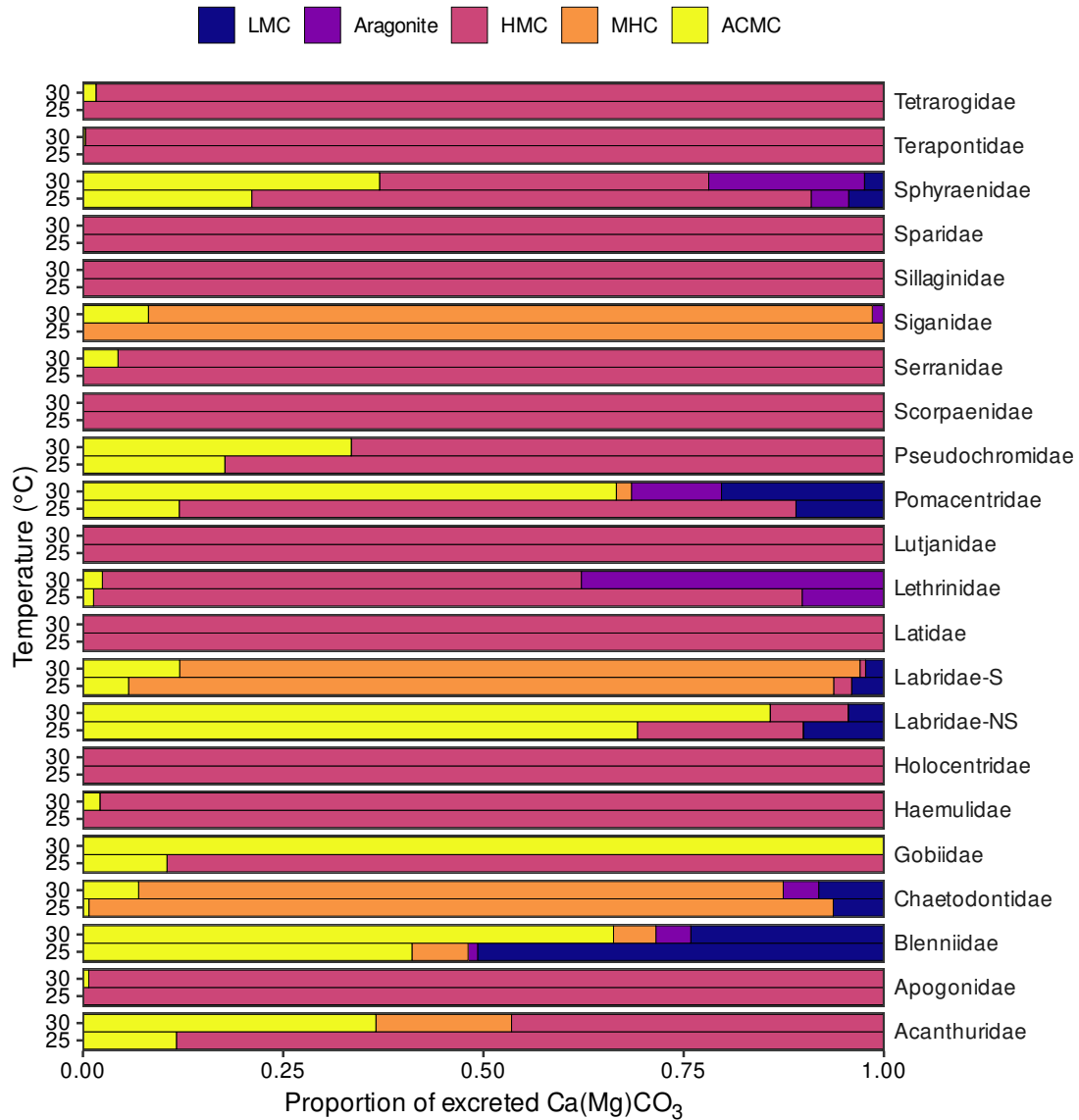
Figure 2.11: Predicted average mineralogical composition of carbonates excreted by 22 fish families at two temperature levels from a Bayesian multivariate hurdle-lognormal model. Predictions are based on average family-level traits for species with genetic information in the Fish Tree of Life (Rabosky et al. 2018). For each family the average biomass of an adult individual of all species was used (considering 1/2 of a species maximum length as representative of an adult individual). LMC, low-magnesium calcite; HMC, high-magnesium calcite; MHC, monohydrocalcite; ACMC, amorphous calcium magnesium carbonate; Labridae-S, scarine Labridae; Labridae-NS, non-scarine Labridae.
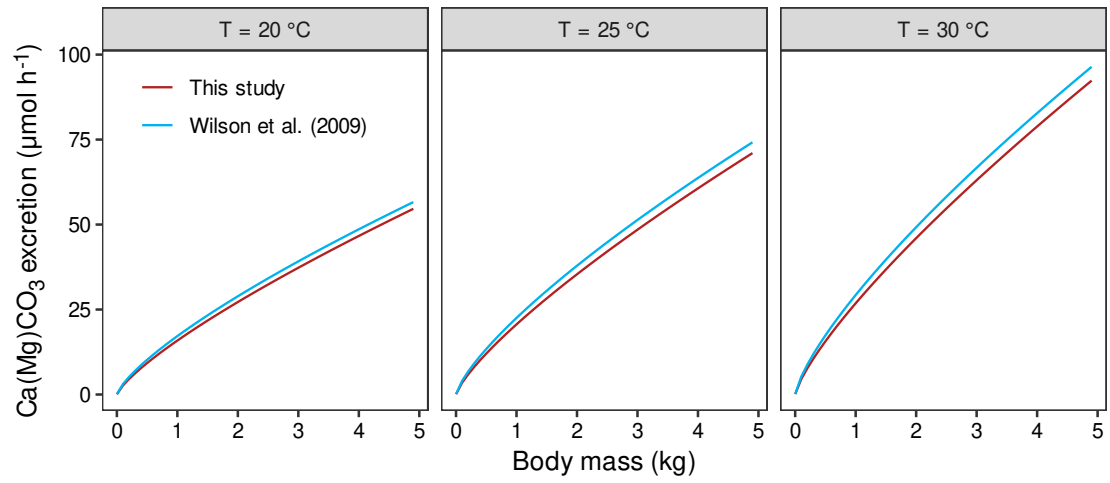
Figure 2.12: Comparison of fish carbonate excretion rate predicted by the model presented in this study and that used by Wilson et al. (2009) at three levels of temperature (T). Estimates of this study are average predictions, thus do not account for the effect of family, for a caudal fin aspect ratio of 1.5 and relative intestinal length of 0.5. Estimates of "Wilson's model" are predictions obtained by setting the constants ρ and α to 1.
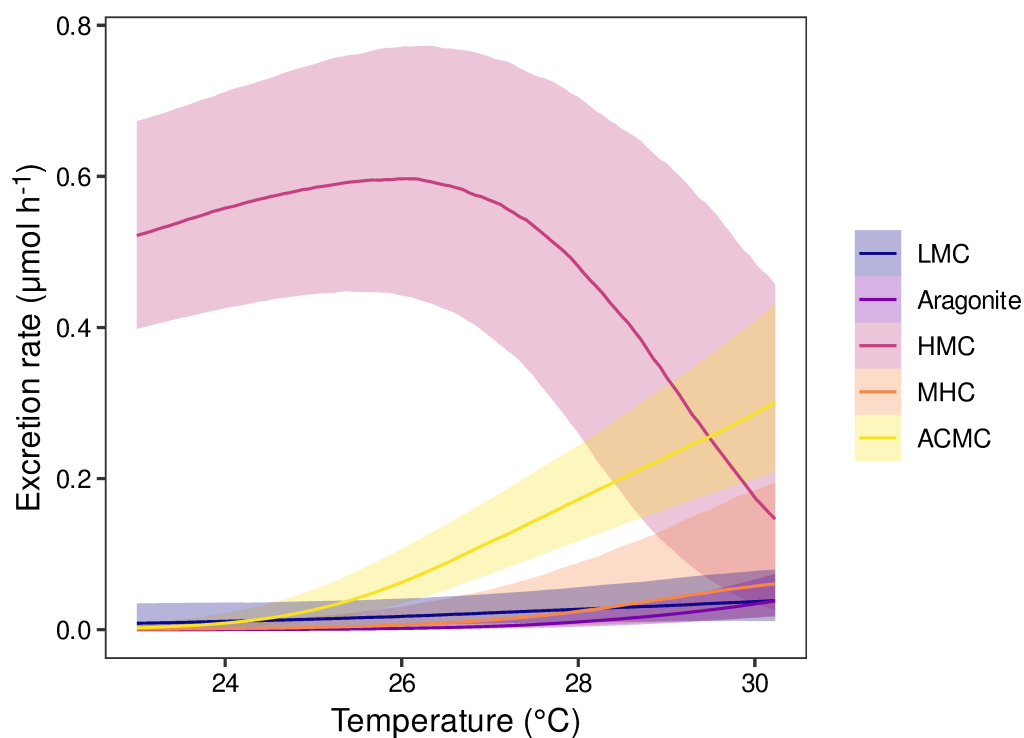
Figure 2.13: Marginal effect of temperature on the excretion rate of five different carbonate polymorphs after controlling for the remaining fixed and group-level effects of a Bayesian multivariate hurdle-lognormal model by standardising the other predictors at their mean values. Coloured lines represent the median predicted fits and the ribbons show the 50% credible intervals around the estimate. LMC, low-magnesium calcite; HMC, high-magnesium calcite; MHC, monohydrocalcite; ACMC, amorphous calcium magnesium carbonate.
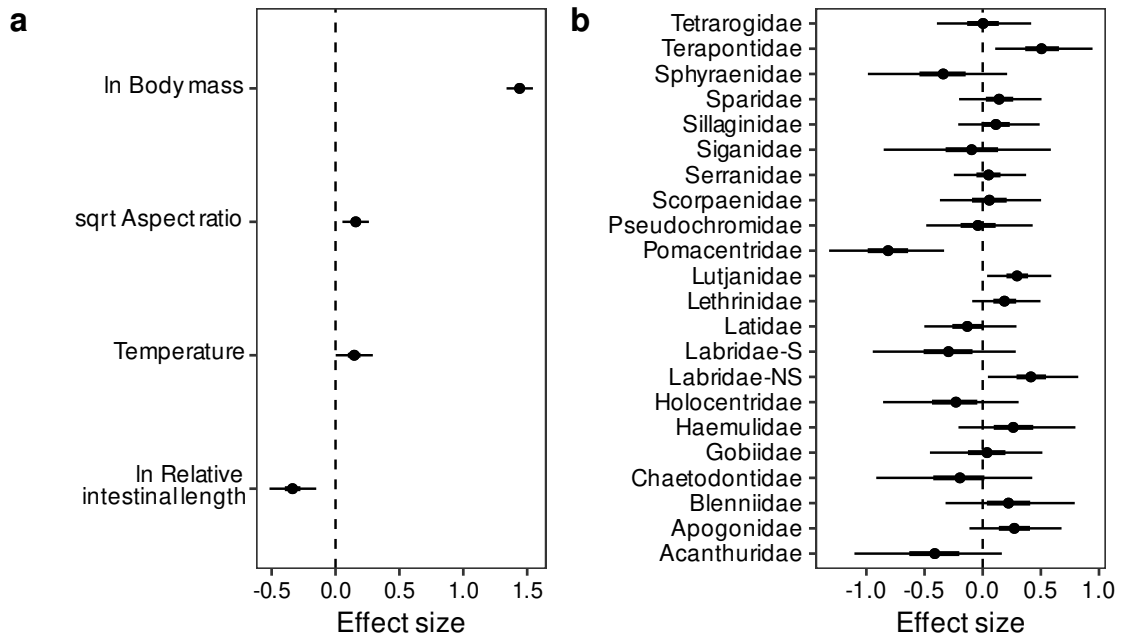
Figure 2.14: Results from a Bayesian multilevel distributional regression model fitted on the corrected data (see Carbonate excretion rates section in the Methods). (**a**) Effects of fish traits and temperature on carbonate excretion rate. (**b**) Family-specific effects on carbonate excretion rate. Estimates are medians (circles), 50% credible intervals (CIs; thick lines; some are too narrow to be seen) and 95% CIs (thin lines) derived from 12,000 posterior draws. All predictors were standardised (mean-centred and scaled by one standard deviation) prior to fitting the model to allow for the comparison of effect sizes. Labridae-S, scarine Labridae; Labridae-NS, non-scarine Labridae.
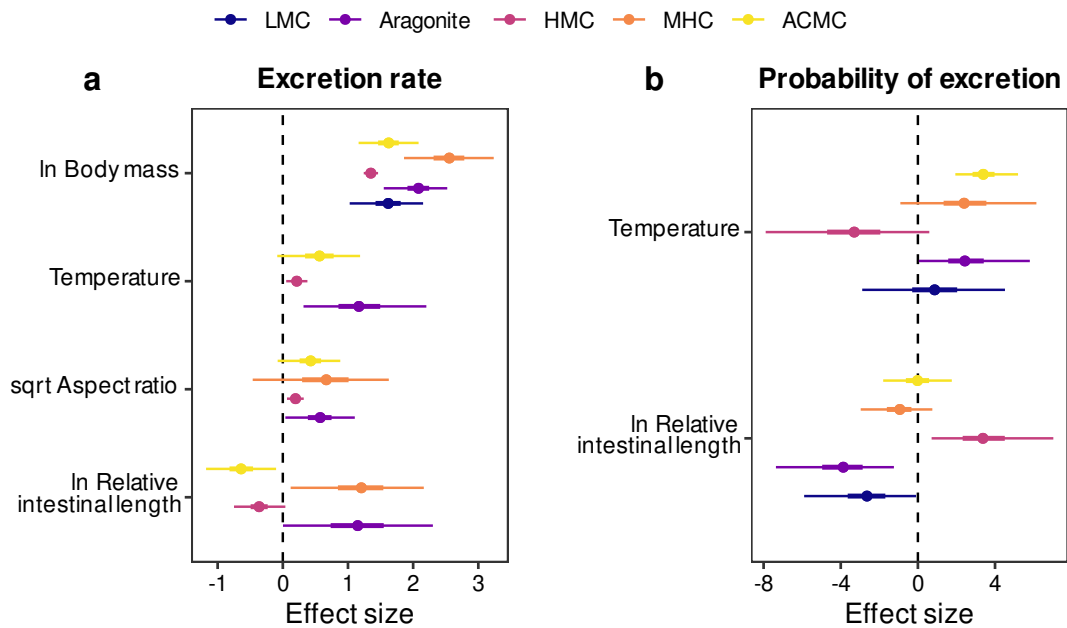
Figure 2.15: Results from a Bayesian multivariate hurdle-lognormal model fitted on the corrected data (see Carbonate excretion rates section in the Methods). (**a**) Effects of fish traits and temperature on the excretion rate of five different carbonate polymorphs. (**b**) Effects of species' relative intestinal length (RIL) and water temperature on the probability of excreting five different carbonate polymorphs. Estimates are medians (circles), 50% credible intervals (CIs; thick lines; some are too narrow to be seen) and 95% CIs (thin lines) derived from 6,000 posterior draws. All predictors were standardised (mean-centred and scaled by one standard deviation) prior to fitting the model to allow for the comparison of effect sizes. Missing estimates correspond to effects excluded from the final model (see the Statistical modelling section in the Methods). LMC, low-magnesium calcite; HMC, high-magnesium calcite; MHC, monohydrocalcite; ACMC, amorphous calcium magnesium carbonate.
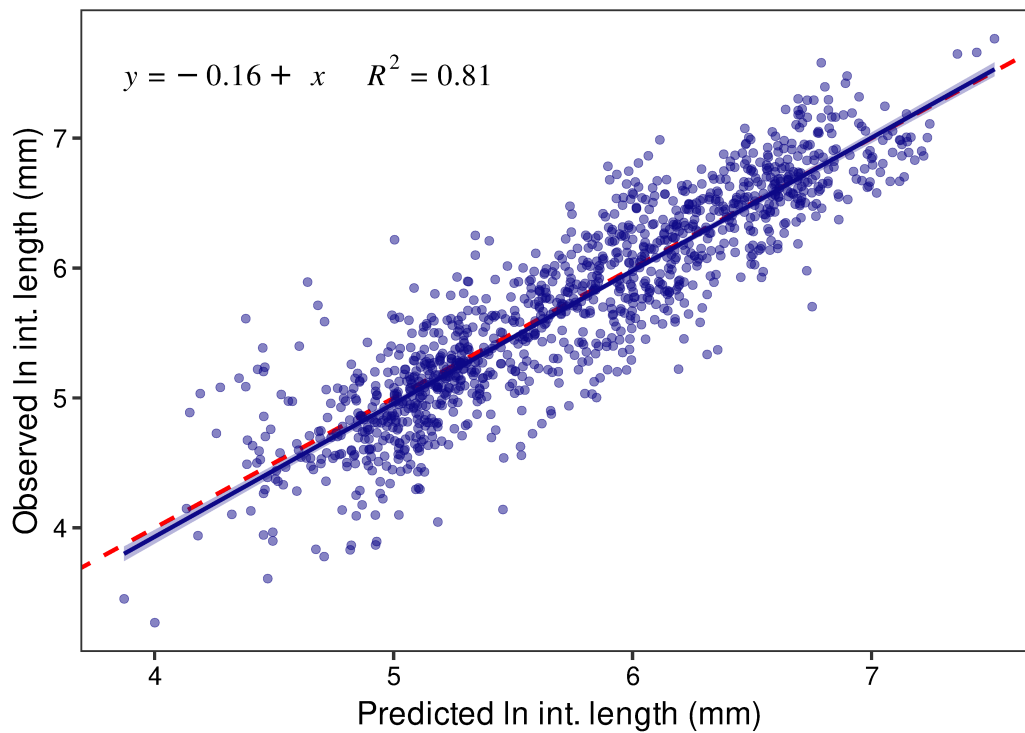
Figure 2.16: Relationship between observed and predicted intestinal length for 1,208 individuals (142 species and 31 families) showing predictive accuracy for unobserved species. The solid line and ribbon show the mean estimate and 95% confidence interval, respectively, of a linear regression, whose equation and goodness of fit (R^2) are shown in the upper left of the panel. Dots represent raw data ($n = 1,208$). The dashed, red line represents the identity line (y = x).
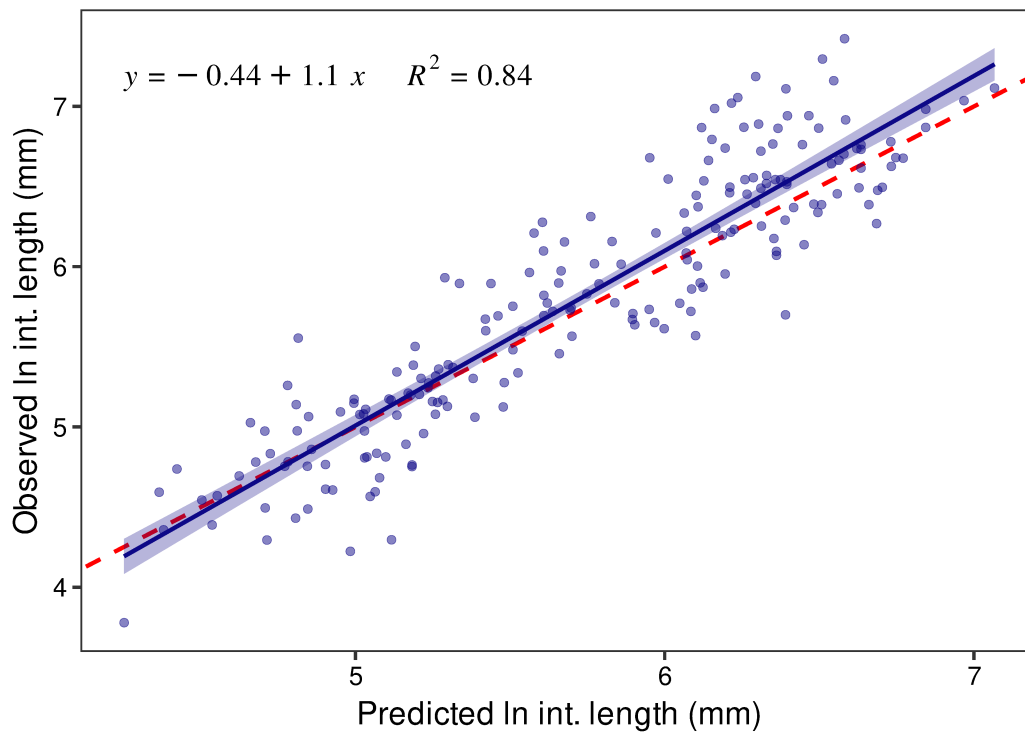
Figure 2.17: Relationship between observed intestinal length and genus-level predictions for 200 individuals of the training dataset for which species names were modified to simulate unidentified species. The solid line and ribbon show the mean estimate and 95% confidence interval, respectively, of a linear regression, whose equation and goodness of fit (R^2) are shown in the upper left of the panel. Dots represent raw data ($n = 200$). The dashed, red line represents the identity line (y = x).

Supplementary Tables

Table 2.1: The number of individuals and groups sampled per species. Included are the region, location, and family for each species. Labridae-S, scarine Labridae; Labridae-NS, non-scarine Labridae.

| Region	Location	Family	Species	# of groups	# of individuals
Australia	Heron Island	Caesionidae	*Caesio cuning*	1	1
Australia	Heron Island	Labridae-NS	*Halichoeres trimaculatus*	4	6
Australia	Heron Island	Labridae-NS	*Thalassoma lunare*	1	1
Australia	Heron Island	Lethrinidae	*Gymnocranius audleyi*	3	4
Australia	Heron Island	Lethrinidae	*Lethrinus miniatus*	9	14
Australia	Heron Island	Lutjanidae	*Lutjanus adetii*	2	3
Australia	Heron Island	Lutjanidae	*Lutjanus carponotatus*	1	1
Australia	Heron Island	Pinguipedidae	*Parapercis queenslandica*	2	2
Australia	Heron Island	Pseudochromidae	*Ogilbyina queenslandiae*	2	2
Australia	Heron Island	Scorpaenidae	*Dendrochirus zebra*	1	1
Australia	Heron Island	Scorpaenidae	*Scorpaenopsis diabolus*	1	1
Australia	Heron Island	Serranidae	*Epinephelus fasciatus*	5	5
Australia	Heron Island	Serranidae	*Epinephelus quoyanus*	1	1
Australia	Heron Island	Serranidae	*Plectropomus leopardus*	3	4
Australia	Heron Island	Sillaginidae	*Sillago sihama*	5	12
Australia	Moreton Bay	Apogonidae	*Ostorhinchus limenus*	1	1
Australia	Moreton Bay	Diodontidae	*Tragulichthys jaculiferus*	1	1
Australia	Moreton Bay	Haemulidae	*Plectorhinchus picus*	1	1
Australia	Moreton Bay	Latidae	*Lates calcarifer*	12	20
Australia	Moreton Bay	Lethrinidae	*Lethrinus genivittatus*	3	16
Australia	Moreton Bay	Lethrinidae	*Lethrinus nebulosus*	3	3
Australia	Moreton Bay	Lutjanidae	*Lutjanus russellii*	11	22
Australia	Moreton Bay	Sillaginidae	*Sillago maculata*	1	4
Australia	Moreton Bay	Sparidae	*Acanthopagrus australis*	4	6
Australia	Moreton Bay	Sparidae	*Pagrus auratus*	5	8
Australia	Moreton Bay	Sparidae	*Rhabdosargus sarba*	2	5
Australia	Moreton Bay	Sygnathidae	*Hippocampus whitei*	1	1
Australia	Moreton Bay	Terapontidae	*Helotes sexlineatus*	4	29
Australia	Moreton Bay	Tetrarogidae	*Centropogon australis*	4	5
Bahamas	Cape Eleuthera	Albulidae	*Albula vulpes*	1	5
Bahamas	Cape Eleuthera	Gerreidae	*Gerres cinereus*	1	2
Bahamas	Cape Eleuthera	Haemulidae	*Haemulon sp.*	1	1
Bahamas	Cape Eleuthera	Lutjanidae	*Lutjanus apodus*	5	26
Bahamas	Cape Eleuthera	Lutjanidae	*Ocyurus chrysurus*	4	25
Bahamas	Cape Eleuthera	Mugilidae	*Mugil sp.*	1	9
Bahamas	Cape Eleuthera	Scorpaenidae	*Pterois volitans*	3	6
Bahamas	Cape Eleuthera	Serranidae	*Cephalopholis cruentata*	3	11
Bahamas	Cape Eleuthera	Serranidae	*Epinephelus guttatus*	1	1
Bahamas	Cape Eleuthera	Sphyraenidae	*Sphyraena barracuda*	4	4
Palau	Koror	Acanthuridae	*Acanthurus nigrofuscus*	2	4
Palau	Koror	Acanthuridae	*Naso annulatus*	1	1
Palau	Koror	Acanthuridae	*Naso vlamingii*	1	1
Palau	Koror	Acanthuridae	*Zebrasoma scopas*	1	1
Palau	Koror	Acanthuridae	*Zebrasoma velifer*	1	1
Palau	Koror	Apogonidae	*Ostorhinchus novemfasciatus*	3	3
Palau	Koror	Apogonidae	*Pristiapogon exostigma*	1	1
Palau	Koror	Apogonidae	*Sphaeramia nematoptera*	1	3
Palau	Koror	Apogonidae	*Sphaeramia orbicularis*	3	9
Palau	Koror	Balistidae	*Rhinecanthus verrucosus*	2	2
Palau	Koror	Blenniidae	*Atrosalarias fuscus*	2	2
Palau	Koror	Blenniidae	*Salarias ceramensis*	3	3
Palau	Koror	Blenniidae	*Salarias fasciatus*	1	1
Palau	Koror	Chaetodontidae	*Chaetodon ephippium*	2	2
Palau	Koror	Chaetodontidae	*Chaetodon lunulatus*	1	1
Palau	Koror	Chaetodontidae	*Chaetodon oxycephalus*	2	2

Table 2.1: *(continued)*

Region	Location	Family	Species	# of groups	# of individuals
Palau	Koror	Gobiidae	*Amblygobius phalaena*	1	1
Palau	Koror	Gobiidae	*Amblygobius semicinctus*	3	4
Palau	Koror	Gobiidae	*Asterropteryx semipunctata*	1	5
Palau	Koror	Gobiidae	*Cryptocentrus cinctus*	1	1
Palau	Koror	Gobiidae	*Valenciennea longipinnis*	3	3
Palau	Koror	Haemulidae	*Plectorhinchus lineatus*	1	1
Palau	Koror	Holocentridae	*Myripristis adusta*	1	3
Palau	Koror	Holocentridae	*Myripristis violacea*	2	2
Palau	Koror	Holocentridae	*Sargocentron spiniferum*	2	2
Palau	Koror	Labridae-S	*Scarus dimidiatus*	2	2
Palau	Koror	Labridae-S	*Scarus globiceps*	1	1
Palau	Koror	Labridae-S	*Scarus scaber*	2	2
Palau	Koror	Lutjanidae	*Lutjanus gibbus*	1	1
Palau	Koror	Mullidae	*Parupeneus barberinus*	1	1
Palau	Koror	Muraenidae	*Gymnothorax javanicus*	1	1
Palau	Koror	Nemipteridae	*Scolopsis margaritifera*	1	1
Palau	Koror	Pomacanthidae	*Pygoplites diacanthus*	1	1
Palau	Koror	Pomacentridae	*Amblyglyphidodon curacao*	3	11
Palau	Koror	Pomacentridae	*Chromis atripectoralis*	3	16
Palau	Koror	Pomacentridae	*Dischistodus perspicillatus*	4	4
Palau	Koror	Pomacentridae	*Pomacentrus bankanensis*	1	1
Palau	Koror	Pseudochromidae	*Pseudochromis fuscus*	1	1
Palau	Koror	Pseudochromidae	*Pseudochromis marshallensis*	1	1
Palau	Koror	Serranidae	*Cephalopholis urodeta*	1	1
Palau	Koror	Serranidae	*Epinephelus merra*	2	2
Palau	Koror	Siganidae	*Siganus doliatus*	1	1
Palau	Koror	Siganidae	*Siganus puellus*	1	1
Palau	Koror	Siganidae	*Siganus punctatus*	1	1
Palau	Koror	Tetraodontidae	*Arothron nigropunctatus*	2	2
Palau	Koror	Zanclidae	*Zanclus cornutus*	1	1

Table 2.2: Comparison between single end point titration and double titration in the carbonate content measured.

Species	Sample ID	Carbonate polymorphs	Single titration (mmol)	Double titration (mmol)	Ratio (single/ double)
Lethrinus atkinsoni	EMP/B-P4	HMC, ARA, ACMC	0.065	0.057	1.141
Lethrinus atkinsoni	EMP/B-P3	HMC, ARA, ACMC	0.113	0.106	1.064
Lethrinus atkinsoni	EMP/B-P2	HMC, ARA, ACMC	0.086	0.079	1.085
Lethrinus atkinsoni	EMP/B-P1	HMC, ARA, ACMC	0.054	0.049	1.108
Cephalopholis cyanostigma	CM/A-P4	HMC	0.269	0.258	1.043
Cephalopholis cyanostigma	CM/A-P3	HMC	0.168	0.157	1.069
Cephalopholis cyanostigma	CM/A-P2	HMC	0.237	0.225	1.053
Cephalopholis cyanostigma	CM/A-P1	HMC	0.212	0.201	1.059
Lutjanus fulvus	SN/C-G-P4	HMC	0.097	0.089	1.091
Lutjanus fulvus	SN/C-G-P3	HMC	0.125	0.117	1.072
Lutjanus fulvus	SN/C-G-P2	HMC	0.164	0.154	1.066
Lutjanus fulvus	SN/C-G-P1	HMC	0.138	0.129	1.068

Abbreviations:

HMC, high-magnesium calcite; ARA, aragonite; ACMC, amorphous calcium magnesium carbonate.

Table 2.3: Leave-one-out (LOO) cross-validation results for 36 Bayesian regression models that examine the drivers of carbonate excretion rate. Each row represents one model, whose formula includes the fixed and random effects specified in the respective columns.

fixed	random	elpd_diff	se_diff	looic	se_looic
log(M) + log(RIL) + T + sqrt(AR)	family	0.00	0.00	485.11	36.03
log(M) + log(RIL) + T + sqrt(AR) + sqrt(ST)	family	-0.29	1.19	485.70	36.69
log(M) + log(RIL) + T	family	-1.43	2.43	487.96	35.15
log(M) + log(RIL) + T + sqrt(ST)	family	-1.99	2.64	489.09	35.89
log(M) + log(RIL) + sqrt(AR) + sqrt(ST)	family	-2.64	2.88	490.38	35.03
log(M) + log(RIL) + sqrt(AR)	family	-2.88	3.13	490.87	33.60
log(M) + log(RIL)	family	-3.14	3.93	491.38	33.36
log(M) + log(RIL) + sqrt(ST)	family	-3.35	3.79	491.82	34.65
log(M) + S + T + sqrt(AR)	family	-5.34	4.15	495.80	35.35
log(M) + S + T + sqrt(AR) + sqrt(ST)	family	-5.57	4.31	496.26	36.12
log(M) + S + sqrt(AR) + sqrt(ST)	family	-5.84	5.13	496.79	35.48
log(M) + S + sqrt(AR)	family	-6.01	5.09	497.14	34.09
log(M)	family	-6.62	5.09	498.34	33.74
log(M) + S + T	family	-7.06	4.97	499.24	34.43
log(M) + S	family	-7.27	5.59	499.65	33.59
log(M) + S + sqrt(ST)	family	-7.42	5.62	499.94	34.82
log(M) + S + T + sqrt(ST)	family	-7.84	5.09	500.79	35.18
log(M) + log(RIL) + sqrt(AR)	-	-17.50	10.06	520.11	33.78
log(M) + log(RIL)	-	-18.27	10.11	521.65	33.20
log(M) + log(RIL) + sqrt(AR) + sqrt(ST)	-	-18.44	9.94	521.99	35.14
log(M) + log(RIL) + sqrt(ST)	-	-19.53	10.01	524.16	33.92
log(M) + log(RIL) + T	-	-19.72	10.13	524.55	33.05
log(M) + log(RIL) + T + sqrt(AR)	-	-19.77	10.22	524.66	34.76
log(M) + S + sqrt(AR)	-	-20.30	10.77	525.71	34.40
log(M) + log(RIL) + T + sqrt(AR) + sqrt(ST)	-	-20.37	10.10	525.86	35.52
log(M) + S	-	-20.80	10.82	526.72	34.27
log(M) + log(RIL) + T + sqrt(ST)	-	-20.85	10.03	526.81	33.71
log(M) + S + sqrt(AR) + sqrt(ST)	-	-20.99	10.75	527.09	35.43
log(M) + S + T + sqrt(AR)	-	-21.78	10.77	528.66	34.62
log(M) + S + sqrt(ST)	-	-21.82	10.82	528.74	35.08
log(M) + S + T	-	-22.05	10.82	529.20	34.21
log(M) + S + T + sqrt(AR) + sqrt(ST)	-	-22.36	10.76	529.83	35.25
log(M) + S + T + sqrt(ST)	-	-22.92	10.84	530.95	34.79
log(M)	-	-28.73	11.90	542.58	36.04
Intercept only	family	-147.32	20.77	779.75	36.10
Intercept only	-	-242.17	21.93	969.45	37.56

Abbreviations:

M, body mass; S, salinity; T, temperature; AR, caudal fin aspect ratio; RIL, relative intestinal length; ST, total sampling period; elpd_diff, difference in expected log pointwise predictive density (ELPD) between each model and the model having the largest ELPD; se_diff, standard error of the difference in ELPD; looic, LOO information criterion; se_loo, LOO standard error.

Table 2.4: Leave-one-out (LOO) cross-validation results for two Bayesian multilevel regression models that examine the drivers of carbonate excretion rate. Each row represents one model, whose formula includes the fixed and random effects specified in the respective columns. The two models differ in that one also estimates the effect of the titration method on the scale parameter σ of the t-distribution (specified in the column "sigma"), while the other does not.

fixed	random	sigma	elpd_diff	se_diff	looic	se_looic
log(M) + log(RIL) + T + sqrt(AR)	family	method	0.00	0.00	451.27	36.70
log(M) + log(RIL) + T + sqrt(AR)	family	-	-16.92	7.61	485.11	36.03

Abbreviations:
M, body mass; RIL, relative intestinal length; T, temperature; AR, caudal fin aspect ratio; elpd_diff, difference in expected log pointwise predictive density (ELPD) between each model and the model having the largest ELPD; se_diff, standard error of the difference in ELPD; looic, LOO information criterion; se_loo, LOO standard error.

3

Global patterns and drivers of reef fish carbonate excretion and mineralogy

Mattia Ghilardi[1,2]*, Matthew McLean[3], Katie Cramer[4], Graham J. Edgar[5], Sebastian C. A. Ferse[1,2], Nicolas Loiseau[6], Valeriano Parravicini[7,8], Loïc Pellissier[9,10], Chris T. Perry[11], Tim Rixen[1], Michael A. Salter[12], Rick D. Stuart-Smith[5], Laure Velez[6], Conor Waldock[13,14], Christian Wild[2], Rod W. Wilson[12], David Mouillot[6,8], Sonia Bejarano[1]

1. Leibniz Centre for Tropical Marine Research (ZMT), FahrenheitstraSSe 6, 28359 Bremen, Germany

2. Department of Marine Ecology, Faculty of Biology and Chemistry, University of Bremen, Leobener StraSSe UFT, 28359 Bremen, Germany

3. Department of Biology and Marine Biology, University of North Carolina Wilmington, Wilmington, NC, USA

4. Global Institute of Sustainability and Innovation, Center for Biodiversity Outcomes, Arizona State University, Tempe, AZ, United States

5. Institute for Marine and Antarctic Studies, University of Tasmania, Hobart, TAS 7001, Australia

6. MARBEC, Univ Montpellier, CNRS, Ifremer, IRD, 34095 Montpellier, France

7. PSL Université Paris: EPHE-UPVD-CNRS, USR3278 CRIOBE, University of Perpignan, 66860 Perpignan, France

8. Institut Universitaire de France, Paris, France

9. Ecosystems and Landscape Evolution, Institute of Terrestrial Ecosystems, Department of Environmental Systems Science, ETH Züurich, 8092 Zürich, Switzerland

10. Unit of Land Change Science, Swiss Federal Research Institute for Forest, Snow and Landscape Research (WSL), 8903 Birmensdorf, Switzerland

11. Geography, University of Exeter, Exeter EX4 4RJ, UK

12. Biosciences, University of Exeter, Exeter EX4 4QD, UK

13. Division of Aquatic Ecology and Evolution, Institute of Ecology and Evolution, University of Bern, Switzerland

14. Department of Fish Ecology and Evolution, Eawag, Swiss Federal Institute of Aquatic Science and Technology, Switzerland

Correspondence: *M. Ghilardi (`mattia.ghilardi91@gmail.com`)

Abstract

Marine fish are important contributors to the inorganic carbon cycle. They excrete diverse carbonate minerals which can be buried within sediments or dissolve and release alkalinity in the water column. Yet, the geographical patterns and drivers underlying fish carbonate excretion and mineralogy remain largely unknown, limiting our understanding of how this may change with ongoing fishing and climate change. Here, we combine data on fish community structure and socio-economic and environmental variables available for 1,412 coral reef sites with carbonate production models to map global carbonate excretion and mineralogy and identify their drivers. We show that carbonate excretion varies primarily as a function of fish community structure and is strongly affected by human gravity (i.e., a proxy for human pressure). Patterns in carbonate mineralogy are primarily driven by sea surface temperature and secondarily by fish community structure. Furthermore, in all regions, excretion is dominated (>50%) by carbonates with high solubility (high-magnesium calcite and amorphous carbonate) and the proportion of the more soluble carbonates increases with temperature. These results have implications for predicting future changes in fish inorganic carbon cycling and how this could be sustained by targeted management measures.

3.1 Introduction

The marine carbon cycle exerts a major control on Earth's climate by regulating atmospheric CO_2 levels. The ocean is currently a sink for ~26% of global anthropogenic CO_2 emissions (Friedlingstein et al. 2022). Fish can influence the ocean's capacity to absorb CO_2 by storing carbon in their bodies and cycling organic and inorganic carbon (Lutz and Martin 2014; Martin et al. 2021; Saba et al. 2021). However, fish carbon cycling has been disrupted by fisheries in the last few decades (Mariani et al. 2020; Cavan and Hill 2021; Bianchi et al. 2021). In this context, understanding the role of fish in the carbon cycle is especially critical to predict how it will change in the future and potentially feedback on atmospheric CO_2 and

climate. Being the dominant vertebrates in the ocean, fish contribute substantially to organic carbon flux through passive (sinking of carcasses and faecal material) and active (diel vertical migration) vertical transport, horizontal transport (migrations or daily movements), and by fuelling primary production (Mariani et al. 2020; Saba et al. 2021; Saba and Steinberg 2012; Hernández-León et al. 2019). Marine bony fish (teleosts) also significantly influence inorganic carbon cycling by continuously excreting intestinally precipitated carbonates as a by-product of osmoregulation (Wilson et al. 2009; Perry et al. 2011; Salter et al. 2017; Salter et al. 2018). While the global relevance of this process is clear (Wilson et al. 2009), little is known about the factors that govern the geographical variability of fish-mediated carbonate production and how ongoing fishing and climate change will affect the role of fish in the inorganic carbon cycle.

Most marine calcifiers produce aragonite (e.g., corals, pteropods) and/or calcite with varying magnesium content (e.g., coralline algae, echinoderms, foraminifera) (Long et al. 2014). Fish produce and excrete a variety of carbonate polymorphs spanning several orders of magnitude of expected solubility (Woosley et al. 2012; Plummer and Busenberg 1982; Breevi and Nielsen 1989; Fukushi et al. 2011). These include stable low-magnesium calcite (LMC; <4 mol% $MgCO_3$) and aragonite, less stable high-magnesium calcite (HMC; >4 mol% $MgCO_3$, but typically >20%), metastable monohydrocalcite (MHC), and highly unstable amorphous calcium magnesium carbonate (ACMC) (Perry et al. 2011; Foran et al. 2013; Salter et al. 2017; Salter et al. 2018; Salter et al. 2019; Ghilardi et al. 2023b). This suggests that fish carbonates are generally more soluble than many other marine carbonates and most will rapidly dissolve while sinking (Wilson et al. 2009; Salter et al. 2017; Salter et al. 2018; Salter et al. 2019), potentially providing an important source of alkalinity in the upper water column (Wilson et al. 2009; Sulpis et al. 2021). Yet, they can also deposit and contribute substantially to fine-grained carbonate sediments at least in shallow tropical environments (Perry et al. 2011). Carbonate mineralogy is highly conserved at the family level (Salter et al. 2018; Salter et al. 2019; Ghilardi et al. 2023b) leading to variability across regions as a function of

fish community composition (Salter et al. 2018), with implications for inorganic carbon cycling. Yet, the geographical patterns in the mineralogical composition of fish carbonates and the underlying drivers remain unknown, but are critical to better understand fish contribution to inorganic carbon flux.

This contribution is expected to be higher in warm regions with high fish biomass (Wilson et al. 2009) and to be influenced by habitat and fish species composition (Salter et al. 2017; Salter et al. 2018). Recent evidence suggests that fish trophic structure may also play an important role in shaping patterns of carbonate excretion and mineralogy, with fish at higher trophic levels excreting more carbonate and different polymorphs than fish at lower trophic levels (Ghilardi et al. 2023b). A relatively high excretion of primarily HMC is thus expected in areas hosting highest proportions of carnivores, such as coral reefs isolated from Quaternary refugia (e.g., Eastern Tropical Pacific and the Atlantic Ocean) (Parravicini et al. 2021). Multiple socio-economic factors influence fish biomass and community composition, and likely carbonate excretion. These include human development, dependency on marine ecosystems, and fisheries management (Cinner et al. 2018; Seguin et al. 2022; Cinner et al. 2022). Carbonate excretion and mineralogy are expected to be severely impacted by fishing, not only through biomass reductions, but also through selective removal of the largest individuals and/or those at high trophic levels, as well as alteration of fish species composition (Jennings and Wilson 2009; Salter et al. 2017; Ghilardi et al. 2023b). Contrarily, carbonate excretion is predicted to increase with climate warming due to increasing metabolic rates, although this positive effect may be offset by a decrease in biomass (Wilson et al. 2009; Lotze et al. 2019). Further, higher temperatures may alter carbonate mineralogy by increasing the excretion of ACMC (Ghilardi et al. 2023b), implying a differential role of fish carbonates across space and time.

Here, focusing on reef fish communities due to the uniquely large amount of standardised and detailed observational data (e.g., Edgar and Stuart-Smith 2014; Barneche et al. 2019; Edgar et al. 2020) and associated ecological, environmental, and social data (e.g., Mora et al. 2011; Duffy et al. 2016; Cinner et al. 2016;

Cinner et al. 2018), we investigate the patterns of fish carbonate excretion and mineralogy across tropical and subtropical reefs and identify their drivers. Combining predictive models based on empirical laboratory data with a reef fish census database of 2,169 transects across 1,412 sites and 59 ecoregions (Spalding et al. 2007), we estimate community-level reef fish carbonate excretion and mineralogical composition. We then use Structural Causal Modelling (SCM, Pearl 2009) to determine how both of these are influenced by key ecological, environmental, and socio-economic factors available for the study sites. We build a Directed Acyclic Graph (DAG) representing the causal structure of reef fish carbonate excretion and estimate unbiased causal effects in a DAG-informed Bayesian framework.

3.2 Methods

3.2.1 Fish and benthic data

We used fish and benthic data from the standardised Reef Life Survey (RLS) monitoring programme (Edgar and Stuart-Smith 2014). Fish were surveyed by experienced scientists and trained recreational divers along 50-m transects laid at consistent depth on shallow reefs (depth range: 0-35 m; mean depth: ~6.6 m). All fishes observed within 5 m of either side of the transects were counted and identified to the lowest possible taxonomic level, and their total length was estimated. Along each of these transects 20 digital photoquadrats (0.3 x 0.3 m) were taken every 2.5 m, and later analysed using a superimposed grid of five points per image (100 points per transect) to derive benthic community data. Full details of census methods, data quality, and training of divers are provided elsewhere (Cresswell et al. 2017; Edgar and Stuart-Smith 2014; Edgar et al. 2020, www.reeflifesurvey.com). Fish taxonomy was harmonised according to FishBase (version April 2021, Froese and Pauly 2021) using the R package *rfishbase* (Boettiger et al. 2012). The estimated length of each fish was then converted into biomass using species-specific length-weight relationships obtained from FishBase. To improve the accuracy in biomass

estimates, estimated sizes were adjusted for the bias in divers' perception of fish size underwater using an empirical calibration (Edgar et al. 2004).

We focus on tropical reef sites (defined by a minimum monthly sea surface temperature > 17 °C, Parravicini et al. 2013) and excluded all elasmobranch fishes in the database as they do not precipitate intestinal carbonates. To prevent bias in the total biomass estimates we also excluded fishes that are likely to be underestimated by visual censuses due to their small size and/or cryptic nature (i.e., recently-settled juveniles, small cryptobenthic fishes, and fishes belonging to the order Anguilliformes, Brandl et al. 2018; Stuart-Smith et al. 2021, see *Supplementary Methods*). As carbonate excretion rate and mineralogy can currently be predicted for fishes belonging to 17 non-cryptic families (Ghilardi et al. 2023b, see *Prediction of carbonate excretion and mineralogy*), we considered only surveys for which these 17 families represented at least 80% of the total fish biomass and abundance. The final dataset thus included 2,169 transects (conducted between 2007 and 2019), encompassing 1,050 taxa identified at the species ($n = 996$) or genus level ($n = 54$) from 1,412 sites and 59 marine ecoregions (Spalding et al. 2007). Benthic data were extracted from photoquadrats scored for a subset of 1,400 of these transects, and were therefore missing for 35.5% ($n = 769$) of the transects. Percent cover was initially recorded for a large set of morphological and functional benthic groups as previously described (Cresswell et al. 2017), but was aggregated into ten broader benthic groups to increase comparability over larger scales for this study (Supplementary Table 3.1).

3.2.2 Fish carbonate excretion and mineralogy

To estimate fish carbonate excretion and mineralogy we first obtained individual-level predictions and then scaled these up to community-level estimates using fish abundance data. Individual-level predictions were obtained using two recently developed Bayesian models (Ghilardi et al. 2023b), which generated estimates for 17 non-cryptic fish families for which empirical data are available (Acanthuridae,

Chaetodontidae, Haemulidae, Holocentridae, Labridae, Latidae, Lethrinidae, Lutjanidae, Pomacentridae, Scorpaenidae, Serranidae, Siganidae, Sillaginidae, Sparidae, Sphyraenidae, Terapontidae, and Tetrarogidae). These models predict carbonate excretion rate (total and per polymorph for LMC, aragonite, HMC, MHC, and ACMC) as a function of fish traits (body mass, relative intestinal length, and caudal fin aspect ratio), water temperature, and fish family. We retrieved species caudal fin aspect ratio from FishBase and extrapolated species-specific relative intestinal length (or genus averages for the 54 taxa identified at genus level) using a Bayesian phylogenetic regression as described in Ghilardi et al. (2023b). We also retrieved the mean SST per site. We then predicted the median and 95% CI carbonate excretion rate and polymorph-specific excretion rates (in μmol h^{-1}) for each species-size-SST combination in our dataset ($n = 106,401$) using 2,000 posterior draws from the models. Median excretion rates were then multiplied by the abundance of the respective species-size combination in each transect and multiplied by 24 to obtain an estimate of excretion rate per day. Excretion rates were finally summed for each transect and divided by the area of the transect (i.e., 500 m^2) to produce community-level estimates of carbonate excretion (in μmol m^2 d^{-1}). Excretion rates per polymorph were computed as proportions dividing them by the total excretion rate of each transect. As the two models predict carbonate excretion rates for fishes close to their resting metabolic rate (Ghilardi et al. 2023b), the community-level carbonate excretion estimated here is highly conservative.

3.2.3 Mapping carbonate excretion and mineralogy

To create maps of carbonate excretion and mineralogy we predicted values at the ecoregion level using Bayesian multilevel regressions. Carbonate excretion was natural-log transformed to ensure normal distribution of residuals, and modelled with an intercept-only regression including a nested group-level effect of sites

within ecoregions:

$$y_i \sim Normal(\mu_i, \sigma)$$
$$\mu_i = \beta_0 + \gamma_{\text{ecor}} + \gamma_{\text{ecor:site}}$$
$$\beta_0 \sim \text{Normal}(0, 5)$$
$$\gamma_{\text{ecor}} \sim \text{Normal}(0, \tau_{\text{ecor}}) \tag{3.1}$$
$$\gamma_{\text{ecor:site}} \sim \text{Normal}(0, \tau_{\text{ecor:site}})$$
$$\tau_{\text{ecor}}, \tau_{\text{ecor:site}} \sim \text{Student}(3, 0, 2.5)$$
$$\sigma \sim \text{Cauchy}(0, 1)$$

where i is the transect index, y_i is the carbonate excretion, μ_i is the average predicted carbonate excretion, β_0 is the global intercept, γ_{ecor} represents ecoregion-level variation from the model intercept, $\gamma_{\text{ecor:site}}$ represents site-level variation from ecoregion-level estimates, τ_{ecor} and $\tau_{\text{ecor:site}}$ are the standard deviations of group-level effects, and σ is the residual standard deviation.

Carbonate mineralogical composition (i.e., continuous proportions of five carbonate polymorphs) was modelled following a Dirichlet distribution with a multivariate logit link function (Douma and Weedon 2019) and the same multilevel structure of equation (3.1). Given that the total carbonate excretion (based on which polymorph-specific proportions were computed) varied largely in our dataset, this may partly influence the precision of the observations (Douma and Weedon 2019). Therefore, we additionally modelled the precision parameter (ϕ) of the Dirichlet distribution as a function of the natural-log transformed total carbonate excretion using a log link function. The model structure was as follows:

$$y_{c,i} \sim \text{Dirichlet}(\mu_{c,i}, \phi_i)$$

$$\mu_{c,i} = \frac{exp(\eta_{c,i})}{\sum_{k=1}^{C} exp(\eta_{k,i})}$$

$$\eta_{c,i} = \beta_{0,c} + \gamma_{\text{ecor},c} + \gamma_{\text{ecor:site},c}$$

$$\log(\phi_i) = \beta_{0,\phi} + \beta_{1,\phi}\text{TotCarb}$$

$$\beta_{0,c}, \beta_{1,\phi} \sim \text{Normal}(0,1) \qquad (3.2)$$

$$\gamma_{\text{ecor},c} \sim \text{Normal}(0, \tau_{\text{ecor},c})$$

$$\gamma_{\text{ecor:site},c} \sim \text{Normal}(0, \tau_{\text{ecor:site},c})$$

$$\tau_{\text{ecor},c}, \tau_{\text{ecor:site},c} \sim \text{Student}(3,0,2.5)$$

$$\beta_{0,\phi} \sim \text{Student}(3,0,5)$$

where c is the carbonate polymorph index ($c = 1,\ldots,C$), i is the transect index, $y_{c,i}$ is the polymorph proportion, $\mu_{c,i}$ is the average predicted polymorph proportion, $\eta_{c,i}$ is the linear predictor, $\beta_{0,c}$ is the global intercept, $\gamma_{\text{ecor},c}$ represents ecoregion-level variation from the model intercept, $\gamma_{\text{ecor:site},c}$ represents site-level variation from ecoregion-level estimates, $\tau_{\text{ecor},c}$ and $\tau_{\text{ecor:site},c}$ are the standard deviations of group-level effects, $\beta_{0,\phi}$ is the intercept for the precision parameter, and $\beta_{1,\phi}$ is the regression coefficient of total carbonate excretion on the precision parameter. One of the carbonate polymorphs (LMC in this case) is defined as the base category b (reference), and η_b is set to 0 to guarantee model identifiability. Thus:

$$\mu_{b,i} = \frac{exp(0)}{\sum_{k=1}^{C} exp(\eta_{k,i})} = \frac{1}{\sum_{k=1}^{C} exp(\eta_{k,i})}. \qquad (3.3)$$

The Dirichlet distribution model proportions defined in the interval (0, 1). However, two carbonate polymorphs, aragonite and MHC, were absent from 411 and 234 transects, respectively. As zero-inflated multilevel Dirichlet regression models have not yet been implemented in R (although progress in this direction has recently been made, Jensen et al. 2022), we overcame this issue by transforming the response according to the following equation:

$$y* = \frac{y(n-1) + \frac{1}{C}}{n}, \qquad (3.4)$$

where y is the proportion of a polymorph, n the total number of transects in the dataset, and C the number of polymorphs (Smithson and Verkuilen 2006), which is commonly used in Beta and Dirichlet regressions (Douma and Weedon 2019; Maier 2014).

3.2.4 Structural causal modelling

The importance of using valid causal inference methods in observational ecological studies has been recently underlined (Arif and MacNeil 2022a). One such method is the SCM framework (Pearl 2009). It uses DAGs to visualise the assumed causal structure of a system or process under study. The sets of variables (adjustment sets) required to determine total causal effects of focal variables (exposures) on the response variable (outcome) are then identified through the backdoor criterion (i.e., blocking all non-causal paths [backdoor paths] between exposure and outcome), and are included into appropriate statistical models to obtain unbiased estimates of exposures' effects.

Causal DAG

Based on past literature and expert discussion we built a causal DAG (available at: dagitty.net/mss1yO7) representing how ecological, environmental, and socio-economic variables are expected to influence reef fish carbonate excretion and mineralogy. The rationale for each arrow in our DAG is provided in Supplementary Table 3.2. The final DAG included 15 key variables of interest expected to directly or indirectly influence fish carbonate excretion and mineralogy. These were: standing biomass, median body mass (i.e., an index of size structure), mean trophic level (MTL; i.e., an index of trophic structure), taxonomic, phylogenetic, and functional diversity, benthic community structure, Sea Surface Temperature (SST), Degree Heating Weeks (DHW), Net Primary Productivity (NPP), depth, human gravity (i.e., a proxy for human pressure considering human population size and accessibility to the reef, Cinner et al. 2018), management type, marine ecosystem dependency, and Human Development Index (HDI). Eight additional

variables were included in the DAG as they may have a confounding effect and should thus be considered in order to obtain unbiased estimates of the causal effects of the key variables of interest. These eight variables were: pH, dissolved oxygen, nitrate and phosphate concentrations, Photosynthetically Available Radiation (PAR), wave energy, upwelling, and latitude. For each transect, we compiled data for all variables, except for upwelling, for which data were lacking at the resolution of our study. Most variables were quantified or derived per transect, while remotely-sensed environmental data, management and gravity were derived per site (i.e., transects within the same site had the same values), and all transects within the country were assigned national HDI and marine ecosystem dependency. In the final dataset values were missing for oxygen, nitrate and phosphate concentrations, as well as PAR, from 35 transects, and wave energy from 20 transects, in addition to missing data for benthic community structure as described above. A detailed description of all variables and data sources, and the test of conditional independencies implied by the DAG is provided in the *Supplementary Methods*.

Covariate selection and Bayesian modelling

We applied the backdoor criterion using the R package *dagitty* to identify the adjustment sets required to estimate the total causal effect of each of the 15 selected variables on carbonate excretion. SST only had one possible adjustment set which included two variables: PAR and upwelling. However, upwelling was unobserved (latent) in our DAG. Consequently, all backdoor paths between SST and carbonate excretion could not be blocked. Since upwelling is a fairly regional phenomenon, its effect on SST in our global dataset is assumed to be relatively low, compared to that of PAR. Therefore, under this assumption, we estimated the effect of SST adjusting only for PAR.

For each selected variable we fitted a Bayesian multilevel regression. The response was the natural-log transformed carbonate excretion as in equation (3.1). The explanatory variables included the variable of interest and the respective set of

covariates identified with the backdoor criterion. We applied natural-log or square-root transformations to explanatory variables that were strongly or moderately right-skewed, respectively. Further, we standardised all continuous variables by subtracting their mean and dividing by two standard deviations to allow direct comparison of effect sizes (Gelman 2008). All models were fitted according to equation (3.1), to which we added fixed effects and, as data were collected at either transect, site, or country level, we replaced *ecoregion* with *country* in the nested group-level effect. Therefore, μ_i was estimated as:

$$\mu_i = \beta_0 + \beta_x X_i + \gamma_{\text{country}} + \gamma_{\text{country:site}}$$
$$\beta_x \sim \text{Normal}(0, 5)$$

(3.5)

where β_x is a vector of regression coefficients associated with the vector of explanatory variables X. In our final models, $\beta_x X$ was as follows:

Biomass (Biom)

$$\beta_x X = \beta_1 \text{Biom} + \beta_2 \text{MedBiom} + \beta_3 \text{MTL} + \beta_4 \text{TD} + \beta_5 \text{PD} + \beta_6 \text{FD} + \beta_7 \text{SST}$$

Median body mass (MedBiom)

$$\beta_x X = \beta_1 \text{MedBiom} + \beta_2 \text{SST} + \beta_3 \text{PC1} + \beta_4 \text{PC2} + \beta_5 \text{PC3} + \beta_6 \text{MPA} + \beta_7 \text{Gravity}$$
$$+ \beta_8 \text{Oxygen}$$

Mean trophic level (MTL)

$$\beta_x X = \beta_1 \text{MTL} + \beta_2 \text{TD} + \beta_3 \text{PD} + \beta_4 \text{FD} + \beta_5 \text{NPP} + \beta_6 \text{PC1} + \beta_7 \text{PC2}$$
$$+ \beta_8 \text{PC3} + \beta_9 \text{MPA} + \beta_{10} \text{Gravity}$$

Taxonomic diversity (TD)

$$\beta_x X = \beta_1 \text{TD} + \beta_2 \text{SST} + \beta_3 \text{PC1} + \beta_4 \text{PC2} + \beta_5 \text{PC3} + \beta_6 \text{MPA} + \beta_7 \text{Gravity}$$
$$+ \beta_8 \text{NPP} + \beta_9 \text{Depth}$$

Phylogenetic diversity (PD)

$$\beta_x X = \beta_1 \text{PD} + \beta_2 \text{SST} + \beta_3 \text{PC1} + \beta_4 \text{PC2} + \beta_5 \text{PC3} + \beta_6 \text{MPA} + \beta_7 \text{Gravity}$$
$$+ \beta_8 \text{NPP} + \beta_9 \text{Depth} + \beta_{10} \text{TD}$$

Functional diversity (FD)

$$\beta_x X = \beta_1 \text{FD} + \beta_2 \text{SST} + \beta_3 \text{PC1} + \beta_4 \text{PC2} + \beta_5 \text{PC3} + \beta_6 \text{MPA} + \beta_7 \text{Gravity}$$
$$+ \beta_8 \text{NPP} + \beta_9 \text{Depth} + \beta_{10} \text{TD}$$

Benthic community structure (PCx = PC1, PC2, PC3)

$$\beta_x X = \beta_1 \text{PCx} + \beta_2 \text{SST} + \beta_3 \text{NPP} + \beta_4 \text{Depth} + \beta_5 \text{Latitude} + \beta_6 \text{Oxygen}$$

SST

$$\beta_x X = \beta_1 \text{SST} + \beta_2 \text{PAR}$$

NPP

$$\beta_x X = \beta_1 \text{NPP} + \beta_2 \text{SST} + \beta_3 \text{Nitrate} + \beta_4 \text{Phosphate} + \beta_5 \text{PAR} + \beta_6 \text{Wave}$$

DHW

$$\beta_x X = \beta_1 \text{DHW} + \beta_2 \text{PAR}$$

Depth

$$\beta_x X = \beta_1 \text{Depth}$$

Management type (MPA)

$$\beta_x X = \beta_1 \text{MPA} + \beta_2 \text{HDI} + \beta_3 \text{MarDep}$$

Gravity

$$\beta_x X = \beta_1 \text{Gravity} + \beta_2 \text{HDI} + \beta_3 \text{Latitude}$$

HDI

$$\beta_x X = \beta_1 \text{HDI} + \beta_2 \text{Latitude}$$

Marine ecosystem dependency (MarDep)

$$\beta_x X = \beta_1 \text{MarDep} + \beta_2 \text{HDI}$$

$$(3.6)$$

where *Latitude* is the absolute latitude and *PC1-3* are the transect scores on the first three dimensions of a PCA on benthic data. For taxonomic, phylogenetic, and functional diversity we used *entropy* indices (i.e., Hill numbers of order $q = 1$).

We filled missing data by performing Bayesian imputation directly within our causal models. To do so, each model containing one or more variables with missing data (i.e., benthic community structure, oxygen, nitrate, phosphate, PAR, and wave energy) as predictors was fitted in a multivariate form. Here, in addition to the main model for carbonate excretion, we fitted multilevel regressions to predict the variables with missing data as functions of other covariates. Other covariates corresponded in this case to those included in the adjustment sets from the DAG. Latitude was used to predict nitrate, phosphate, and PAR, SST and NPP to predict oxygen, depth to predict wave energy, and benthic community structure was predicted as a function of NPP, SST, depth, and latitude. For benthic community structure, which was collected at the transect level, we used the same group-level effect of the main model (i.e., sites nested within countries). For the other variables (i.e., oxygen, nitrate, phosphate, PAR, and wave energy) we only included a group-level effect of *country* as transects within the same site had the same values. The model used to estimate the causal effect of DHW on carbonate excretion is provided in the *Supplementary Methods* as an example of the Bayesian imputation procedure, and the imputed missing values for benthic community structure are shown in Supplementary Fig. 3.15.

We used the same DAG and the same adjustments sets to estimate the causal effects on carbonate mineralogical composition. For each variable, we fitted equation (3.2) adding the fixed effects from equation (3.6) and replacing *ecoregion* with *country*, as for carbonate excretion. Due to the high computational costs of Bayesian imputation and Bayesian multilevel Dirichlet regressions with a large dataset, we fitted these models on a filtered dataset with complete observations ($n = 1,374$), thus avoiding imputation.

Finally, from each fitted model, we only extracted the effect of the focal variable (β_1 in equation (3.6)) to create figures, and ignored the other variables which are included only to avoid bias in the estimated causal effect.

Sensitivity analyses

We performed a series of sensitivity analyses to assess the robustness of our results. Firstly, we tested the sensitivity of the results to the Bayesian imputation by refitting all the models for carbonate excretion using a filtered dataset including only transects with complete observations ($n = 1,374$). Secondly, we tested how the benthic classification affected the results. We refitted all models including benthic community structure, either as the main predictor or as confounding variable, using the transect scores on the first three axes of a PCA based on five broad benthic groups (Supplementary Table 3.1). Thirdly, we tested how the selection of biodiversity indices affects the results by refitting all models including taxonomic, phylogenetic, or functional diversity, either as the main predictor or as confounding variables, using *richness* indices (i.e., Hill numbers of order $q = 0$). All sensitivity analyses were performed using the filtered dataset with complete observations to avoid the computational costs of Bayesian imputation.

3.2.5   Software environment and model specifications

All analyses were performed in R (version 4.1.3; R Core Team (2021)) and all models were fitted in Stan (Carpenter et al. 2017) using the R package *brms* (Bürkner 2017), which uses a Hamiltonian Monte Carlo sampler algorithm (MCMC) to estimate the posterior distributions of model parameters. All causal models for carbonate excretion fitted on the full dataset (with imputation) were run for four chains, each with 2,000 iterations and a warm-up of 1,000 iterations, whereas 3,000 iterations were used for all other models. All models were examined for evidence of convergence using trace plots and scale reduction factors (Rhat) and we used posterior predictive plots to check for models' fit.

3.3 Results

3.3.1 Patterns of carbonate excretion and mineralogy

Reef fish excrete an average of 25.75 μmol m^{-2} d^{-1} (95% credible interval (CI): 20.78, 31.85) on tropical reefs. Carbonate excretion varied greatly across marine ecoregions (Fig. 3.1), from 5.55 μmol m^{-2} d^{-1} (CI: 4.32, 7.17) in the Houtman ecoregion (Western Australia) to 101.82 μmol m^{-2} d^{-1} (CI: 61.16, 170.90) in the Cortezian ecoregion (Gulf of California). Excretion rates were generally highest near the Equator, although some ecoregions at higher latitudes, such as Cortezian and Floridian, also displayed atypically high values (>50 μmol m^{-2} d^{-1}). The five ecoregions with the highest excretion rates were all located in the Eastern Tropical Pacific realm (Fig. 3.1), but values were highly variable among their sites (Supplementary Fig. 3.6).

Figure 3.1: Map of fish carbonate excretion across tropical and subtropical reefs. Dots indicate ecoregions where fish surveys were conducted, while dot size and colour represent ecoregion-level average predictions of fish carbonate excretion.

Although also variable across ecoregions, the mineralogical composition of reef fish carbonates was generally dominated by the least stable carbonate polymorphs. HMC and ACMC for instance, accounted for >50% of the excreted carbonate in all ecoregions (Fig. 3.2). Close to the Equator, MHC was excreted in respectable proportions, accounting for up to 36.9% of the total reef fish carbonate in the Phoenix/Tokelau/Northern Cook Islands ecoregion (Central Pacific). More stable
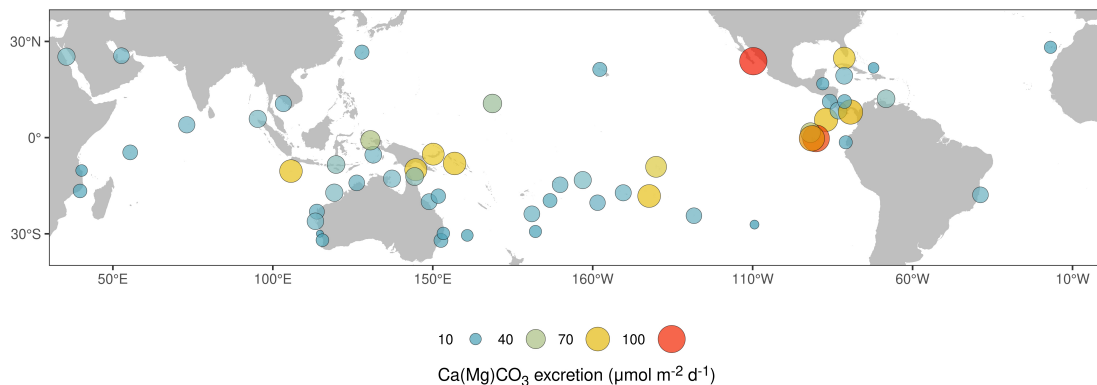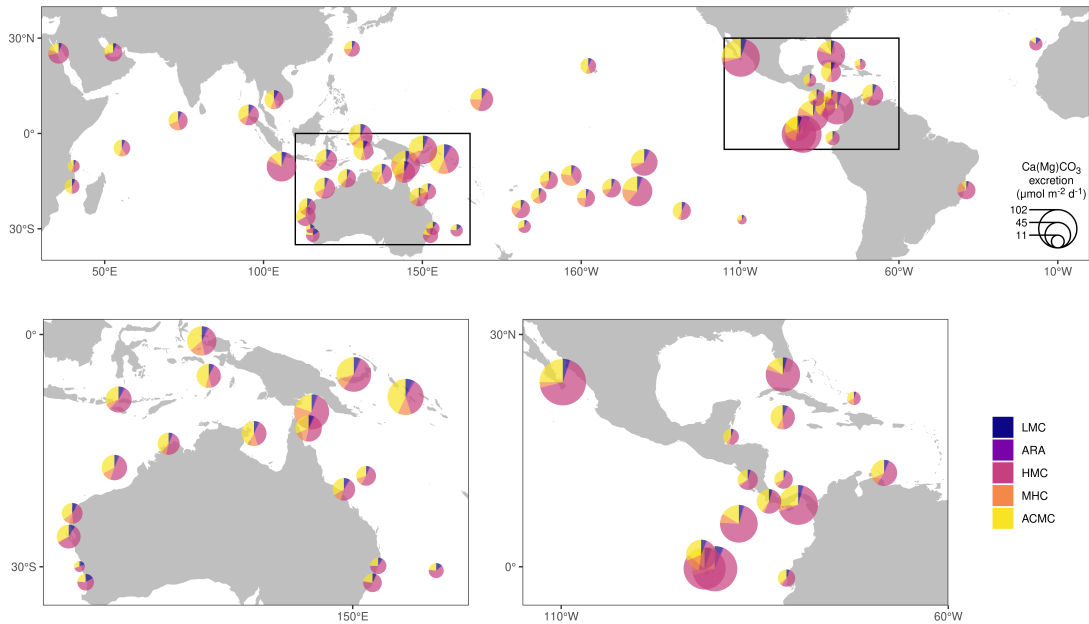
Figure 3.2: Map of fish carbonate mineralogy across tropical and subtropical reefs. Pies indicate ecoregions where fish surveys were conducted, with pie size representing ecoregion-level average predictions of fish carbonate excretion, and colours representing ecoregion-level average predictions of fish carbonate mineralogical composition. Insets allow better visualisation of overlapping pies around Australia and in the Eastern Tropical Pacific and Caribbean. LMC, low-Mg calcite; ARA, aragonite; HMC, high-Mg calcite; MHC, monohydrocalcite; ACMC, amorphous Ca-Mg carbonate.

polymorphs, such as aragonite and LMC generally represented a minor proportion of the excreted carbonate (typically <10% combined), although they added up to 18.8% in the Houtman ecoregion.

3.3.2 Drivers of carbonate excretion and mineralogy

Predictably, we found that fish biomass was the strongest driver of carbonate excretion (Fig. 3.3). Indeed, fish biomass is commonly used as a proxy for coral reef functioning (Mora et al. 2011; Duffy et al. 2016; Brandl et al. 2019; Cinner et al. 2020). However, as observed for several other functions sustained by reef fish (Schiettekatte et al. 2022a), the relationship between carbonate excretion and biomass was allometric. Specifically, the slope of natural-log transformed biomass was 0.88 (CI: 0.87, 0.89). This reiterates the inappropriate use of fish biomass as proxy for ecosystem functioning.
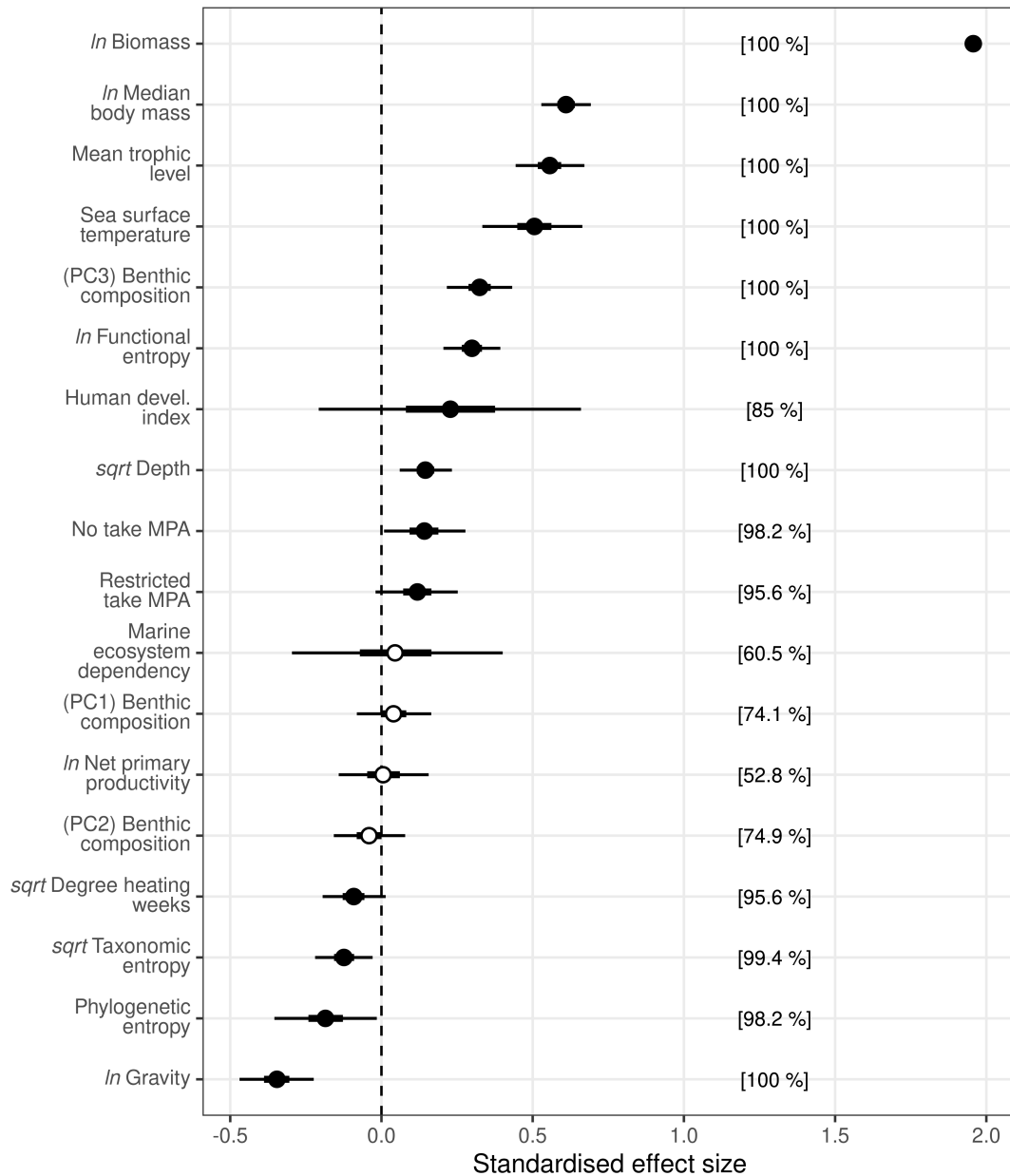
Figure 3.3: Drivers of reef fish carbonate excretion. Estimates are posterior medians (circles), 50% credible intervals (CIs; thick lines; some are too narrow to be seen) and 95% CIs (thin lines) from DAG-informed Bayesian multilevel regressions fitted to the entire dataset, and represent total causal effects. White circles depict effects with a 50% CI overlapping zero. Percentages represent the posterior probability that an effect is either positive (when the median in above zero) or negative (when the median is below zero). PC1-PC3 are the transect scores on the first three axes of a principal component analysis of benthic composition classified into ten groups. MPA, Marine Protected Area.
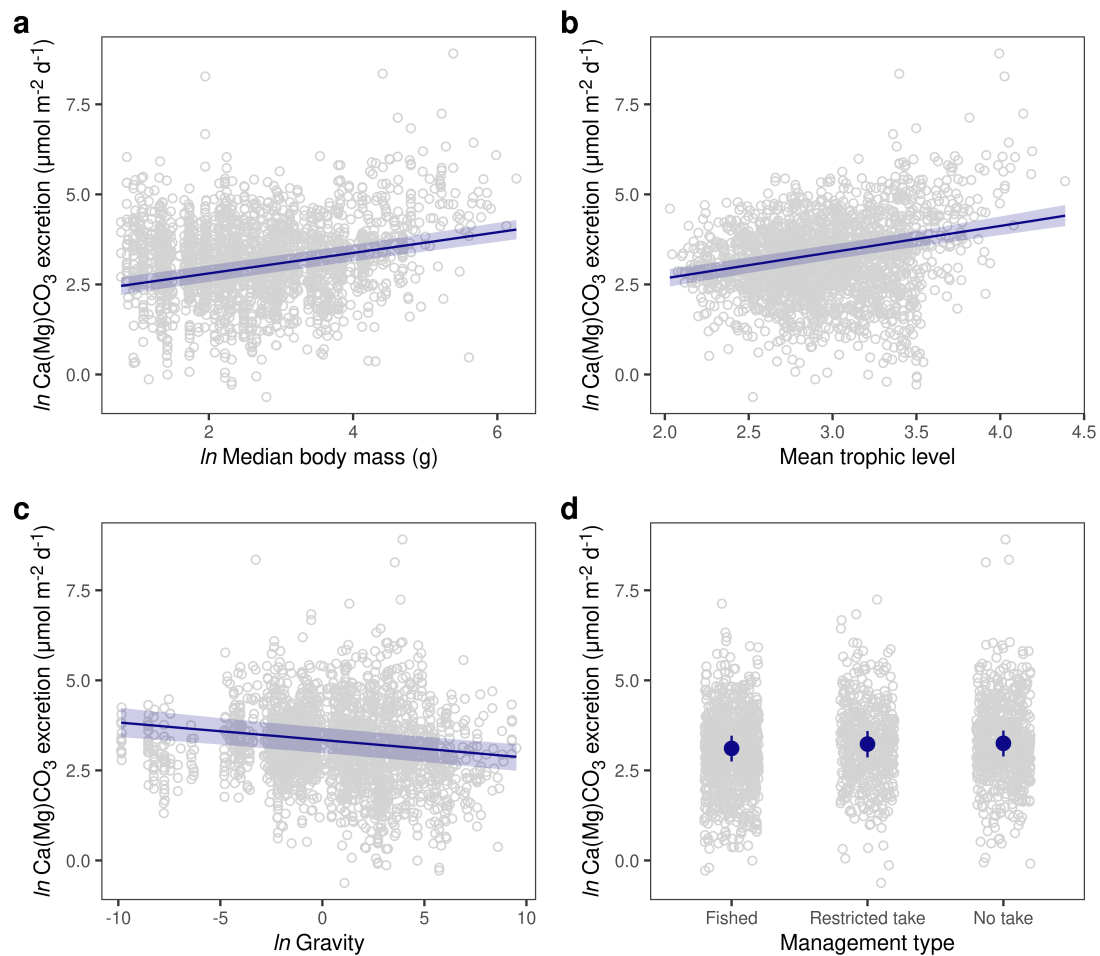
Figure 3.4: Estimated causal effect of reef fish community structure and humans on carbonate excretion. Fitted lines and ribbons in **a-c**, as well as large circles and lines in **d**, are posterior medians and 95% credible intervals, respectively, from DAG-informed Bayesian multilevel regressions fitted to the entire dataset, and represent conditional effects after accounting for the influence of all confounding variables, which were set to their mean values. Grey circles are observed data.

Beyond total biomass, MTL and median body mass had a strong positive effect on fish carbonate excretion (Figs. 3.3-3.4). Human gravity had the strongest negative effect on carbonate excretion, which largely exceeded the weak positive effect of management in the form of restricted-take (e.g., ban on certain fishing gears, effort and size limits) or no-take areas (Figs. 3.3-3.4). These findings were consistent when models were fitted also on a filtered dataset including only transects with complete observations (i.e., $n = 1{,}374$ without missing data; Supplementary Fig. 3.7).

The trophic structure of fish communities also largely influenced carbonate mineralogy. Specifically, communities dominated by herbivores (low MTL) excrete a mix of ACMC, HMC, and MHC, whereas communities dominated by high trophic level fishes (high MTL) excrete predominantly HMC (Fig. 3.5 and Supplementary Fig. 3.8). Opposite to the patterns observed for carbonate excretion, human gravity and management had very little or no effect on carbonate mineralogy (Fig. 3.5 and Supplementary Fig. 3.8).

Further, carbonate excretion increased with increasing SST (Fig. 3.3). However, the strength of this relationship was to some extent sensitive to the size of the dataset used (Supplementary Fig. 3.7). Importantly, SST was the strongest driver of carbonate mineralogy (Supplementary Fig. 3.8). Specifically, HMC is the dominant carbonate polymorph in colder waters, whereas a mix of HMC, ACMC, and MHC is excreted in warmer waters (Fig. 3.5).

Finally, fish biodiversity and benthic community structure had a relatively weak influence on carbonate excretion and mineralogy. The effect of diversity was contingent upon whether the metric considered was taxonomic, phylogenetic, or functional and upon whether indices focused on common (entropy) or rare (richness) species. This calls for caution when interpreting biodiversity-ecosystem functioning relationships obtained from single facets of diversity. Particularly, functional diversity had a consistent positive effect on carbonate excretion, whereas phylogenetic and taxonomic diversity had contrasting effects (weakly negative for entropy and strongly positive for richness), with the latter also having contrasting effects on carbonate mineralogy (Fig. 3.3 and Supplementary Figs. 3.9-3.10-3.11). This suggests that communities with high carbonate excretion rates are dominated by a few common species and lineages, but not necessarily by a few functional entities (Supplementary Fig. 3.10). Furthermore, carbonate excretion was higher where the benthos was covered mostly by living organisms, in particular crustose coralline algae (CCA), than in places dominated by bare rock, sand, and rubble (PC3 in Fig. 3.3 and Supplementary Figs. 3.7 and 3.12, and PC2 in Supplementary Figs. 3.13-3.14). Carbonate excretion and mineralogy were
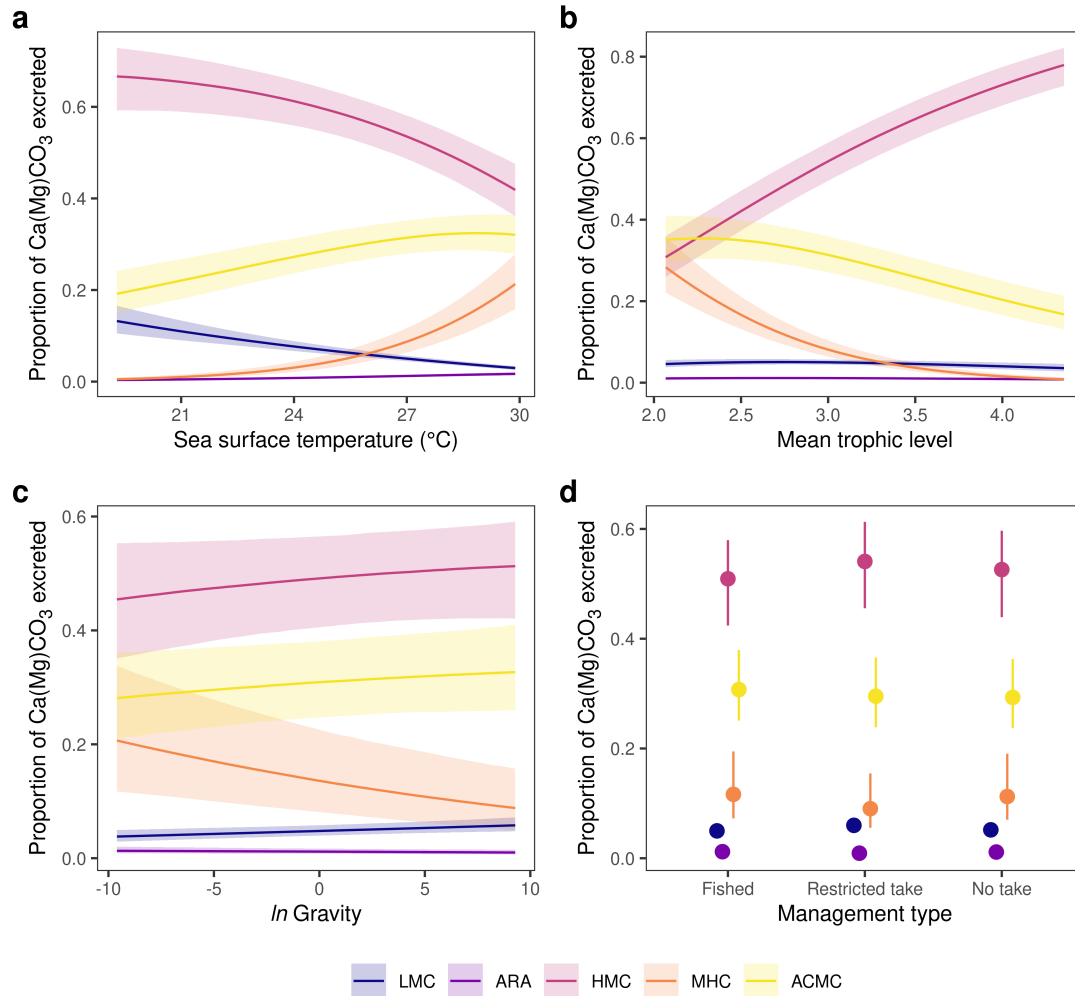
Figure 3.5: Reef fish carbonate mineralogy is largely influenced by temperature and fish community structure but only weakly by humans. Fitted lines and ribbons in **a-c**, as well as circles and lines in **d**, are posterior medians and 95% credible intervals (some are too narrow to be seen) from DAG-informed Bayesian multilevel Dirichlet regressions fitted to a filtered dataset with complete observations ($n = 1{,}374$), and represent conditional effects after accounting for the influence of all confounding variables, which were set to their mean values. LMC, low-Mg calcite; ARA, aragonite; HMC, high-Mg calcite; MHC, monohydrocalcite; ACMC, amorphous Ca-Mg carbonate.

relatively consistent across reefs regardless of the dominant benthic group, yet excretion rates were slightly higher on reefs containing more algal turfs (PC1), macroalgae and CCA (PC2), than on reefs with more live corals (Fig. 3.3 and Supplementary Figs. 3.7 and 3.12). However, aggregating the three algal groups resulted in a larger positive effect of the benthos on carbonate excretion (PC1 in Supplementary Figs. 3.13-3.14).

3.4 Discussion

By mapping fish carbonate excretion and mineralogy, we provide evidence of large variability in the amount and composition of excreted carbonates at global-scale. These observations support recent local- and regional-scale analyses which suggested that the role of fish in inorganic carbon cycling could be more complex than previously thought (Salter et al. 2017; Salter et al. 2018). Further, our maps highlight that fish consistently excrete large proportions of ACMC across global reefs, and often also MHC. This implies that a large proportion of excreted carbonates, which can reach up to ~50% in some regions (e.g., Western Indian Ocean), and up to 85% at specific sites, will likely dissolve in surface waters. The remainder will likely dissolve over a depth range subject to local carbonate saturation states. Some carbonate may contribute to fine-grained sediment formation where the seafloor is above the carbonate saturation depth, thus this may represent a large proportion including HMC in shallow environments.

Through causal inference, we also demonstrate that fish carbonate excretion rates are primarily driven by variation in fish community structure and human pressure, whereas carbonate mineralogy follow the SST gradient and are secondarily driven by fish community structure. These findings have strong implications for predicting the impacts of fishing and climate change on fish contributions to the inorganic carbon cycle.

Following our expectations, fish carbonate excretion is highest on reefs with high fish biomass, median body mass and MTL, where predominantly HMC is

excreted. These conditions are promoted by isolation and low human pressure (Cinner et al. 2018; Lefcheck et al. 2021), but are not necessarily preserved by current management strategies (D'Agata et al. 2016), as shown by the positive but weak effect of restricted-take and no-take areas. Such reefs are mainly found in the highly productive Eastern Tropical Pacific where pH levels are generally low. The low pH and shallow HMC saturation horizon (Sulpis et al. 2021) suggest rapid dissolution of excreted carbonates within the first 200 m of the water column. Shallow dissolution of fish carbonates implies these may not reduce surface water alkalinity or have a ballast effect on faecal pellets (in which they are embedded), thus limiting the export of both inorganic and organic carbon to the seafloor. However, the alkalinity released by HMC dissolution may buffer against further decreases in pH. The Eastern Tropical Pacific is thus highlighted here as a hotspot of fish-mediated carbonate production, but with limited potential for sedimentation and carbon export via this pathway.

Size-selective fishing erodes carbon sequestration in the deep sea by preventing sinking of large-bodied fish carcasses and reducing the production and downward export of faecal pellets (Mariani et al. 2020; Saba et al. 2021). Further, it impacts fish carbon storage by removing biomass which has the potential to store carbon for decades (depending of species' lifespan). Our findings show that the selective removal of large-bodied fish at upper trophic levels also reduces overall fish carbonate excretion by decreasing the median body mass and MTL of the community (Jennings and Wilson 2009) and alters the mineralogical composition of excreted carbonates thereby increasing their dissolution potential. These combined effects on carbonate excretion and mineralogy exacerbate the fishing-induced reduction in fish carbon sequestration potential and their contribution to the marine carbon cycle.

Climate warming is expected to increase fish-mediated carbonate production by increasing metabolic and carbonate excretion rates at the individual level (Ghilardi et al. 2023b). However, the decrease in fish size and biomass with temperature (Lotze et al. 2019; Salvatteci et al. 2022) may offset the positive temperature

effect through metabolism (Wilson et al. 2009). We found that sea surface temperature is a positive driver of carbonate excretion, but, as observed in other marine calcifiers (Figuerola et al. 2023), fishes excrete more soluble carbonate polymorphs in warmer waters. Therefore, while increasing seawater temperatures may increase fish-mediated carbonate production, climate warming is expected to alter fish role in inorganic carbon cycling. Excreted carbonates will dissolve faster and/or at shallower depth, thereby reducing their sedimentation potential. Further, warming is associated with an increase in dissolved CO_2 and acidification, which will accelerate carbonate dissolution. The more soluble polymorphs produced by fish could then partially buffer further acidification.

Climate change is also restructuring coral reefs into novel configurations impacting ecosystem functioning (Stuart-Smith et al. 2018; Williams and Graham 2019). Particularly, climate-induced coral bleaching can result in coral–macroalgal regime shifts and associated changes in fish community structure and composition (Graham et al. 2015). Nevertheless, regime-shifted reefs can still sustain ecosystem functions and services. For instance, following coral loss reefs can remain important sources of micronutrients for fisheries and sustain high catch levels thanks to higher biomass production driven by increased abundance of herbivorous species (Robinson et al. 2019; Morais et al. 2020a; Robinson et al. 2022; Hamilton et al. 2022). However, this translates in lower MTL which may result in lower carbonate excretion and higher solubility. Although we did not directly compare reefs pre- and post-regime shifts, our global analysis shows that fish carbonate excretion is higher in reefs covered more by algae than on reefs with more corals, with no major differences in the mineralogy. This suggest that, contrary to expectations, this ecosystem function could be maintained after climate-driven coral mortality, possibly through higher biomass of herbivores.

Our (conservative) estimates suggest that fish contribution to the overall carbonate production is generally low on coral reefs relative to other marine calcifiers and potentially negligible in many sites. However, the distinct size and mineralogy of fish carbonates suggest that they probably contribute significantly to the

production of the more soluble carbonate polymorphs (HMC, ACMC, and MHC) and fine-grained carbonate sediments in shallow reef environments (Perry et al. 2011). Such contribution is likely to increase with increasing water temperatures and reef degradation (decrease in corals' contribution), but the sedimentation potential will decrease.

Although we focused on coral reefs, our findings could be largely generalised and used to understand how fish may contribute to inorganic carbon cycling in other ecosystems. For instance, the strong temperature dependence of fish carbonate excretion and mineralogy suggests that, at higher latitudes, fish likely excrete relatively less carbonate. These excreted carbonates will be mainly composed by calcite, with an increasing proportion of LMC with decreasing temperature. This is supported by empirical observations of fish carbonates in temperate settings (Salter et al. 2019). At higher latitudes fish carbonates are thus expected to have a higher sedimentation potential, although carbonate saturation states are lower in colder waters (Jiang et al. 2015). Instead, pelagic fish are expected to predominantly excrete HMC as they typically occupy middle and high trophic levels. However, magnesium content may vary across latitude as a function of temperature (Salter et al. 2019). This would imply that the contribution of fish to the inorganic carbon cycle in the open ocean reflects the initial hypothesis of Wilson et al. (2009) which was based on the assumption that fish excrete only HMC.

Our analysis identifies the conditions under which fish contribution to inorganic carbon cycling is maintained and provides insight into how it may change under increasing anthropogenic pressure. While climate change and fishing can severely affect fish inorganic carbon cycling, our results shows that human gravity has a strong impact on carbonate excretion, likely reflecting its impact on fish biomass (Cinner et al. 2016; Seguin et al. 2022). Restricted-take and no-take areas have however limited capacity to sustain carbonate excretion. With the human population steadily increasing, the role of fish in the carbon cycle is expected to decrease. The protection of large carnivores could be a win-win strategy to enhance fish contribution to both inorganic and organic ocean carbon fluxes.

Acknowledgements

References

Ankan, Ankur, Inge M.N. Wortel, and Johannes Textor (2021). "Testing Graphical Causal Models Using the R Package dagitty". In: *Current Protocols* 1, e45. DOI: `10.1002/cpz1.45`.

Arif, Suchinta and Aaron MacNeil (2022a). "Predictive models aren't for causal inference". In: *Ecology Letters* 25, pp. 1741–1745. DOI: `10.1111/ele.14033`.

Assis, Jorge et al. (2018). "Bio-ORACLE v2.0: Extending marine data layers for bioclimatic modelling". In: *Global Ecology and Biogeography* 27.3, pp. 277–284. DOI: `10.1111/geb.12693`.

Barkley, Hannah C. et al. (2015). "Changes in coral reef communities across a natural gradient in seawater pH". In: *Science Advances* 1, e1500328. DOI: `10.1126/sciadv.1500328`.

Barlow, Jos et al. (2018). "The future of hyperdiverse tropical ecosystems". In: *Nature* 559.7715, pp. 517–526. DOI: `10.1038/s41586-018-0301-1`.

Barneche, D. R. et al. (2019). "Body size, reef area and temperature predict global reef-fish species richness across spatial scales". In: *Global Ecology and Biogeography* 28.3, pp. 315–327. DOI: `10.1111/geb.12851`.

Behrenfeld, Michael J. and Paul G. Falkowski (1997). "Photosynthetic rates derived from satellite-based chlorophyll concentration". In: *Limnology and Oceanography* 42.1, pp. 1–20. DOI: `10.4319/lo.1997.42.1.0001`.

Bianchi, Daniele et al. (2021). "Estimating global biomass and biogeochemical cycling of marine fish with and without fishing". In: *Science Advances* 7, eabd7554. DOI: `10.1126/sciadv.abd7554`.

Boettiger, Carl, D. T. Lang, and P. C. Wainwright (2012). "Rfishbase: Exploring, manipulating and visualizing FishBase data from R". In: *Journal of Fish Biology* 81.6, pp. 2030–2039. DOI: `10.1111/j.1095-8649.2012.03464.x`.

Brandl, Simon J et al. (2019). "Demographic dynamics of the smallest marine vertebrates fuel coral-reef ecosystem functioning". In: *Science* 364.6446, pp. 1189–1192. DOI: `10.1126/science.aav3384`.

Brandl, Simon J. et al. (2018). "The hidden half: Ecology and evolution of cryptobenthic fishes on coral reefs". In: *Biological Reviews* 93.4, pp. 1846–1873. DOI: `10.1111/brv.12423`.

Breevi, Ljerka and Arne Erik Nielsen (1989). "Solubility of amorphous calcium carbonate". In: *Journal of Crystal Growth* 98, pp. 504–510.

Burkepile, Deron E. and Mark E. Hay (2006). "Herbivore vs. nutrient control of marine primary producers: Context-dependent effects". In: *Ecology* 87.12, pp. 3128–3139. DOI: `10.1890/0012-9658(2006)87[3128:HVNCOM]2.0.CO;2`.

Bürkner, Paul Christian (2017). "brms: An R package for Bayesian multilevel models using Stan". In: *Journal of Statistical Software* 80.1, pp. 1–28. DOI: `10.18637/jss.v080.i01`.

Campbell, Janet W. and Thorkild Aarup (1989). "Photosynthetically available radiation at high latitudes". In: *Limnology and Oceanography* 34.8, pp. 1490–1499. DOI: `10.4319/lo.1989.34.8.1490`.

Cardinale, Bradley J. et al. (2006). "Effects of biodiversity on the functioning of trophic groups and ecosystems". In: *Nature* 443, pp. 989–992. DOI: `10.1038/nature05202`.

Carpenter, Bob et al. (2017). "Stan: A probabilistic programming language". In: *Journal of Statistical Software* 76.1, pp. 1–32. DOI: `10.18637/jss.v076.i01`.

Cavan, Emma L. and Simeon L. Hill (2021). "Commercial fishery disturbance of the global ocean biological carbon sink". In: *Global Change Biology* 28.4, pp. 1212–1221. DOI: `10.1111/gcb.16019`.

Chao, Anne, Chun Huo Chiu, and Lou Jost (2010). "Phylogenetic diversity measures based on Hill numbers". In: *Philosophical Transactions of the Royal Society B: Biological Sciences* 365.1558, pp. 3599–3609. DOI: `10.1098/rstb.2010.0272`.

— (2014). "Unifying species diversity, phylogenetic diversity, functional diversity, and related similarity and differentiation measures through hill numbers". In: *Annual Review of Ecology, Evolution, and Systematics* 45, pp. 297–324. DOI: `10.1146/annurev-ecolsys-120213-091540`.

Chao, Anne et al. (2019). "An attribute-diversity approach to functional diversity, functional beta diversity, and related (dis)similarity measures". In: *Ecological Monographs* 89.2, e01343. DOI: `10.1002/ecm.1343`.

Cinner, Joshua E et al. (2016). "Bright spots among the world's coral reefs". In: *Nature* 535.7612, pp. 416–419. DOI: `10.1038/nature18607`.

Cinner, Joshua E. et al. (2018). "Gravity of human impacts mediates coral reef conservation gains". In: *Proceedings of the National Academy of Sciences of the United States of America* 115.27, E6116–E6125. DOI: `10.1073/pnas.1708001115`.

Cinner, Joshua E. et al. (2020). "Meeting fisheries, ecosystem function, and biodiversity goals in a human-dominated world". In: *Science* 368.6488, pp. 307–311. DOI: `10.1126/science.aax9412`.

Cinner, Joshua E. et al. (2022). "Linking key human-environment theories to inform the sustainability of coral reefs". In: *Current Biology* 32.12, 2610–2620.e4. DOI: `10.1016/j.cub.2022.04.055`.

Cresswell, Anna K. et al. (2017). "Translating local benthic community structure to national biogenic reef habitat types". In: *Global Ecology and Biogeography* 26.10, pp. 1112–1125. DOI: `10.1111/geb.12620`.

D'Agata, Stephanie et al. (2016). "Marine reserves lag behind wilderness in the conservation of key functional roles". In: *Nature Communications* 7, p. 12000. DOI: `10.1038/ncomms12000`.

D'Agata, Stéphanie et al. (2014). "Human-mediated loss of phylogenetic and functional diversity in coral reef fishes". In: *Current Biology* 24.5, pp. 555–560. DOI: 10.1016/j.cub.2014.01.049.

D'Angelo, Cecilia and Jörg Wiedenmann (2014). "Impacts of nutrient enrichment on coral reefs: New perspectives and implications for coastal management and reef survival". In: *Current Opinion in Environmental Sustainability* 7.2, pp. 82–93. DOI: 10.1016/j.cosust.2013.11.029.

Darling, Emily S. et al. (2017). "Relationships between structural complexity, coral traits, and reef fish assemblages". In: *Coral Reefs* 36.2, pp. 561–575. DOI: 10.1007/s00338-017-1539-z.

Douma, Jacob C. and James T. Weedon (2019). "Analysing continuous proportions in ecology and evolution: A practical introduction to beta and Dirichlet regression". In: *Methods in Ecology and Evolution* 10.9, pp. 1412–1430. DOI: 10.1111/2041-210X.13234.

Duffy, J. Emmett et al. (2016). "Biodiversity enhances reef fish biomass and resistance to climate change". In: *Proceedings of the National Academy of Sciences of the United States of America* 113.22, pp. 6230–6235. DOI: 10.1073/pnas.1524465113.

Edgar, Graham J., Neville S. Barrett, and Alastair J. Morton (2004). "Biases associated with the use of underwater visual census techniques to quantify the density and size-structure of fish populations". In: *Journal of Experimental Marine Biology and Ecology* 308.2, pp. 269–290. DOI: 10.1016/j.jembe.2004.03.004.

Edgar, Graham J. and Rick D. Stuart-Smith (2014). "Systematic global assessment of reef fish communities by the Reef Life Survey program". In: *Scientific Data* 1, p. 140007. DOI: 10.1038/sdata.2014.7.

Edgar, Graham J. et al. (2020). "Reef Life Survey: Establishing the ecological basis for conservation of shallow marine life". In: *Biological Conservation* 252.June, p. 108855. DOI: 10.1016/j.biocon.2020.108855.

Edwards, C. B. et al. (2014). "Global assessment of the status of coral reef herbivorous fishes: Evidence for fishing effects". In: *Proceedings of the Royal Society B: Biological Sciences* 281.1774, pp. 7–11. DOI: 10.1098/rspb.2013.1835.

Emslie, Michael J. et al. (2015). "Expectations and outcomes of reserve network performance following re-zoning of the Great Barrier Reef Marine Park". In: *Current Biology* 25.8, pp. 983–992. DOI: 10.1016/j.cub.2015.01.073.

Falkowski, Paul G. (2012). "The Global Carbon Cycle: Biological Processes". In: *Fundamentals of Geobiology*, pp. 5–19. DOI: 10.1002/9781118280874.ch2.

Figuerola, Blanca et al. (2023). "Temperature as a likely driver shaping global patterns in mineralogical composition in bryozoans: implications for marine calcifiers under global change". In: *Ecography* 2023, e06381. DOI: 10.1111/ecog.06381.

Foran, Elizabeth, Steve Weiner, and Maoz Fine (2013). "Biogenic fish-gut calcium carbonate is a stable amorphous phase in the gilt-head seabream, sparus aurata". In: *Scientific Reports* 3, p. 1700. DOI: 10.1038/srep01700.

Fox, Helen E. et al. (2012). "Explaining global patterns and trends in marine protected area (MPA) development". In: *Marine Policy* 36.5, pp. 1131–1138. DOI: 10.1016/j.marpol.2012.02.007.

Friedlingstein, Pierre et al. (2022). "Global Carbon Budget 2022". In: *Earth System Science Data* 14.11, pp. 4811–4900.

Froese, Rainer and Daniel Pauly (2021). *FishBase*. version (04/2021). URL: www.fishbase.org.

Fukushi, Keisuke et al. (2011). "Monohydrocalcite: A promising remediation material for hazardous anions". In: *Science and Technology of Advanced Materials* 12.6, p. 064702. DOI: `10.1088/1468-6996/12/6/064702`.

Furnas, Miles J. et al. (1990). "Phytoplankton biomass and primary production in semi-enclosed reef lagoons of the central Great Barrier Reef, Australia". In: *Coral Reefs* 9, pp. 1–10. DOI: `10.1007/BF00686716`.

Gelman, Andrew (2008). "Scaling regression inputs by dividing by two standard deviations". In: *Statistics in Medicine* 27, pp. 2865–2873. DOI: `10.1002/sim`.

Ghilardi, Mattia et al. (2021b). "Phylogeny, body morphology, and trophic level shape intestinal traits in coral reef fishes". In: *Ecology and Evolution* 11.19, pp. 13218–13231. DOI: `10.1002/ece3.8045`.

Ghilardi, Mattia et al. (2023b). "Temperature, species identity and morphological traits predict carbonate excretion and mineralogy in tropical reef fishes". In: *Nature Communications* 14, p. 985. DOI: `10.1038/s41467-023-36617-7`.

Graham, N. A.J. et al. (2005). "Size-spectra as indicators of the effects of fishing on coral reef fish assemblages". In: *Coral Reefs* 24.1, pp. 118–124. DOI: `10.1007/s00338-004-0466-y`.

Graham, Nicholas A.J. et al. (2015). "Predicting climate-driven regime shifts versus rebound potential in coral reefs". In: *Nature* 518.7537, pp. 94–97. DOI: `10.1038/nature14140`.

Graham, Nicholas A.J. et al. (2017). "Human Disruption of Coral Reef Trophic Structure". In: *Current Biology* 27.2, pp. 231–236. DOI: `10.1016/j.cub.2016.10.062`.

Graham, Nicholas A.J. et al. (2018). "Seabirds enhance coral reef productivity and functioning in the absence of invasive rats". In: *Nature* 559.7713, pp. 250–253. DOI: `10.1038/s41586-018-0202-3`.

Hamilton, Mark et al. (2022). "Climate impacts alter fisheries productivity and turnover on coral reefs". In: *Coral Reefs* 41.4, pp. 921–935. DOI: `10.1007/s00338-022-02265-4`.

Heenan, Adel, Gareth J. Williams, and Ivor D. Williams (2019). "Natural variation in coral reef trophic structure across environmental gradients". In: *Frontiers in Ecology and the Environment* 18.2, pp. 69–75. DOI: `10.1002/fee.2144`.

Hernández-León, Santiago et al. (2019). "Zooplankton and Micronekton Active Flux Across the Tropical and Subtropical Atlantic Ocean". In: *Frontiers in Marine Science* 6.September, pp. 1–20. DOI: `10.3389/fmars.2019.00535`.

Heuer, Rachael M. et al. (2016). "Changes to intestinal transport physiology and carbonate production at various CO2 levels in a marine teleost, the Gulf Toadfish (*Opsanus beta*)". In: *Physiological and Biochemical Zoology* 89.5, pp. 402–416. DOI: `10.1086/688235`.

Hughes, Terry P. et al. (2017b). "Global warming and recurrent mass bleaching of corals". In: *Nature* 543.7645, pp. 373–377. DOI: `10.1038/nature21707`.

Hughes, Terry P. et al. (2018a). "Global warming transforms coral reef assemblages". In: *Nature* 556, pp. 492–496. DOI: `10.1038/s41586-018-0041-2`.

Jennings, Simon and Rod W. Wilson (2009). "Fishing impacts on the marine inorganic carbon cycle". In: *Journal of Applied Ecology* 46.5, pp. 976–982. DOI: `10.1111/j.1365-2664.2009.01682.x`.

Jensen, Alexander J et al. (2022). "Introducing zoid : A mixture model and R package for modeling proportional data with zeros and ones in ecology". In: *Ecology* April, e3804. DOI: 10.1002/ecy.3804.

Jiang, Li Qing et al. (2015). "Climatological distribution of aragonite saturation state in the global oceans". In: *Global Biogeochemical Cycles* 29.10, pp. 1656–1673. DOI: 10.1002/2015GB005198.

Jiang, Li Qing et al. (2019). "Surface ocean pH and buffer capacity: past, present and future". In: *Scientific Reports* 9, p. 18624. DOI: 10.1038/s41598-019-55039-4.

Karkarey, Rucha et al. (2022). "Spatial decoupling of α and β diversity suggest different management needs for coral reef fish along an extensive mid-oceanic ridge". In: *Global Ecology and Conservation* 36, e02110. DOI: 10.1016/j.gecco.2022.e02110.

Koop, K. et al. (2001). "ENCORE: The effect of nutrient enrichment on coral reefs. Synthesis of results and conclusions". In: *Marine Pollution Bulletin* 42.2, pp. 91–120. DOI: 10.1016/S0025-326X(00)00181-8.

Kummu, Matti and Olli Varis (2011). "The world by latitudes: A global analysis of human population, development level and environment across the north-south axis over the past half century". In: *Applied Geography* 31.2, pp. 495–507. DOI: 10.1016/j.apgeog.2010.10.009.

Lange, Ines D. et al. (2021). "Wave exposure shapes reef community composition and recovery trajectories at a remote coral atoll". In: *Coral Reefs* 40.6, pp. 1819–1829. DOI: 10.1007/s00338-021-02184-w.

Lefcheck, Jonathan S. et al. (2021). "Species richness and identity both determine the biomass of global reef fish communities". In: *Nature Communications* 12, p. 6875. DOI: 10.1038/s41467-021-27212-9.

Levitus, Sydney et al. (1993). "Distribution of nitrate, phosphate and silicate in the world oceans". In: *Progress in Oceanography* 31.3, pp. 245–273. DOI: 10.1016/0079-6611(93)90003-V.

Li, Daijiang (2018). "hillR: taxonomic, functional, and phylogenetic diversity and similarity through Hill Numbers". In: *Journal of Open Source Software* 3.31, p. 1041. DOI: 10.21105/joss.01041.

Liu, Gang et al. (2014). "Reef-scale thermal stress monitoring of coral ecosystems: New 5-km global products from NOAA coral reef watch". In: *Remote Sensing* 6.11, pp. 11579–11606. DOI: 10.3390/rs61111579.

Long, Xia, Yurong Ma, and Limin Qi (2014). "Biogenic and synthetic high magnesium calcite - A review". In: *Journal of Structural Biology* 185.1, pp. 1–14. DOI: 10.1016/j.jsb.2013.11.004.

Lotze, Heike K. et al. (2019). "Global ensemble projections reveal trophic amplification of ocean biomass declines with climate change". In: *Proceedings of the National Academy of Sciences of the United States of America* 116.26, pp. 12907–12912. DOI: 10.1073/pnas.1900194116.

Lutz, S. J. and A. H. Martin (2014). *Fish Carbon: Exploring Marine Vertebrate Carbon Services*. Arendal, Norway: GRID-Arendal.

MacNeil, M. Aaron et al. (2015). "Recovery potential of the world's coral reef fishes". In: *Nature* 520.7547, pp. 341–344. DOI: 10.1038/nature14358.

Magneville, Camille et al. (2022). "mFD: an R package to compute and illustrate the multiple facets of functional diversity". In: *Ecography* 2022.1, pp. 1–15. DOI: 10.1111/ecog.05904.

Maier, Marco J (2014). *DirichletReg : Dirichlet Regression for Compositional Data in R*. Tech. rep. January. WU Vienna: University of Economics, Business Institute for Statistics, and Mathematics.

Maire, Eva et al. (2016). "How accessible are coral reefs to people? A global assessment based on travel time". In: *Ecology Letters* 19.4, pp. 351–360. DOI: `10.1111/ele.12577`.

Mariani, Gaël et al. (2020). "Let more big fish sink: Fisheries prevent blue carbon sequestration-half in unprofitable areas". In: *Science Advances* 6.44, pp. 1–9. DOI: `10.1126/sciadv.abb4848`.

Martin, Angela Helen et al. (2021). "Integral functions of marine vertebrates in the ocean carbon cycle and climate change mitigation". In: *One Earth* 4.5, pp. 680–693. DOI: `10.1016/j.oneear.2021.04.019`.

Micheli, Fiorenza and Benjamin S. Halpern (2005). "Low functional redundancy in coastal marine assemblages". In: *Ecology Letters* 8.4, pp. 391–400. DOI: `10.1111/j.1461-0248.2005.00731.x`.

Mora, Camilo et al. (2011). "Global human footprint on the linkage between biodiversity and ecosystem functioning in reef fishes". In: *PLoS Biology* 9.4, e1000606. DOI: `10.1371/journal.pbio.1000606`.

Morais, Renato A et al. (2020a). "Severe coral loss shifts energetic dynamics on a coral reef". In: *Functional Ecology* 34, pp. 1507–1518. DOI: `10.1111/1365-2435.13568`.

Nakamura, Gabriel, Aline Richter, and Bruno E. Soares (2021). "FishPhyloMaker: An R package to generate phylogenies for ray-finned fishes". In: *Ecological Informatics* 66.June, p. 101481. DOI: `10.1016/j.ecoinf.2021.101481`.

Orio, Alessandro, Yvette Heimbrand, and Karin Limburg (2022). "Deoxygenation impacts on Baltic Sea cod: Dramatic declines in ecosystem services of an iconic keystone predator". In: *Ambio* 51.3, pp. 626–637. DOI: `10.1007/s13280-021-01572-4`.

Oschlies, Andreas et al. (2018). "Drivers and mechanisms of ocean deoxygenation". In: *Nature Geoscience* 11.7, pp. 467–473. DOI: `10.1038/s41561-018-0152-2`.

Parravicini, V. et al. (2021). "Coral reef fishes reveal strong divergence in the prevalence of traits along the global diversity gradient". In: *Proceedings of the Royal Society B: Biological Sciences* 288, p. 20211712. DOI: `10.1098/rspb.2021.1712`.

Parravicini, Valeriano et al. (2013). "Global patterns and predictors of tropical reef fish species richness". In: *Ecography* 36.12, pp. 1254–1262. DOI: `10.1111/j.1600-0587.2013.00291.x`.

Parravicini, Valeriano et al. (2020). "Delineating reef fish trophic guilds with global gut content data synthesis and phylogeny". In: *PLoS Biology* 18.12, e3000702. DOI: `10.1371/journal.pbio.3000702`.

Pearl, Judea (2009). *Causality: models, reasoning and inference*. 2nd. Cambridge, UK: Cambridge University Press.

Péquignet, A. C. et al. (2011). "The dissipation of wind wave energy across a fringing reef at Ipan, Guam". In: *Coral Reefs* 30.SUPPL. 1, pp. 71–82. DOI: `10.1007/s00338-011-0719-5`.

Pereira, Pedro Henrique Cipresso et al. (2018). "Effects of depth on reef fish communities: Insights of a deep refuge hypothesis from Southwestern Atlantic reefs". In: *PLoS ONE* 13.9, e0203072. DOI: `10.1371/journal.pone.0203072`.

Perry, Chris T. et al. (2011). "Fish as major carbonate mud producers and missing components of the tropical carbonate factory". In: *Proceedings of the National Academy of Sciences* 108.10, pp. 3865–3869. DOI: 10.1073/pnas.1015895108.

Plummer, L. Niel and Eurybiades Busenberg (1982). "The solubilities of calcite, aragonite and vaterite in CO2-H2O solutions between 0 and 90řC, and an evaluation of the aqueous model for the system CaCO3-CO2-H2O". In: *Geochimica et Cosmochimica Acta* 46.6, pp. 1011–1040. DOI: 10.1016/0016-7037(82)90056-4.

Pu, Zhichao et al. (2014). "Phylogenetic diversity stabilizes community biomass". In: *Journal of Plant Ecology* 7.2, pp. 176–187. DOI: 10.1093/jpe/rtt071.

Qu, Bo (2015). "Photosynthetically Active Radiation, Ice Cover, and Sea Surface Temperature". In: *The Impact of Melting Ice on the Ecosystems in Greenland Sea: Correlations on Ice Cover, Phytoplankton Biomass, AOD and PAR*, pp. 49–63. DOI: 10.1007/978-3-642-54498-9_4.

R Core Team (2021). *R: a language and environment for statistical computing*.

Rabosky, Daniel L. et al. (2018). "An inverse latitudinal gradient in speciation rate for marine fishes". In: *Nature* 559.7714, pp. 392–395. DOI: 10.1038/s41586-018-0273-1.

Robinson, James P.W. et al. (2017). "Fishing degrades size structure of coral reef fish communities". In: *Global Change Biology* 23.3, pp. 1009–1022. DOI: 10.1111/gcb.13482.

Robinson, James P.W. et al. (2018). "Environmental conditions and herbivore biomass determine coral reef benthic community composition: implications for quantitative baselines". In: *Coral Reefs* 37.4, pp. 1157–1168. DOI: 10.1007/s00338-018-01737-w.

Robinson, James P.W. et al. (2019). "Productive instability of coral reef fisheries after climate-driven regime shifts". In: *Nature Ecology and Evolution* 3.2, pp. 183–190. DOI: 10.1038/s41559-018-0715-z.

Robinson, James P.W. et al. (2022). "Climate-induced increases in micronutrient availability for coral reef fisheries". In: *One Earth* 5.1, pp. 98–108. DOI: 10.1016/j.oneear.2021.12.005.

Rogers, Alice, Julia L. Blanchard, and Peter J. Mumby (2014). "Vulnerability of coral reef fisheries to a loss of structural complexity". In: *Current Biology* 24.9, pp. 1000–1005. DOI: 10.1016/j.cub.2014.03.026.

Russ, Garry R. et al. (2021). "Coral cover a stronger driver of reef fish trophic biomass than fishing". In: *Ecological Applications* 31.1, e02224. DOI: 10.1002/eap.2224.

Saba, Grace K. and Deborah K. Steinberg (2012). "Abundance, composition, and sinking rates of fish fecal pellets in the santa barbara channel". In: *Scientific Reports* 2, p. 716. DOI: 10.1038/srep00716.

Saba, Grace K. et al. (2021). "Toward a better understanding of fish-based contribution to ocean carbon flux". In: *Limnology and Oceanography* 66.5, pp. 1639–1664. DOI: 10.1002/lno.11709.

Salter, Michael A., Chris T. Perry, and Abigail M. Smith (2019). "Calcium carbonate production by fish in temperate marine environments". In: *Limnology and Oceanography* 64.6, pp. 2755–2770. DOI: 10.1002/lno.11339.

Salter, Michael A. et al. (2017). "Phase heterogeneity in carbonate production by marine fish influences their roles in sediment generation and the inorganic carbon cycle". In: *Scientific Reports* 7.1, pp. 1–15. DOI: 10.1038/s41598-017-00787-4.

Salter, Michael A. et al. (2018). "Reef fish carbonate production assessments highlight regional variation in sedimentary significance". In: *Geology* 46.8, pp. 699–702. DOI: `10.1130/G45286.1`.

Salvatteci, Renato et al. (2022). "Smaller fish species in a warm and oxygen-poor Humboldt Current system". In: *Science* 375.6576, pp. 101–104. DOI: `10.1126/science.abj0270`.

Schiettekatte, Nina M D et al. (2022a). "Biological trade-offs underpin coral reef ecosystem functioning". In: *Nature Ecology and Evolution*. DOI: `10.1038/s41559-022-01710-5`.

Schulz, Kai G., Simon Hartley, and Bradley Eyre (2019). "Upwelling Amplifies Ocean Acidification on the East Australian Shelf: Implications for Marine Ecosystems". In: *Frontiers in Marine Science* 6, p. 636. DOI: `10.3389/fmars.2019.00636`.

Seguin, Raphael et al. (2022). "Towards process-oriented management of tropical reefs in the anthropocene". In: *Nature Sustainability*. DOI: `10.1038/s41893-022-00981-x`.

Selig, Elizabeth R. et al. (2019). "Mapping global human dependence on marine ecosystems". In: *Conservation Letters* 12.2, pp. 1–10. DOI: `10.1111/conl.12617`.

Sing Wong, Amy, Spyridon Vrontos, and Michelle L. Taylor (2022). "An assessment of people living by coral reefs over space and time". In: *Global Change Biology* 28.23, pp. 7139–7153. DOI: `10.1111/gcb.16391`.

Smithson, Michael and Jay Verkuilen (2006). "A better lemon squeezer? Maximum-likelihood regression with beta-distributed dependent variables". In: *Psychological Methods* 11.1, pp. 54–71. DOI: `10.1037/1082-989X.11.1.54`.

Soler, German A. et al. (2015). "Reef fishes at all trophic levels respond positively to effective marine protected areas". In: *PLoS ONE* 10.10, pp. 1–12. DOI: `10.1371/journal.pone.0140270`.

Spalding, Mark D. et al. (2007). "Marine ecoregions of the world: A bioregionalization of coastal and shelf areas". In: *BioScience* 57.7, pp. 573–583. DOI: `10.1641/B570707`.

Stefanoudis, Paris V. et al. (2019). "Depth-dependent structuring of reef fish assemblages from the shallows to the rariphotic zone". In: *Frontiers in Marine Science* 6, p. 307. DOI: `10.3389/fmars.2019.00307`.

Stuart-Smith, Rick D et al. (2018). "Ecosystem restructuring along the Great Barrier Reef following mass coral bleaching". In: *Nature* 560, pp. 92–96. DOI: `10.1038/s41586-018-0359-9`.

Stuart-Smith, Rick D. et al. (2021). "Habitat loss and range shifts contribute to ecological generalization among reef fishes". In: *Nature Ecology and Evolution* 5.5, pp. 656–662. DOI: `10.1038/s41559-020-01342-7`.

Sulpis, Olivier et al. (2021). "Calcium carbonate dissolution patterns in the ocean". In: *Nature Geoscience* 14.6, pp. 423–428. DOI: `10.1038/s41561-021-00743-y`.

Textor, Johannes et al. (2016). "Robust causal inference using directed acyclic graphs: the R package 'dagitty'". In: *International Journal of Epidemiology* 45.6, pp. 1887–1894. DOI: `10.1093/ije/dyw341`.

Tittensor, Derek P. et al. (2010). "Global patterns and predictors of marine biodiversity across taxa". In: *Nature* 466.7310, pp. 1098–1101. DOI: `10.1038/nature09329`.

Topor, Zachary M. et al. (2019). "Marine protected areas enhance coral reef functioning by promoting fish biodiversity". In: *Conservation Letters* 12, e12638. DOI: `10.1111/conl.12638`.

Villéger, Sébastien et al. (2017). "Functional ecology of fish: current approaches and future challenges". In: *Aquatic Sciences* 79.4, pp. 783–801. DOI: 10.1007/s00027-017-0546-z.

Weiss, R. F. (1974). "Carbon dioxide in water and seawater: the solubility of a non-ideal gas". In: *Marine Chemistry1* 2.3, pp. 203–215. DOI: 10.5194/bg-13-841-2016.

Williams, Gareth J. and Nicholas A.J. Graham (2019). "Rethinking coral reef functional futures". In: *Functional Ecology* 33.6, pp. 942–947. DOI: 10.1111/1365-2435.13374.

Williams, Gareth J. et al. (2015). "Local human impacts decouple natural biophysical relationships on Pacific coral reefs". In: *Ecography* 38.8, pp. 751–761. DOI: 10.1111/ecog.01353.

Wilson, Rod W. et al. (2009). "Contribution of fish to the marine inorganic carbon cycle". In: *Science* 323.January, pp. 359–362. DOI: 10.1126/science.1157972.

Woosley, Ryan J., Frank J. Millero, and Martin Grosell (2012). "The solubility of fish-produced high magnesium calcite in seawater". In: *Journal of Geophysical Research: Oceans* 117.4, pp. 1–5. DOI: 10.1029/2011JC007599.

Wootton, Henry F. et al. (2022). "Smaller adult fish size in warmer water is not explained by elevated metabolism". In: *Ecology Letters* January, pp. 1–12. DOI: 10.1111/ele.13989.

Yeager, Lauren A. et al. (2017). "Marine Socio-Environmental Covariates: queryable global layers of environmental and anthropogenic variables for marine ecosystem studies". In: *Ecology* 98.7, p. 1976. DOI: 10.1002/ecy.1884.

Supplementary information

Supplementary Methods

RLS data curation

To prevent bias in the total biomass estimates we cleaned the raw RLS database by removing: (i) small fishes likely to be recently-settled juveniles (defined as all fishes in the 2.5 cm size class and fishes in the 5 cm size classes belonging to species with a maximum body size $\geq$ 25 cm, Stuart-Smith et al. 2021), (ii) small cryptobenthic reef fishes (defined here as all fishes belonging to the 17 core families identified by Brandl et al. (2018)) as they are largely underestimated by visual censuses due to their small size and highly cryptic nature (Brandl et al. 2018), (iii) fish belonging to the order Anguilliformes, likely underestimated due to their cryptic behaviour, and (iv) implausible estimated body sizes (defined by an estimated size more than twice the maximum body size of the species, or more than the maximum body size plus 50 cm, for fish in size classes below and above 50 cm, respectively, $n = 166$).

Description of potential drivers and other covariates

Ecological variables

From each RLS transect we computed the i) fish standing biomass, ii) median body mass (as an index of size structure), iii) biomass-weighted mean trophic level based on species-specific trophic levels obtained from FishBase (Froese and Pauly 2021) (as an index of trophic structure), and iv) six complementary indices of taxonomic, phylogenetic, and functional diversity. For each diversity component, we calculated attribute diversity based on Hill numbers of order q (Chao et al. 2014) for $q = 0$ (richness) and $q = 1$ (entropy). For taxonomic diversity, $q = 0$ is equivalent to species richness, while $q = 1$ to the exponential of Shannon entropy (Chao et al. 2014), and they represent the effective number of species. We calculated phylogenetic diversity (i.e., effective number of equally distinct lineages) using the R package *HillR* (Chao et al. 2010; Li 2018). For this we built a

phylogeny using the R package *FishPhyloMaker* (Nakamura et al. 2021) which uses the phylogeny of the Fish Tree of Life (Rabosky et al. 2018) as a backbone and inserts taxa in a sequential order based on their taxonomic hierarchy. Of the 1,050 taxa in our dataset, 791 where present in the Fish Tree of Life, 242 where inserted as congeners, and 17 at the family level. Fish functional diversity was calculated based on four traits: (i) maximum total length; (ii) trophic guild (i.e., sessile invertivores, herbivores/microvores/detritivores, corallivores, piscivores, microinvertivores, macroinvertivores, crustacivores, and planktivores) (Parravicini et al. 2020); (iii) period of activity (i.e., diurnal, nocturnal, or both); and (iv) vertical position in the water column (i.e., pelagic, bentho-pelagic, or benthic). We computed the Gower distance between all pairs of species and computed Chao's $^qFD(\Delta(\tau))$ index (Chao et al. 2019) for $q = 0$ and $q = 1$, which can be interpreted as the effective number of functionally equally distinct species, using the R package *mFD* (Magneville et al. 2022). We used the average functional distance as the level of threshold distinctiveness (τ). All indices of order $q = 1$ were computed weighting species by their relative biomass.

Environmental variables

Depth and geographic coordinates of the transects were recorded *in situ* by the RLS divers. Additionally, we compiled data for the following variables per site: SST, DHW, NPP, pH, dissolved oxygen, nitrate and phosphate concentrations, PAR, and wave energy. SST and DHW (a measure of accumulated thermal stress) were sourced from CoralReefWatch v3.1 (Liu et al. 2014), NPP based on Standard Vertically Generalized Production Model (VGPM) (Behrenfeld and Falkowski 1997) from Ocean Productivity (`http://sites.science.oregonstate.edu/ocean.productivity/`), pH from the Norwegian Earth System Model forced ocean simulation (NorESM2) (`https://wiki.met.no/noresm/start`), and all four variables were averaged across 5-year periods prior to the surveys. Mean oxygen, nitrate and phosphate concentrations, as well as PAR were extracted from Bio-Oracle through the R package *sdmpredictors* (Assis et al. 2018). Values for these four variables were missing from 35 transects in the final dataset. Wave energy

was obtained from the MSEC database (Yeager et al. 2017) and this variable was missing from 20 transects. To characterise benthic community structure we performed two separate PCAs based on ten and five benthic groups (Supplementary Table 3.1, Supplementary Figs. 3.13 and 3.14). We then extracted the coordinates of each transect on the first three axes, which collectively explained 61% and 99% of the variation in the dataset for the ten and five group classifications, respectively. The coordinates from the PCA based on ten benthic groups were used in the main analysis, and a sensitivity analysis was performed using the coordinates from the PCA based on five benthic groups.

Socio-economic variables

The type of management at the time of survey (i.e., fished: area open to fishing without restrictions; restricted-take: area subject to some form of fishing restrictions, e.g., size or effort limits; no-take: area where fishing is prohibited) was determined for each site based on expert opinion of the RLS data curators and checked with the World Database on Protected Areas (`http://protectedplanet.net/`). Additionally, we calculated the total human gravity within 500 km of each reef site, an indicator of the amount of human pressure on a reef (Cinner et al. 2018). Gravity integrates both the size of the human population and a surrogate for distance, travel time, which also accounts for landscape heterogeneity, road networks, and coastline tortuosity (Maire et al. 2016). For every 1-by-1 km grid cell within a 500 km radius of a reef site, we calculated gravity by dividing the population size of that cell by the squared travel time between the cell and the reef site (Maire et al. 2016). We then summed the gravity values of all cells within 500 km of the reef site. A 500 km radius was chosen as the maximum distance within which any fishing or land use activities could influence tropical and subtropical reefs (Cinner et al. 2018; Seguin et al. 2022). For each country, we also retrieved data for national Human Development Index (HDI) and the degree of human dependence on marine ecosystems, which integrates nutritional, economic, and coastal protection dependence (Selig et al. 2019).

Testing DAG-data consistency

Our final DAG implied 500 conditional independencies. To ensure DAG-data consistency we tested all the 500 independencies against our data through linear tests using the R package *dagitty* (Textor et al. 2016). For this step we used a filtered dataset of 1,374 transects with complete observations (i.e., no missing data). Due to the relatively large size of our dataset even very weak associations between variables may yield small p-values (Ankan et al. 2021). Therefore, to identify violations of implied independencies we focused on absolute effect sizes (partial correlation coefficients) greater than 0.3. These represented ~3.2% ($n = 16$) of all tests and mainly showed modest correlations (<0.4). Only 4 independencies were relatively strongly contradicted by the data with absolute effect sizes between 0.42 and 0.76, suggesting association, conditional on PAR, between pH and a few variables (HDI, latitude, and marine ecosystem dependency), and between SST and latitude. However, no direct link exists between any of these variables. Instead, these violated independencies are readily explained by the low resolution of remotely-sensed PAR data, which do not reflect well the indirect link between latitude and SST through solar radiation. Therefore, we ignored these residual correlations and did not add unsupported links to our DAG.

Example of Bayesian imputation

The causal effect of DHW on carbonate excretion was modelled as follows:

$$\text{carb}_i \sim \text{Normal}(\mu_i, \sigma)$$

$$\mu_i = \beta_0 + \beta_1 \text{DHW}_i + \beta_2 \text{PAR}_i + \gamma_{\text{country}} + \gamma_{\text{country:site}}$$

$$\text{PAR}_i \sim \text{Normal}(\nu_i, \sigma_{\text{PAR}})$$

$$\nu_i = \beta_{0,\text{PAR}} + \beta_{1,\text{PAR}} \text{Latitude}_i + \gamma_{\text{country,PAR}}$$

$$\beta_{0,\text{PAR}} \sim \text{Normal}(0, 1) \tag{S3.1}$$

$$\beta_{1,\text{PAR}} \sim \text{Normal}(0, 1)$$

$$\gamma_{\text{country,PAR}} \sim \text{Normal}(0, \tau_{\text{country,PAR}})$$

$$\tau_{\text{country,PAR}} \sim \text{Student}(3, 0, 2.5)$$

$$\sigma_{\text{PAR}} \sim \text{Cauchy}(0, 1)$$

where ν_i is the average predicted PAR, $\beta_{0,\text{PAR}}$ is the global intercept for PAR, $\beta_{1,\text{PAR}}$ is the regression coefficient of latitude on PAR, $\gamma_{\text{country,PAR}}$ represents country-level variation in PAR, $\tau_{\text{country,PAR}}$ is the standard deviations of the group-level effect, and σ_{PAR} is the residual standard deviation for PAR. Remaining priors were as described in equations (3.1) and (3.5) in the main text.

Supplementary Figures
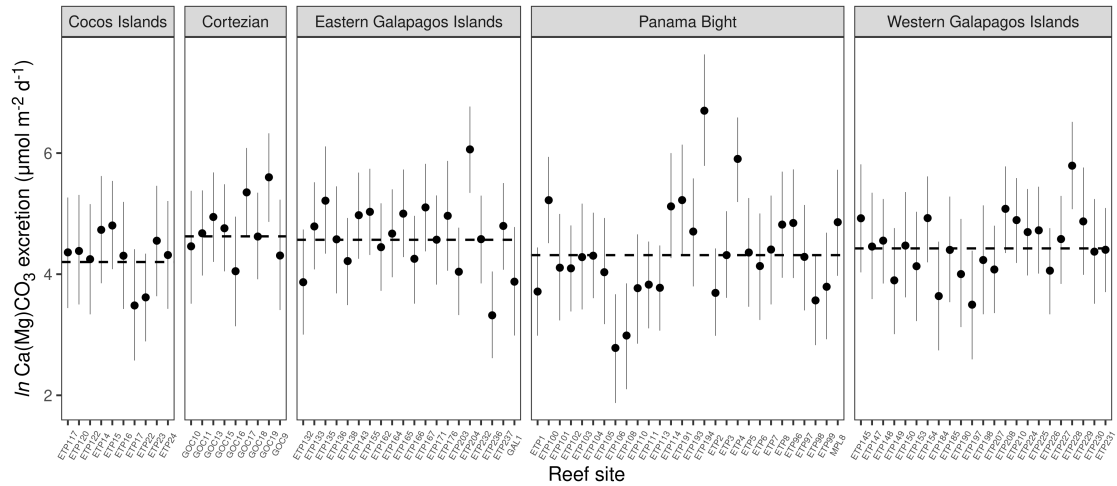
Figure 3.6: Variability in reef fish carbonate excretion within ecoregions of the Tropical Eastern Pacific realm. Circles and lines represent site-level predictions of fish carbonate excretion (medians and 95% credible intervals, respectively), whereas dashed lines represent ecoregion-level median predictions.
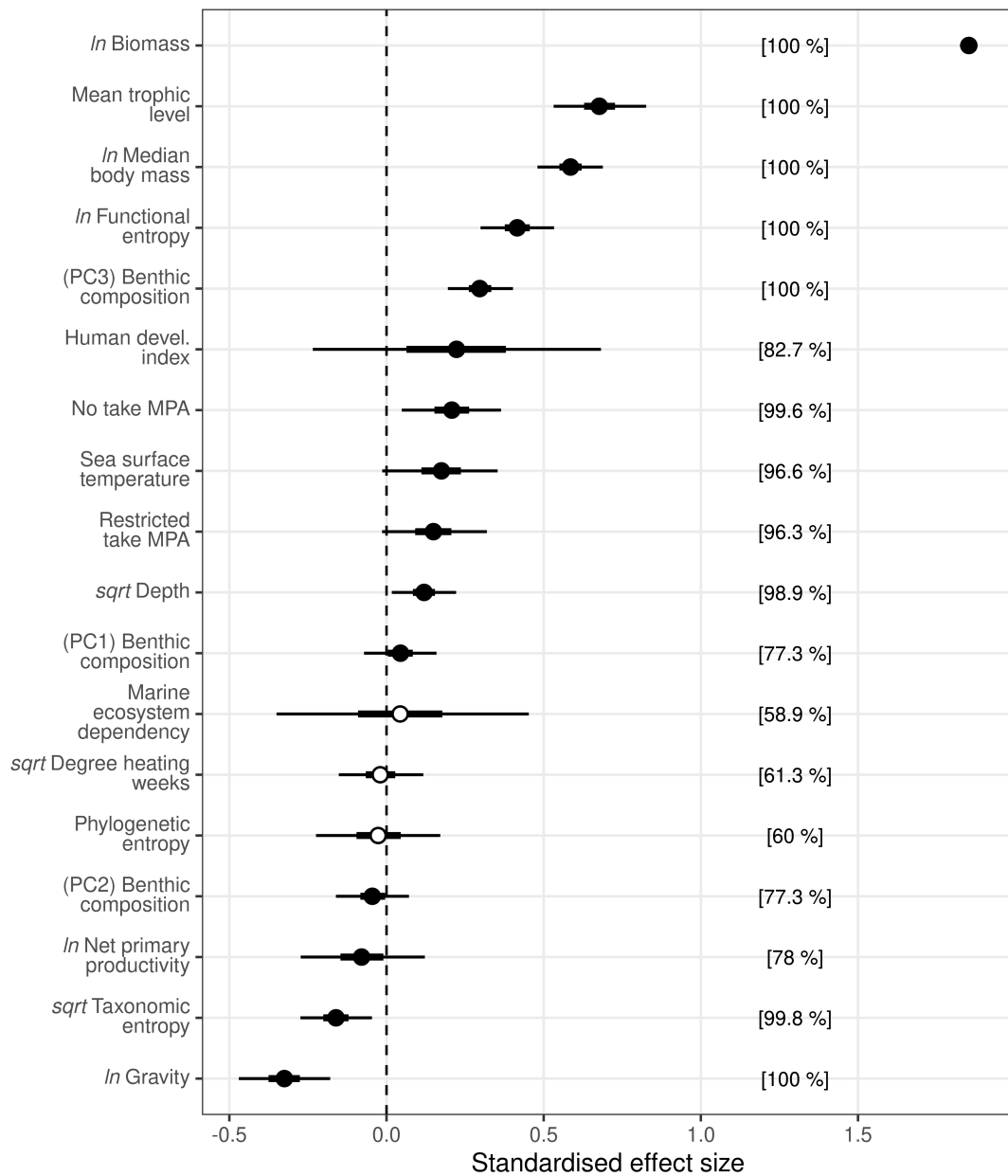
Figure 3.7: Drivers of reef fish carbonate excretion using a filtered dataset.
Estimates are posterior medians (circles), 50% credible intervals (CIs; thick lines; some
are too narrow to be seen) and 95% CIs (thin lines) from DAG-informed Bayesian
multilevel regressions fitted to a filtered dataset with complete observations ($n = 1{,}374$),
and represent total causal effects. White circles depict effects with a 50% CI overlapping
zero. Percentages represent the posterior probability that an effect is either positive
(when the median in above zero) or negative (when the median is below zero). PC1-PC3
are the transect scores on the first three axes of a principal component analysis of benthic
composition classified into ten groups. MPA, Marine Protected Area.

Figure 3.8: Drivers of reef fish carbonate mineralogy. Estimates are posterior medians (circles) and 95% credible intervals (CIs; lines) from DAG-informed Bayesian multilevel Dirichlet regressions fitted to a filtered dataset with complete observations ($n = 1,374$), and represent total causal effects. White circles depict effects with a CI overlapping zero. PC1-PC3 are the transect scores on the first three axes of a principal component analysis of benthic composition classified into ten groups. MPA, Marine Protected Area. LMC, low-Mg calcite; ARA, aragonite; HMC, high-Mg calcite; MHC, monohydrocalcite; ACMC, amorphous Ca-Mg carbonate.
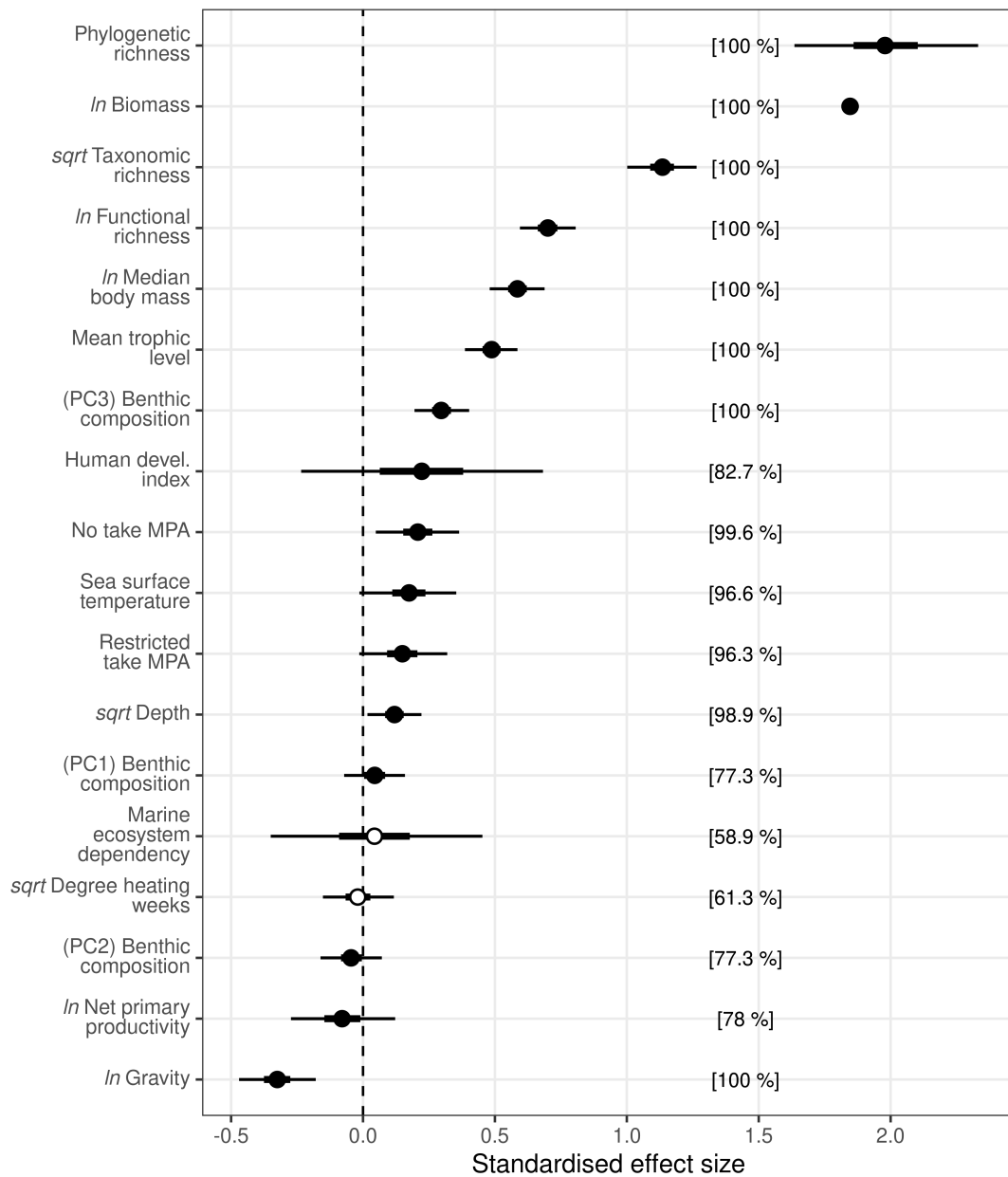
Figure 3.9: Drivers of reef fish carbonate excretion using *richness* indices of biodiversity. Estimates are posterior medians (circles), 50% credible intervals (CIs; thick lines; some are too narrow to be seen) and 95% CIs (thin lines) from DAG-informed Bayesian multilevel regressions fitted to a filtered dataset with complete observations (n = 1,374), and represent total causal effects. White circles depict effects with a 50% CI overlapping zero. Percentages represent the posterior probability that an effect is either positive (when the median in above zero) or negative (when the median is below zero). PC1-PC3 are the transect scores on the first three axes of a principal component analysis of benthic composition classified into ten groups. MPA, Marine Protected Area.

Figure 3.10: Relationship between reef fish carbonate excretion and biodiversity. The three transects with the highest carbonate excretion are labelled with their respective ecoregion name. Each point is coloured by the number of neighboring points.
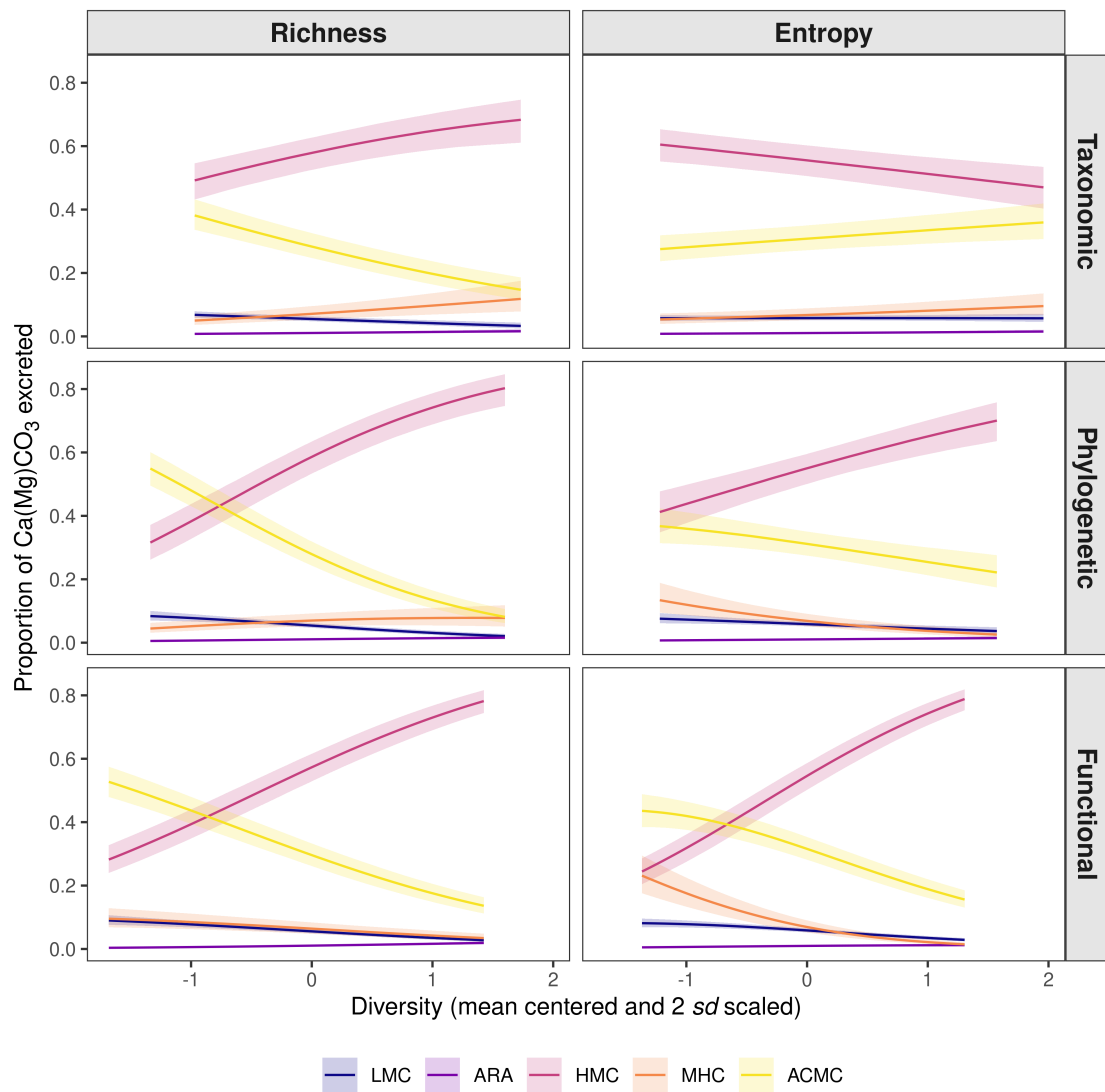
Figure 3.11: Causal effects of biodiversity on reef fish carbonate mineralogy.
Fitted lines and ribbons are posterior medians and 95% credible intervals from DAG-informed Bayesian multilevel Dirichlet regressions fitted to a filtered dataset with complete observations ($n = 1{,}374$), and represent conditional effects after accounting for the influence of all confounding variables, which were set to their mean values. LMC, low-Mg calcite; ARA, aragonite; HMC, high-Mg calcite; MHC, monohydrocalcite; ACMC, amorphous Ca-Mg carbonate.
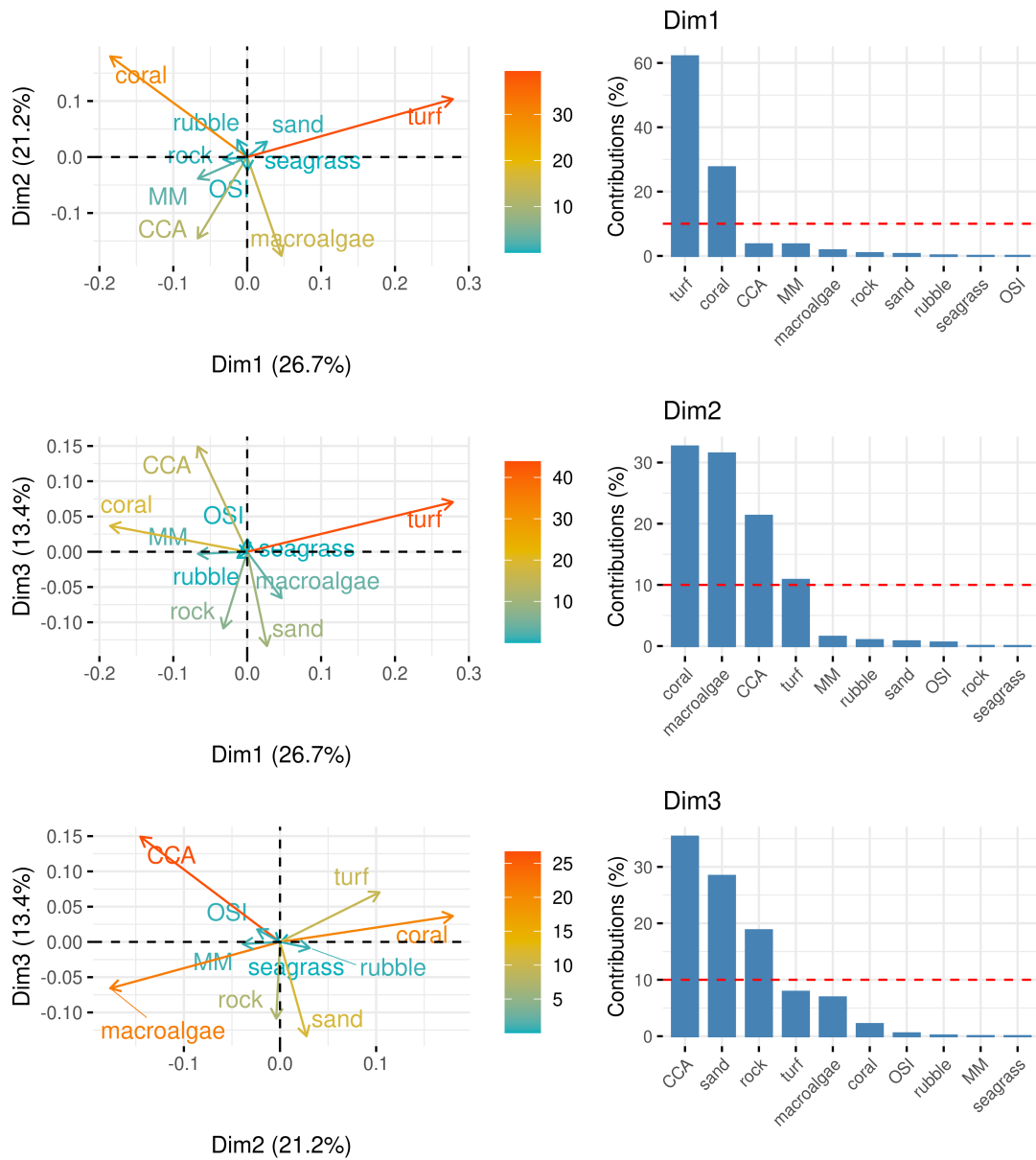
Figure 3.12: Principal Component Analysis (PCA) of benthic composition classified into ten groups. Graphs of variables show the direction of each benthic group along the first three dimensions of the PCA, coloured by their relative contributions. Barplots show the relative contribution of benthic groups to each of the first three dimensions of the PCA. Red dashed lines correspond to the expected value if the contributions were uniform. CCA, Crustose Coralline Algae; MM, Microalgal Mats; OSI, Other Sessile Invertebrates.
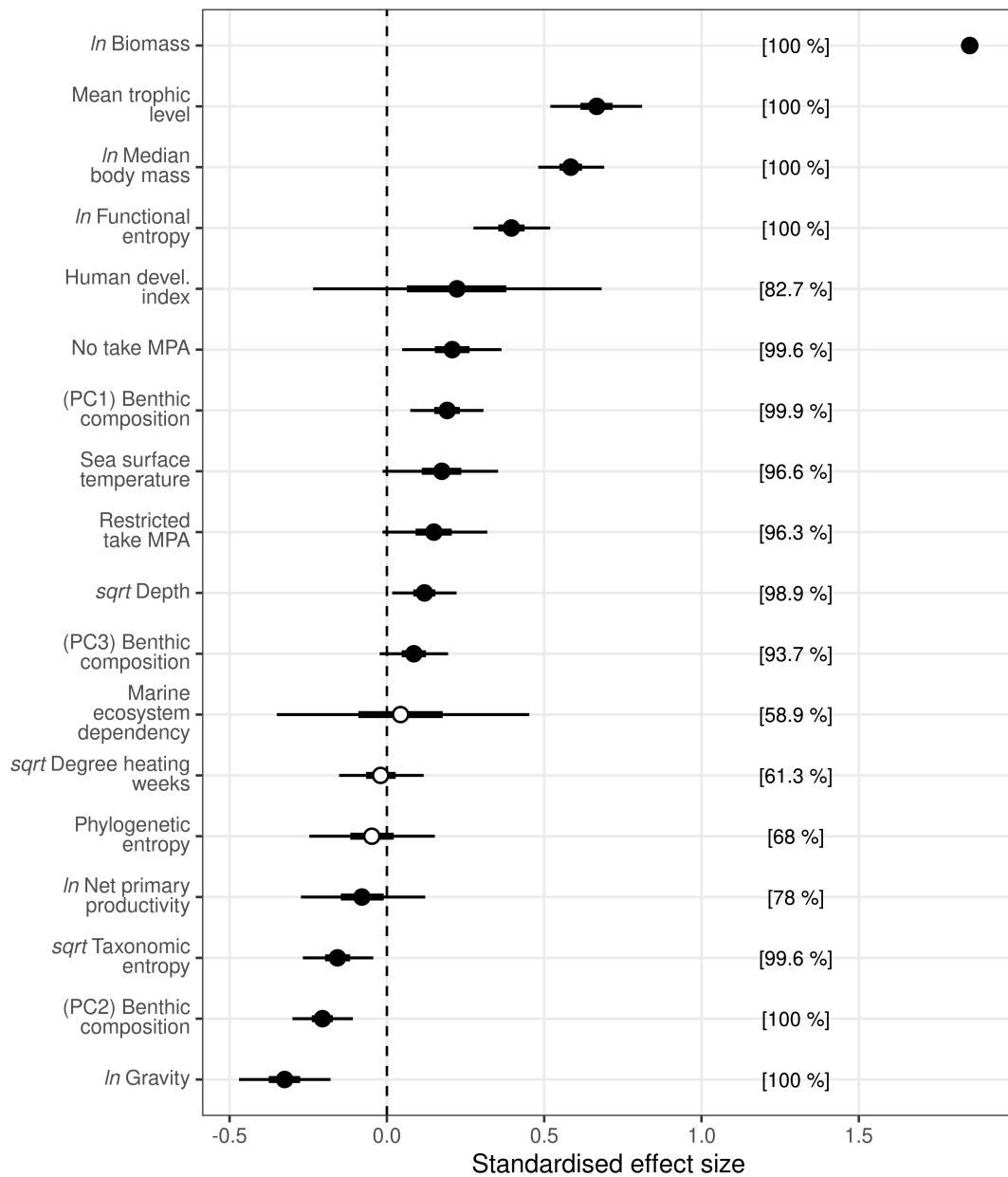
Figure 3.13: Drivers of reef fish carbonate excretion using a broader benthic classification. Estimates are posterior medians (circles), 50% credible intervals (CIs; thick lines; some are too narrow to be seen) and 95% CIs (thin lines) from DAG-informed Bayesian multilevel regressions fitted to a filtered dataset with complete observations (n = 1,374), and represent total causal effects. White circles depict effects with a 50% CI overlapping zero. Percentages represent the posterior probability that an effect is either positive (when the median in above zero) or negative (when the median is below zero). PC1-PC3 are the transect scores on the first three axes of a principal component analysis of benthic composition classified into five groups. MPA, Marine Protected Area.
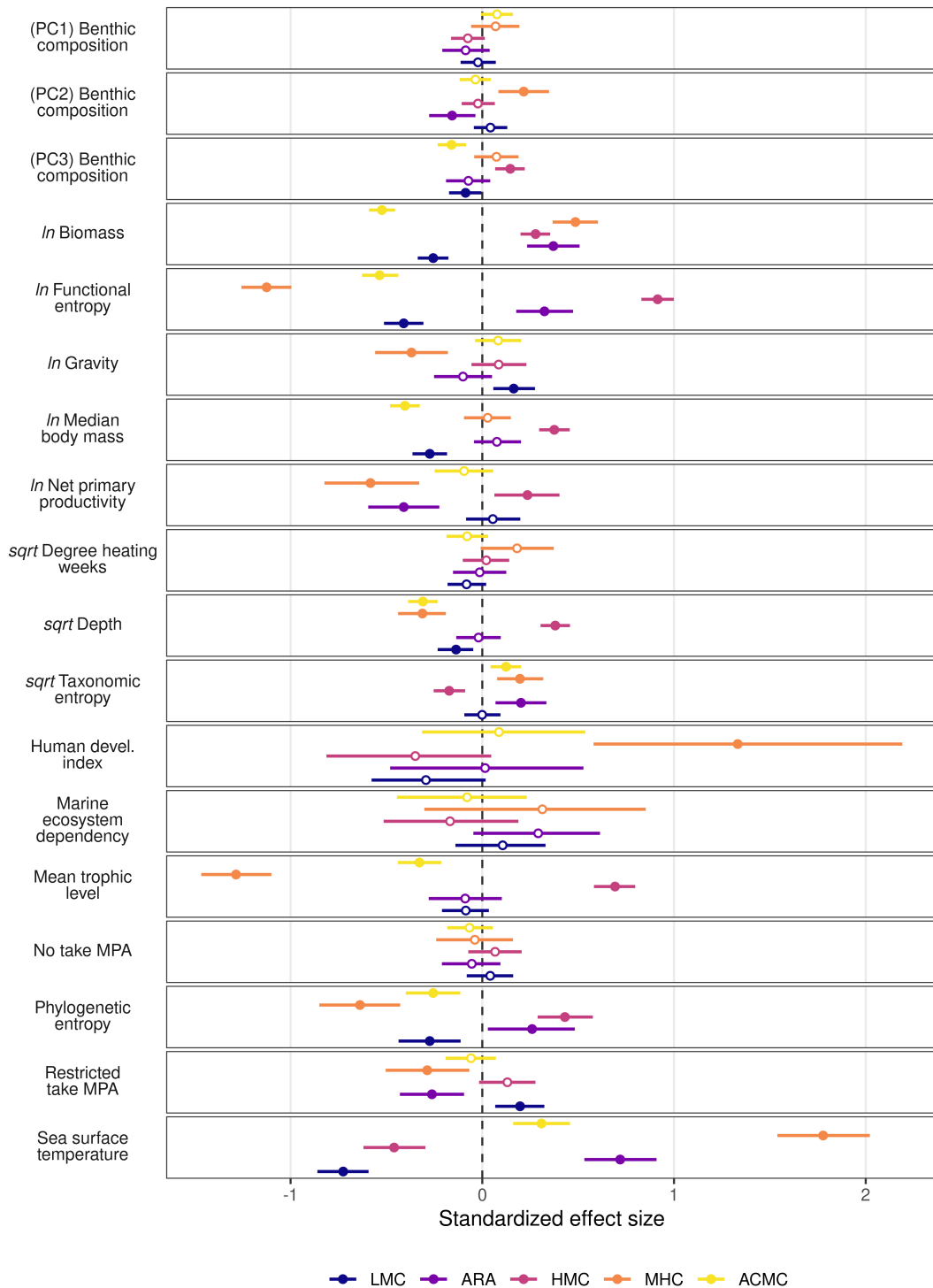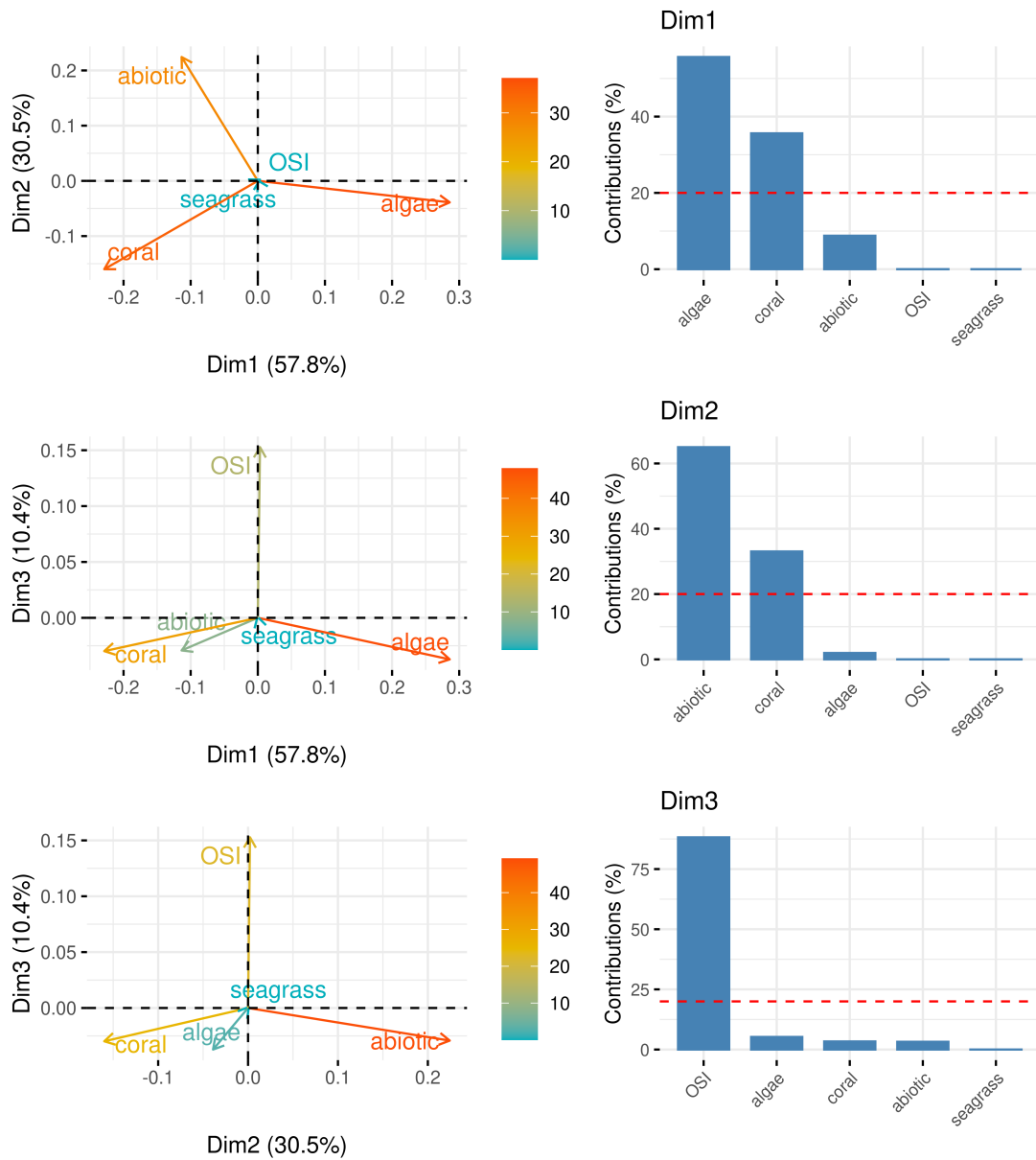
Figure 3.14: Principal Component Analysis (PCA) of benthic composition classified into five groups. Graphs of variables show the direction of each benthic group along the first three dimensions of the PCA, coloured by their relative contributions. Barplots show the relative contribution of benthic groups to each of the first three dimensions of the PCA. Red dashed lines correspond to the expected value if the contributions were uniform. OSI, Other Sessile Invertebrates.
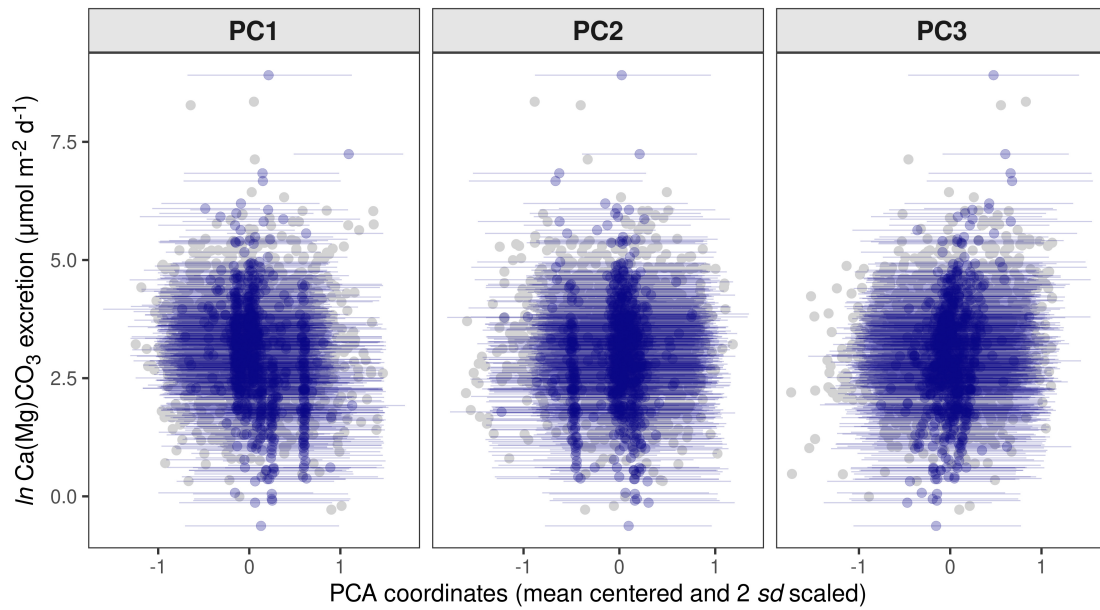
Figure 3.15: Relationship between reef fish carbonate excretion and benthic community structure showing imputed missing values. Benthic community structure is represented by the transect scores on the first three dimensions of a PCA based on ten benthic groups. Grey points ($n = 1,400$) are observed data, whereas coloured points ($n = 769$) and lines are posterior means and 95% credible intervals, respectively, of imputed benthic community structure as a function of sea surface temperature, net primary productivity, depth, latitude, country, and reef site.

Supplementary Tables

Table 3.1: Benthic classification from photoquadrats.

5 categories	10 categories
algae	crustose coralline algae (CCA)
	macroalgae
	microalgal mats
	turf
coral	coral
other sessile invertebrates	other sessile invertebrates
abiotic	rock
	rubble
	sand
seagrass	seagrass

Table 3.2: Justification for the causal links in our Directed Acyclic Graph.

Causal link	Rationale
Fish biomass -> Carbonate	Carbonate excretion rate is inherently related to body mass (Wilson et al. 2009; Ghilardi et al. 2023b) and linked to fish abundance. Fish communities with higher biomass are expected to excrete more carbonate, regardless of the structure and composition of the community.
Median body mass -> Carbonate	Smaller individuals excrete more carbonate per unit mass than larger individuals (Wilson et al. 2009; Ghilardi et al. 2023b). Consequently, fish communities with higher median body mass are expected to excrete less carbonate per unit biomass than those with lower median body mass. Body mass is positively related to the excretion rate of all carbonate forms produced by fish, but variability in the strength of that relationship can lead to changes in the carbonate composition along median body mass gradients (Ghilardi et al. 2023b).
Mean trophic level -> Carbonate	The trophic level is negatively related to the relative intestinal length (Ghilardi et al. 2021b), which has a negative effect on individual carbonate excretion rates and influences the mineralogical composition of excreted carbonates (Ghilardi et al. 2023b).
Fish biodiversity -> Carbonate	Taxonomic diversity can influence carbonate excretion as fish families differ in their carbonate excretion rate and mineralogical composition (Salter et al. 2018; Ghilardi et al. 2023b). Moreover, multiple facets of biodiversity are often linked to ecosystem functions on coral reefs, and could also influence carbonate excretion (Villéger et al. 2017). Functional diversity, for instance, likely influence carbonate excretion and mineralogy as these are linked to multiple fish traits (Ghilardi et al. 2023b).
SST -> Carbonate	Individual carbonate excretion rate increases with temperature, which also influences the mineralogical composition of the excreted carbonates (Wilson et al. 2009; Heuer et al. 2016; Ghilardi et al. 2023b).
Mean trophic level -> Fish biomass	Fish trophic structure can influence reef fish biomass. The highest biomass can be found in reefs dominated by intermediate consumer levels (e.g., planktivores) which can sustain high biomass of predators (Heenan et al. 2019). However, when sharks and pelagic fish are not considered, such as in our analysis, communities with low mean trophic level generally lead to higher biomass through large abundance and biomass of herbivores (Graham et al. 2017).
Median body mass -> Fish biomass	Median body mass influences fish standing biomass primarily through the presence or absence of large-bodied fishes (Lefcheck et al. 2021).
Fish biodiversity -> Fish biomass Fish biodiversity -> Mean trophic level	Higher biodiversity (in species, traits and lineages) can increase the likelihood of complementary resource use, positive interactions like facilitation, and the presence of particular species in the community which in turn, influence fish biomass and trophic structure (Cardinale et al. 2006; Pu et al. 2014; Duffy et al. 2016).
Depth -> Fish biomass Depth -> Fish biodiversity	Deeper reefs lead to higher fish biomass and diversity through the reduction of fishing pressure (Duffy et al. 2016; Pereira et al. 2018; Stefanoudis et al. 2019).

Causal link	Rationale
Marine ecosystem dependency -> Fish biomass	Marine ecosystem dependency is obtained from nutritional, economic (fisheries), and coastal protection dependence on marine ecosystems (Selig et al. 2019). Countries which are more dependent on marine ecosystems influences fish biomass through higher fishing pressure.
Oxygen -> Fish biomass Oxygen -> Median body mass	Oxygen-poor waters are unsuitable to many species and reduce fish growth leading to smaller fish size and lower biomass (Orio et al. 2022; Salvatteci et al. 2022).
NPP -> Fish biomass NPP -> Mean trophic level NPP -> Fish biodiversity	Areas with higher net primary productivity (NPP) are able to support a larger fish biomass, particularly at high trophic levels (Heenan et al. 2019; Graham et al. 2017). High primary production can also promote biodiversity by sustaining large population sizes, thereby averting extinction and promoting niche specialists (Tittensor et al. 2010; Graham et al. 2018).
Human gravity -> Fish biomass Human gravity -> Median body mass Human gravity -> Mean trophic level Human gravity -> Fish biodiversity	Higher human gravity is associated with increased fishing pressure and other negative human impacts (e.g., habitat degradation, pollution, tourism), which in turn reduces reef fish biomass (Cinner et al. 2016; Cinner et al. 2018; Cinner et al. 2020) and can influence fish taxonomic, functional, and phylogenetic diversity (D'Agata et al. 2014), as well as their size and trophic structure through the selective removal of large individuals and predators (Graham et al. 2005; Edwards et al. 2014; Graham et al. 2017; Robinson et al. 2017; Cinner et al. 2020; Lefcheck et al. 2021).
Fisheries management -> Fish biomass Fisheries management -> Median body mass Fisheries management -> Mean trophic level Fisheries management -> Fish biodiversity	Fishing restrictions and no-take MPAs generally lead to higher reef fish biomass and increases in biodiversity and abundance of large individuals and predators through the reduction of fishing pressure (Edwards et al. 2014; Soler et al. 2015; MacNeil et al. 2015; Emslie et al. 2015; Topor et al. 2019; Cinner et al. 2020).
Benthic composition -> Fish biomass Benthic composition -> Median body mass Benthic composition -> Mean trophic level Benthic composition -> Fish biodiversity	Benthic composition, especially the cover of hard corals, determines the physical three-dimensional structure (or structural complexity) of coral reefs and reefs with higher cover of hard corals provide more habitats and refuges for reef fishes which can result in higher fish biomass and diversity (Darling et al. 2017) and influence fish size structure (Rogers et al. 2014). Benthic composition also affects fish trophic structure, with a greater proportion of herbivores in algal-dominated reefs and a greater proportion of planktivores, corallivores and predators in coral-dominated reefs (Russ et al. 2021).
Taxonomic diversity -> Functional/Phylogenetic diversity	The addition of new species in a community is likely to increase the number of functional traits and lineages represented in the community (Micheli and Halpern 2005).
SST -> Fish biodiversity	Temperature is a major control of diversity on global scale. The underlying assumption of this relationship is that higher temperature would accelerate the metabolic rate which would allow for a higher rate of speciation (Tittensor et al. 2010; Duffy et al. 2016).
SST -> Median body mass	Fishes in warmer waters have typically smaller adult size mainly because they reach maturity earlier than in cooler water (Wootton et al. 2022).
HDI -> Marine ecosystem dependency	Countries with a lower HDI are more nutritionally and economically dependent on marine ecosystems (Selig et al. 2019).

Table 3.2: *(continued)*

Causal link	Rationale
HDI -> Fisheries management	Countries with a higher HDI are likely to have a greater capacity to manage their environment and consequently their reefs are expected to have more protection (Fox et al. 2012; Barlow et al. 2018)
Marine ecosystem dependency -> Fisheries management	Countries that are more dependent on marine ecosystems, such as small island developing states, are likely to be more inclined to manage their marine resources.
PAR -> SST	SST increases with increasing solar radiation and therefore Photosynthetically Available Radiation (PAR) (Qu 2015).
PAR -> DHW	Higher solar radiation, and therefore higher PAR, is expected to increase the likelihood of accumulating Degree Heating Weeks (DHW).
Latitude -> PAR	Latitudinal differences in solar elevation affect the quantity and quality of PAR entering the water column, and higher latitudes have greater seasonal variability in PAR (Campbell and Aarup 1989).
Latitude -> HDI	HDI is positively correlated with the distance from the equator (Kummu and Varis 2011).
Latitude -> Human gravity	Human population density is related to latitude (Kummu and Varis 2011). Human gravity on coral reefs was strongly related to latitude (Karkarey et al. 2022).
HDI -> Human gravity	Lower-middle-income countries are the income group with the highest human population within 5-100 km from coral reefs, and low-income countries have the highest human population density within 5 km from coral reefs (Sing Wong et al. 2022). HDI is therefore expected to have a negative effect on human gravity.
Latitude -> Nitrate / Phosphate	Nitrate and phosphate have higher concentrations at high latitudes (Levitus et al. 1993).
PAR -> NPP Nitrate / Phosphate -> NPP SST -> NPP	Light, nutrients, and temperature are the major limiting factors for NPP (Falkowski 2012).
Wave energy -> NPP	Wave exposed reefs are subject to high flushing rates, leading to lower planktonic abundance and primary productivity (Furnas et al. 1990).
Depth -> Wave energy	Wave energy on the reef is strongly depth-limited and decreases with depth (Péquignet et al. 2011).
PAR -> Benthic composition Nitrate / Phosphate -> Benthic composition	PAR and nutrients can influence benthic composition by stimulating algal growth (Burkepile and Hay 2006). Increased nutrients also affect coral physiological performance (D'Angelo and Wiedenmann 2014) and limit coral growth rates (Koop et al. 2001).
NPP -> Benthic composition SST -> Benthic composition Wave energy -> Benthic composition	SST, NPP and wave energy are primary drivers of benthic composition on coral reefs. Reefs dominated by reef-building organisms occurring in warm, productive regions with low wave energy and algal-dominated reefs occurring at lower temperatures and productivity (Williams et al. 2015; Robinson et al. 2018). Benthic community composition largely differ between wave exposed and sheltered reef sites (Lange et al. 2021).
pH -> Benthic composition	Coral reef benthic communities shift across a natural gradient in seawater pH (Barkley et al. 2015).
DHW -> Benthic composition	DHW influences coral abundance through bleaching and mortality, thereby altering benthic composition (Hughes et al. 2017b; Hughes et al. 2018a).

Causal link	Rationale
SST -> pH	Temperature controls the surface pH through two processes: directly through the temperature dependence of the seawater CO_2 chemistry, which results in a positive effect on the pH, and indirectly through the air-sea exchange of CO_2, whereby a increase in temperature decreases the solubility of CO_2 in sea water and favours the outgassing of CO_2 into the atmosphere thus increasing the pH (Weiss 1974; Jiang et al. 2019).
SST -> Oxygen	Sea surface temperature is a primary driver of surface-water oxygen concentrations, and oxygen solubility decreases with increasing temperatures (Oschlies et al. 2018).
NPP -> Oxygen	As photosynthesis consumes CO_2 and releases oxygen, NPP is expected to positively affect oxygen concentrations in seawater.
Upwelling -> SST Upwelling -> Nitrate / Phosphate Upwelling -> pH Upwelling -> Oxygen	Upwelling brings to the surface cold water rich in nutrients and dissolved CO_2 and poor in oxygen (Schulz et al. 2019).

Abbreviations:

SST, sea surface temperature; NPP, net primary productivity; HDI, human development index; PAR, photosynthetically available radiation; DHW, degree heating weeks.

4

Evaluating the effects of human pressure and protection on fish inorganic carbon cycling on Australian coral reefs

Anaëlle Durfort[1,2#], Mattia Ghilardi[2,3#*], Graham J. Edgar[4], Sebastian C. A. Ferse[2,3], Valeriano Parravicini[5,6], Rick D. Stuart-Smith[4], Laure Velez[2], David Mouillot[2,6], Sonia Bejarano[2]

1. MARBEC, Univ Montpellier, CNRS, Ifremer, IRD, 34095 Montpellier, France

2. Leibniz Centre for Tropical Marine Research (ZMT), FahrenheitstraSSe 6, 28359 Bremen, Germany

3. Department of Marine Ecology, Faculty of Biology and Chemistry, University of Bremen, Leobener StraSSe UFT, 28359 Bremen, Germany

4. Institute for Marine and Antarctic Studies, University of Tasmania, Hobart, TAS 7001, Australia.

5. PSL Université Paris: EPHE-UPVD-CNRS, USR3278 CRIOBE, University of Perpignan, 66860 Perpignan, France

6. Institut Universitaire de France, Paris, France

Correspondence: *M. Ghilardi (`mattia.ghilardi91@gmail.com`)

\# These authors contributed equally to this work.

Abstract

Conserving coral reef ecosystem functioning is a key management objective. Measures that consider multiple functions are required. Carbonate excretion is an important function underpinned by reef fishes as it contributes to the inorganic carbon cycle. Yet the extent to which common conservation measures preserve fish-mediated carbonate production is unknown. Using Australian reefs as a case study, we investigate how this biogeochemical function is affected by human pressure and protection level. We use structural equation models to disentangle the indirect effects of human gravity (i.e., a proxy for human pressure) and fisheries management on carbonate excretion and mineralogy. We find a strong negative effect of human gravity on fish-mediated carbonate production, mainly driven by a direct effect on fish biomass. A decrease in biomass is related to both the proximity of humans to reefs and population density. Gravity also has a weak effect on the mineralogical composition of excreted carbonates, decreasing carbonate preservation within sediments. Fisheries management has a weak positive effect on fish biodiversity, but no effect on carbonate excretion and mineralogy. These findings highlight that in countries with relatively low fishing pressure current management measures do not support the production and accumulation of fish carbonates.

4.1   Introduction

Coral reefs are hyperdiverse ecosystems and provide many functions and services to coastal populations (Moberg and Folke 1999). Yet reefs are transforming rapidly in response to increasing anthropogenic disturbances (Hughes et al. 2017a; Hughes et al. 2018a; Stuart-Smith et al. 2018). They are subject to heavy functional reorganisation (Williams and Graham 2019) with implications for the ecosystem services they provide (Woodhead et al. 2019; Eddy et al. 2021). Coral reef integrity and functioning has been internationally recognised as a conservation priority and integrated in the post-2020 global biodiversity framework (`https://www.iucn congress2020.org/motion/122`). Understanding which functions should be

prioritised for conservation is a key challenge (Bellwood et al. 2019a). The core processes underlying the provision of many ecosystem services have been identified (Brandl et al. 2019), but it is now clear that not all functions can be locally maximised (Cinner et al. 2020) due to biological trade-offs (Schiettekatte et al. 2022a). Conservation of coral reefs towards a desirable functional future requires integrated management of multiple functions and an understanding of the context under which certain functions can be sustained.

In addition to their key role in food provisioning, fish also mediate numerous critical ecosystem processes on coral reefs, including geo-ecological functions (Perry et al. 2022). While the role of coral reef fish in bioerosion and sediment reworking is relatively well understood (e.g., Yarlett et al. 2018; Lange et al. 2020), less is known about their contribution to the inorganic carbon cycle. All marine teleosts (bony fish) continuously excrete carbonate that they precipitate in their intestine as a by-product of osmoregulation (Walsh et al. 1991; Wilson et al. 2002). The potential significance of this process for the marine inorganic carbon cycle has been recognised (Wilson et al. 2009). Conservative estimates suggest that fish potentially account for 3-15% of total carbonate production in the world's surface oceans (Wilson et al. 2009). Further, because fish carbonates are high in magnesium content and more soluble than other marine carbonates, they may represent an important source of alkalinity at shallow depth (Wilson et al. 2009). Yet, the role of fish within the carbonate cycle of shallow reefs is poorly understood. While fish contribution to total carbonate production may be relevant where other marine calcifiers are less abundant (Perry et al. 2011), it is potentially trivial on coral reefs. Fish generate reef sediments through bioerosion and framework breakage, with low contributions from intestinal carbonate (Yarlett et al. 2021; Perry et al. 2022). However, these contributions are higher when considering only mud-grade sediment due to the distinct size spectrum of fish carbonate (Perry et al. 2011; Salter et al. 2014).

Fish excrete a diverse range of carbonate polymorphs, including aragonite, low- and high-magnesium calcite (LMC and HMC, respectively), monohydrocalcite

(MHC), and amorphous calcium magnesium carbonate (ACMC) (Foran et al. 2013; Salter et al. 2017; Salter et al. 2018; Salter et al. 2019; Ghilardi et al. 2023b). Existing knowledge suggests that they should have very different dissolution rates. Aragonite and calcite should rapidly sink in the water column and be preserved in sediments in shallow reef environments (Perry et al. 2011). Amorphous carbonate and MHC are unstable carbonate polymorphs and should dissolve rapidly in the water column or after reaching the substrate, or transform into calcite or aragonite (Fukushi et al. 2011; Foran et al. 2013). In high energy settings, fish carbonates may be partially transported offshore where the most stable mineral forms will sink into deeper waters, contributing to carbon export (Salter et al. 2014; Saba et al. 2021).

The mineralogical composition of carbonates excreted by fishes depends on the species, with many families excreting predominantly HMC with generally >20% magnesium content (Perry et al. 2011; Salter et al. 2018; Ghilardi et al. 2023b). This mineral would constitute the largest proportion of fish carbonate accumulated in shallow reef sediments. As HMC is more soluble than aragonite and LMC, it may provide a first line of response against the decreasing saturation state of seawater caused by increasing partial pressure of atmospheric CO_2 and ocean acidification (Morse et al. 2006; Roberts et al. 2017). Indeed, carbonate minerals should dissolve sequentially in response to acidification according to their stability, with initial removal of the most soluble forms (Morse et al. 2006). Therefore, fish carbonates could partially buffer the effects of acidification on other reef organisms whose skeleton or shell consists of aragonite or LMC, although experiments are required to support this hypothesis. Fish carbonate excretion rate and mineralogical composition are linked to fish traits and species identity (Ghilardi et al. 2023b), and are affected by human pressure through changes in fish community structure (Jennings and Wilson 2009). It is therefore urgent to understand the human impact on this fish biogeochemical function and to what extent it is addressed by common management measures such as no-take or restricted-take (i.e., open to some form of fishing) Marine Protected Areas (MPAs).

Tropical and subtropical reefs in Australia provide an ideal case study to assess how human pressure and protection affect ecosystem functioning. They constitute the largest reef area in the world (Burke et al. 2011) and their fish communities have been extensively surveyed, producing large databases suited to quantify ecosystem dynamics through space and time (Edgar et al. 2020). Australian reefs are subject to varying levels of human pressure (through fishing, pollution, sedimentation, coastal development, and tourism) and protection. Australia has implemented a large network of MPAs that together cover about 45% of its waters (`https://parksaustralia.gov.au/marine/`), including the Great Barrier Reef in Queensland and Ningaloo Reef in Western Australia. However, only one quarter of this network is fully protected (i.e., no-take), while the remainder is under partial protection (i.e., restricted-take), where fishing is allowed but subject to some form of restrictions such as gear, size, and effort limits (Roberts et al. 2020).

Here, we investigate how the role of reef fish in the inorganic carbon cycle is affected by the level of protection and human pressure at 796 reef sites in Australia. Specifically, we used Structural Equation Models (SEMs) to: (1) disentangle the mechanisms through which human gravity (i.e., a proxy for human pressure) and fisheries management (i.e., degree of fishing permitted) affect fish carbonate excretion rate and mineralogy; (2) determine whether the effect of human gravity is due to isolation (i.e., travel time to reefs from nearest human settlement), human population density, or both, and whether pathways of influence vary by management category; (3) assess the indirect effects of the MPA age and size on fish carbonate excretion rate and mineralogy; and (4) investigate how this biogeochemical function performed by fish is affected by the cumulative effects of four key MPA features (i.e., no-take, well-enforced, >10 years old, >100 km^2 large) (Edgar and Stuart-Smith 2014).

4.2   Methods

4.2.1   Fish data

We used data from the standardised Reef Life Survey (RLS) monitoring programme (Edgar and Stuart-Smith 2014), in which experienced scientists and trained volunteer divers survey fishes along 50 m transects laid at a consistent depth on shallow reefs. Divers count and estimate the total length of all fishes observed within 5 m of either side of the transect, identifying them to the lowest possible taxonomic level. Full details of census methods, data quality, and training of divers are provided elsewhere (Edgar and Stuart-Smith 2014; Edgar et al. 2020, www.reeflifesurvey.com). We harmonised fish taxonomy according to FishBase (version April 2021, Froese and Pauly 2021). The estimated length of each fish was then converted into biomass using species-specific length-weight relationships obtained from FishBase and adjusting for the bias in divers' perception of fish size underwater using an empirical calibration (Edgar et al. 2004). For these analyses, we focus on tropical and subtropical reef sites (defined by a minimum monthly Sea Surface Temperature (SST) >17 °C, Parravicini et al. 2013) and excluded fishes which do not precipitate intestinal carbonates (i.e., elasmobranchs) and fishes that are likely to be underestimated by visual censuses due to their small size and/or cryptic nature (i.e., recently-settled juveniles, small cryptobenthic fishes, and fishes belonging to the order Anguilliformes, Brandl et al. 2018; Stuart-Smith et al. 2021). As carbonate excretion rate and mineralogy can currently be predicted for fishes belonging to 17 non-cryptic families (Ghilardi et al. 2023b), we considered only surveys for which these 17 families represented at least 80% of the total fish biomass and abundance. The final dataset thus included 1,277 surveys (conducted between 2008 and 2019) from 796 sites and 15 marine ecoregions (Spalding et al. 2007) (Fig. 4.1). As sites were characterised by a different number of surveys (range: 1 - 5, mean: 1.6, median: 2), and human pressure and protection variables were
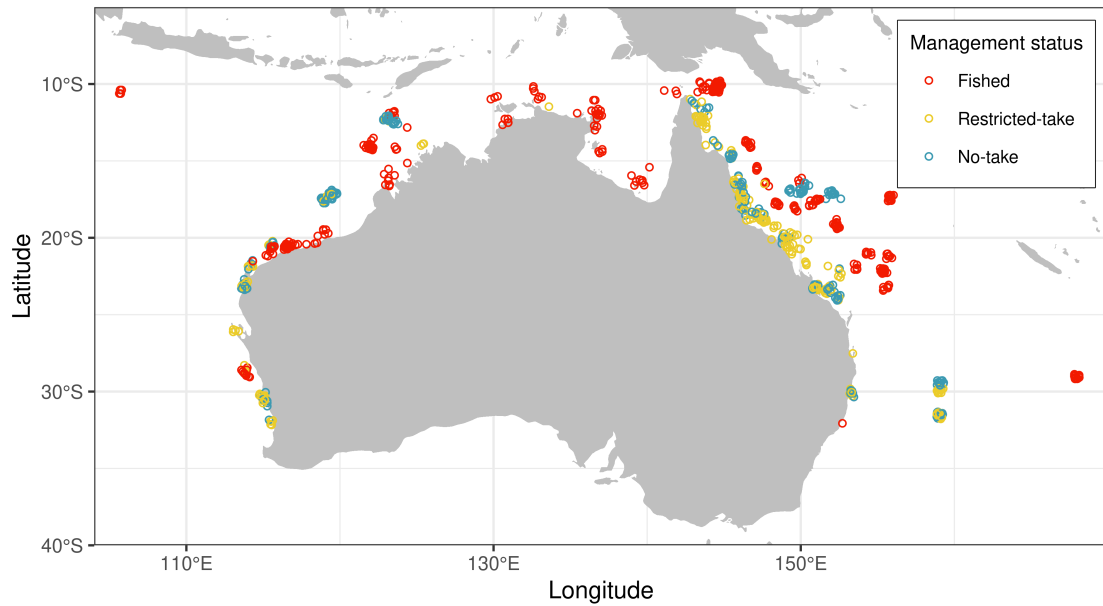
Figure 4.1: Location of study sites coloured by the type of management at the time of survey (Fished, $n = 317$; Restricted-take, $n = 231$; No-take, $n = 248$). Points are jittered to allow better visualisation.

obtained at the site level, we averaged the biomass and abundance of each species-size combination across surveys at each site, and all analyses were performed at the site level.

4.2.2 Fish carbonate excretion and mineralogy

To estimate fish carbonate excretion and mineralogy we first obtained individual-level predictions using two recently developed Bayesian models (Ghilardi et al. 2023b) and then scaled these up to community-level estimates using fish abundance data. These models predict carbonate excretion rate (total and per polymorph for LMC, aragonite, HMC, MHC, and ACMC) as a function of fish traits (body mass, relative intestinal length, and caudal fin aspect ratio), water temperature, and fish family. For each species in the RLS database, we retrieved the caudal fin aspect ratio from FishBase and extrapolated species-specific relative intestinal length following Ghilardi et al. (2023b). We also retrieved the mean SST per site. Then, we used 2,000 posterior draws from the models to predict the median carbonate excretion rate (in μmol h^{-1}) and the median polymorph-specific excretion

rates for each species-size-SST combination in our dataset ($n = 59{,}893$). Median excretion rates were then multiplied by the abundance of the respective species-size combination at each site and multiplied by 24 to obtain an estimate of excretion rate per day. Community-level estimates of carbonate excretion (in μmol m^{-2} d^{-1}) were then obtained by summing individual-level excretion rates and dividing by the area of the survey (i.e., 500 m^2). Polymorph-specific excretion rates were computed as proportions dividing them by the total excretion rate of each site.

4.2.3   Selection of variables included in the models

The primary response variables in all of our analyses were community-level carbonate excretion rate and mineralogical composition. We collated data for three human pressure and four protection variables per site and for eight ecological and environmental factors mediating their effect on carbonate excretion and mineralogy. We provide here a brief overview of these variables, with a detailed description in the Supplementary Methods.

Fish community structure

Individual-level fish carbonate excretion rate is related to body mass, intestinal length, activity level, and species identity (Ghilardi et al. 2023b). We thus assumed that community-level carbonate excretion depends on characteristics of fish assemblages such as biomass, size and trophic structure (as diet is related to intestinal length, Ghilardi et al. 2021b), and biodiversity. Therefore, for each site we computed five metrics defining fish community structure: standing biomass, median body mass (as an index of size structure), mean trophic level (as an index of trophic structure), taxonomic and functional diversity.

Environmental variables

Environmental conditions are also expected to influence community-level carbonate excretion and mineralogy through both direct and indirect effects. We included the mean depth of the transects, SST, and Net Primary Productivity

(NPP) because they influence fish community structure and composition (Duffy et al. 2016), and temperature affects individual-level carbonate excretion rate and mineralogical composition (Wilson et al. 2009; Ghilardi et al. 2023b).

Human pressure and protection variables

Humans can indirectly impact fish carbonate cycling through changes in community structure and composition. These may result from direct extractive activities (fishing) or from the effects of anthropogenic habitat and water quality deterioration. Human gravity is an indicator of the amount of human pressure on reefs (Cinner et al. 2018). Gravity accounts for both the size of the human population and the travel time necessary to reach the reef, with higher gravity values (higher population and/or shorter travel time) indicating higher human pressure. Travel time is not only based on linear distance, but also accounts for landscape heterogeneity, road networks, and coastline tortuosity (Maire et al. 2016). Following previous studies (Cinner et al. 2016; Cinner et al. 2018; Cinner et al. 2020; Seguin et al. 2022), we used the cumulative gravity within a 500 km radius of a given reef, with a squared exponent for the travel time. In addition, we used the travel time to the nearest human settlement and the total population within 500 km separately. A 500 km radius was chosen as the maximum distance within which any fishing or land use activities could influence tropical and subtropical reefs (Cinner et al. 2018; Seguin et al. 2022).

The primary goals of MPAs are to act as fishery reserves and protect biodiversity, which may positively affect the rate of key ecological processes (Topor et al. 2019). However, the ecological outcomes of MPAs are linked to multiple features, such as no-take regulations, well-enforced compliance, >10 years old, and >100 km^2 large (Edgar and Stuart-Smith 2014). We used the management status at the time of survey (i.e., fished: site open to fishing without restrictions; restricted-take: site within an MPA but where fishing is allowed with varying restrictions, e.g., size or effort limits; no-take: site within a no-take MPA where fishing is prohibited) and tested the effect of MPA age and size within restricted-take and

no-take MPAs. Further, to assess whether the benefits of management increase with the accumulation of four key features, we assigned a value from 0 to 4 based on how many of these MPA features (i.e., no-take, well-enforced, >10 years old, >100 km² large) characterise each site.

4.2.4 Statistical analysis

To uncover the pathways by which human pressure and fisheries management affect fish carbonate cycling, we used Bayesian SEMs, which provide a flexible modelling framework that allows to incorporate a wide variety of model structures and distributions, and to estimate the full posterior distributions of parameters. We built a causal Directed Acyclic Graph (DAG) (available at: `http://dagitty.net/mdKVBtK`) representing the influence of human pressure and fisheries management on fish carbonate excretion and mineralogy as mediated by fish community structure and composition and environmental variables (see Supplementary Table 4.1 for a description of assumed relationships). Based on the DAG, we then fitted a series of SEMs where we: 1) investigate the indirect effects of human gravity and fisheries management on carbonate excretion and mineralogy; 2) replace human gravity with travel time and human population density to evaluate the effects of the two gravity components individually; 3) fit the second SEM separately for each management category to test whether the effects of travel time and human population density on fish community structure and carbonate cycling are contingent on the management category, while also testing the effects of MPA age and size within restricted-take and no-take areas; 4) assess the indirect effects of the total number of key MPA features.

We applied natural-log or square-root transformations to response and predictor variables that were strongly or moderately right-skewed, respectively. Further, all continuous response and predictor variables were standardised by subtracting their mean and dividing by two standard deviations to allow direct comparison of effect sizes, including for categorical variables (i.e., management category) (Gelman 2008). All sub-models had a multilevel structure, including ecoregion as a group-level effect

to account for the spatial structure in the data. Carbonate mineralogical composition (i.e., continuous proportions of five carbonate polymorphs) was modelled following a Dirichlet distribution with a multivariate logit link function (Douma and Weedon 2019), while all other variables were modelled following a Gaussian distribution. The models were fitted using a Hamiltonian Monte Carlo sampler algorithm in Stan (Carpenter et al. 2017) with the R package *brms* (Bürkner 2017), running three parallel chains, each with 2,000 iterations and a warm-up of 1,000 iterations. We used the following priors for all models: Normal(0, 1) for all intercepts and slopes, Student-t(3, 0, 2.5) for standard deviations of group-level effects and residual standard deviations, and Student-t(3, 0, 5) for the precision parameter (ϕ) of the Dirichlet distribution. We examined models for evidence of convergence using trace plots and scale reduction factor (Rhat) and checked model fit using posterior predictive plots.

We then extracted the standardised effects for each predictor in the Gaussian models. For each predictor in the Dirichlet model, we computed linearised standardised effects comparable to those of Gaussian models using the observed-empirical approach to standardisation, which was proposed for binary outcomes but suggested to be appropriate also for models with multiple nominal responses (Grace et al. 2018). Using these standardised effects, we calculated the indirect effects of each predictor on carbonate excretion and mineralogy by multiplying the coefficients along the respective pathways while propagating uncertainty. For variables that influence carbonate excretion and mineralogy both directly and indirectly, we also computed their total effects by summing direct and indirect effects. To test whether the effects of travel time and human population density on each fish community structure variable vary under different management categories, we tested the null hypothesis that the difference between slopes equals zero using the entire posterior distribution of parameters.

All statistical analyses and data visualisation were performed in R (version 4.1.3, R Core Team 2021).
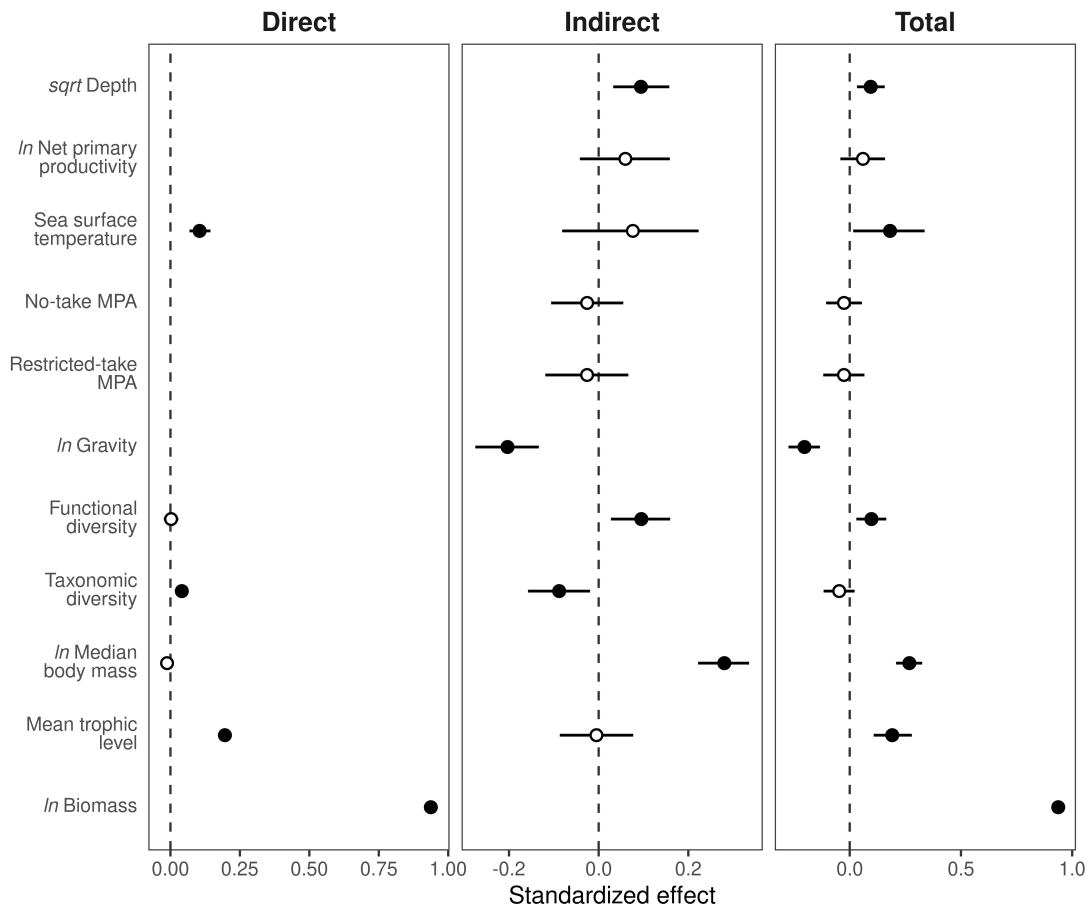
Figure 4.2: Direct, indirect and total (direct + indirect) standardised effects of different predictors on fish carbonate excretion. Estimates are mean (circles) and 95% credible intervals (CI; lines; some are too narrow to be seen) from a structural equation model including human gravity and fisheries management category. White circles depict effects with a CI overlapping zero. Values are missing when a variable does not have a direct or an indirect effect on carbonate excretion. Note that the scale differs among the three panels. MPA, marine protected area.

4.3 Results

4.3.1 Effects of fish community structure and environment

Fish carbonate excretion rate was strongly correlated with biomass, as community-level excretion rates are the sum of the excretion rate of each individual (Fig. 4.2). Further, mean trophic level, SST, and taxonomic diversity had a direct positive effect on carbonate excretion rate. The positive direct effect of taxonomic diversity was however offset by its negative indirect effect, mainly due to a negative

relationship with median body mass (Figs. 4.2 and 4.3). Functional diversity and median body mass did not directly influence carbonate excretion rate, but they had a positive indirect effect through mean trophic level and standing biomass, respectively (Figs. 4.2 and 4.3). Carbonate excretion rate was positively and indirectly affected by water depth, mainly through an increase in biomass (Supplementary Table 4.2), but unaffected by NPP.

Fish community structure and SST also influenced carbonate mineralogy (Fig. 4.4). HMC and ACMC consistently accounted for the largest proportion of carbonate excreted, and their proportions typically covaried over the range of each predictor. HMC, for instance, increased with increasing biomass, mean trophic level and functional diversity, but decreased with increasing SST and taxonomic diversity, while ACMC followed the exact opposite pattern. MHC was excreted in relatively high proportions by fishes at low mean trophic levels, but these proportions decreased steeply at trophic levels $\geq$ 2.5. Biomass and taxonomic diversity had a weak positive effect on MHC. A relatively high proportion of LMC was excreted at an SST of 23 °C, but it decreased in warmer waters. As observed for carbonate excretion rate, the median body mass of fish communities did not affect carbonate mineralogy directly, but had an indirect effect through biomass (Fig. 4.3 and Supplementary Fig. 4.6).

4.3.2 Indirect effects of human pressure

Human pressure had a strong negative effect on fish carbonate excretion rate and weakly influenced the mineralogical composition of the excreted carbonate. The indirect standardised effect of human gravity on carbonate excretion rate, combining all the pathways of influence, was -0.20 (95% credible interval: -0.28, -0.13) (Fig. 4.2). This effect resulted almost entirely from a single pathway, i.e., the effect of human gravity on carbonate excretion rate mediated by fish biomass (Fig. 4.3a). Human gravity had a negative direct effect on biomass (-0.22 [-0.29, -0.15]), resulting in an average standardised effect of -0.21 on carbonate excretion rate through this pathway. The remaining variables were only weakly affected by

Figure 4.3: Directed acyclic graphs from structural equation models representing the indirect effects of (a) human gravity and (b) human population density and travel time on fish carbonate excretion. Black and grey arrows represent positive and negative relationships, respectively. Line thickness is proportional to the mean standardised effect (Supplementary Tables 4.2-4.3). Dashed lines represent effects with a 95% credible interval overlapping zero.
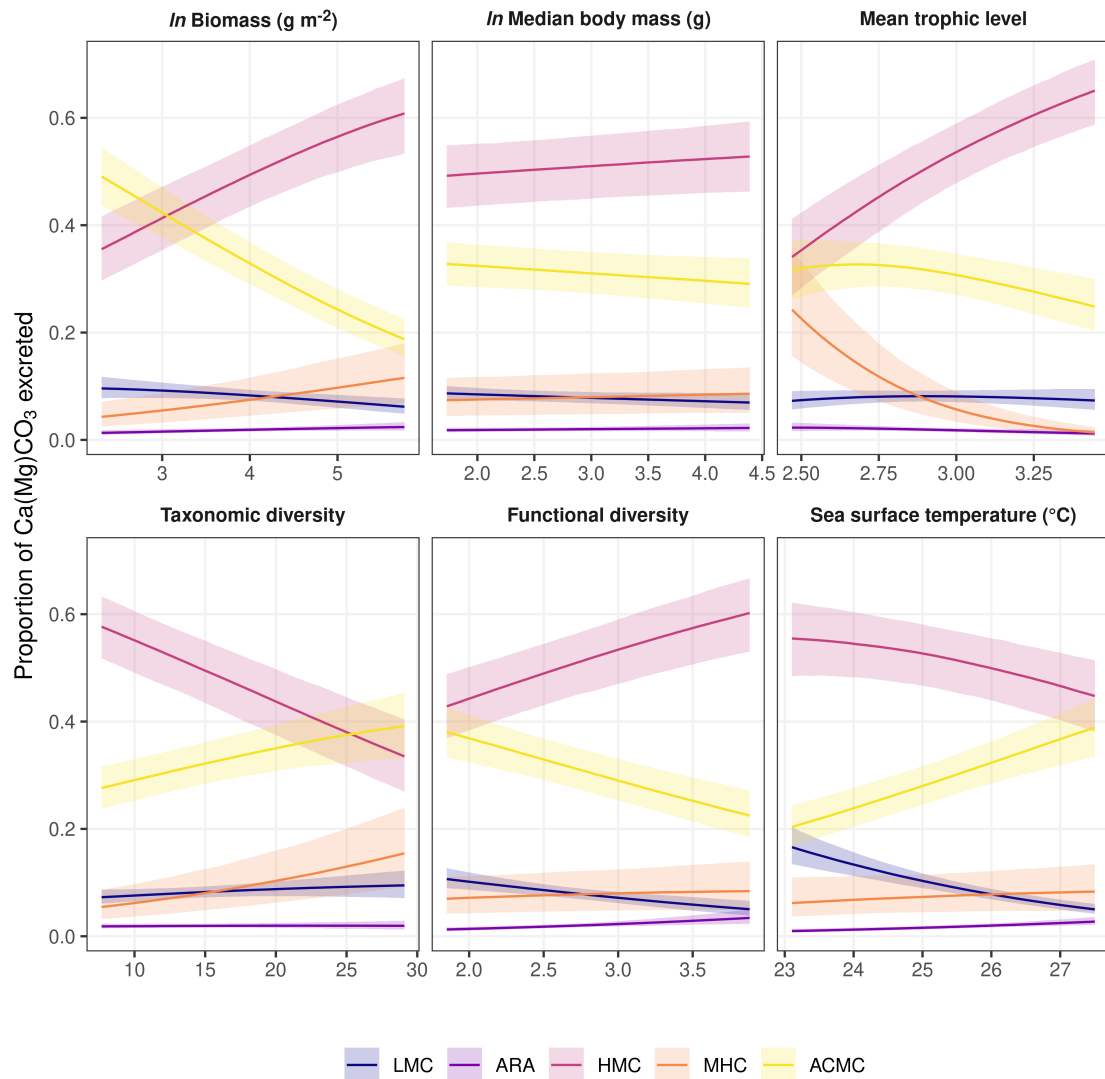
Figure 4.4: Direct effects of five community structure variables and temperature on carbonate mineralogy. Fitted lines and ribbons are posterior medians and 95% credible intervals from a multilevel Dirichlet regression within a Bayesian structural equation model, and represent conditional effects after accounting for the influence of all covariates, which were set to their mean values. LMC, low-magnesium calcite; ARA, aragonite; HMC, high-magnesium calcite; MHC, monohydrocalcite; ACMC, amorphous calcium magnesium carbonate.

human gravity, with the strongest direct effects on mean trophic level, functional diversity, and NPP. Human gravity also affected carbonate mineralogy by reducing standing biomass, and to a lesser extent by increasing mean trophic level and decreasing functional diversity. Specifically, increasing human gravity resulted in higher proportions of ACMC and LMC and lower proportions of HMC, MHC and aragonite (Supplementary Fig. 4.6).

The effect of human gravity on carbonate excretion rate and mineralogy was driven by both components (human population density and travel time). Reef sites that are further away from humans had higher fish biomass and had more taxonomically diverse fish communities. Larger human populations around reefs were associated with lower fish biomass and lower median body mass (Fig. 4.3b). These translate into an indirect positive effect of travel time and negative effect of human population density on carbonate excretion rate (Supplementary Fig. 4.7). Further, carbonate mineralogy was more affected by human population density than by travel time, with a higher proportion of ACMC and LMC and lower proportion of HMC being produced in more densely populated areas (Supplementary Fig. 4.8).

In general, the direct effects of travel time and human population density on fish community structure were consistent across the three management categories, with one exception. The effect of travel time on taxonomic diversity differed between no-take and fished sites (0.21 [0.01, 0.41]; null hypothesis: "β(No-take) - β(Fished) = 0"). Specifically, taxonomic diversity increased with increasing travel time in no-take MPAs, but not in fished areas (Supplementary Fig. 4.9). The indirect effect of travel time and human population density on carbonate excretion rate also varied among management categories. Travel time had a positive effect on carbonate excretion rate in restricted-take MPAs, but had no effect in fished areas and no-take MPAs. Human population density had a negative effect on carbonate excretion rate in fished areas and no-take MPAs, but had no effect in restricted-take MPAs (Supplementary Fig. 4.10).

4.3.3 Indirect effects of fisheries management

After accounting for travel time and human population density, fish communities within restricted-take and no-take MPAs had on average 18% smaller median body mass compared to those in fished areas (Fig. 4.5a). However, they did not directly differ in standing biomass. Only no-take MPAs (not restricted-take MPAs) had higher levels of taxonomic diversity compared to fished areas (28% higher on average). Fisheries management categories had no indirect effect on carbonate excretion rate or mineralogy (Fig. 4.2 and Supplementary Figs. 4.6). The number of key MPA features also had a negative effect on median body mass and positive effect on taxonomic diversity, but no effect on carbonate excretion rate or mineralogy (Supplementary Fig. 4.11). Considering management categories separately, MPA age had a negative effect on taxonomic diversity only within no-take MPAs (Supplementary Fig. 4.12). Carbonate excretion rate and mineralogy were thus unaffected by MPA age or size (Supplementary Fig. 4.10).

4.4 Discussion

Our results demonstrate that fish carbonate excretion on tropical and subtropical reefs in Australia is strongly affected by humans, but fisheries management does not reduce this impact. Human pressure altered multiple characteristics of reef fish communities, but the decrease in carbonate excretion was mainly driven by the well-known direct effect of gravity on fish biomass (Cinner et al. 2016; Seguin et al. 2022). This effect results from the combined effects of isolation and human population density. Reefs closest to humans are known to host lower fish biomass (D'Agata et al. 2016), which further decreases as surrounding human population density increases (Mora et al. 2011; Brewer et al. 2012; Duffy et al. 2016; Lefcheck et al. 2021). A decrease in standing biomass translates directly into a decrease in the level of numerous ecosystem functions and services provided by fish (McClanahan et al. 2011; Bellwood et al. 2012), such as the excretion of carbonate which contributes to carbon cycling.
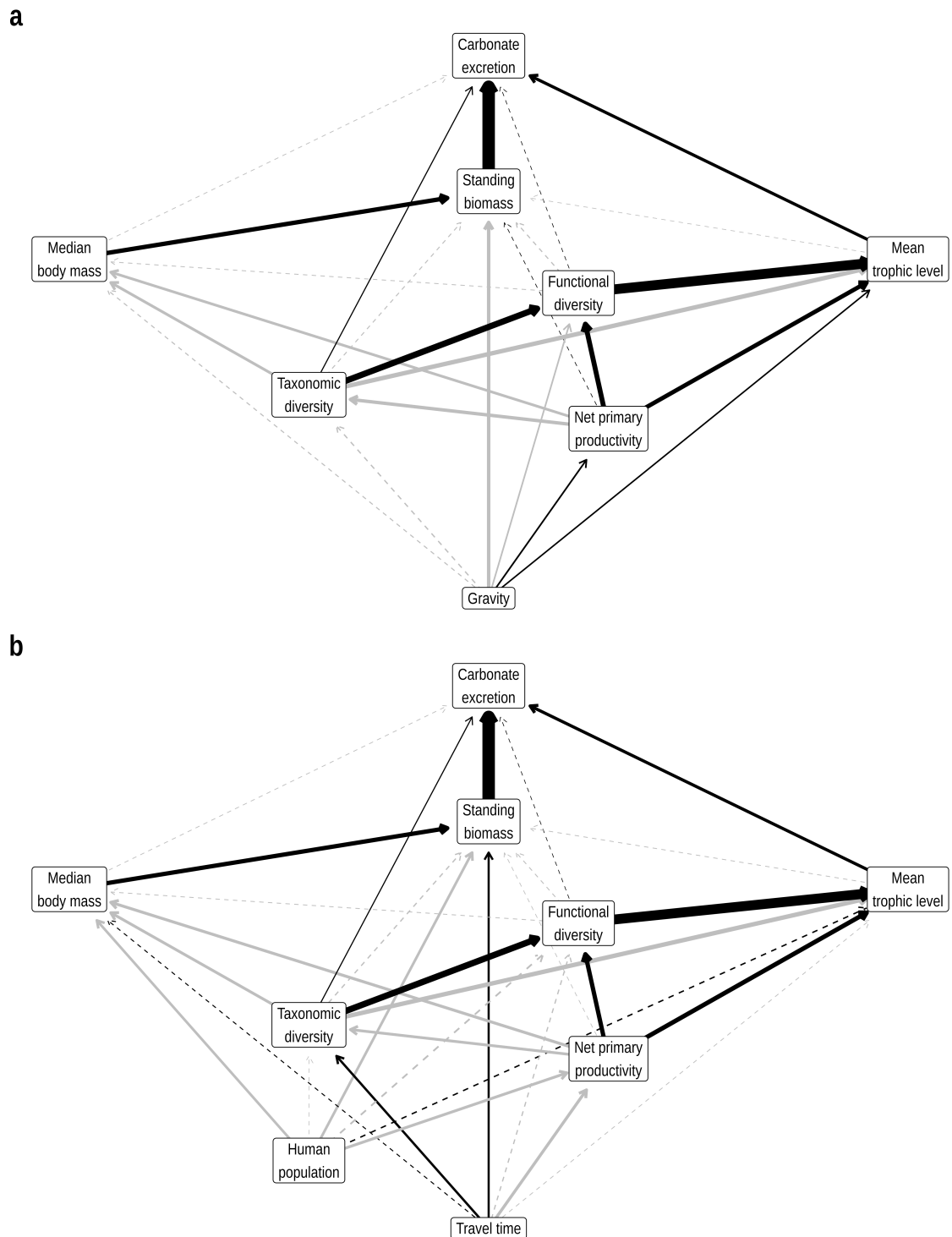
a

b
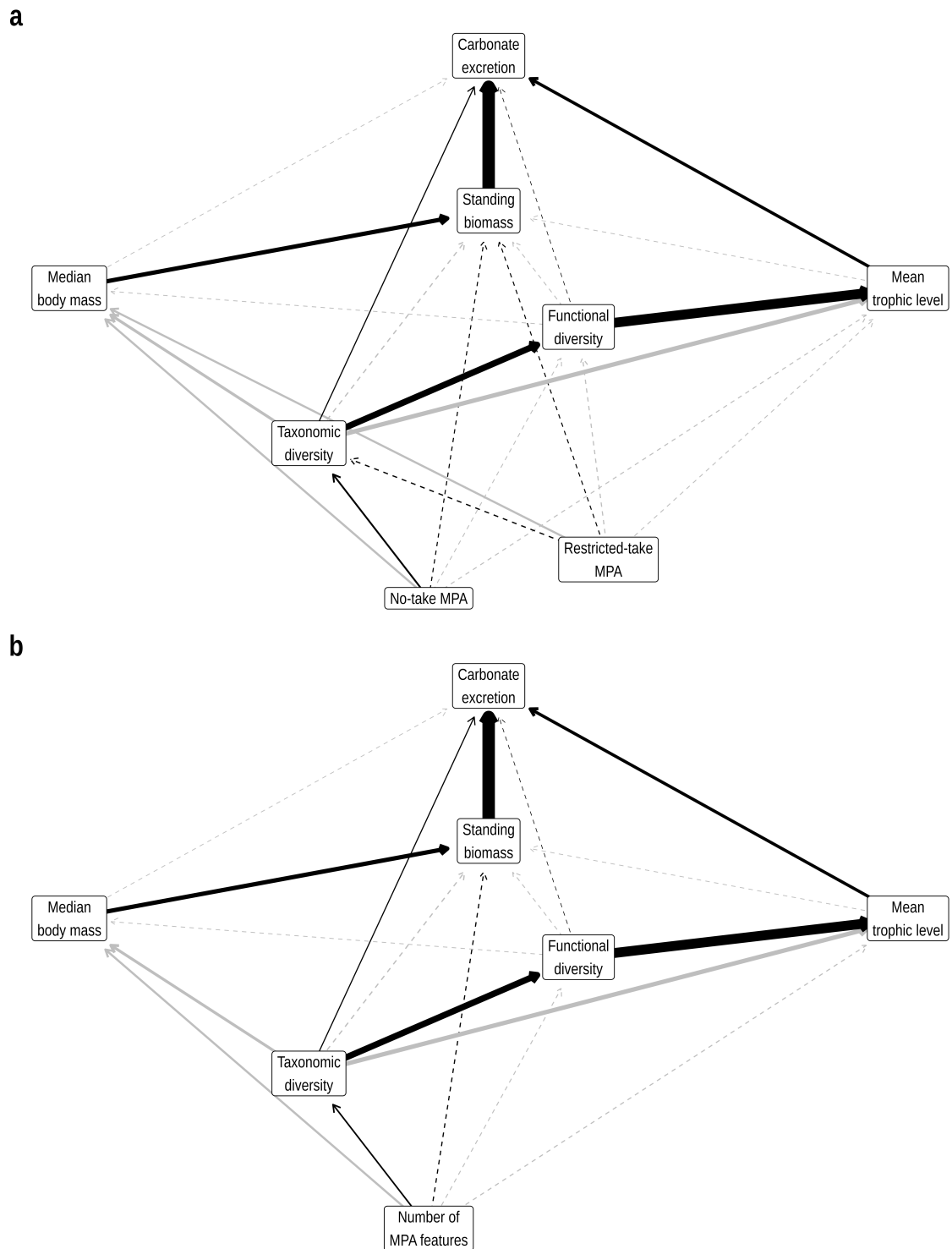
Figure 4.5: Directed acyclic graphs from structural equation models representing the indirect effects of (a) fisheries management and (b) number of MPA features on fish carbonate excretion. Black and grey arrows represent positive and negative relationships, respectively. Line thickness is proportional to the mean standardised effect (Supplementary Tables 4.3-4.4). Dashed lines represent effects with a 95% credible interval overlapping zero.

The nature of fish contribution to the inorganic carbon cycle depends on the mineralogical composition of the excreted carbonate. The most unstable carbonate polymorphs (ACMC and MHC) should dissolve rapidly post-excretion, acting as a localised source of alkalinity. Aragonite and calcite sink and contribute to the formation of fine-grained carbonate sediment on shallow reefs, or are transported offshore where they contribute to carbon export into deeper waters (Perry et al. 2011; Salter et al. 2014). By affecting fish biomass and community attributes, human pressure also influences carbonate mineralogy. A higher proportion of ACMC and LMC and a smaller proportion of other carbonate forms is produced in reefs under high versus low human pressure. These effects are, however, much smaller than those of SST. This suggests that human influence on carbonate mineralogy is more pronounced through global ocean warming (resulting from anthropogenic release of CO_2) than through local alteration of fish community structure and composition. Increases in SST and human population density both result in the excretion of a higher proportion of ACMC, thereby increasing carbonate dissolution and decreasing preservation into sediments.

In this analysis, we used human gravity as an index of human pressure. Gravity is derived from the travel time required to reach the reef from the nearest human settlement and the human population density in the surrounding area (Cinner et al. 2018). It is thus a proxy of collective human impacts, including fishing, coastal development, land use, pollution and tourism (Mora et al. 2011). Many studies have demonstrated human impacts on fish biomass, particularly through selective removal of large individuals (Jackson et al. 2001; Mora et al. 2011; Duffy et al. 2016; Mellin et al. 2016a; Zgliczynski and Sandin 2017). However, this phenomenon does not seem to be the underlying cause of human-induced biomass decreases in tropical and subtropical reefs in Australia. Human gravity drives the probability of occurrence and the abundance of large individuals of fished species in the Australian continental shelf (Bosch et al. 2022). Yet, the median body size of fish communities in our study did not correlate with human gravity, although a weak negative relationship exists with human population density. After accounting

for the size structure of fish communities, gravity directly affected fish biomass. This pattern may have resulted from multiple human activities affecting coral reefs (Mora et al. 2011). These activities are likely of particular significance in Australia where approximately 80% of the human population is concentrated within 25 km of the coast (Chen and McAneney 2006).

This may also help explain why fish carbonate excretion and mineralogy did not differ among fished reefs, restricted-take and no-take MPAs. While the benefits of these management tools for fisheries and biodiversity in tropical and sub-tropical reefs have been largely demonstrated (e.g., McClanahan et al. 2007; Russ et al. 2008; Edgar and Stuart-Smith 2014; MacNeil et al. 2015; Mellin et al. 2016b), the magnitude of these effects depends on the intensity of fishing pressure and the diversity of catches. Limited benefits are provided where fishing effort is relatively low, targets a narrow range of species, and destructive techniques are prohibited, such as in Australia (Emslie et al. 2015). Several studies have shown that the density and size of the most heavily targeted species within Australia's fisheries are greater in no-take MPAs than on fished reefs (Miller et al. 2012; Emslie et al. 2015; Bosch et al. 2022; Hall et al. 2023). These effects are less evident in partially protected zones (Hall et al. 2023). In contrast, there are no clear differences in the density, biomass and diversity of non-target fish species between protected and unprotected reefs (Emslie et al. 2015; Hall et al. 2023). The effect of fisheries management in preserving fish contributions to inorganic carbon cycling can be imperceptible (or is overwhelmed by overall human pressure) where or when reliance of the human population on fishing is low. However, restricted-take and no-take MPAs may be effective tools where fishing pressure is high and a broad range of species are exploited (Jennings and Wilson 2009; MacNeil et al. 2015).

In addition to the Australian socio-economic setting, the spatial and temporal scale of our analysis may contribute to explaining the lack of an effect of fisheries management on fish standing biomass and carbonate excretion rate. Reefs were surveyed throughout tropical and subtropical regions of Australia over the course of 12 years (2008-2019). During this time, they experienced multiple severe disturbances,

including marine heatwaves and cyclones, with mass coral bleaching followed by ecosystem restructuring (Hughes et al. 2017b; Hughes et al. 2018a; Hughes et al. 2018b; Stuart-Smith et al. 2018). No-take and restricted-take MPAs cannot protect reefs from these large-scale disturbances. Therefore, the effect of fisheries management can be trivial compared to the huge variation in ecological conditions resulting from these events within each management category. This may be an artefact of the spatial scale covered here (i.e., regional). More localised comparisons of fish carbonate excretion rate before and after the implementation of an MPA or between an MPA and adjacent fished reefs could reach different conclusions.

The degree of fishing permitted is only one of several protection features that are required to achieve the desired conservation benefits of MPAs (Edgar and Stuart-Smith 2014). Considering restricted-take and no-take MPAs separately, we found that larger and older MPAs do not necessarily enhance carbonate excretion rate, and overall we found no effect of the accumulation of multiple key MPA features (regulations, age, size, enforcement). These results can also be explained by the fact that about 71% of reef sites in restricted-take or no-take MPAs have been protected for >10 years, 94% are within MPAs of >100 km^2, and regulations are generally well enforced. Therefore, the effect of the number of features mainly reflects that of no-take MPAs, as the majority of no-take sites also have the other three features.

Nevertheless, our study reveals some management effects on fish community structure and composition. A primary objective of most MPAs is to conserve and protect marine biodiversity to maintain ecological processes and associated services. We show that reefs within no-take MPAs host a higher fish taxonomic diversity than fished reefs and this effect is stronger on more isolated reefs (higher travel time). This demonstrates that Australian no-take MPAs are performing as expected with regard to biodiversity conservation. However, diversity is not higher under partial protection through fishing restrictions compared to fished reefs. Contrary to expectations, median body mass in partially and fully protected reefs is smaller than in fished reefs. As a common achievement of MPAs, including in Australia, is the increase in the density and biomass of large fishes, mainly from

target species (Emslie et al. 2015; Turnbull et al. 2021; Bosch et al. 2022; Hall et al. 2023), the size structure of fish communities is expected to differ between protected and unprotected reefs. Protected reefs should display higher median body mass as large fishes increase in density, unless there is a concomitant increase in small non-target fishes. To understand the observed effect we modelled the density, median body mass, and biomass of each fish family (Supplementary Methods) and found very little variation among management categories, particularly for the families of the main target species (i.e., snappers, emperors, groupers) (Supplementary Fig. 4.13). The lower median body mass observed at protected sites might result from higher density and biomass of the smallest fishes (i.e., wrasses, damselfishes) than at fished sites. This is unlikely to be explained by reduced top-down control as there was no significant variation in density of predators (e.g., groupers). These small fishes are often associated with corals and high structural complexity (Wilson et al. 2006; Graham and Nash 2013), suggesting a potential bottom-up response. MPAs can reduce the damage caused by fishing gear and recreational activities on corals, especially those more easily damaged, such as branching corals (McManus et al. 1997; Strain et al. 2019; Stevens 2021). However, a global assessment showed limited effect of MPAs in enhancing total coral cover and branching coral cover (Strain et al. 2019). MPA placement in areas with high coral cover and structural complexity, and potentially high conservation value, may be a presumed factor underlying the observed patterns in fish size structure.

4.5 Conclusions

Effective MPAs have been promoted as a viable adaptation strategy to climate change based on their capacity to support ecosystem functions and services, including the accumulation of fish carbonates in shelf sediments (by rebuilding fish populations) with a potential role in the adaptation to ocean acidification (Roberts et al. 2017). Our study highlights that well-managed MPAs in developed countries with relatively low fishing pressure do not appear to support fish-mediated carbonate production and accumulation in shallow reef settings. This finding does

not undermine the many benefits effective MPAs provide to coral reefs (Russ et al. 2008; Edgar and Stuart-Smith 2014; MacNeil et al. 2015; Mellin et al. 2016a), and reapplying our analysis to other tropical regions with higher fishing pressure may reveal a positive effect of fisheries management, as the effects of management vary depending on socio-economic context (Cinner et al. 2020). If the maintenance of biogeochemical functions is to be prioritised in coral reef conservation (Bellwood et al. 2019a), then our results suggest that current fisheries management is not sufficient at least in the Australian context. Maintenance of this ecosystem function would require effective, context-tailored management actions integrating fisheries regulations and conservation strategies aimed at reducing the negative effects of socioeconomic drivers (Cinner et al. 2022).

Acknowledgements

References

Andradi-Brown, Dominic A. et al. (2016). "Reef fish community biomass and trophic structure changes across shallow to upper- Mesophotic reefs in the mesoamerican barrier reef, Caribbean". In: *PLoS ONE* 11.6, e0156641. DOI: `10.1371/journal.pone.0156641`.

Behrenfeld, Michael J. and Paul G. Falkowski (1997). "Photosynthetic rates derived from satellite-based chlorophyll concentration". In: *Limnology and Oceanography* 42.1, pp. 1–20. DOI: `10.4319/lo.1997.42.1.0001`.

Bellwood, David R., Andrew S. Hoey, and Terence P. Hughes (2012). "Human activity selectively impacts the ecosystem roles of parrotfishes on coral reefs". In: *Proceedings of the Royal Society B: Biological Sciences* 279.1733, pp. 1621–1629. DOI: `10.1098/rspb.2011.1906`.

Bellwood, David R. et al. (2019a). "Coral reef conservation in the Anthropocene: Confronting spatial mismatches and prioritizing functions". In: *Biological Conservation* 236.March, pp. 604–615. DOI: 10.1016/j.biocon.2019.05.056.

Boettiger, Carl, D. T. Lang, and P. C. Wainwright (2012). "Rfishbase: Exploring, manipulating and visualizing FishBase data from R". In: *Journal of Fish Biology* 81.6, pp. 2030–2039. DOI: 10.1111/j.1095-8649.2012.03464.x.

Bosch, Nestor E. et al. (2022). "Effects of human footprint and biophysical factors on the body-size structure of fished marine species". In: *Conservation Biology* 36.2, e13807. DOI: 10.1111/cobi.13807.

Brandl, Simon J et al. (2019). "Demographic dynamics of the smallest marine vertebrates fuel coral-reef ecosystem functioning". In: *Science* 364.6446, pp. 1189–1192. DOI: 10.1126/science.aav3384.

Brandl, Simon J. et al. (2018). "The hidden half: Ecology and evolution of cryptobenthic fishes on coral reefs". In: *Biological Reviews* 93.4, pp. 1846–1873. DOI: 10.1111/brv.12423.

Brewer, Tom D. et al. (2012). "Market access, population density, and socioeconomic development explain diversity and functional group biomass of coral reef fish assemblages". In: *Global Environmental Change* 22.2, pp. 399–406. DOI: 10.1016/j.gloenvcha.2012.01.006.

Burke, Lauretta et al. (2011). *Reefs At Risk Revisited*. Tech. rep. Washington (USA), p. 130. DOI: 10.1016/0022-0981(79)90136-9.

Bürkner, Paul Christian (2017). "brms: An R package for Bayesian multilevel models using Stan". In: *Journal of Statistical Software* 80.1, pp. 1–28. DOI: 10.18637/jss.v080.i01.

Carpenter, Bob et al. (2017). "Stan: A probabilistic programming language". In: *Journal of Statistical Software* 76.1, pp. 1–32. DOI: 10.18637/jss.v076.i01.

Chao, Anne, Chun Huo Chiu, and Lou Jost (2014). "Unifying species diversity, phylogenetic diversity, functional diversity, and related similarity and differentiation measures through hill numbers". In: *Annual Review of Ecology, Evolution, and Systematics* 45, pp. 297–324. DOI: 10.1146/annurev-ecolsys-120213-091540.

Chao, Anne et al. (2019). "An attribute-diversity approach to functional diversity, functional beta diversity, and related (dis)similarity measures". In: *Ecological Monographs* 89.2, e01343. DOI: 10.1002/ecm.1343.

Chen, Keping and John McAneney (2006). "High-resolution estimates of Australia's coastal population". In: *Geophysical Research Letters* 33.16. DOI: 10.1029/2006GL026981.

Cinner, Joshua E et al. (2016). "Bright spots among the world's coral reefs". In: *Nature* 535.7612, pp. 416–419. DOI: 10.1038/nature18607.

Cinner, Joshua E. et al. (2018). "Gravity of human impacts mediates coral reef conservation gains". In: *Proceedings of the National Academy of Sciences of the United States of America* 115.27, E6116–E6125. DOI: 10.1073/pnas.1708001115.

Cinner, Joshua E. et al. (2020). "Meeting fisheries, ecosystem function, and biodiversity goals in a human-dominated world". In: *Science* 368.6488, pp. 307–311. DOI: 10.1126/science.aax9412.

Cinner, Joshua E. et al. (2022). "Linking key human-environment theories to inform the sustainability of coral reefs". In: *Current Biology* 32.12, 2610–2620.e4. DOI: 10.1016/j.cub.2022.04.055.

D'Agata, Stephanie et al. (2016). "Marine reserves lag behind wilderness in the conservation of key functional roles". In: *Nature Communications* 7, p. 12000. DOI: `10.1038/ncomms12000`.

D'Agata, Stéphanie et al. (2014). "Human-mediated loss of phylogenetic and functional diversity in coral reef fishes". In: *Current Biology* 24.5, pp. 555–560. DOI: `10.1016/j.cub.2014.01.049`.

Douma, Jacob C. and James T. Weedon (2019). "Analysing continuous proportions in ecology and evolution: A practical introduction to beta and Dirichlet regression". In: *Methods in Ecology and Evolution* 10.9, pp. 1412–1430. DOI: `10.1111/2041-210X.13234`.

Duffy, J. Emmett et al. (2016). "Biodiversity enhances reef fish biomass and resistance to climate change". In: *Proceedings of the National Academy of Sciences of the United States of America* 113.22, pp. 6230–6235. DOI: `10.1073/pnas.1524465113`.

Eddy, Tyler D. et al. (2021). "Global decline in capacity of coral reefs to provide ecosystem services". In: *One Earth* 4.9, pp. 1278–1285. DOI: `10.1016/j.oneear.2021.08.016`.

Edgar, Graham J., Neville S. Barrett, and Alastair J. Morton (2004). "Biases associated with the use of underwater visual census techniques to quantify the density and size-structure of fish populations". In: *Journal of Experimental Marine Biology and Ecology* 308.2, pp. 269–290. DOI: `10.1016/j.jembe.2004.03.004`.

Edgar, Graham J. and Rick D. Stuart-Smith (2009). "Ecological effects of marine protected areas on rocky reef communities-A continental-Scale analysis". In: *Marine Ecology Progress Series* 388.4, pp. 51–62. DOI: `10.3354/meps08149`.

— (2014). "Systematic global assessment of reef fish communities by the Reef Life Survey program". In: *Scientific Data* 1, p. 140007. DOI: `10.1038/sdata.2014.7`.

Edgar, Graham J. et al. (2014). "Global conservation outcomes depend on marine protected areas with five key features". In: *Nature* 506.7487, pp. 216–220. DOI: `10.1038/nature13022`.

Edgar, Graham J. et al. (2020). "Reef Life Survey: Establishing the ecological basis for conservation of shallow marine life". In: *Biological Conservation* 252.June, p. 108855. DOI: `10.1016/j.biocon.2020.108855`.

Edwards, C. B. et al. (2014). "Global assessment of the status of coral reef herbivorous fishes: Evidence for fishing effects". In: *Proceedings of the Royal Society B: Biological Sciences* 281.1774, pp. 7–11. DOI: `10.1098/rspb.2013.1835`.

Emslie, Michael J. et al. (2015). "Expectations and outcomes of reserve network performance following re-zoning of the Great Barrier Reef Marine Park". In: *Current Biology* 25.8, pp. 983–992. DOI: `10.1016/j.cub.2015.01.073`.

Feng, Jianfeng et al. (2021). "A Threshold Sea-Surface Temperature at 14řC for Phytoplankton Nonlinear Responses to Ocean Warming". In: *Global Biogeochemical Cycles* 35.5, e2020GB006808. DOI: `10.1029/2020GB006808`.

Foran, Elizabeth, Steve Weiner, and Maoz Fine (2013). "Biogenic fish-gut calcium carbonate is a stable amorphous phase in the gilt-head seabream, sparus aurata". In: *Scientific Reports* 3, p. 1700. DOI: `10.1038/srep01700`.

Froese, Rainer and Daniel Pauly (2021). *FishBase.* version (04/2021). URL: `www.fishbase.org`.

Fukushi, Keisuke et al. (2011). "Monohydrocalcite: A promising remediation material for hazardous anions". In: *Science and Technology of Advanced Materials* 12.6, p. 064702. DOI: `10.1088/1468-6996/12/6/064702`.

Gelman, Andrew (2008). "Scaling regression inputs by dividing by two standard deviations". In: *Statistics in Medicine* 27, pp. 2865–2873. DOI: `10.1002/sim`.

Ghilardi, Mattia et al. (2021b). "Phylogeny, body morphology, and trophic level shape intestinal traits in coral reef fishes". In: *Ecology and Evolution* 11.19, pp. 13218–13231. DOI: `10.1002/ece3.8045`.

Ghilardi, Mattia et al. (2023b). "Temperature, species identity and morphological traits predict carbonate excretion and mineralogy in tropical reef fishes". In: *Nature Communications* 14, p. 985. DOI: `10.1038/s41467-023-36617-7`.

Grace, James B. et al. (2018). "Quantifying relative importance: computing standardized effects in models with binary outcomes". In: *Ecosphere* 9.6, e02283. DOI: `10.1002/ecs2.2283`.

Graham, N. A.J. and K. L. Nash (2013). "The importance of structural complexity in coral reef ecosystems". In: *Coral Reefs* 32.2, pp. 315–326. DOI: `10.1007/s00338-012-0984-y`.

Graham, N. A.J. et al. (2005). "Size-spectra as indicators of the effects of fishing on coral reef fish assemblages". In: *Coral Reefs* 24.1, pp. 118–124. DOI: `10.1007/s00338-004-0466-y`.

Graham, Nicholas A.J. et al. (2017). "Human Disruption of Coral Reef Trophic Structure". In: *Current Biology* 27.2, pp. 231–236. DOI: `10.1016/j.cub.2016.10.062`.

Graham, Nicholas A.J. et al. (2018). "Seabirds enhance coral reef productivity and functioning in the absence of invasive rats". In: *Nature* 559.7713, pp. 250–253. DOI: `10.1038/s41586-018-0202-3`.

Hall, April E., Katie T. Sievers, and Michael J. Kingsford (2023). "Conservation benefits of no-take marine reserves outweigh modest benefits of partially protected areas for targeted coral reef fishes". In: *Coral Reefs*. DOI: `10.1007/s00338-022-02340-w`.

Heenan, Adel, Gareth J. Williams, and Ivor D. Williams (2019). "Natural variation in coral reef trophic structure across environmental gradients". In: *Frontiers in Ecology and the Environment* 18.2, pp. 69–75. DOI: `10.1002/fee.2144`.

Heuer, Rachael M. et al. (2016). "Changes to intestinal transport physiology and carbonate production at various CO2 levels in a marine teleost, the Gulf Toadfish (*Opsanus beta*)". In: *Physiological and Biochemical Zoology* 89.5, pp. 402–416. DOI: `10.1086/688235`.

Hughes, Terry P. et al. (2017a). "Coral reefs in the Anthropocene". In: *Nature* 546.7656, pp. 82–90. DOI: `10.1038/nature22901`.

Hughes, Terry P. et al. (2017b). "Global warming and recurrent mass bleaching of corals". In: *Nature* 543.7645, pp. 373–377. DOI: `10.1038/nature21707`.

Hughes, Terry P. et al. (2018a). "Global warming transforms coral reef assemblages". In: *Nature* 556, pp. 492–496. DOI: `10.1038/s41586-018-0041-2`.

Hughes, Terry P. et al. (2018b). "Spatial and temporal patterns of mass bleaching of corals in the Anthropocene". In: *Science* 359.6371, pp. 80–83. DOI: `10.1126/science.aan8048`.

Jackson, Jeremy B.C. et al. (2001). "Historical overfishing and the recent collapse of coastal ecosystems". In: *Science* 293.5530, pp. 629–637. DOI: `10.1126/science.1059199`. arXiv: `484`.

Jennings, Simon and Rod W. Wilson (2009). "Fishing impacts on the marine inorganic carbon cycle". In: *Journal of Applied Ecology* 46.5, pp. 976–982. DOI: `10.1111/j.1365-2664.2009.01682.x`.

Lange, Ines D. et al. (2020). "Site-level variation in parrotfish grazing and bioerosion as a function of species-specific feeding metrics". In: *Diversity* 12, p. 379. DOI: 10.3390/d12100379.

Lefcheck, Jonathan S. et al. (2021). "Species richness and identity both determine the biomass of global reef fish communities". In: *Nature Communications* 12, p. 6875. DOI: 10.1038/s41467-021-27212-9.

Liu, Gang et al. (2014). "Reef-scale thermal stress monitoring of coral ecosystems: New 5-km global products from NOAA coral reef watch". In: *Remote Sensing* 6.11, pp. 11579–11606. DOI: 10.3390/rs61111579.

MacNeil, M. Aaron et al. (2015). "Recovery potential of the world's coral reef fishes". In: *Nature* 520.7547, pp. 341–344. DOI: 10.1038/nature14358.

Magneville, Camille et al. (2022). "mFD: an R package to compute and illustrate the multiple facets of functional diversity". In: *Ecography* 2022.1, pp. 1–15. DOI: 10.1111/ecog.05904.

Maire, Eva et al. (2016). "How accessible are coral reefs to people? A global assessment based on travel time". In: *Ecology Letters* 19.4, pp. 351–360. DOI: 10.1111/ele.12577.

McClanahan, Tim R. et al. (2007). "Toward pristine biomass: Reef fish recovery in coral reef marine protected areas in Kenya". In: *Ecological Applications* 17.4, pp. 1055–1067. DOI: 10.1890/06-1450.

McClanahan, Tim R. et al. (2011). "Critical thresholds and tangible targets for ecosystem-based management of coral reef fisheries". In: *Proceedings of the National Academy of Sciences of the United States of America* 108.41, pp. 17230–17233. DOI: 10.1073/pnas.1106861108.

McManus, John W, Rodolfo B Reyes, and Cleto L Nanola (1997). "Effects of some destructive fishing methods on coral cover and potential rates of recovery". In: *Environmental Management* 21.1, pp. 69–78. DOI: 10.1007/s002679900006.

Mellin, Camille et al. (2016a). "Humans and seasonal climate variability threaten large-bodied coral reef fish with small ranges". In: *Nature Communications* 7, p. 10491. DOI: 10.1038/ncomms10491.

Mellin, Camille et al. (2016b). "Marine protected areas increase resilience among coral reef communities". In: *Ecology Letters* 19.6, pp. 629–637. DOI: 10.1111/ele.12598.

Micheli, Fiorenza and Benjamin S. Halpern (2005). "Low functional redundancy in coastal marine assemblages". In: *Ecology Letters* 8.4, pp. 391–400. DOI: 10.1111/j.1461-0248.2005.00731.x.

Miller, Ian et al. (2012). "Ongoing effects of no-take marine reserves on commercially exploited coral trout populations on the Great Barrier Reef". In: *Marine Environmental Research* 79, pp. 167–170. DOI: 10.1016/j.marenvres.2012.05.008.

Moberg, Fredrik and Carl Folke (1999). "Ecological goods and services of coral reef ecosystems". In: *Ecological Economics* 29.2, pp. 215–233. DOI: 10.1016/S0921-8009(99)00009-9.

Mora, Camilo et al. (2011). "Global human footprint on the linkage between biodiversity and ecosystem functioning in reef fishes". In: *PLoS Biology* 9.4, e1000606. DOI: 10.1371/journal.pbio.1000606.

Morse, John W., Andreas J. Andersson, and Fred T. Mackenzie (2006). "Initial responses of carbonate-rich shelf sediments to rising atmospheric pCO_2 and "ocean

acidification": Role of high Mg-calcites". In: *Geochimica et Cosmochimica Acta* 70, pp. 5814–5830. DOI: `10.1016/j.gca.2006.08.017`.

Parravicini, V. et al. (2021). "Coral reef fishes reveal strong divergence in the prevalence of traits along the global diversity gradient". In: *Proceedings of the Royal Society B: Biological Sciences* 288, p. 20211712. DOI: `10.1098/rspb.2021.1712`.

Parravicini, Valeriano et al. (2013). "Global patterns and predictors of tropical reef fish species richness". In: *Ecography* 36.12, pp. 1254–1262. DOI: `10.1111/j.1600-0587.2013.00291.x`.

Parravicini, Valeriano et al. (2020). "Delineating reef fish trophic guilds with global gut content data synthesis and phylogeny". In: *PLoS Biology* 18.12, e3000702. DOI: `10.1371/journal.pbio.3000702`.

Pereira, Pedro Henrique Cipresso et al. (2018). "Effects of depth on reef fish communities: Insights of a deep refuge hypothesis from Southwestern Atlantic reefs". In: *PLoS ONE* 13.9, e0203072. DOI: `10.1371/journal.pone.0203072`.

Perry, Chris T. et al. (2011). "Fish as major carbonate mud producers and missing components of the tropical carbonate factory". In: *Proceedings of the National Academy of Sciences* 108.10, pp. 3865–3869. DOI: `10.1073/pnas.1015895108`.

Perry, Chris T. et al. (2022). "Geo-ecological functions provided by coral reef fishes vary among regions and impact reef carbonate cycling regimes". In: *Ecosphere* 13, e4288. DOI: `10.1002/ecs2.4288`.

Pritchard, T. R. et al. (2003). "Phytoplankton responses to nutrient sources in coastal waters off southeastern Australia". In: *Aquatic Ecosystem Health and Management* 6.2 SPEC. ISS. Pp. 105–117. DOI: `10.1080/14634980301469`.

R Core Team (2021). *R: a language and environment for statistical computing.*

Rice, Jake and Henrik Gislason (1996). "Patterns of change in the size spectra of numbers and diversity of the North Sea fish assemblage, as reflected in surveys and models". In: *ICES Journal of Marine Science* 53.6, pp. 1214–1225. DOI: `10.1006/jmsc.1996.0146`.

Roberts, Callum M. et al. (2017). "Marine reserves can mitigate and promote adaptation to climate change". In: *Proceedings of the National Academy of Sciences* 114.24, pp. 6167–6175. DOI: `10.1073/pnas.1701262114`.

Roberts, Kelsey E., Olivia Hill, and Carly N. Cook (2020). "Evaluating perceptions of marine protection in Australia: Does policy match public expectation?" In: *Marine Policy* 112.November 2019, p. 103766. DOI: `10.1016/j.marpol.2019.103766`.

Robinson, James P.W. et al. (2017). "Fishing degrades size structure of coral reef fish communities". In: *Global Change Biology* 23.3, pp. 1009–1022. DOI: `10.1111/gcb.13482`.

Russ, Garry R. et al. (2008). "Rapid increase in fish numbers follows creation of world's largest marine reserve network". In: *Current Biology* 18.12, pp. 514–515. DOI: `10.1016/j.cub.2008.04.016`.

Saba, Grace K. et al. (2021). "Toward a better understanding of fish-based contribution to ocean carbon flux". In: *Limnology and Oceanography* 66.5, pp. 1639–1664. DOI: `10.1002/lno.11709`.

Salter, Michael A., Chris T. Perry, and Abigail M. Smith (2019). "Calcium carbonate production by fish in temperate marine environments". In: *Limnology and Oceanography* 64.6, pp. 2755–2770. DOI: `10.1002/lno.11339`.

Salter, Michael A., Chris T. Perry, and Rod W. Wilson (2014). "Size fraction analysis of fish-derived carbonates in shallow sub-tropical marine environments and a

potentially unrecognised origin for peloidal carbonates". In: *Sedimentary Geology* 314, pp. 17–30. DOI: 10.1016/j.sedgeo.2014.10.005.

Salter, Michael A. et al. (2017). "Phase heterogeneity in carbonate production by marine fish influences their roles in sediment generation and the inorganic carbon cycle". In: *Scientific Reports* 7.1, pp. 1–15. DOI: 10.1038/s41598-017-00787-4.

Salter, Michael A. et al. (2018). "Reef fish carbonate production assessments highlight regional variation in sedimentary significance". In: *Geology* 46.8, pp. 699–702. DOI: 10.1130/G45286.1.

Schiettekatte, Nina M D et al. (2022a). "Biological trade-offs underpin coral reef ecosystem functioning". In: *Nature Ecology and Evolution*. DOI: 10.1038/s41559-022-01710-5.

Seguin, Raphael et al. (2022). "Towards process-oriented management of tropical reefs in the anthropocene". In: *Nature Sustainability*. DOI: 10.1038/s41893-022-00981-x.

Soler, German A. et al. (2015). "Reef fishes at all trophic levels respond positively to effective marine protected areas". In: *PLoS ONE* 10.10, pp. 1–12. DOI: 10.1371/journal.pone.0140270.

Spalding, Mark D. et al. (2007). "Marine ecoregions of the world: A bioregionalization of coastal and shelf areas". In: *BioScience* 57.7, pp. 573–583. DOI: 10.1641/B570707.

Stevens, Bradley G. (2021). "The ups and downs of traps: Environmental impacts, entanglement, mitigation, and the future of trap fishing for crustaceans and fish". In: *ICES Journal of Marine Science* 78.2, pp. 584–596. DOI: 10.1093/icesjms/fsaa135.

Strain, Elisabeth M.A. et al. (2019). "A global assessment of the direct and indirect benefits of marine protected areas for coral reef conservation". In: *Diversity and Distributions* 25.1, pp. 9–20. DOI: 10.1111/ddi.12838.

Stuart-Smith, Rick D et al. (2018). "Ecosystem restructuring along the Great Barrier Reef following mass coral bleaching". In: *Nature* 560, pp. 92–96. DOI: 10.1038/s41586-018-0359-9.

Stuart-Smith, Rick D. et al. (2021). "Habitat loss and range shifts contribute to ecological generalization among reef fishes". In: *Nature Ecology and Evolution* 5.5, pp. 656–662. DOI: 10.1038/s41559-020-01342-7.

Tanner, Susanne E. et al. (2019). "Regional climate, primary productivity and fish biomass drive growth variation and population resilience in a small pelagic fish". In: *Ecological Indicators* 103.April, pp. 530–541. DOI: 10.1016/j.ecolind.2019.04.056.

Tittensor, Derek P. et al. (2010). "Global patterns and predictors of marine biodiversity across taxa". In: *Nature* 466.7310, pp. 1098–1101. DOI: 10.1038/nature09329.

Topor, Zachary M. et al. (2019). "Marine protected areas enhance coral reef functioning by promoting fish biodiversity". In: *Conservation Letters* 12, e12638. DOI: 10.1111/conl.12638.

Turnbull, John W., Emma L. Johnston, and Graeme F. Clark (2021). "Evaluating the social and ecological effectiveness of partially protected marine areas". In: *Conservation Biology* 35.3, pp. 921–932. DOI: 10.1111/cobi.13677.

Villéger, Sébastien et al. (2017). "Functional ecology of fish: current approaches and future challenges". In: *Aquatic Sciences* 79.4, pp. 783–801. DOI: 10.1007/s00027-017-0546-z.

Walsh, Patrick J. et al. (1991). "Carbonate deposits in marine fish intestines: A new source of biomineralization". In: *Limnology and Oceanography* 36.6, pp. 1227–1232. DOI: 10.4319/lo.1991.36.6.1227.

Williams, Gareth J. and Nicholas A.J. Graham (2019). "Rethinking coral reef functional futures". In: *Functional Ecology* 33.6, pp. 942–947. DOI: 10.1111/1365-2435.13374.

Wilson, Rod W., Jonathan M. Wilson, and Martin Grosell (2002). "Intestinal bicarbonate secretion by marine teleost fish-why and how?" In: *Biochimica et Biophysica Acta* 1566, pp. 182–193. DOI: 10.1016/s0005-2736(02)00600-4.

Wilson, Rod W. et al. (2009). "Contribution of fish to the marine inorganic carbon cycle". In: *Science* 323.January, pp. 359–362. DOI: 10.1126/science.1157972.

Wilson, Shaun K. et al. (2006). "Multiple disturbances and the global degradation of coral reefs: Are reef fishes at risk or resilient?" In: *Global Change Biology* 12.11, pp. 2220–2234. DOI: 10.1111/j.1365-2486.2006.01252.x.

Woodhead, Anna J. et al. (2019). "Coral reef ecosystem services in the Anthropocene". In: *Functional Ecology* 33.6, pp. 1023–1034. DOI: 10.1111/1365-2435.13331.

Wootton, Henry F. et al. (2022). "Smaller adult fish size in warmer water is not explained by elevated metabolism". In: *Ecology Letters* January, pp. 1–12. DOI: 10.1111/ele.13989.

Yarlett, Robert T., Chris T. Perry, and Rod W. Wilson (2021). "Quantifying production rates and size fractions of parrotfish-derived sediment: A key functional role on Maldivian coral reefs". In: *Ecology and Evolution* 11.22, pp. 16250–16265. DOI: 10.1002/ece3.8306.

Yarlett, Robert T. et al. (2018). "Constraining species-size class variability in rates of parrotfish bioerosion on Maldivian coral reefs: Implications for regional-scale bioerosion estimates". In: *Marine Ecology Progress Series* 590, pp. 155–169. DOI: 10.3354/meps12480.

Zgliczynski, Brian J. and Stuart A. Sandin (2017). "Size-structural shifts reveal intensity of exploitation in coral reef fisheries". In: *Ecological Indicators* 73, pp. 411–421. DOI: 10.1016/j.ecolind.2016.09.045.

Supplementary information

Supplementary Methods

Ecological and environmental variables

Biomass: total fish biomass (in kg/m^2) of the species retained at each site obtained by summing the biomass of all individuals and dividing by the survey area (i.e., 500 m^2). Individual biomass was calculated from the estimated total length recorded in the RLS database and species-specific length–weight relationships obtained from FishBase (Froese and Pauly 2021).

Median body mass: median body mass (in g) among all individuals recorded in each site.

Mean trophic level: biomass-weighted mean trophic level based on species-specific trophic levels obtained from FishBase (Froese and Pauly 2021) using the R package *rfishbase* (Boettiger et al. 2012).

Taxonomic diversity: effective number of species, computed as the exponential of Shannon entropy (Chao et al. 2014).

Functional diversity: effective number of functionally equally distinct species, computed as the Chao's $^qFD(\Delta(\tau))$ index (Chao et al. 2019) for *q = 1* using the R package *mFD* (Magneville et al. 2022). We used the mean functional distance as the level of threshold distinctiveness (τ) and weighted species by their relative biomass. Fish functional diversity was calculated based on four traits: (i) maximum total length; (ii) trophic guilds defined by Parravicini et al. (2020); (iii) period of activity (i.e., diurnal, nocturnal, or both); and (iv) vertical position in the water column (i.e., pelagic, bentho-pelagic, or benthic).

Depth: depth at which the survey was conducted in metres. When several surveys had been conducted on the same site, we took the average depth. All surveys were conducted in shallow reefs (depth range: 0-21 m; mean depth: ~6.2 m).

Sea Surface Temperature (SST): mean SST (in °C) across 5-year periods prior to the surveys using daily SST data sourced from CoralReefWatch v3.1 (Liu et al. 2014) (`https://coralreefwatch.noaa.gov/product/5km/index.php`).

Net Primary Productivity (NPP): mean NPP (in $mgC/m^2/day$) across 5-year periods prior to the surveys using monthly NPP data based on Standard Vertically Generalized Production Model (VGPM) (Behrenfeld and Falkowski 1997) sourced from Ocean Productivity (`http://sites.science.oregonstate.edu/ocean.productivity/`).

Human pressure and protection variables

Management: type of management at the time of survey: fished, site open to fishing without restrictions; restricted-take, site located within an MPA but with some fishing methods allowed; no-take, site within a no-take MPA. Sites located within an MPA, but where surveys were conducted prior to MPA implementation, were considered open to fishing. Classification was based on expert opinion of the RLS data curators and checked with the World Database on Protected Areas (`http://protectedplanet.net/`).

MPA size: surface of MPAs (in km^2) obtained from the World Database on Protected Areas (`http://protectedplanet.net/`).

MPA age: number of years between the implementation of the MPA and the time of the survey.

MPA features: total number of key MPA features: no-take, well-enforced, >10 years old, >100 km^2 large (Edgar and Stuart-Smith 2014).

Travel time: travel time between the reef site and the nearest populated pixel within a 500 km radius calculated using a cost-distance algorithm that computes the least 'cost' (in minutes) of travelling to the reef site (Maire et al. 2016). Cost was based on a raster grid of land cover, road networks, and shorelines data and estimated travel time over different surfaces.

Population: summed human population estimates (from 1-by-1 km grid) within 500 km from the reef site using LandScan 2011 database (`https://landscan.ornl.gov/`).

Gravity: total human gravity is an indicator of the amount of human pressure on a reef (Cinner et al. 2018). Gravity integrates both the size of the human population and a surrogate for distance: travel time. The gravity value of a reef site is the sum of the gravity calculated within all cells (1-by-1 km grid) in a 500 km radius. The gravity value for each cell is the population of the given cell divided by the squared time travel between the cell and the site. A 500 km radius was chosen as the maximum distance any fishing or land use activities could influence tropical and subtropical reefs (Cinner et al. 2018; Seguin et al. 2022).

Modelling density, median body mass, and biomass of fish families

To understand the negative effect of management on the median body mass of fish communities yielded by the structural equation model, we investigated whether fish families differed in density, median body mass, and total biomass under different types of management. We computed the three metrics per family and reef site. Then, we fitted three separate Bayesian multilevel regression, one for each metric. We included management as a fixed effect and allowed the slope to vary by family (group-level effect). Additionally, we included environmental variables (depth, SST, NPP) and human pressure (travel time, human population) as fixed effects, and ecoregion as a group-level effect to account for the spatial structure in the data and control for different environmental conditions and human impact. Models were fitted with the R package *brms* (Bürkner 2017), running two parallel chains, each with 2,000 iterations and a warm-up of 1,000 iterations, and using uninformative priors. Convergence and model fit was examined using trace plots, scale reduction factor (Rhat) and posterior predictive plots.

Supplementary Figures
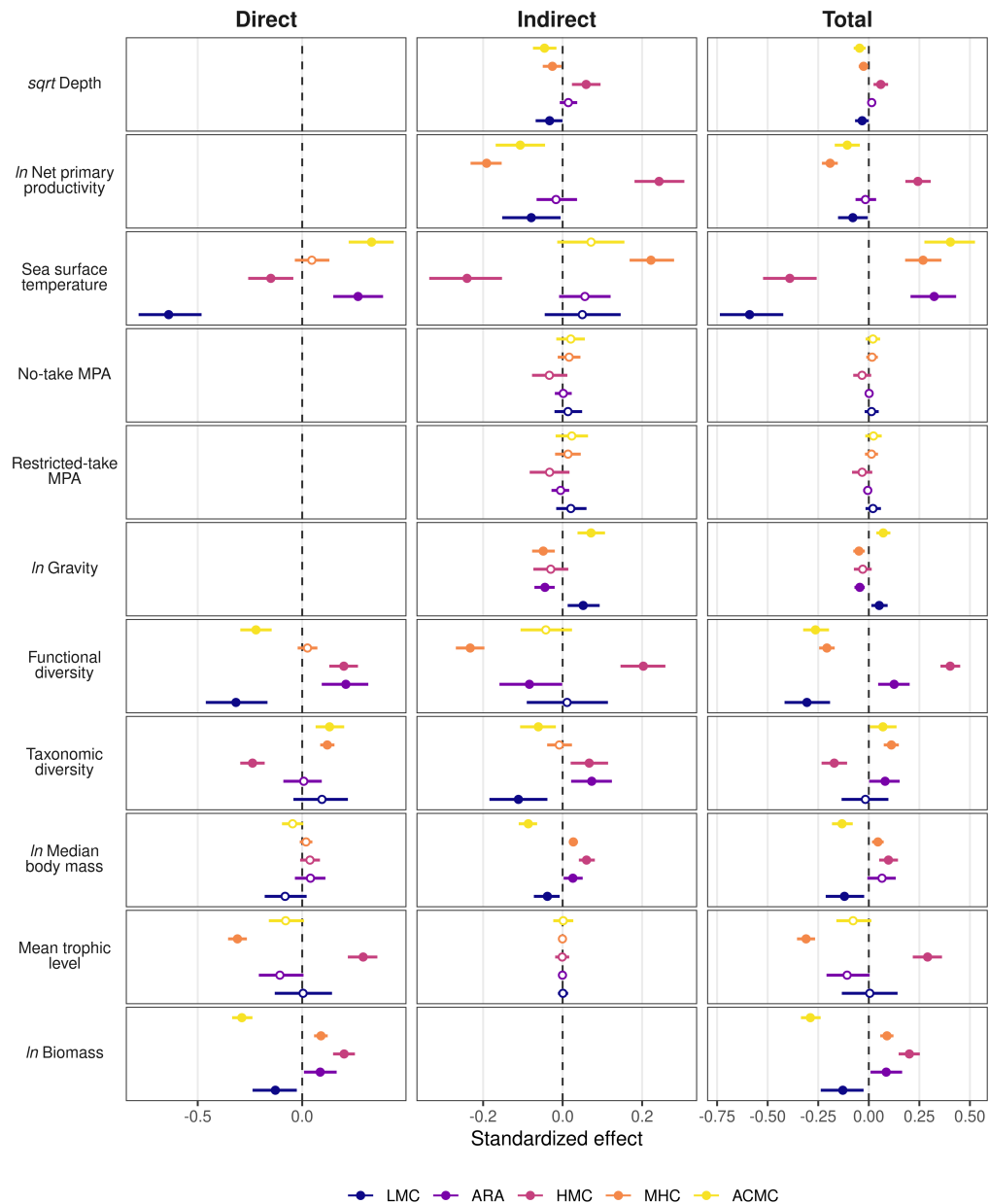
Figure 4.6: Direct, indirect and total (direct + indirect) standardised effects of different predictors on fish carbonate mineralogy. Estimates are mean (circles) and 95% credible intervals (CI; lines; some are too narrow to be seen) from a structural equation model including human gravity and fisheries management. White circles depict effects with a CI overlapping zero. Values are missing when a variable does not have a direct or an indirect effect on carbonate mineralogy. Note that the scale differs among the three panels. MPA, marine protected area; LMC, low-magnesium calcite; ARA, aragonite; HMC, high-magnesium calcite; MHC, monohydrocalcite; ACMC, amorphous calcium magnesium carbonate.

Figure 4.7: Direct, indirect and total (direct + indirect) standardised effects of different predictors on fish carbonate excretion. Estimates are mean (circles) and 95% credible intervals (CI; lines; some are too narrow to be seen) from a structural equation model including travel time, human population size and fisheries management. White circles depict effects with a CI overlapping zero. Values are missing when a variable does not have a direct or an indirect effect on carbonate excretion. Note that the scale differs among the three panels. MPA, marine protected area.
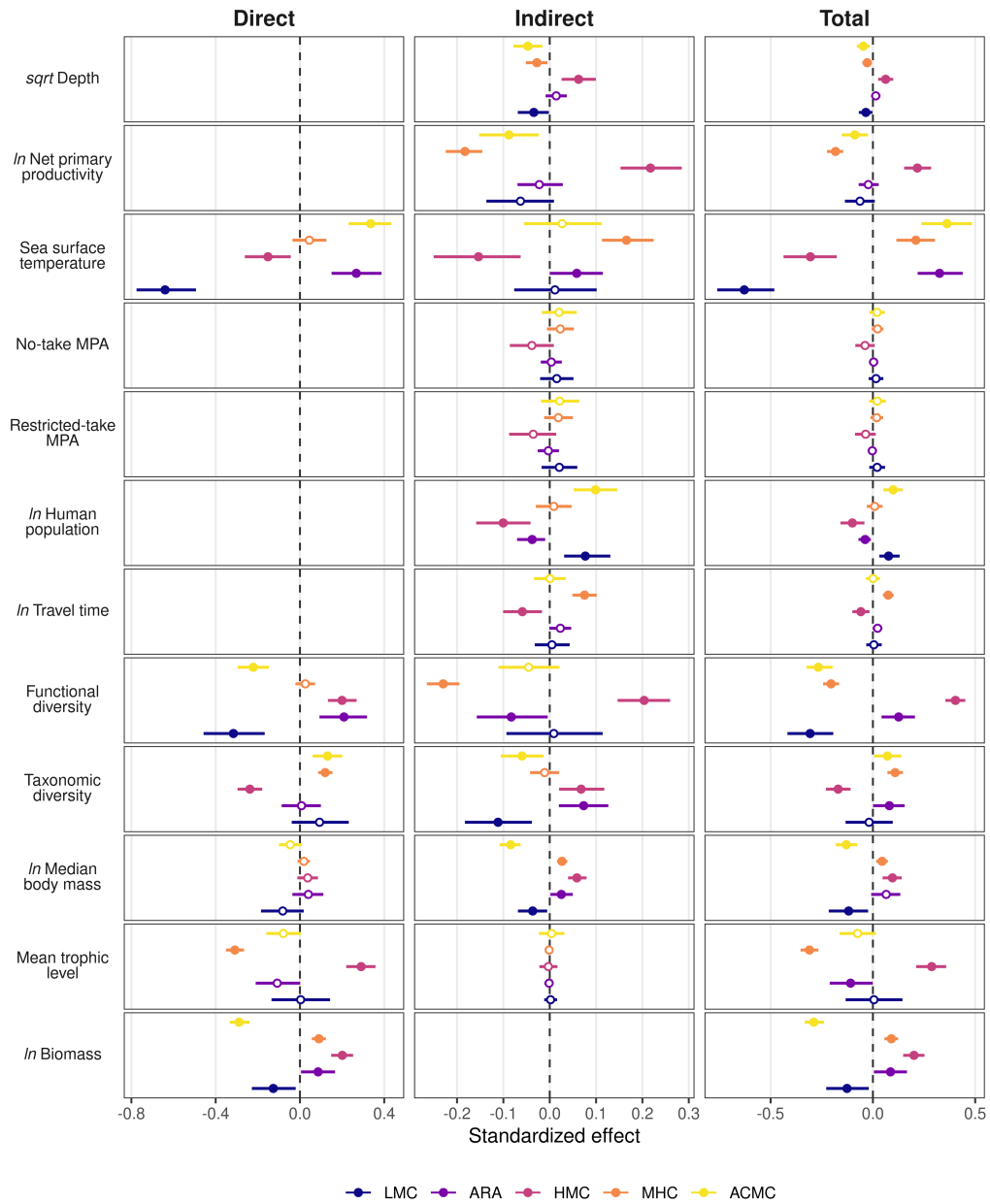
Figure 4.8: Direct, indirect and total (direct + indirect) standardised effects of different predictors on fish carbonate mineralogy. Estimates are mean (circles) and 95% credible intervals (CI; lines; some are too narrow to be seen) from a structural equation model including travel time, human population size and fisheries management. White circles depict effects with a CI overlapping zero. Values are missing when a variable does not have a direct or an indirect effect on carbonate mineralogy. Note that the scale differs among the three panels. MPA, marine protected area; LMC, low-magnesium calcite; ARA, aragonite; HMC, high-magnesium calcite; MHC, monohydrocalcite; ACMC, amorphous calcium magnesium carbonate.

Figure 4.9: Conditional effects of travel time and human population size on five community structure variables for each management category. Effects are from three separate structural equation models, one for each management category. Lines and ribbons represent the median predicted model fits and 95% credible intervals, respectively, after accounting for the influence of all confounding variables, which were set to their mean values in the full dataset to allow comparison among management categories. Asterisks indicate those metrics for which the difference between two slopes has a 95% credible interval that does not overlap zero.
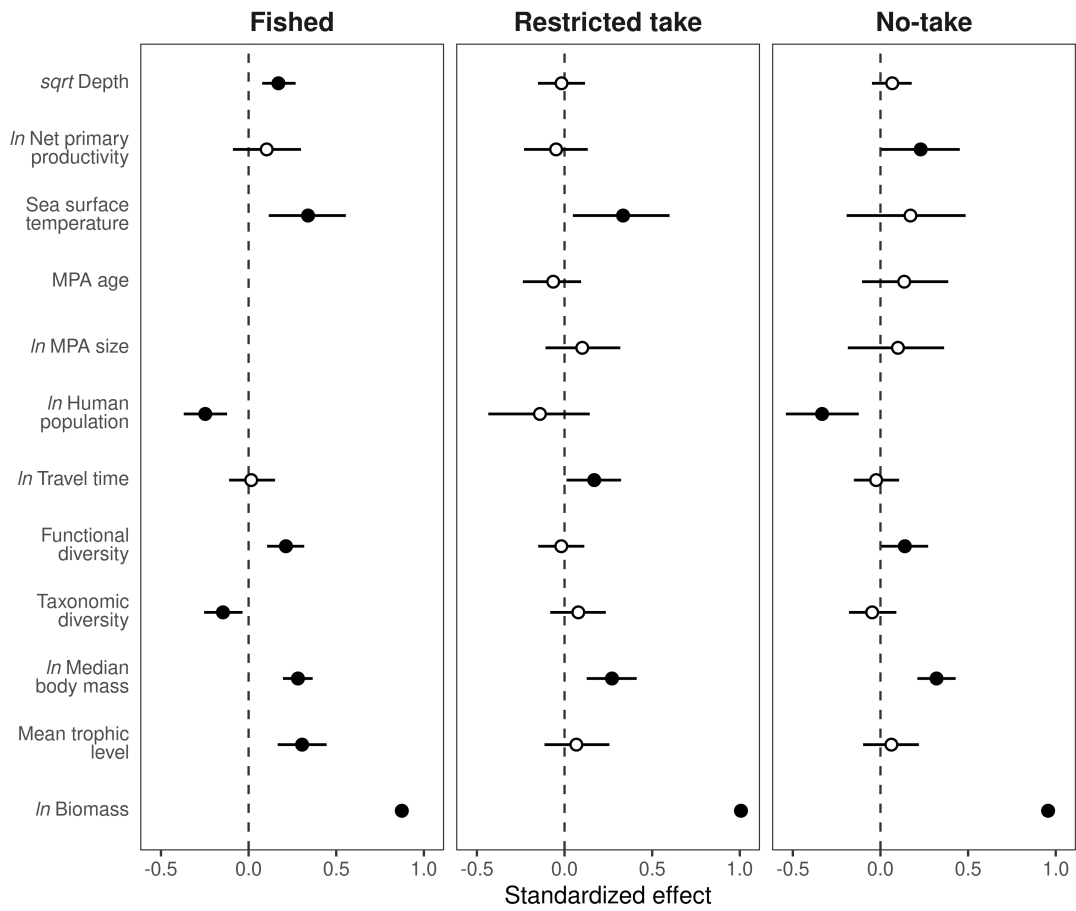
Figure 4.10: Total (direct + indirect) standardised effects of different predictors on fish carbonate excretion. Estimates are mean (circles) and 95% credible intervals (CI; lines; some are too narrow to be seen) from three structural equation models fitted separately for each fisheries management category. White circles depict effects with a CI overlapping zero. Values are missing when a variable does not have a direct or an indirect effect on carbonate excretion. Note that the scale differs among the three panels. MPA, marine protected area.
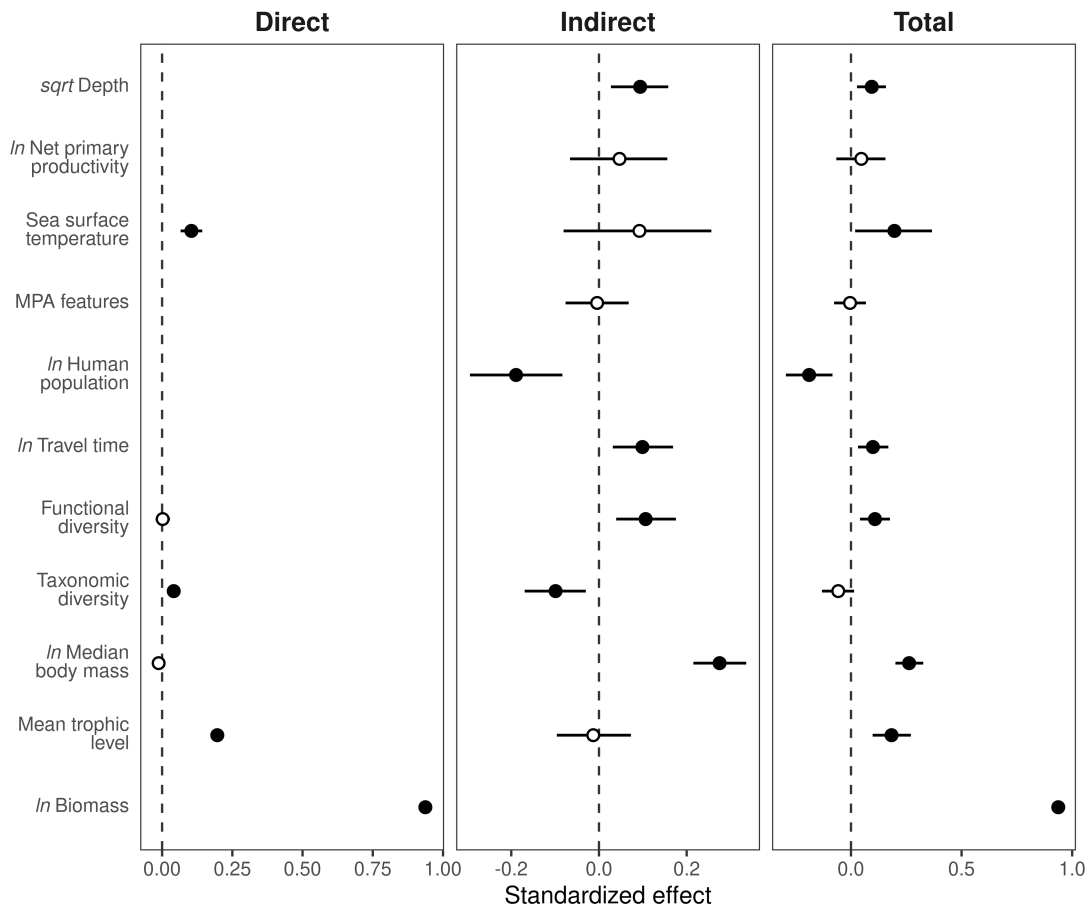
Figure 4.11: Direct, indirect and total (direct + indirect) standardised effects of different predictors on fish carbonate excretion. Estimates are mean (circles) and 95% credible intervals (CI; lines; some are too narrow to be seen) from a structural equation model including travel time, human population size and number of MPA features. White circles depict effects with a CI overlapping zero. Values are missing when a variable does not have a direct or an indirect effect on carbonate excretion. Note that the scale differs among the three panels. MPA, marine protected area.
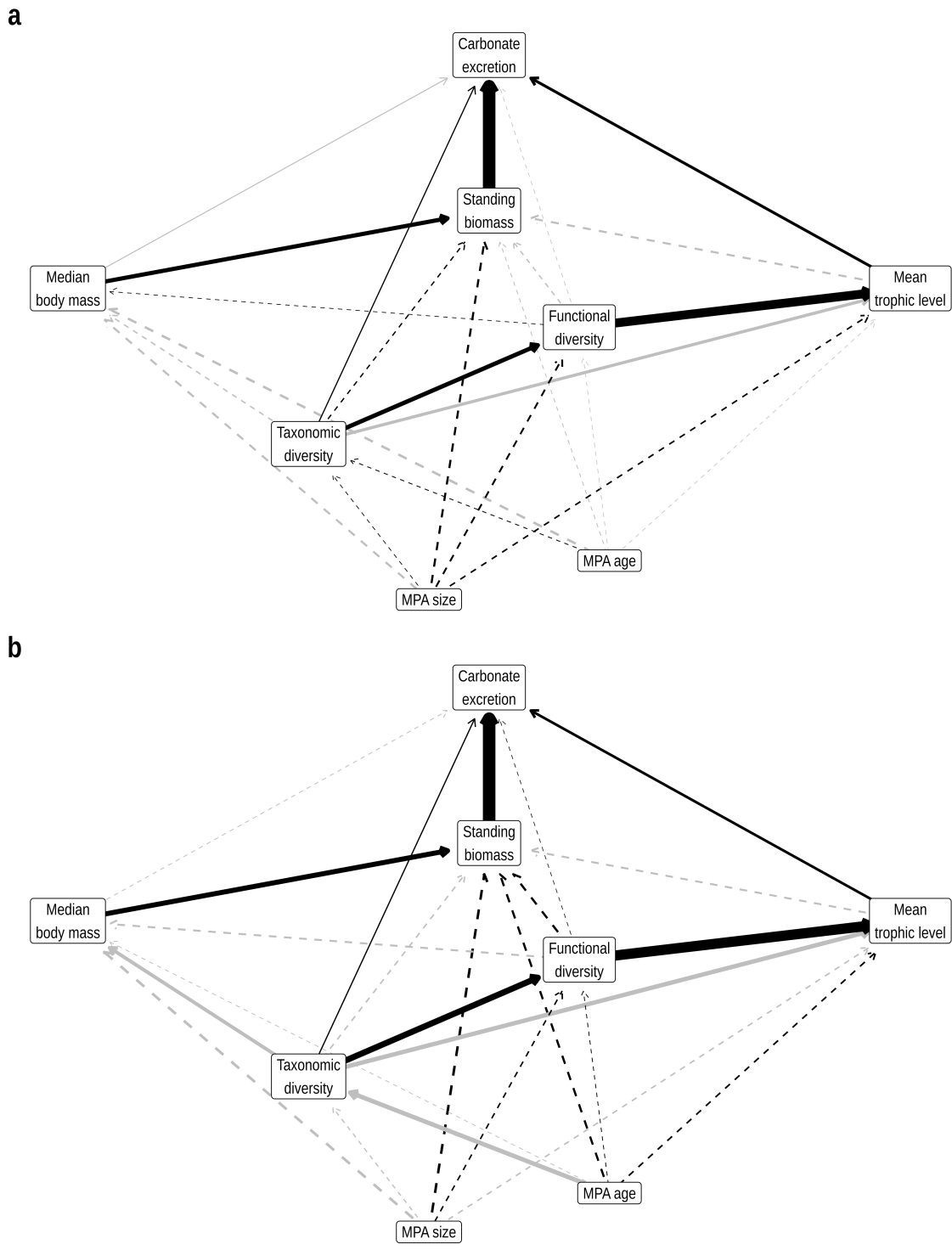
Figure 4.12: Directed acyclic graphs from structural equation models representing the indirect effects of MPA age and size on fish carbonate excretion in (a) restricted take and (b) no-take MPAs. Black and grey arrows represent positive and negative relationships, respectively. Line thickness is proportional to the mean standardised effect. Dashed lines represent effects with a 95% credible interval overlapping zero.
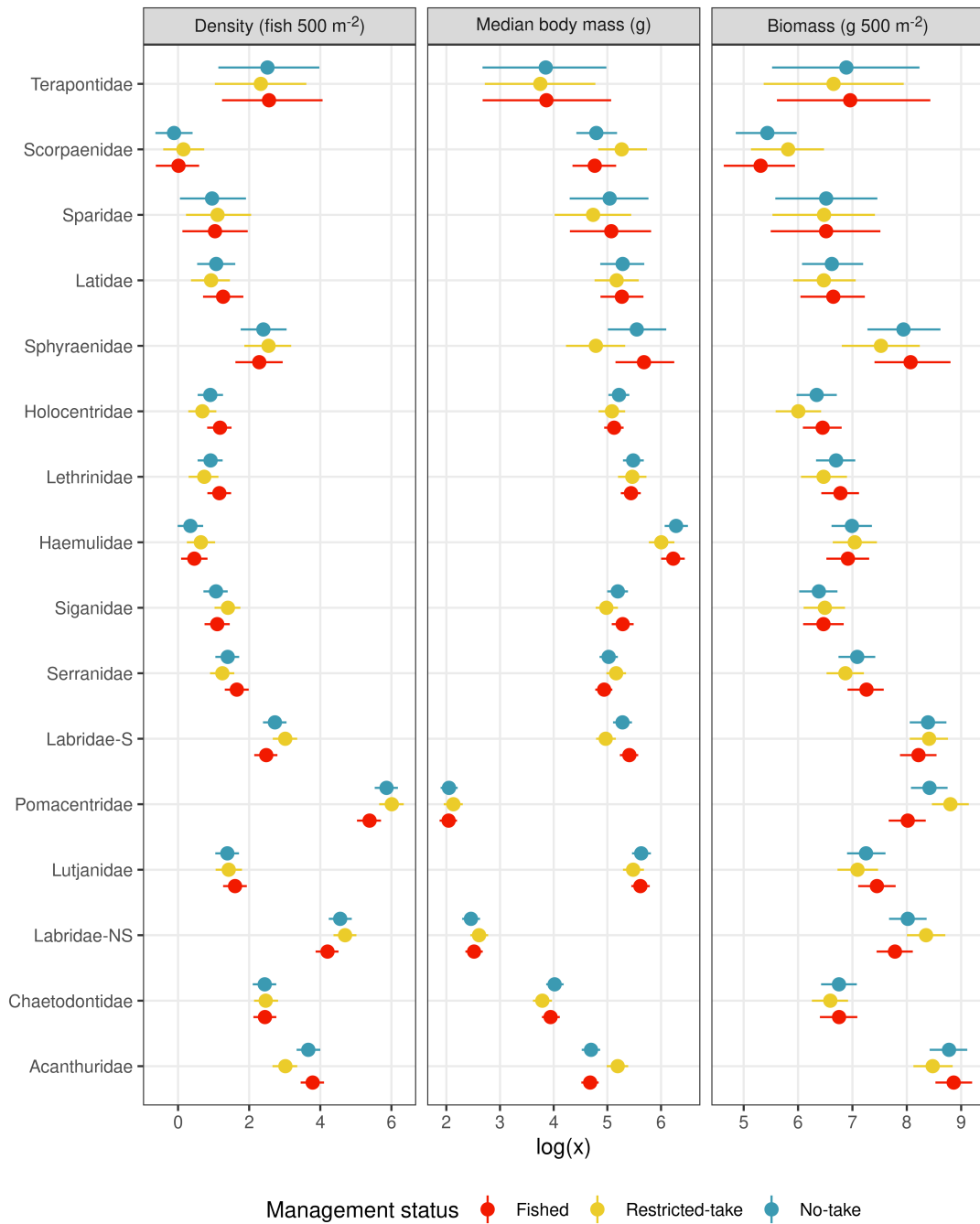
Figure 4.13: Density, median body mass, and biomass of fish families in three management categories. Circles and lines represent mean predicted values and 95% credible intervals from Bayesian linear multilevel regressions (see Supplementary Methods). Labridae-NS, non-scarine Labridae; Labridae-S, scarine Labridae.

Supplementary Tables

Table 4.1: Description of assumed relationships between predictors and responses (in bold) in the Directed Acyclic Graph.

Predictor	Description	Expected effect	Reference
CaCO3 excretion			
Biomass	Carbonate excretion rate is inherently related to fish standing biomass. Fish communities with higher biomass are expected to excrete more carbonate, regardless of the structure and composition of the community.	Positive	Wilson et al. (2009)
Mean trophic level	The trophic level is negatively related to the relative intestinal length, which has a negative effect on carbonate excretion rate at the individual level. Thus, fish communities with higher mean trophic level are expected to excrete relatively more carbonate than those with lower mean trophic level.	Positive	Ghilardi et al. (2021b), Ghilardi et al. (2023b)
Median body mass	Smaller individuals excrete more carbonate per unit mass than larger individuals. Consequently, fish communities with higher median body mass are expected to excrete relatively less carbonate than those with lower median body mass after accounting for standing biomass.	Negative	Ghilardi et al. (2023b)
Taxonomic and functional diversity	Carbonate excretion rate vary across fish families. Thus, taxonomic diversity is expected to influence community-level carbonate excretion. Moreover, both taxonomic and functional diversity are often positively linked to ecosystem functions on coral reefs, and could also have a positive effect on fish carbonate excretion.	Positive	Villéger et al. (2017), Ghilardi et al. (2023b)
SST	Temperature is expected to positively affect community-level carbonate production, as it is known to have a positive effect at the individual-level by increasing metabolic rate.	Positive	Wilson et al. (2009), Heuer et al. (2016), Ghilardi et al. (2023b)
CaCO3 composition			

Predictor	Description	Expected effect	Reference
Biomass	Although there is no apparent direct link between standing biomass and the mineralogical composition of fish carbonate, biomass varies three orders of magnitude across the sites included in the study. Therefore, we need to account for the confounding effect of biomass to correctly assess the effect of the community structure and composition.	Unknown	
Mean trophic level	The mineralogical composition of fish carbonate is influenced by relative intestinal length. Specifically, fish with short intestines excrete more ACMC and LMC, while fish with long intestines excrete more MHC.ă HMC and aragonite have the highest excretion rates in fish with intermediate intestinal length. Thus, as trophic level is negatively related to intestinal length, communities with high mean trophic level are expected to produce a greater proportion of ACMC and HMC than those with lower mean trophic level, which are instead expected to produce a greater proportion of MHC.ă	Varying by carbonate mineral form	Ghilardi et al. (2021b), Ghilardi et al. (2023b)
Median body mass	Body mass is positively related to the excretion rate of all carbonate forms produced by fish, but variability in the strength of that relationship can lead to changes in the carbonate composition along median body mass gradients.	Varying by carbonate mineral form	Ghilardi et al. (2023b)
Taxonomic and functional diversity	The mineralogical composition of fish carbonate is generally highly conserved at the family level, but may largely differ among families. Thus, a higher diversity is expected to result in a more diverse mineralogical composition of the excreted carbonate. Conversely, fish communities with low diversity are expected to mainly produce the most common fish carbonate polymorphs, particularly HMC (the main form produced by most fish families), but also ACMC.	Varying by carbonate mineral form	Salter et al. (2018), Ghilardi et al. (2023b)

Table 4.1: *(continued)*

Predictor	Description	Expected effect	Reference
SST	As temperature influences the excretion rate of different carbonate forms at the individual level, community-level carbonate mineralogy is expected to vary along temperature gradients. Particularly, temperature has a strong positive effect on the excretion rate of ACMC, thus fish communities at higher temperatures are expected to excrete a greater proportion of this carbonate form.	Varying by carbonate mineral form	Ghilardi et al. (2023b)
Biomass			
Human pressure	Reefs under a higher human pressure are known to have lower biomass due to direct exploitation and indirect effects through habitat degradation, pollution, land use and tourism.	Negative	Mora et al. (2011), Duffy et al. (2016), Cinner et al. (2016)
Management	Protected areas are expected to have higher overall biomass as extractive activities are restricted or banned. This effect should increase with increasing effectiveness (higher number of MPA features).	Positive	Edgar et al. (2014), Cinner et al. (2018)
Mean trophic level	Communities with low mean trophic level generally lead to higher biomass through large abundance and biomass of herbivores.	Negative	Graham et al. (2017)
Median body mass	Variations in fish community biomass are driven by the presence or absence of large-bodied fishes.	Positive	Lefcheck et al. (2021)
Taxonomic and functional diversity	Taxonomic and functional diversity are known to enhance reef fish community biomass. This relationships have been explained through complementary resource use and positive interaction between species like facilitation.	Positive	Duffy et al. (2016), Lefcheck et al. (2021)
SST	Temperature is a known driver of fish biomass.	Positive	Duffy et al. (2016)
NPP	Areas with higher net primary productivity are able to support a larger fish biomass.	Positive	Graham et al. (2018), Heenan et al. (2019)
Depth	Deeper reefs lead to higher fish biomass through the reduction of fishing pressure.	Positive	Duffy et al. (2016)

Table 4.1: *(continued)*

Predictor	Description	Expected effect	Reference
Mean trophic level			
Human pressure	Fishing generally targets high trophic level fishes or large herbivorous species like parrotfishes. Fishing is thus expected to modify the trophic structure of fish communities by removing biomass at high and low trophic levels. This could result in an increased mean trophic level at high fishing pressure due to higher proportion of biomass at mid trophic levels.	Positive or negative	Edwards et al. (2014), Graham et al. (2017), Cinner et al. (2018)
Management	Restrictions on extractive activities is expected to act in the opposite direction of fishing. Protected areas often display different trophic structure than fished areas.	Positive or negative	Soler et al. (2015), Graham et al. (2017), Cinner et al. (2018)
Taxonomic and functional diversity	More diverse communities support higher proportions of biomass at high trophic levels.	Positive	Villéger et al. (2017)
NPP	High primary productivity is able to sustain communities with large biomass at high trophic levels.	Positive	Heenan et al. (2019)
Depth	Herbivores are less abundant in deeper reefs due to limiting resources while high trophic level fishes are more abundant.	Positive	Andradi-Brown et al. (2016)
Median body mass			
Human pressure	Fishing is generally size-selective, thus modifying the size structure of the fish community by directly removing the biggest individuals (regardless of the trophic group, i.e., large-bodied individuals are targeted among both carnivores and herbivores). Evolution would also favour fast growing fishes with smaller adult sizes.	Negative	Graham et al. (2005), Robinson et al. (2017)
Management	Alleviation of the fishing pressure through protection measures allow fishes to grow older before being fished or dying, thus protection is expected to increase the median body-mass of the community.	Positive	Edgar and Stuart-Smith (2009), Edgar et al. (2014)

Table 4.1: *(continued)*

Predictor	Description	Expected effect	Reference
Taxonomic and functional diversity	There are more small species than large species, thus the diversity is usually higher among small-bodied fishes. The median body-mass is expected to decrease along biodiversity gradients	Negative	Rice and Gislason (1996), Parravicini et al. (2021)
SST	Fishes in warmer waters have typically smaller adult size mainly because they reach maturity earlier than in cooler water.	Negative	Wootton et al. (2022)
NPP	Primary productivity affects fish growth. High food availability increases fish growth, but high primary productivity may have negative effects on fish growth, potentially by altering the food web.	Negative	Tanner et al. (2019)
Depth	Larger fishes are more abundant in deeper reefs due to reduced fishing pressure.	Positive	Pereira et al. (2018)
Taxonomic diversity			
Management	Protected areas are an efficient tool to protect/restore biodiversity, including for coral reef fish communities.	Positive	Topor et al. (2019), Cinner et al. (2020)
Human pressure	Anthropogenic pressures are largely related to biodiversity loss (taxonomic and functional) including in reef fish communities.	Negative	D'Agata et al. (2014)
NPP	Highly productive coral reefs display higher biodiversity. High primary production can sustain large population size, averting extinction and promoting niche specialists.	Positive	Tittensor et al. (2010), Graham et al. (2018)
SST	Temperature is a major control of diversity on global scale. The underlying assumption of this relationship is that higher temperature would accelerate the metabolic rate which would allow for a higher rate of speciation.	Positive	Tittensor et al. (2010), Duffy et al. (2016)
Depth	Deeper reefs lead to higher fish diversity through the reduction of fishing pressure.	Positive	Duffy et al. (2016), Pereira et al. (2018)
Functional diversity			

Table 4.1: *(continued)*

Predictor	Description	Expected effect	Reference
Taxonomic diversity	Taxonomic and functional diversity are positively related as the addition of new species in a community is likely to increase the number of functional traits represented in the community.	Positive	Micheli and Halpern (2005)
Same predictors as for taxonomic diversity	Same assumptions as for taxonomic diversity.		
NPP			
SST	Temperature decreases primary productivity by increasing water stratification which reduces nutrients flux.	Negative	Feng et al. (2021)
Human pressure	Anthropogenic discharges (sewage water, agricultural runoffs) in coastal areas can increase nutrients levels and primary productivity.	Positive	Pritchard et al. (2003)

Abbreviations:
SST, sea surface temperature; NPP, net primary productivity.

Table 4.2: Standardised effects of structural equation model testing the indirect effects of human gravity and fisheries management on fish carbonate excretion and mineralogy.

Response	Predictor	Estimate	2.5%	25%	75%	97.5%
LMC	ln(Biomass)	-0.128	-0.238	-0.165	-0.091	-0.026
LMC	MTL	0.004	-0.131	-0.047	0.055	0.143
LMC	ln(Median biomass)	-0.082	-0.180	-0.118	-0.047	0.021
LMC	Taxonomic diversity	0.095	-0.042	0.049	0.142	0.219
LMC	Functional diversity	-0.317	-0.461	-0.371	-0.264	-0.166
LMC	SST	-0.639	-0.783	-0.690	-0.591	-0.482
ARA	ln(Biomass)	0.086	0.008	0.059	0.114	0.165
ARA	MTL	-0.107	-0.208	-0.146	-0.070	0.006
ARA	ln(Median biomass)	0.040	-0.035	0.013	0.066	0.111
ARA	Taxonomic diversity	0.007	-0.090	-0.023	0.038	0.094
ARA	Functional diversity	0.209	0.093	0.169	0.249	0.316
ARA	SST	0.267	0.148	0.229	0.307	0.387
HMC	ln(Biomass)	0.201	0.148	0.182	0.219	0.252
HMC	MTL	0.292	0.218	0.267	0.317	0.360
HMC	ln(Median biomass)	0.037	-0.010	0.021	0.053	0.085
HMC	Taxonomic diversity	-0.238	-0.297	-0.257	-0.218	-0.180
HMC	Functional diversity	0.199	0.130	0.176	0.223	0.267
HMC	SST	-0.150	-0.258	-0.189	-0.111	-0.043
MHC	ln(Biomass)	0.090	0.057	0.078	0.101	0.122
MHC	MTL	-0.310	-0.355	-0.324	-0.295	-0.265
MHC	ln(Median biomass)	0.018	-0.012	0.008	0.028	0.049
MHC	Taxonomic diversity	0.120	0.086	0.108	0.131	0.154
MHC	Functional diversity	0.025	-0.022	0.009	0.042	0.073
MHC	SST	0.046	-0.035	0.018	0.073	0.130
ACMC	ln(Biomass)	-0.289	-0.336	-0.306	-0.272	-0.238
ACMC	MTL	-0.079	-0.160	-0.109	-0.050	0.008
ACMC	ln(Median biomass)	-0.046	-0.097	-0.064	-0.027	0.005
ACMC	Taxonomic diversity	0.131	0.064	0.107	0.155	0.201
ACMC	Functional diversity	-0.221	-0.296	-0.249	-0.194	-0.146
ACMC	SST	0.332	0.222	0.295	0.369	0.438
ln(Carbonate excretion)	ln(Biomass)	0.937	0.919	0.931	0.944	0.955
ln(Carbonate excretion)	MTL	0.196	0.171	0.187	0.204	0.221
ln(Carbonate excretion)	ln(Median biomass)	-0.012	-0.030	-0.019	-0.006	0.005
ln(Carbonate excretion)	Taxonomic diversity	0.041	0.019	0.033	0.049	0.062
ln(Carbonate excretion)	Functional diversity	0.002	-0.024	-0.006	0.011	0.028
ln(Carbonate excretion)	SST	0.105	0.068	0.092	0.118	0.144
ln(Biomass)	MTL	-0.005	-0.092	-0.035	0.026	0.082
ln(Biomass)	ln(Median biomass)	0.299	0.237	0.279	0.320	0.358
ln(Biomass)	Taxonomic diversity	-0.030	-0.115	-0.057	-0.002	0.047
ln(Biomass)	Functional diversity	-0.043	-0.135	-0.074	-0.012	0.048
ln(Biomass)	SST	0.244	0.054	0.182	0.311	0.419
ln(Biomass)	ln(NPP)	0.005	-0.103	-0.033	0.043	0.108
ln(Biomass)	sqrt(Depth)	0.122	0.059	0.100	0.144	0.187
ln(Biomass)	ln(Gravity)	-0.221	-0.293	-0.245	-0.196	-0.151
ln(Biomass)	Restricted take MPA	0.011	-0.080	-0.020	0.042	0.105
ln(Biomass)	No-take MPA	0.013	-0.068	-0.015	0.042	0.096
MTL	Taxonomic diversity	-0.299	-0.358	-0.320	-0.279	-0.239
MTL	Functional diversity	0.734	0.683	0.716	0.752	0.785
MTL	ln(NPP)	0.290	0.222	0.266	0.314	0.359
MTL	sqrt(Depth)	0.044	-0.003	0.028	0.060	0.092

Response	Predictor	Estimate	2.5%	25%	75%	97.5%
MTL	ln(Gravity)	0.071	0.014	0.052	0.090	0.127
MTL	Restricted take MPA	-0.021	-0.093	-0.044	0.003	0.050
MTL	No-take MPA	-0.030	-0.090	-0.052	-0.009	0.031
ln(Median biomass)	Taxonomic diversity	-0.169	-0.247	-0.197	-0.141	-0.087
ln(Median biomass)	Functional diversity	-0.018	-0.091	-0.042	0.007	0.056
ln(Median biomass)	SST	-0.328	-0.506	-0.386	-0.267	-0.162
ln(Median biomass)	ln(NPP)	-0.163	-0.288	-0.206	-0.118	-0.041
ln(Median biomass)	sqrt(Depth)	-0.137	-0.208	-0.161	-0.112	-0.063
ln(Median biomass)	ln(Gravity)	-0.036	-0.118	-0.064	-0.007	0.045
ln(Median biomass)	Restricted take MPA	-0.101	-0.199	-0.136	-0.065	0.003
ln(Median biomass)	No-take MPA	-0.104	-0.191	-0.134	-0.074	-0.015
Taxonomic diversity	SST	0.214	0.052	0.157	0.272	0.369
Taxonomic diversity	ln(NPP)	-0.219	-0.321	-0.256	-0.183	-0.116
Taxonomic diversity	sqrt(Depth)	0.049	-0.013	0.026	0.071	0.110
Taxonomic diversity	ln(Gravity)	-0.053	-0.124	-0.079	-0.027	0.021
Taxonomic diversity	Restricted take MPA	0.031	-0.059	0.000	0.063	0.121
Taxonomic diversity	No-take MPA	0.070	-0.008	0.043	0.097	0.151
Functional diversity	Taxonomic diversity	0.438	0.365	0.412	0.464	0.510
Functional diversity	SST	0.155	-0.035	0.097	0.218	0.324
Functional diversity	ln(NPP)	0.338	0.230	0.300	0.376	0.442
Functional diversity	sqrt(Depth)	0.108	0.044	0.086	0.129	0.172
Functional diversity	ln(Gravity)	-0.079	-0.156	-0.106	-0.053	-0.004
Functional diversity	Restricted take MPA	-0.034	-0.128	-0.068	-0.001	0.060
Functional diversity	No-take MPA	-0.013	-0.093	-0.042	0.015	0.070
ln(NPP)	SST	-1.169	-1.271	-1.204	-1.133	-1.067
ln(NPP)	ln(Gravity)	0.083	0.036	0.066	0.100	0.131

Abbreviations:

LMC, low-magnesium calcite; ARA, aragonite; HMC, high-magnesium calcite; MHC, monohydrocalcite; ACMC, amorphous calcium magnesium carbonate; MTL, mean trophic level; SST, sea surface temperature; NPP, net primary productivity.

Table 4.3: Standardised effects of structural equation model testing the indirect effects of travel time, human population size and fisheries management on fish carbonate excretion and mineralogy.

Response	Predictor	Estimate	2.5%	25%	75%	97.5%
LMC	ln(Biomass)	-0.127	-0.228	-0.162	-0.092	-0.020
LMC	MTL	0.003	-0.135	-0.044	0.049	0.143
LMC	ln(Median biomass)	-0.082	-0.185	-0.117	-0.046	0.018
LMC	Taxonomic diversity	0.093	-0.039	0.046	0.140	0.232
LMC	Functional diversity	-0.316	-0.457	-0.368	-0.266	-0.167
LMC	SST	-0.640	-0.776	-0.689	-0.593	-0.493
ARA	ln(Biomass)	0.086	0.005	0.056	0.116	0.166
ARA	MTL	-0.108	-0.210	-0.146	-0.071	0.001
ARA	ln(Median biomass)	0.040	-0.036	0.014	0.066	0.111
ARA	Taxonomic diversity	0.007	-0.087	-0.025	0.040	0.099
ARA	Functional diversity	0.209	0.093	0.171	0.249	0.318
ARA	SST	0.267	0.150	0.227	0.305	0.387
HMC	ln(Biomass)	0.201	0.148	0.183	0.220	0.252
HMC	MTL	0.290	0.219	0.267	0.315	0.358
HMC	ln(Median biomass)	0.037	-0.013	0.021	0.053	0.085
HMC	Taxonomic diversity	-0.238	-0.296	-0.258	-0.218	-0.179
HMC	Functional diversity	0.200	0.133	0.176	0.224	0.269
HMC	SST	-0.152	-0.262	-0.189	-0.116	-0.043
MHC	ln(Biomass)	0.090	0.056	0.079	0.102	0.123
MHC	MTL	-0.309	-0.351	-0.324	-0.294	-0.265
MHC	ln(Median biomass)	0.019	-0.012	0.009	0.029	0.047
MHC	Taxonomic diversity	0.120	0.087	0.108	0.132	0.155
MHC	Functional diversity	0.025	-0.022	0.010	0.041	0.072
MHC	SST	0.044	-0.035	0.017	0.072	0.125
ACMC	ln(Biomass)	-0.289	-0.333	-0.306	-0.273	-0.239
ACMC	MTL	-0.079	-0.160	-0.107	-0.052	0.006
ACMC	ln(Median biomass)	-0.046	-0.100	-0.064	-0.027	0.009
ACMC	Taxonomic diversity	0.131	0.060	0.107	0.155	0.201
ACMC	Functional diversity	-0.221	-0.295	-0.248	-0.196	-0.147
ACMC	SST	0.335	0.231	0.301	0.371	0.434
ln(Carbonate excretion)	ln(Biomass)	0.937	0.919	0.931	0.943	0.955
ln(Carbonate excretion)	MTL	0.197	0.172	0.188	0.205	0.220
ln(Carbonate excretion)	ln(Median biomass)	-0.012	-0.030	-0.018	-0.007	0.005
ln(Carbonate excretion)	Taxonomic diversity	0.041	0.021	0.034	0.049	0.063
ln(Carbonate excretion)	Functional diversity	0.002	-0.023	-0.007	0.011	0.027
ln(Carbonate excretion)	SST	0.105	0.069	0.092	0.117	0.143
ln(Biomass)	MTL	-0.015	-0.110	-0.046	0.019	0.079
ln(Biomass)	ln(Median biomass)	0.292	0.232	0.270	0.314	0.353
ln(Biomass)	Taxonomic diversity	-0.050	-0.137	-0.079	-0.021	0.036
ln(Biomass)	Functional diversity	-0.024	-0.122	-0.056	0.010	0.075
ln(Biomass)	SST	0.226	0.023	0.159	0.292	0.414
ln(Biomass)	ln(NPP)	-0.007	-0.128	-0.048	0.034	0.113
ln(Biomass)	sqrt(Depth)	0.118	0.051	0.095	0.140	0.184
ln(Biomass)	ln(Travel time)	0.121	0.048	0.097	0.145	0.198
ln(Biomass)	ln(Human population)	-0.155	-0.268	-0.192	-0.117	-0.051
ln(Biomass)	Restricted take MPA	0.033	-0.056	0.002	0.064	0.124
ln(Biomass)	No-take MPA	0.036	-0.047	0.008	0.064	0.116
MTL	Taxonomic diversity	-0.299	-0.361	-0.319	-0.278	-0.236
MTL	Functional diversity	0.731	0.680	0.713	0.749	0.784

Response	Predictor	Estimate	2.5%	25%	75%	97.5%
MTL	ln(NPP)	0.307	0.230	0.280	0.332	0.384
MTL	sqrt(Depth)	0.043	-0.003	0.027	0.059	0.093
MTL	ln(Travel time)	-0.013	-0.068	-0.031	0.005	0.041
MTL	ln(Human population)	0.064	-0.019	0.037	0.091	0.143
MTL	Restricted take MPA	-0.023	-0.093	-0.046	0.001	0.042
MTL	No-take MPA	-0.032	-0.093	-0.053	-0.010	0.028
ln(Median biomass)	Taxonomic diversity	-0.174	-0.259	-0.203	-0.146	-0.088
ln(Median biomass)	Functional diversity	-0.018	-0.093	-0.044	0.008	0.057
ln(Median biomass)	SST	-0.330	-0.510	-0.392	-0.268	-0.147
ln(Median biomass)	ln(NPP)	-0.184	-0.315	-0.228	-0.139	-0.054
ln(Median biomass)	sqrt(Depth)	-0.136	-0.210	-0.161	-0.109	-0.065
ln(Median biomass)	ln(Travel time)	0.033	-0.050	0.006	0.060	0.116
ln(Median biomass)	ln(Human population)	-0.153	-0.280	-0.195	-0.111	-0.034
ln(Median biomass)	Restricted take MPA	-0.115	-0.220	-0.149	-0.080	-0.017
ln(Median biomass)	No-take MPA	-0.119	-0.211	-0.150	-0.087	-0.029
Taxonomic diversity	SST	0.182	0.019	0.130	0.238	0.330
Taxonomic diversity	ln(NPP)	-0.170	-0.276	-0.205	-0.134	-0.066
Taxonomic diversity	sqrt(Depth)	0.039	-0.024	0.016	0.061	0.104
Taxonomic diversity	ln(Travel time)	0.135	0.065	0.111	0.159	0.206
Taxonomic diversity	ln(Human population)	-0.004	-0.106	-0.038	0.030	0.097
Taxonomic diversity	Restricted take MPA	0.050	-0.039	0.020	0.079	0.139
Taxonomic diversity	No-take MPA	0.093	0.008	0.065	0.121	0.171
Functional diversity	Taxonomic diversity	0.447	0.377	0.423	0.471	0.516
Functional diversity	SST	0.187	-0.011	0.130	0.249	0.360
Functional diversity	ln(NPP)	0.295	0.183	0.256	0.332	0.411
Functional diversity	sqrt(Depth)	0.114	0.049	0.091	0.137	0.178
Functional diversity	ln(Travel time)	-0.049	-0.127	-0.075	-0.022	0.028
Functional diversity	ln(Human population)	-0.089	-0.191	-0.123	-0.054	0.018
Functional diversity	Restricted take MPA	-0.040	-0.137	-0.072	-0.008	0.058
Functional diversity	No-take MPA	-0.023	-0.110	-0.054	0.006	0.062
ln(NPP)	SST	-0.975	-1.082	-1.012	-0.939	-0.867
ln(NPP)	ln(Travel time)	-0.186	-0.227	-0.200	-0.171	-0.142
ln(NPP)	ln(Human population)	-0.174	-0.239	-0.196	-0.152	-0.110

Abbreviations:
LMC, low-magnesium calcite; ARA, aragonite; HMC, high-magnesium calcite; MHC, monohydrocalcite; ACMC, amorphous calcium magnesium carbonate; MTL, mean trophic level; SST, sea surface temperature; NPP, net primary productivity.

Table 4.4: Standardised effects of structural equation model testing the indirect effects of travel time, human population size and number of MPA features on fish carbonate excretion and mineralogy.

Response	Predictor	Estimate	2.5%	25%	75%	97.5%
LMC	ln(Biomass)	-0.128	-0.236	-0.165	-0.092	-0.024
LMC	MTL	0.008	-0.135	-0.040	0.058	0.148
LMC	ln(Median biomass)	-0.082	-0.182	-0.118	-0.044	0.018
LMC	Taxonomic diversity	0.096	-0.041	0.050	0.140	0.224
LMC	Functional diversity	-0.321	-0.474	-0.374	-0.269	-0.162
LMC	SST	-0.634	-0.775	-0.689	-0.583	-0.472
ARA	ln(Biomass)	0.086	0.004	0.060	0.113	0.165
ARA	MTL	-0.107	-0.213	-0.142	-0.071	0.000
ARA	ln(Median biomass)	0.039	-0.035	0.014	0.065	0.111
ARA	Taxonomic diversity	0.007	-0.086	-0.023	0.038	0.096
ARA	Functional diversity	0.208	0.098	0.171	0.247	0.317
ARA	SST	0.269	0.146	0.230	0.309	0.391
HMC	ln(Biomass)	0.200	0.146	0.183	0.218	0.251
HMC	MTL	0.291	0.221	0.267	0.315	0.365
HMC	ln(Median biomass)	0.037	-0.009	0.022	0.053	0.085
HMC	Taxonomic diversity	-0.238	-0.295	-0.258	-0.218	-0.178
HMC	Functional diversity	0.200	0.131	0.177	0.223	0.267
HMC	SST	-0.152	-0.260	-0.190	-0.114	-0.041
MHC	ln(Biomass)	0.090	0.057	0.079	0.102	0.121
MHC	MTL	-0.310	-0.353	-0.324	-0.296	-0.267
MHC	ln(Median biomass)	0.019	-0.010	0.009	0.029	0.048
MHC	Taxonomic diversity	0.120	0.083	0.108	0.132	0.154
MHC	Functional diversity	0.026	-0.020	0.009	0.043	0.073
MHC	SST	0.043	-0.038	0.015	0.070	0.128
ACMC	ln(Biomass)	-0.289	-0.334	-0.306	-0.273	-0.238
ACMC	MTL	-0.078	-0.161	-0.107	-0.050	0.006
ACMC	ln(Median biomass)	-0.047	-0.098	-0.065	-0.029	0.007
ACMC	Taxonomic diversity	0.131	0.062	0.106	0.154	0.200
ACMC	Functional diversity	-0.221	-0.292	-0.247	-0.197	-0.142
ACMC	SST	0.335	0.224	0.300	0.373	0.437
ln(Carbonate excretion)	ln(Biomass)	0.937	0.919	0.931	0.943	0.955
ln(Carbonate excretion)	MTL	0.196	0.173	0.188	0.205	0.221
ln(Carbonate excretion)	ln(Median biomass)	-0.012	-0.029	-0.018	-0.006	0.005
ln(Carbonate excretion)	Taxonomic diversity	0.041	0.021	0.034	0.049	0.063
ln(Carbonate excretion)	Functional diversity	0.002	-0.023	-0.007	0.011	0.028
ln(Carbonate excretion)	SST	0.104	0.066	0.090	0.117	0.143
ln(Biomass)	MTL	-0.014	-0.103	-0.045	0.018	0.077
ln(Biomass)	ln(Median biomass)	0.294	0.229	0.271	0.316	0.358
ln(Biomass)	Taxonomic diversity	-0.050	-0.129	-0.078	-0.022	0.028
ln(Biomass)	Functional diversity	-0.025	-0.119	-0.057	0.007	0.069
ln(Biomass)	SST	0.225	0.025	0.159	0.291	0.419
ln(Biomass)	ln(NPP)	0.000	-0.117	-0.041	0.040	0.120
ln(Biomass)	sqrt(Depth)	0.120	0.054	0.098	0.142	0.185
ln(Biomass)	ln(Travel time)	0.120	0.050	0.095	0.144	0.189
ln(Biomass)	ln(Human population)	-0.154	-0.260	-0.191	-0.118	-0.045
ln(Biomass)	MPA features	0.044	-0.027	0.020	0.069	0.116
MTL	Taxonomic diversity	-0.297	-0.359	-0.319	-0.276	-0.241
MTL	Functional diversity	0.731	0.681	0.712	0.748	0.782
MTL	ln(NPP)	0.303	0.228	0.277	0.329	0.379

Response	Predictor	Estimate	2.5%	25%	75%	97.5%
MTL	sqrt(Depth)	0.042	-0.007	0.026	0.059	0.091
MTL	ln(Travel time)	-0.012	-0.066	-0.031	0.007	0.041
MTL	ln(Human population)	0.061	-0.018	0.036	0.088	0.138
MTL	MPA features	-0.038	-0.090	-0.056	-0.019	0.016
ln(Median biomass)	Taxonomic diversity	-0.174	-0.265	-0.204	-0.143	-0.085
ln(Median biomass)	Functional diversity	-0.017	-0.094	-0.044	0.008	0.061
ln(Median biomass)	SST	-0.322	-0.514	-0.384	-0.263	-0.136
ln(Median biomass)	ln(NPP)	-0.191	-0.322	-0.236	-0.147	-0.063
ln(Median biomass)	sqrt(Depth)	-0.138	-0.214	-0.163	-0.112	-0.064
ln(Median biomass)	ln(Travel time)	0.039	-0.041	0.010	0.066	0.121
ln(Median biomass)	ln(Human population)	-0.149	-0.274	-0.191	-0.106	-0.028
ln(Median biomass)	MPA features	-0.120	-0.196	-0.149	-0.093	-0.042
Taxonomic diversity	SST	0.179	0.019	0.121	0.235	0.344
Taxonomic diversity	ln(NPP)	-0.172	-0.283	-0.209	-0.136	-0.068
Taxonomic diversity	sqrt(Depth)	0.039	-0.024	0.018	0.060	0.101
Taxonomic diversity	ln(Travel time)	0.129	0.057	0.105	0.155	0.202
Taxonomic diversity	ln(Human population)	-0.005	-0.108	-0.039	0.028	0.093
Taxonomic diversity	MPA features	0.074	0.002	0.051	0.099	0.145
Functional diversity	Taxonomic diversity	0.448	0.375	0.422	0.472	0.522
Functional diversity	SST	0.199	0.005	0.140	0.261	0.365
Functional diversity	ln(NPP)	0.294	0.179	0.254	0.333	0.408
Functional diversity	sqrt(Depth)	0.112	0.048	0.089	0.136	0.175
Functional diversity	ln(Travel time)	-0.047	-0.123	-0.073	-0.021	0.028
Functional diversity	ln(Human population)	-0.088	-0.194	-0.125	-0.052	0.019
Functional diversity	MPA features	-0.028	-0.107	-0.057	0.000	0.048
ln(NPP)	SST	-0.976	-1.086	-1.012	-0.940	-0.869
ln(NPP)	ln(Travel time)	-0.185	-0.226	-0.200	-0.171	-0.143
ln(NPP)	ln(Human population)	-0.173	-0.237	-0.195	-0.150	-0.112

Abbreviations:

LMC, low-magnesium calcite; ARA, aragonite; HMC, high-magnesium calcite; MHC, monohydro-calcite; ACMC, amorphous calcium magnesium carbonate; MTL, mean trophic level; SST, sea surface temperature; NPP, net primary productivity.

Synthesis

Towards a comprehensive understanding of fish contribution to the inorganic carbon cycle

The rapid transformations faced by ecosystems globally in response to climate change and anthropogenic disturbances has led to calls for a shift in conservation practices towards the prioritisation of ecosystem functioning to sustain the provision of ecosystem services (Hughes et al. 2017a; Bellwood et al. 2019a; Williams and Graham 2019; Duarte et al. 2020). Understanding and conserving the functioning of the marine carbon cycle is of primary importance in an era of global climate change. Marine fish are an important component of the carbon cycle (Lutz and Martin 2014; Martin et al. 2021; Saba et al. 2021). Among the many functions and services they sustain, fish continuously excrete carbonates at high rates as a waste product of their physiological processes (Wilson et al. 2002). Given the huge abundance and biomass of fish in the ocean, they can greatly contribute to the inorganic carbon cycle (Wilson et al. 2009). Research in this field has grown rapidly in recent years, mainly advancing our understanding of the physiological process itself and the diversity of carbonate polymorphs produced. However, if we are to sustain this ecosystem service, knowledge of its drivers is required. Through a multilevel assessment of the drivers of fish carbonate excretion rate and mineralogy, this thesis fast-tracks our understanding of the role fish play in the marine inorganic carbon cycle. The results provide a detailed and spatially comprehensive overview of the drivers at the individual and community levels. It thus improves the quantification of current levels of this biogeochemical function and facilitates the prediction of future changes in the services it provides (Figure 4.14).
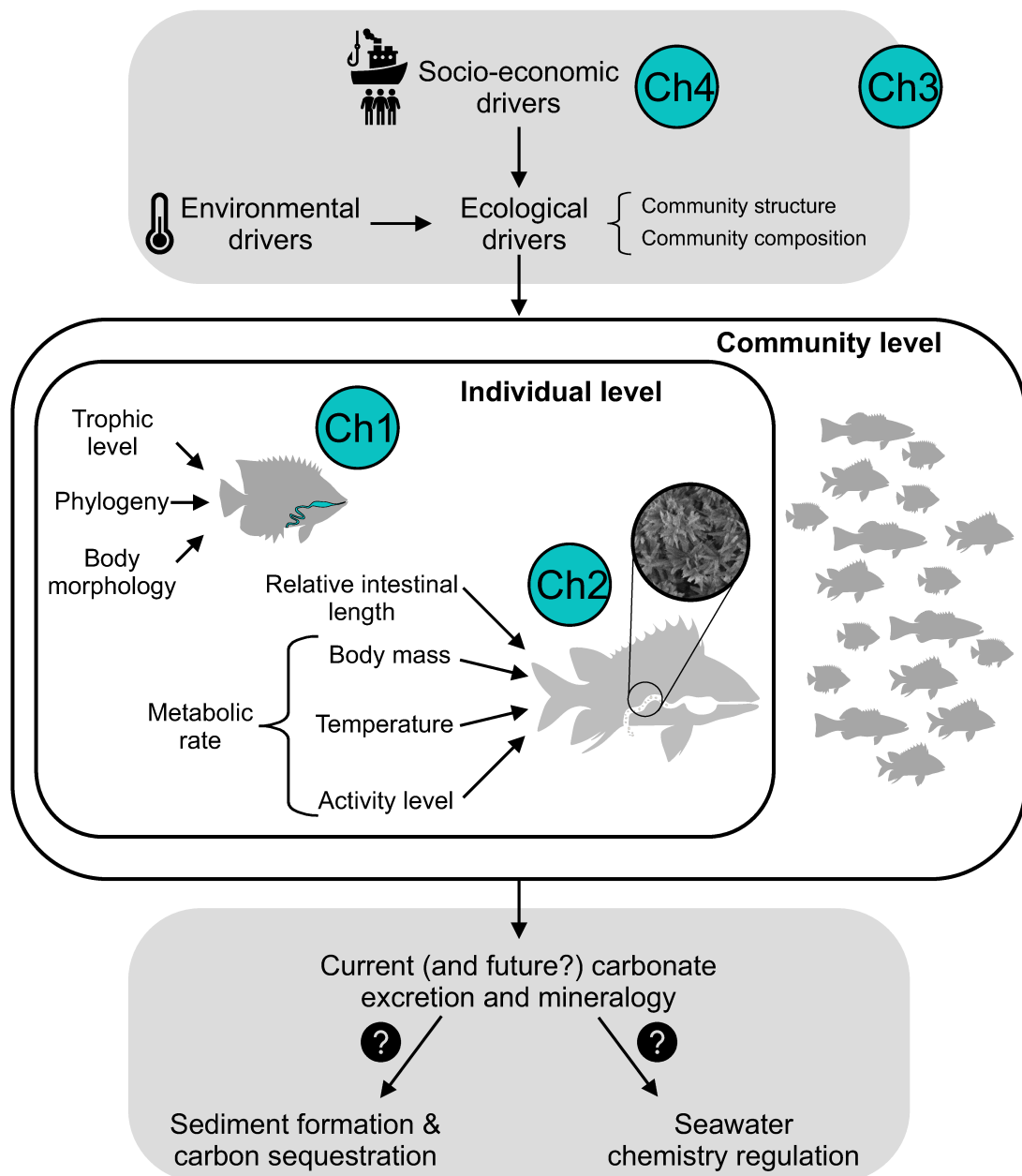
Figure 4.14: Schematic diagram of the contribution of this thesis in understanding the role of fish in the inorganic carbon cycle. At the individual level, the major drivers of intestinal morphology and carbonate excretion rates and mineralogy were identified (*Chapters 1* and *2*, respectively). At the community level, a global-scale analysis indicated that current carbonate excretion and mineralogy are primarily driven by fish community structure, sea surface temperature, and human pressure (*Chapter 3*). The impact of human pressure is mediated by a reduction in fish biomass, despite fishing pressure being relatively low in the Australian coral reef context (*Chapter 4*). Coupled with predictive models, these findings could yield solid predictions of future levels of this function. However, our understanding of the services provided by fish carbonates remain limited by knowledge gaps on their fate post-excretion, as indicated by question marks.

Drivers of individual-level carbonate excretion and mineralogy

The physiological mechanisms of carbonate precipitation and excretion suggest that this process may be regulated by several intrinsic and extrinsic factors that govern the amount of ingested calcium and magnesium by fish. Elevated salinity, for instance, increases osmotic water loss and drinking rates, leading to higher carbonate excretion rates (Genz et al. 2008; Mekuchi et al. 2010; Schauer et al. 2018). Elevated temperature increases osmotic water loss and carbonate excretion rates by increasing gill ventilation and metabolic rate (Wilson et al. 2009; Heuer et al. 2016). Temperature is also known to influence the mineralogy of other biogenic carbonates (Figuerola et al. 2023), but this is less evident in fish (Salter et al. 2019). These factors have typically been tested separately on individual species. A first comprehensive assessment of the drivers of carbonate excretion rate and mineralogical composition has been undertaken across numerous species and families of tropical reef fishes (*Chapter 2*). This study reached three key conclusions: (1) carbonate excretion rate scales proportionally to metabolic rate, (2) intestinal length is a major driver of carbonate excretion rate, and (3) the mineralogical composition of the excreted carbonates depends on the intestinal length and water temperature as well as on the family of the fish.

Given the direct effect of fish metabolic rate on drinking rate, a relationship between carbonate excretion rate and metabolic rate has long been hypothesised but never empirically tested (Takei and Tsukada 2001; Jennings and Wilson 2009; Wilson et al. 2009). Evidence of this relationship is crucial for quantifying fish-mediated carbonate production and for validating previous global estimates based on this assumption (Wilson et al. 2009). Demonstrating this relationship has also implications for the assumed impact of ongoing fishing and climate change on fish contribution to carbon cycling. Using three key drivers of metabolic rate (i.e., body mass, temperature, and aspect ratio of caudal fin), this thesis finds that the metabolism-carbonate excretion rate link is consistent across species and families (*Chapter 2*). Specifically, carbonate excretion rate per unit mass increases with

temperature and activity level of the fish (linked to aspect ratio), but decreases with increasing body mass. Thus, as fishing removes larger individuals, carbonate excretion decreases at a slower rate than fish biomass (Jennings and Wilson 2009). This concept has also been observed in other fish functions, such as biomass productivity (Morais and Bellwood 2020). Industrial fishing of pelagic species, which have the highest activity levels, has likely impacted carbonate production for decades by depleting the biomass of these high carbonate producers (Christensen et al. 2014). This adds to the reduction in sinking of fish carcasses and associated carbon sequestration in the deep sea caused by fishing (Mariani et al. 2020). Global warming will increase the metabolic and carbonate excretion rates of individual fishes, but this positive effect may be offset by a decrease in community biomass (Wilson et al. 2009; Lotze et al. 2019; Salvatteci et al. 2022). This thesis demonstrates that community-level carbonate excretion rates are higher in warmer waters, at least on tropical and subtropical reefs (*Chapter 3*).

The strong negative relationship between carbonate excretion rate and intestinal length identified in *Chapter 2* shows that intestinal morphology, in addition to being tightly linked to digestion and assimilation, plays an important role in osmoregulation. There is scope for physiological research to examine the mechanisms underlying this observation. Intestinal length is highly conserved across the fish phylogeny and strongly related to body size and shape as well as to trophic level (*Chapter 1*). Herbivores have longer intestines and thus lower carbonate excretion rates than higher trophic level fishes (Al-Hussaini 1947; Elliott and Bellwood 2003; Wagner et al. 2009; Steinberg 2018, *Chapter 1*). This implies spatial variation in fish carbonate excretion as a function of the trophic structure of fish communities (*Chapter 3*), and cascading effects of disturbances altering fish trophic structure. *Chapter 3* thus sheds light over the potential effects of fishing on carbonate excretion. Explicitly, it predicts that carbonate excretion would be highest in top-heavy (i.e., more biomass in high trophic levels, >4) and lowest in bottom-heavy (i.e., more biomass in low trophic levels, <2.5) fish

communities. Depletion of high trophic level fishes would thus disproportionately decrease carbonate excretion rates.

Although it is important to understand the drivers of fish carbonate excretion rates, it is equally important to understand the drivers of the mineralogical composition of the excreted carbonates. Indeed, the global significance of fish carbonates lies precisely in their mineralogy which dictates their solubility. Fish carbonate mineralogy suggests a relatively high solubility compared to other biogenic carbonates (Woosley et al. 2012), leading to the hypothesis that they provide an important source of upper ocean dissolution (Wilson et al. 2009; Sulpis et al. 2021). Fish produce a wide variety of carbonate polymorphs (Walsh et al. 1991; Perry et al. 2011; Salter et al. 2012; Foran et al. 2013; Salter et al. 2017; Salter et al. 2018; Salter et al. 2019), but the composition of the excreted carbonates shows a high degree of consistency within families (Salter et al. 2017; Salter et al. 2018; Salter et al. 2019, *Chapter 2*). However, this thesis finds that further interspecific variation exists and is explained by temperature and relative intestinal length (*Chapter 2*). The excretion rate of unstable amorphous calcium magnesium carbonate (ACMC) is highest in warm waters and in fishes with short intestines (i.e., high trophic level), while monohydrocalcite (MHC) is excreted more by fishes with long intestines (i.e., low trophic level). Therefore, spatial variation in carbonate mineralogy is driven by temperature and variation in fish community structure and composition (*Chapter 3*) and may shift in response to climate change and other disturbances. In warmer waters, for instance, excreted carbonates would contain more ACMC suggesting higher dissolution and at shallower depth. These findings suggest that the role of fish in the inorganic carbon cycle is more complex than previously thought. It changes spatially and temporally as a function of the excretion rates and the mineralogical composition of fish carbonates. Integration of carbonate mineralogy into production models is thus required to better understand this process.

Determining the mechanistic aspects of different forms of carbon released by fish (e.g., dissolved and particulate organic carbon) has been identified as a high priority research need to improve estimation of fish carbon cycling (Saba et al.

2021). We now have identified the fish traits and environmental variables that control carbonate excretion and mineralogy and quantified their relationships. This empirically-derived information is new and useful for the parameterisation of global biogeochemical models. With this information we can start refining estimates of the contribution of fish to particulate inorganic carbon. We can also determine the potential impacts of fishing and climate change on this function, and infer its roles as a potential buffer for ocean acidification and as a sediment source. These steps are facilitated by recently published models (*Chapter 2*). While currently limited in geographic and taxonomic scope, these can be updated as data for new regions and species become available.

Drivers of community-level carbonate excretion and mineralogy

Determining the mechanisms underlying individual-level processes is a necessary task towards the understanding of ecosystem functioning. A logical next step is to move from the individual to the community level, and identify the factors (e.g., ecological, environmental, socio-economic) shaping spatial and temporal patterns of ecosystem functions. Such information would lead to better maps of current levels of ecosystem functions and services and facilitate the prediction of their future levels under different socio-economic and climate change scenarios (Shared Socioeconomic Pathway-Representative Concentration Pathway, SSP-RCP, van Vuuren et al. 2014). This could help to inform management strategies that aim to sustain ecosystem services.

Large spatial scale (regional to global) analyses are regularly performed to investigate the factors influencing properties of fish communities (e.g., Parravicini et al. 2013; Mellin et al. 2016a; McLean et al. 2021; Parravicini et al. 2021), including ecosystem functions (e.g., Cinner et al. 2020; Schiettekatte et al. 2022a; Seguin et al. 2022). Fish functions involved in carbon cycling lag behind in this respect do to our limited ability to quantify them for entire fish communities. Studies are mainly limited to fish biomass (e.g., Mora et al. 2011; Duffy et al. 2016;

Cinner et al. 2016; McClanahan et al. 2019; Fontoura et al. 2022), which represent a snapshot of the amount of carbon stored in fish bodies, or biomass production (Morais et al. 2020b; Morais et al. 2021; Seguin et al. 2022), which represent the carbon storage potential. Extending large-scale analysis to the excretion and egestion of organic carbon by fish is now more feasible following improvements in modelling fish nutrient fluxes (Schiettekatte et al. 2020).

Carbonate production by fish has been estimated at regional scale in Bahamian and Australian reefs (Perry et al. 2011; Salter et al. 2017; Salter et al. 2018). While these studies have not directly investigated the drivers of the observed spatial patterns, several interesting observations have emerged. The first, although evident given that carbonate excretion rates are linked to fish size and abundance, is that excretion rates vary among locations as a function of fish biomass. Second, excretion rates vary among habitat types as these support different levels of biomass and species composition (Perry et al. 2011; Salter et al. 2017). Third, given that different species produce different carbonate polymorphs, carbonate mineralogy and its significance for sediment production and inorganic carbon cycling varies regionally and among habitats as a function of fish community composition (Salter et al. 2017; Salter et al. 2018). Fourth, fishing impacts carbonate excretion on Bahamian reefs by removing fish biomass and alters the mineralogical composition through selective removal of certain families (Salter et al. 2017).

Chapter 3 of this thesis combined new carbonate production models (*Chapter 2*) with a global reef fish survey database to map carbonate excretion and mineralogy across tropical reefs. Applying causal inference this chapter provided a first evaluation of the drivers of fish inorganic carbon cycling. While biomass is the main determinant of spatial variation in carbonate excretion rates, several ecological, environmental and socio-economic drivers were identified. Fish community structure is key in determining carbonate excretion and mineralogy. Communities characterised by large-bodied and high trophic level fish have the highest excretion rates and excrete predominantly high-magnesium calcite (HMC). Communities dominated by herbivores excrete less carbonate and a combination

257

of carbonate polymorphs. These findings reflect the influence of intestinal length on fish carbonate excretion and mineralogy (*Chapter 2*). Although larger fish have lower excretion rates per unit mass than smaller fish (*Chapter 2*), they contribute disproportionately to total fish biomass (Lefcheck et al. 2021). Hence there is indirect positive effect of community median body mass on carbonate excretion rate (*Chapter 4*). Of the environmental factors, temperature exerts the strongest influence on carbonate excretion by influencing the metabolic and drinking rates of fish. Temperature also appears as the strongest driver of patterns in carbonate mineralogy. Proportions of highly soluble carbonates (ACMC and MHC) increase in warmer waters due to a direct effect of temperature on the excretion of ACMC (*Chapter 2*) and to an indirect effect on MHC mediated by fish biodiversity (*Chapter 4*). Rising temperatures may thus increase the carbonate production by fish, but carbonate would dissolve faster, thereby releasing alkalinity at shallower depths and reducing both its sedimentation potential and its ballast effect on gravitational organic carbon.

Chapter 3 also showed that at the global scale carbonate excretion rate is strongly affected by human gravity (i.e., an index of human pressure). This effect largely exceeded the weak positive effect of fisheries management, whether it was fishing restrictions such as size or effort limits, or no-take areas (*Chapter 3*). Focusing on a smaller geographic scale (i.e., Australian reefs) as a case study, *chapter 4* reached a similar conclusion regarding the relative role of fisheries management and human gravity on fish carbonate excretion. Despite the relatively low fishing pressure afforded by Australian reefs, the effect of human gravity was strong and mediated by a reduction in fish biomass. This highlights that human pressure has a pervasive impact on reef fish communities and the services they provide. This effect is not exclusively attributable to fishing pressure, but also to multiple human impacts, including coastal development, land use, pollution and tourism (Mora et al. 2011).

Partial or complete closure to fishing has been shown to weakly increase carbonate excretion on reefs at global scale (*Chapter 3*). However, the effects of

management vary depending on the socio-economic context (Cinner et al. 2018). Although marine protected areas in Australia are typically well-managed, no positive effect on fish carbonate excretion rate was detected (*Chapter 4*). This is likely a result of relatively low fishing pressure targeting a narrow range of species. Where fishing pressure is higher a positive effect of fisheries management may be observed (Salter et al. 2017). In The Bahamas, for instance, fish biodiversity and the biomass of commercially important large-bodied species is significantly higher in a no-take marine reserve compared to unprotected reefs (Mumby et al. 2006; Harborne et al. 2008). As a result, fish carbonate excretion rates inside the no-take reserve double those outside (Salter et al. 2017). Further, selective removal of species may drive changes in carbonate mineralogy altering the nature of fish carbonate contribution to inorganic carbon cycling (Salter et al. 2017). It is therefore clear that effective management actions adapted to the socio-economic context would be required to maintain this ecosystem function.

Current and future fish contribution to inorganic carbon cycling

Marine fish have been estimated to contribute 3-15% to the current global carbonate production in surface oceans, with less conservative estimates up to 45% (Wilson et al. 2009). These early estimates were based on the assumed proportional relationship between carbonate excretion rate and metabolic rate, which has recently been demonstrated (*Chapter 2*). However, evidence of additional relationships between carbonate excretion rate and fish traits suggests that carbonate production by fish may have been overestimated (*Chapter 2*). Estimating the global production rate is important to highlight the scale of the process. Fully understanding fish contribution to the inorganic carbon cycle, however, requires information on where the carbonate is excreted and its mineralogical composition.

Fish carbonate excretion rates vary primarily as a function of fish biomass (Salter et al. 2018, *Chapter 3*). The highest excretion rates are found in highly productive areas of the ocean that support high fish biomass, such as upwelling

regions, including the Eastern Tropical Pacific (Wilson et al. 2009, *Chapter 3*). These regions are hotspots of fish carbonate excretion. As they typically support high biomass of high trophic level fishes and water temperature is relatively low (Salinas-De-León et al. 2016), the main carbonate form excreted is HMC (*Chapter 3*). This suggests that in upwelling regions fish excrete large amounts of HMC which, given the low pH and shallow HMC saturation horizon (Sulpis et al. 2021), are likely to dissolve within a few hundred metres, releasing alkalinity and buffering against further decreases in pH.

Fish carbonate excretion rates also vary across latitude as a function of temperature, with higher rates per unit of biomass at lower latitudes (Wilson et al. 2009, *Chapter 3*). Here, ACMC and MHC are excreted in relatively higher proportions than at higher latitudes (*Chapter 3*) suggesting rapid dissolution of a large proportion of excreted carbonates. At higher latitudes, where temperatures are lower, fish excrete lower amounts of carbonate per unit of biomass and this mainly consist of calcite, including a relatively large proportion of low-magnesium calcite (LMC) (*Chapter 3*, Salter et al. 2019). A greater sedimentation potential of fish carbonates thus exists at higher latitudes. These however should be less stable as carbonate saturation states are lower in colder waters (Jiang et al. 2015).

The above interpretations are complicated by the fact that carbonate excretion rate and mineralogy depend on fish community structure and composition (*Chapter 3*). Large variability may occur within regions. This is particularly true for coral reefs (*Chapter 3*) and probably other coastal habitats where the trophic structure of fish communities is highly variable (Heenan et al. 2019), resulting in variable carbonate mineralogy at relatively small spatial scales. Fish trophic structure in open waters is less variable and typically dominated by middle and high trophic level fish (planktivores and predators). This means that pelagic fish should predominantly excrete HMC, although the magnesium content may vary across latitude as a function of temperature (Salter et al. 2019). This remains to be determined, and if true, then pelagic fish would contribute to the inorganic carbon cycle as previously hypothesised by Wilson et al. (2009).

Historical overfishing and collapse of fish stocks worldwide (Jackson et al. 2001; Christensen et al. 2014) mean that fish currently contribute less to the inorganic carbon cycle than in the past. Their role has likely changed through altered community structure and changes in carbonate mineralogy. By the 1990s, fishing is thought to have halved fish biomass and biogeochemical cycling compared to pre-exploitation (Bianchi et al. 2021). This has also likely resulted in halving of fish inorganic carbon cycling. In addition to the direct effect of fishing, coastal ecosystems are subject to a multitude of disturbances related to human population density which affect carbonate excretion rates (*Chapter 3*, *Chapter 4*). With the human population projected to reach nearly 10 billion people by 2050 (UN Department of Economic and Social Affairs - Population Division 2021), and population densities increasing on the coasts (Sing Wong et al. 2022), the impact on fish populations is only expected to increase, further decreasing the production of carbonate by fish.

Instead, fish carbonate excretion rates are expected to increase with increasing sea temperatures and dissolved CO_2 caused by anthropogenic climate change (Wilson et al. 2009; Grosell 2019). These expectations are based on their direct effects on individual fish. However, global fish biomass is projected to decrease with climate change (Lotze et al. 2019; Salvatteci et al. 2022) potentially offsetting its individual level effect. Further, fish species are shifting their distributions in response to climate change, leading to spatial changes in fish biomass and community structure and composition (e.g., Perry et al. 2005; Cheung et al. 2013; Campana et al. 2020; Antão et al. 2020). This will redistribute the spatial patterns in fish carbonate excretion rates and mineralogical composition. The proportions of the more soluble carbonate polymorphs produced by fish are predicted to increase with increasing temperatures (*Chapter 3*), changing the role of fish carbonates in the inorganic carbon cycle.

Limitations and research needs

The findings of this thesis certainly contribute to a better understanding of the role of fish in the marine inorganic carbon cycle. They have also highlighted

significant limitations and knowledge gaps that hamper our understanding of the services provided by fish carbonates and our ability to quantify fish contribution to inorganic carbon cycling outside tropical coastal areas. Opportunities for future research on the mechanisms of carbonate precipitation have also emerged from key findings of the thesis.

Fate of fish carbonates

The potentially significant role of fish carbonates in inorganic carbon cycling has been recognised. But our knowledge of the fate of fish carbonates post-excretion is extremely limited. This restricts our understanding of their significance in the regulation of ocean chemistry and carbon sequestration through sedimentation and enhancement of downward organic carbon export. To date, our interpretations are mainly based on solubility data from other biogenic carbonates. A single study measured the solubility of fish carbonates, testing HMC produced by the Gulf toadfish (*Opsanus beta*) (Woosley et al. 2012). Results indicate that fish-derived HMC is nearly twice as soluble as aragonite, and solubility is broadly comparable to HMC generated on the Bahamas Banks from other sources. However, HMC may vary in magnesium content, the primary factor influencing solubility, and more measurement across a spectrum of magnesium content are required. The mineralogy of fish carbonates is highly diverse and determines how rapidly and/or to which depth they dissolve and release alkalinity. Therefore, determining solubility of different carbonate polymorphs produced by fish is of primary importance. Priority should be given to the predominant polymorphs HMC and ACMC, which typically account for >50% of excreted carbonates (*Chapter 3*), but other carbonate polymorphs should also be analysed, particularly metastable MHC.

Further, new evidence suggests that we have yet to discover the full array of fish carbonate products. Analysing samples collected in Palau (*Chapter 2*) a new form of carbonate produced by fish was discovered – nesquehonite ($MgCO_3 \cdot 3H_2O$) – a form of hydrated magnesium carbonate mineral. This mineral is uncommon in the ocean, but it can be found as evaporative films on the wetland

water surface (Power et al. 2007). To the best of the author's knowledge, there is only one observation of bio-precipitation of nesquehonite, induced by the probiotic *Bacillus licheniformis* SRB2 (Zhao et al. 2019). This author cultured bacteria at 37°C at different Mg/Ca ratios and nesquehonite was precipitated only at Mg/Ca ratio $\geq$ 10 alongside MHC. The proportion of nesquehonite in that case increased with increasing Mg/Ca ratio (Zhao et al. 2019). Crystals of nesquehonite are prismatic, elongated, and a few hundred ʈm long (Figure 4.15). They were found in carbonates produced by four individual fishes belonging to three different species and families. In all cases, nesquehonite was produced alongside MHC in fishes with relatively long intestines. In two blackspotted pufferfish (*Arothron nigropunctatus*, f. Tetraodontidae, Figure 4.15) and a regal angelfish (*Pygoplites diacanthus*, f. Pomacanthidae) nesquehonite was the dominant carbonate form (60-75% of carbonate), while MHC represented a secondary product. Nesquehonite was also found in a sample of a bignose unicornfish (*Naso vlamingii*, f. Acanthuridae), in which MHC represented the dominant carbonate form. The Mg/Ca ratio in the fish intestine is often $\geq$ 10 (Grosell et al. 2001; Taylor and Grosell 2006), but nesquehonite has not been found in the carbonates of most species. The precipitation of nesquehonite may potentially require very high Mg/Ca ratios which might occur after the precipitation of MHC in fishes with relatively long intestines. Further, the high water temperature in Palau temperature (i.e., ~30°C) might have played a role in promoting nesquehonite precipitation. The mechanisms of nesquehonite precipitation in the fish intestine remain to be determined. Nevertheless, the fact that it has been found in carbonates of several species and families, and typically in large proportions, suggests that nesquehonite may not be irrelevant in the fish contribution to inorganic carbon cycling and should be further explored.

Database expansion

The current carbonate database is mainly limited to tropical and subtropical reef fishes. Additional data are needed to increase its taxonomic scope and thermal range and broaden the predictions to high-latitude and pelagic environments. Data
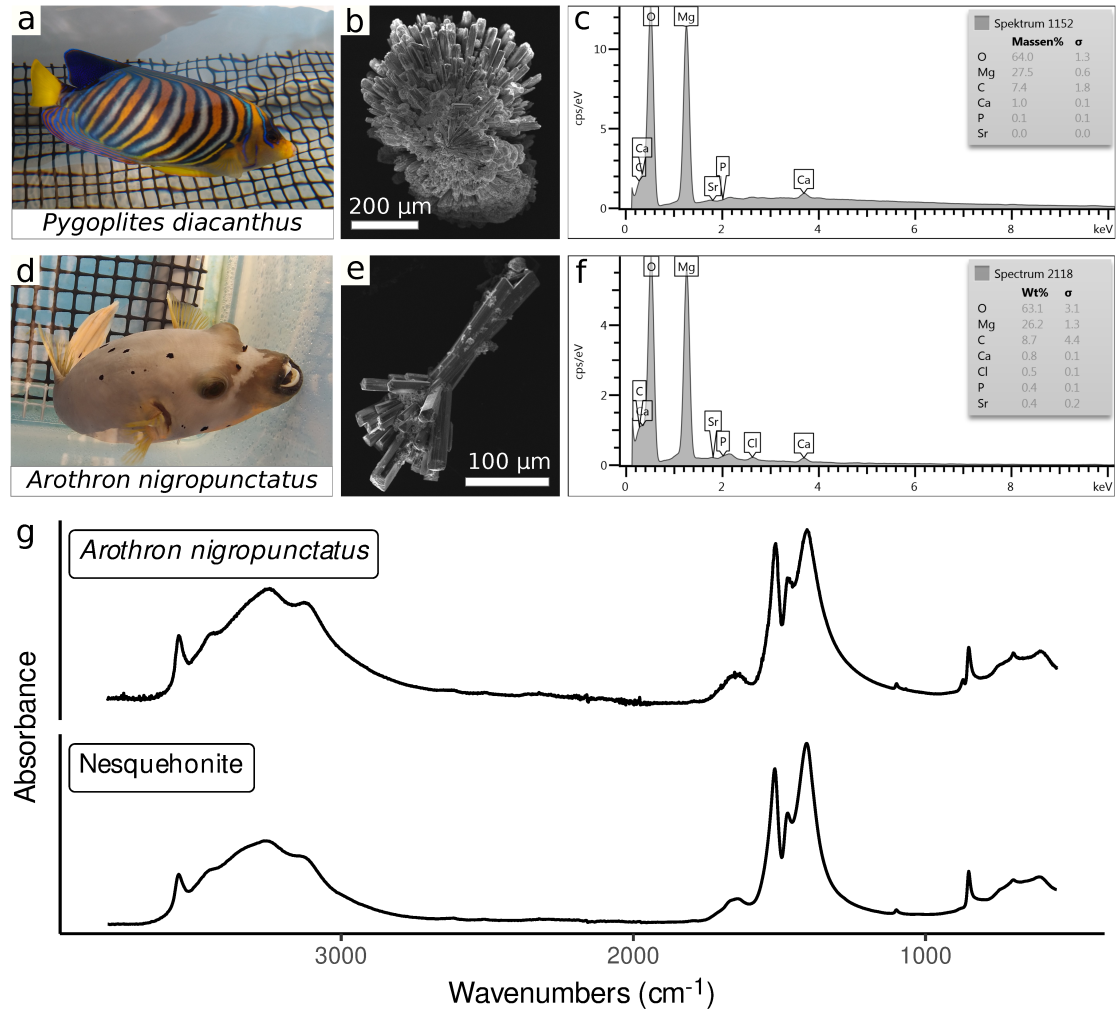
Figure 4.15: a-f Fish images, scanning electron microscope images, and energy-dispersive X-ray (EDX) spectra of nesquehonite crystals produced by the regal angelfish (*Pygoplites diacanthus*; **a-c**) and the blackspotted pufferfish (*Arothron nigropunctatus*; **d-f**). **g** Comparison between spectra obtained from Attenuated total reflectance Fourier transform infrared (ATR-FTIR) analysis of fish-produced nesquehonite and the same mineral from the University of Arizona Mineral Museum. Nesquehonite ATR-FTIR spectrum was dowloaded from the RRUFF database (`https://rruff.info/Nesquehonite/R050639`).

collection campaigns should be targeted to: 1) fish families representing large proportion of biomass in the ocean (small pelagic and mesopelagic fishes), 2) temperate and high-latitude environments, 3) high and low salinity areas (e.g., Red Sea, Mediterranean, Baltic Sea). This would open the possibility of testing the robustness of recent findings and refining both regional and global estimates of carbonate excretion rates and mineralogy. Progress in this direction has been made and mineralogical data now exist for several temperate species (Salter et al. 2019). If associated excretion rate data become available, predictions could be initially extended to temperate regions.

Model improvements

An expansion of the carbonate excretion rate database to include further species and families would certainly allow for improvements of current carbonate production models. Data from temperate and high-latitude areas would refine the temperature relationship and allow more accurate predictions. Other known drivers could be included as predictors in the models. For instance, salinity would improve predictions for high and low salinity areas and can easily be integrated if data from these areas (e.g., Red Sea, Mediterranean, Baltic Sea) become available. Current models make predictions for fish that are at rest and should be improved to predict carbonate excretion rates for fish in their natural habitat and activity levels. This may not be trivial and at best requires knowledge of field metabolic rates, diet, feeding rates, the elemental composition of the food, and the proportion of food-derived calcium that is precipitated. In addition to the improvement of current models, the creation of new models, such as bioenergetic models, is encouraged.

Laboratory experiments

Climate change is predicted to affect fish carbonate excretion rates and mineralogy. Therefore, there is a need for additional experiments to test fish carbonate excretion and dissolution under climate change relevant scenarios of temperature and CO_2 in representative species from different climate regions. Further, experiments

on fish that are not fasted are particularly important to allow model parameterisation to predict carbonate excretion and mineralogy in fish in natural conditions.

Physiological research

Findings within this thesis identified a strong relationship between relative intestinal length and the excretion rate and mineralogical composition of fish carbonates. Hypotheses are proposed here to explain these relationships. Interspecific variability in intestinal water absorption efficiency and gut residence times are two potential viable explanations. Data on these fish traits are limited and further research is required to test these hypotheses or formulate new ones and understand the mechanistic links underlying the observed patterns.

Causal inference in ecosystem functioning research

Causal questions are central in ecology and ecosystem functioning research. In certain contexts, randomised controlled experiments are used to answer cause and effect relationships, such as the effect of biodiversity on ecosystem functioning (e.g., Veen et al. 2018; Jochum et al. 2020). Observational data may prove useful in answering causal questions in ecology when these experiments are not feasible. However, conclusions regarding ecological relationships are commonly drawn from observational data by applying statistical techniques which are not valid for causal inference, such as predictive techniques (Arif and MacNeil 2022a). Causal inference methods are regularly employed in other fields, such as in the social sciences (Gangl 2010), but the importance of their application to ecological research has only recently been underlined (Arif and MacNeil 2022a).

The Structural Causal Modelling (SCM) framework (Pearl 2009) is one of several causal inference method and has recently been introduced in ecology (Cronin and Schoolmaster 2018; Schoolmaster et al. 2020; Arif et al. 2022; Arif and MacNeil 2022a). This framework allows researchers to determine the variables required to answer specific causal questions, given a hypothesised causal structure, through a two-step process. First a Directed Acyclic Graph (DAG) is created to visualise

the assumed causal relationships in the study system reflecting current domain knowledge. Then, the backdoor criterion is applied to determine 1) whether the hypothesised causal effect of X on Y can be accurately estimated given a set of observed variables and, if so, 2) which variables are required to estimate the causal effect without bias. The backdoor criterion is the process of blocking all non-causal paths (backdoor paths) between X and Y, while leaving all causal paths open. This removes common statistical biases such as collider, confounding, and overcontrol bias. It is not the purpose of this section to provide a detailed explanation of how to construct DAGs and apply the backdoor criterion, so I refer interested readers to studies in which these have been thoroughly explained (Cronin and Schoolmaster 2018; Schoolmaster et al. 2020; Arif et al. 2022; Arif and MacNeil 2022a). The set of variables identified through the backdoor criterion is then included into an appropriate statistical model which can assume any form and distribution. From this model, only the effect of X (the variable of interest) is interpreted. The other predictor variables act as controls. This approach differs from the one common in ecology, where all hypothesised predictors are included into one model and all effects are interpreted. This also includes the models in the first two chapters of this thesis. Reanalysing our data within a causal framework may reveal further insights as observed in other studies (Arif et al. 2022).

In *Chapter 3* of this thesis we applied the SCM framework to estimate the causal effects of a set of ecological, environmental and socio-economic variables on fish carbonate excretion rate and mineralogy. This study represents one of the first applications of causal inference in ecology and specifically in ecosystem functioning research (Arif and MacNeil 2022b). DAGs representing the causal structure underlying ecosystem functions are likely to be complex given the many relevant variables that should be included to obtain accurate estimates of causal effects. This is particularly true for complex social-ecological systems such as coral reefs. Our study sets as an example for future research aimed at determining drivers of ecosystem functions and use them to predict future levels of ecosystem functioning. Indeed, results from causal inference can be used to inform predictive

approaches. Our results, for instance, can be used to select predictors which should be included in a predictive model to quantify how fish inorganic carbon cycling may change under different scenarios. Included predictors would be variables shown to have a causal effect on the response (Arif et al. 2022).

Conclusions

This thesis identifies the drivers of the role of fish in the marine inorganic carbon cycle at different ecological levels and spatial scales. It provides much needed knowledge to improve the quantification of fish inorganic carbon cycling and predict future changes in ecosystem functioning and services. Beyond identifying the drivers of fish carbonate excretion rates, this work takes a novel step further providing a thorough analysis of the drivers of the mineralogy of excreted carbonates. This increases the value of the results in the context of comprehending the services sustained by this ecosystem function.

The compilation and analysis of a large database of intestinal morphology demonstrated that whilst intestinal length, diameter, and surface area are phylogenetically conserved and depend on body morphology, they are strongly related to trophic level (*Chapter 1*). Building on this, a first comprehensive assessment of potential drivers of fish carbonate excretion rates and mineralogy provided empirical evidence in support of the link between metabolic rate and carbonate excretion rate. While it supports earlier estimates of carbonate production, it also identified new traits underpinning this function that warrant a refinement of these estimates (*Chapter 2*). This analysis also provided new predictive models for the quantification of carbonate excretion rate and mineralogy. Combining these models with a global database of reef fish surveys led to the production of the first global scale maps of reef fish carbonate excretion and mineralogy (*Chapter 3*). The application of a causal inference approach revealed the ecological, environmental, and socio-economic drivers underlying the observed spatial patterns. This analysis showed a strong impact of human pressure on fish carbonate excretion rate and a

weak management effect. A follow up study focused on Australian reefs revealed that the human impact on fish inorganic carbon cycling is mediated by a decrease in fish biomass, but this is not necessarily a result of fishing pressure (*Chapter 4*). In areas were fishing pressure is relatively low fish carbonate excretion rate may still be impacted by high human densities and a number of related disturbances. In this context current management measures do not support fish inorganic carbon cycling. Context-tailored conservation strategies aimed at reducing the negative effects of socio-economic factors would be required alongside fisheries regulations to sustain this ecosystem function.

Although this thesis focused on tropical and subtropical reef fish, the findings should be broadly applicable as the underlying mechanisms are common to fish in general, but their robustness should be tested with additional data. The new predictive models (*Chapter 2*) are an important step forward in the quantification of fish inorganic carbon cycling as they can compute excretion rates of different carbonate polymorphs for individual fishes. Their taxonomic and thermal scope is still limited and targeted data collection campaigns are needed to increase the proportion of biomass in the ocean for which predictions can be made.

It is now clear that fish play a much more complex role in the inorganic carbon cycle than previously thought. Their contribution is highly variable through space and most likely over time both for the quantity of carbonate produced and for its mineralogical composition. This thesis provides a solid foundation to understand this complexity, and highlights key outstanding knowledge gaps on the fate of fish carbonates. This is the next required step to understand this process well enough to inform, together with other fish carbon services, effective policies and management of fish populations as an additional nature-based solution for climate change mitigation and adaptation (Lutz and Martin 2014; Martin et al. 2021; Saba et al. 2021).

References

Antão, Laura H. et al. (2020). "Temperature-related biodiversity change across temperate marine and terrestrial systems". In: *Nature Ecology and Evolution* 4.7, pp. 927–933. DOI: 10.1038/s41559-020-1185-7.

Arif, Suchinta and Aaron MacNeil (2022a). "Predictive models aren't for causal inference". In: *Ecology Letters* 25, pp. 1741–1745. DOI: 10.1111/ele.14033.

Arif, Suchinta and M. Aaron MacNeil (2022b). "Utilizing causal diagrams across quasi-experimental approaches". In: *Ecosphere* 13, e4009. DOI: 10.1002/ecs2.4009.

Arif, Suchinta et al. (2022). "Causal drivers of climate-mediated coral reef regime shifts". In: *Ecosphere* 13.3, e3956. DOI: 10.1002/ecs2.3956.

Bellwood, David R. et al. (2019a). "Coral reef conservation in the Anthropocene: Confronting spatial mismatches and prioritizing functions". In: *Biological Conservation* 236.March, pp. 604–615. DOI: 10.1016/j.biocon.2019.05.056.

Bianchi, Daniele et al. (2021). "Estimating global biomass and biogeochemical cycling of marine fish with and without fishing". In: *Science Advances* 7, eabd7554. DOI: 10.1126/sciadv.abd7554.

Campana, Steven E. et al. (2020). "Shifting fish distributions in warming sub-Arctic oceans". In: *Scientific Reports* 10, p. 16448. DOI: 10.1038/s41598-020-73444-y.

Cheung, William W.L. et al. (2013). "Shrinking of fishes exacerbates impacts of global ocean changes on marine ecosystems". In: *Nature Climate Change* 3.3, pp. 254–258. DOI: 10.1038/nclimate1691.

Christensen, Villy et al. (2014). "A century of fish biomass decline in the ocean". In: *Marine Ecology Progress Series* 512, pp. 155–166. DOI: 10.3354/meps10946.

Cinner, Joshua E et al. (2016). "Bright spots among the world's coral reefs". In: *Nature* 535.7612, pp. 416–419. DOI: 10.1038/nature18607.

Cinner, Joshua E. et al. (2018). "Gravity of human impacts mediates coral reef conservation gains". In: *Proceedings of the National Academy of Sciences of the United States of America* 115.27, E6116–E6125. DOI: 10.1073/pnas.1708001115.

Cinner, Joshua E. et al. (2020). "Meeting fisheries, ecosystem function, and biodiversity goals in a human-dominated world". In: *Science* 368.6488, pp. 307–311. DOI: 10.1126/science.aax9412.

Cronin, James Patrick and Donald R. Jr. Schoolmaster (2018). "A causal partition of trait correlations: using graphical models to derive statistical models from theoretical language". In: *Ecosphere* 9.9, e02422. DOI: 10.1002/ecs2.2422.

Duarte, Carlos M. et al. (2020). "Rebuilding marine life". In: *Nature* 580.7801, pp. 39–51. DOI: 10.1038/s41586-020-2146-7.

Duffy, J. Emmett et al. (2016). "Biodiversity enhances reef fish biomass and resistance to climate change". In: *Proceedings of the National Academy of Sciences of the United States of America* 113.22, pp. 6230–6235. DOI: 10.1073/pnas.1524465113.

Elliott, J. P. and D. R. Bellwood (2003). "Alimentary tract morphology and diet in three coral reef fish families". In: *Journal of Fish Biology* 63, pp. 1598–1609. DOI: 10.1046/j.1095-8649.2003.00272.x.

Figuerola, Blanca et al. (2023). "Temperature as a likely driver shaping global patterns in mineralogical composition in bryozoans: implications for marine calcifiers under global change". In: *Ecography* 2023, e06381. DOI: 10.1111/ecog.06381.

Fontoura, Luisa et al. (2022). "Protecting connectivity promotes successful biodiversity and fisheries conservation". In: *Science* 375, pp. 336–340. DOI: `10.1126/science.abg4351Protecting`.

Foran, Elizabeth, Steve Weiner, and Maoz Fine (2013). "Biogenic fish-gut calcium carbonate is a stable amorphous phase in the gilt-head seabream, sparus aurata". In: *Scientific Reports* 3, p. 1700. DOI: `10.1038/srep01700`.

Gangl, Markus (2010). "Causal inference in sociological research". In: *Annual Review of Sociology* 36, pp. 21–47. DOI: `10.1146/annurev.soc.012809.102702`.

Genz, J., J. R. Taylor, and M. Grosell (2008). "Effects of salinity on intestinal bicarbonate secretion and compensatory regulation of acid-base balance in *Opsanus beta*". In: *Journal of Experimental Biology* 211.14, pp. 2327–2335. DOI: `10.1242/jeb.016832`.

Grosell, Martin (2019). "CO2 and calcification processes in fish". In: *Fish Physiology.* Ed. by Martin Grosell et al. 1st ed. Vol. 37. Elsevier Inc., pp. 133–159. DOI: `10.1016/bs.fp.2019.07.002`.

Grosell, Martin et al. (2001). "Intestinal HCO3- secretion in marine teleost fish: Evidence for an apical rather than a basolateral Cl-/HCO3- exchanger". In: *Fish Physiology and Biochemistry* 24.2, pp. 81–95. DOI: `10.1023/A:1011994129743`.

Harborne, Alastair R. et al. (2008). "Reserve effects and natural variation in coral reef communities". In: *Journal of Applied Ecology* 45.4, pp. 1010–1018. DOI: `10.1111/j.1365-2664.2008.01490.x`.

Heenan, Adel, Gareth J. Williams, and Ivor D. Williams (2019). "Natural variation in coral reef trophic structure across environmental gradients". In: *Frontiers in Ecology and the Environment* 18.2, pp. 69–75. DOI: `10.1002/fee.2144`.

Heuer, Rachael M. et al. (2016). "Changes to intestinal transport physiology and carbonate production at various CO2 levels in a marine teleost, the Gulf Toadfish (*Opsanus beta*)". In: *Physiological and Biochemical Zoology* 89.5, pp. 402–416. DOI: `10.1086/688235`.

Hughes, Terry P. et al. (2017a). "Coral reefs in the Anthropocene". In: *Nature* 546.7656, pp. 82–90. DOI: `10.1038/nature22901`.

Al-Hussaini, A. H. (1947). "The feeding habits and the morphology of the alimentary tract of some teleosts living in the neighbourhood of the Marine Biological Station, Ghardaga, Red Sea." In: *Publications of the Marine Biology Station, Ghardaga, Red Sea* 5, pp. 1–61.

Jackson, Jeremy B.C. et al. (2001). "Historical overfishing and the recent collapse of coastal ecosystems". In: *Science* 293.5530, pp. 629–637. DOI: `10.1126/science.1059199`. arXiv: `484`.

Jennings, Simon and Rod W. Wilson (2009). "Fishing impacts on the marine inorganic carbon cycle". In: *Journal of Applied Ecology* 46.5, pp. 976–982. DOI: `10.1111/j.1365-2664.2009.01682.x`.

Jiang, Li Qing et al. (2015). "Climatological distribution of aragonite saturation state in the global oceans". In: *Global Biogeochemical Cycles* 29.10, pp. 1656–1673. DOI: `10.1002/2015GB005198`.

Jochum, Malte et al. (2020). "The results of biodiversity–ecosystem functioning experiments are realistic". In: *Nature ecology & evolution* 4.11, pp. 1485–1494.

Lefcheck, Jonathan S. et al. (2021). "Species richness and identity both determine the biomass of global reef fish communities". In: *Nature Communications* 12, p. 6875. DOI: `10.1038/s41467-021-27212-9`.

Lotze, Heike K. et al. (2019). "Global ensemble projections reveal trophic amplification of ocean biomass declines with climate change". In: *Proceedings of the National Academy of Sciences of the United States of America* 116.26, pp. 12907–12912. DOI: `10.1073/pnas.1900194116`.

Lutz, S. J. and A. H. Martin (2014). *Fish Carbon: Exploring Marine Vertebrate Carbon Services*. Arendal, Norway: GRID-Arendal.

Mariani, Gaël et al. (2020). "Let more big fish sink: Fisheries prevent blue carbon sequestration-half in unprofitable areas". In: *Science Advances* 6.44, pp. 1–9. DOI: `10.1126/sciadv.abb4848`.

Martin, Angela Helen et al. (2021). "Integral functions of marine vertebrates in the ocean carbon cycle and climate change mitigation". In: *One Earth* 4.5, pp. 680–693. DOI: `10.1016/j.oneear.2021.04.019`.

McClanahan, Tim R. et al. (2019). "Global baselines and benchmarks for fish biomass: Comparing remote reefs and fisheries closures". In: *Marine Ecology Progress Series* 612, pp. 167–192. DOI: `10.3354/meps12874`.

McLean, Matthew et al. (2021). "Trait similarity in reef fish faunas across the world's oceans". In: *Proceedings of the National Academy of Sciences of the United States of America* 118.12, e2012318118. DOI: `10.1073/pnas.2012318118`.

Mekuchi, Miyuki, Tamao Hatta, and Toyoji Kaneko (2010). "Mg-calcite, a carbonate mineral, constitutes Ca precipitates produced as a byproduct of osmoregulation in the intestine of seawater-acclimated Japanese eel *Anguilla japonica*". In: *Fisheries Science* 76.2, pp. 199–205. DOI: `10.1007/s12562-009-0199-5`.

Mellin, Camille et al. (2016a). "Humans and seasonal climate variability threaten large-bodied coral reef fish with small ranges". In: *Nature Communications* 7, p. 10491. DOI: `10.1038/ncomms10491`.

Mora, Camilo et al. (2011). "Global human footprint on the linkage between biodiversity and ecosystem functioning in reef fishes". In: *PLoS Biology* 9.4, e1000606. DOI: `10.1371/journal.pbio.1000606`.

Morais, Renato A. and David R. Bellwood (2020). "Principles for estimating fish productivity on coral reefs". In: *Coral Reefs* 39.5, pp. 1221–1231. DOI: `10.1007/s00338-020-01969-9`.

Morais, Renato A., Sean R. Connolly, and David R. Bellwood (2020b). "Human exploitation shapes productivitybiomass relationships on coral reefs". In: *Global Change Biology* 26.3, pp. 1295–1305. DOI: `10.1111/gcb.14941`.

Morais, Renato A. et al. (2021). "Spatial subsidies drive sweet spots of tropical marine biomass production". In: *PLoS Biology* 19.11, pp. 4–6. DOI: `10.1371/journal.pbio.3001435`.

Mumby, Peter J. et al. (2006). "Fishing, trophic cascades, and the process of grazing on coral reefs". In: *Science* 311.5757, pp. 98–101. DOI: `10.1126/science.1121129`.

Parravicini, V. et al. (2021). "Coral reef fishes reveal strong divergence in the prevalence of traits along the global diversity gradient". In: *Proceedings of the Royal Society B: Biological Sciences* 288, p. 20211712. DOI: `10.1098/rspb.2021.1712`.

Parravicini, Valeriano et al. (2013). "Global patterns and predictors of tropical reef fish species richness". In: *Ecography* 36.12, pp. 1254–1262. DOI: `10.1111/j.1600-0587.2013.00291.x`.

Pearl, Judea (2009). *Causality: models, reasoning and inference*. 2nd. Cambridge, UK: Cambridge University Press.

Perry, Allison L. et al. (2005). "Climate change and distribution shifts in marine fishes". In: *Science* 308.5730, pp. 1912–1915. DOI: `10.1126/science.1111322`.

Perry, Chris T. et al. (2011). "Fish as major carbonate mud producers and missing components of the tropical carbonate factory". In: *Proceedings of the National Academy of Sciences* 108.10, pp. 3865–3869. DOI: `10.1073/pnas.1015895108`.

Power, Ian M. et al. (2007). "Biologically induced mineralization of dypingite by cyanobacteria from an alkaline wetland near Atlin, British Columbia, Canada". In: *Geochemical Transactions* 8.February. DOI: `10.1186/1467-4866-8-13`.

Saba, Grace K. et al. (2021). "Toward a better understanding of fish-based contribution to ocean carbon flux". In: *Limnology and Oceanography* 66.5, pp. 1639–1664. DOI: `10.1002/lno.11709`.

Salinas-De-León, Pelayo et al. (2016). "Largest global shark biomass found in the northern Galápagos Islands of Darwin and Wolf". In: *PeerJ* 4, e1911. DOI: `10.7717/peerj.1911`.

Salter, Michael A., Chris T. Perry, and Abigail M. Smith (2019). "Calcium carbonate production by fish in temperate marine environments". In: *Limnology and Oceanography* 64.6, pp. 2755–2770. DOI: `10.1002/lno.11339`.

Salter, Michael A., Christopher T. Perry, and Rod W. Wilson (2012). "Production of mud-grade carbonates by marine fish: Crystalline products and their sedimentary significance". In: *Sedimentology* 59.7, pp. 2172–2198. DOI: `10.1111/j.1365-3091.2012.01339.x`.

Salter, Michael A. et al. (2017). "Phase heterogeneity in carbonate production by marine fish influences their roles in sediment generation and the inorganic carbon cycle". In: *Scientific Reports* 7.1, pp. 1–15. DOI: `10.1038/s41598-017-00787-4`.

Salter, Michael A. et al. (2018). "Reef fish carbonate production assessments highlight regional variation in sedimentary significance". In: *Geology* 46.8, pp. 699–702. DOI: `10.1130/G45286.1`.

Salvatteci, Renato et al. (2022). "Smaller fish species in a warm and oxygen-poor Humboldt Current system". In: *Science* 375.6576, pp. 101–104. DOI: `10.1126/science.abj0270`.

Schauer, Kevin L. et al. (2018). "Interrogation of the Gulf toadfish intestinal proteome response to hypersalinity exposure provides insights into osmoregulatory mechanisms and regulation of carbonate mineral precipitation". In: *Comparative Biochemistry and Physiology - Part D: Genomics and Proteomics* 27.June, pp. 66–76. DOI: `10.1016/j.cbd.2018.06.004`.

Schiettekatte, Nina M D et al. (2022a). "Biological trade-offs underpin coral reef ecosystem functioning". In: *Nature Ecology and Evolution*. DOI: `10.1038/s41559-022-01710-5`.

Schiettekatte, Nina M.D. et al. (2020). "Nutrient limitation, bioenergetics and stoichiometry: A new model to predict elemental fluxes mediated by fishes". In: *Functional Ecology* 34.9, pp. 1857–1869. DOI: `10.1111/1365-2435.13618`.

Schoolmaster, Donald R. Jr., Chad R. Zirbel, and James Patrick Cronin (2020). "A graphical causal model for resolving species identity effects and biodiversityecosystem function correlations". In: *Ecology* 101.8, e03070. DOI: `10.1002/ecy.3070`.

Seguin, Raphael et al. (2022). "Towards process-oriented management of tropical reefs in the anthropocene". In: *Nature Sustainability*. DOI: `10.1038/s41893-022-00981-x`.

Sing Wong, Amy, Spyridon Vrontos, and Michelle L. Taylor (2022). "An assessment of people living by coral reefs over space and time". In: *Global Change Biology* 28.23, pp. 7139–7153. DOI: 10.1111/gcb.16391.

Steinberg, Christian E.W. (2018). "Diets and Digestive Tracts Your Food Determines Your Intestine'". In: *Aquatic Animal Nutrition: A Mechanistic Perspective from Individuals to Generations*. Springer International Publishing, pp. 9–59. DOI: 10.1007/978-3-319-91767-2.

Sulpis, Olivier et al. (2021). "Calcium carbonate dissolution patterns in the ocean". In: *Nature Geoscience* 14.6, pp. 423–428. DOI: 10.1038/s41561-021-00743-y.

Takei, Yoshio and Takehiro Tsukada (2001). "Ambient temperature regulates drinking and arterial pressure in eels". In: *Zoological Science* 18.7, pp. 963–967. DOI: 10.2108/zsj.18.963.

Taylor, Josi R. and Martin Grosell (2006). "Feeding and osmoregulation: Dual function of the marine teleost intestine". In: *Journal of Experimental Biology* 209.15, pp. 2939–2951. DOI: 10.1242/jeb.02342.

UN Department of Economic and Social Affairs - Population Division (2021). *Global Population Growth and Sustainable Development*. Tech. rep. UN DESA/POP/2021/TR/NO. 2. URL: www.unpopulation.org..

Van Vuuren, Detlef P et al. (2014). "A new scenario framework for Climate Change Research : scenario matrix architecture". In: *Climate Change* 122, pp. 373–386. DOI: 10.1007/s10584-013-0906-1.

Veen, G. F., Wim H. van der Putten, and T. Martijn Bezemer (2018). "Biodiversity-ecosystem functioning relationships in a long-term non-weeded field experiment". In: *Ecology* 99.8, pp. 1836–1846. DOI: 10.1002/ecy.2400.

Wagner, Catherine E et al. (2009). "Diet predicts intestine length in Lake Tanganyika' s cichlid fishes". In: *Functional Ecology* 23, pp. 1122–1131. DOI: 10.1111/j.1365-2435.2009.01589.x.

Walsh, Patrick J. et al. (1991). "Carbonate deposits in marine fish intestines: A new source of biomineralization". In: *Limnology and Oceanography* 36.6, pp. 1227–1232. DOI: 10.4319/lo.1991.36.6.1227.

Williams, Gareth J. and Nicholas A.J. Graham (2019). "Rethinking coral reef functional futures". In: *Functional Ecology* 33.6, pp. 942–947. DOI: 10.1111/1365-2435.13374.

Wilson, Rod W., Jonathan M. Wilson, and Martin Grosell (2002). "Intestinal bicarbonate secretion by marine teleost fish-why and how?" In: *Biochimica et Biophysica Acta* 1566, pp. 182–193. DOI: 10.1016/s0005-2736(02)00600-4.

Wilson, Rod W. et al. (2009). "Contribution of fish to the marine inorganic carbon cycle". In: *Science* 323.January, pp. 359–362. DOI: 10.1126/science.1157972.

Woosley, Ryan J., Frank J. Millero, and Martin Grosell (2012). "The solubility of fish-produced high magnesium calcite in seawater". In: *Journal of Geophysical Research: Oceans* 117.4, pp. 1–5. DOI: 10.1029/2011JC007599.

Zhao, Yanyang et al. (2019). "Bio-precipitation of calcium and magnesium ions through extracellular and intracellular process induced by bacillus licheniformis SRB2". In: *Minerals* 9.9, pp. 1–23. DOI: 10.3390/min9090526.

Universität Bremen
Fachbereich 2
Prüfungsamt Chemie
z. Hd. Frau Frauke Ernst
Leobener Straße

28359 Bremen
Deutschland

.

Prüfungsamt
Chemie

Frauke Ernst
Geschäftsstelle
Fachbereich 02
Leobener Str. / NW2
D-28359 Bremen

Verwaltungspavillon 06
Tel. 0421 218-62802
Fax 0421 218-9862802
frauke.ernst@uni-bremen.de
www.fb2.uni-bremen.de

<u>Versicherung an Eides Statt</u>

Name, Vorname	Ghilardi, Mattia
Matrikel-Nr.	
Straße	Hollerallee 30E
Ort, PLZ	Bremen, 28209

Ich, Mattia Ghilardi (Vorname, Name)

versichere an Eides Statt durch meine Unterschrift, dass ich die vorstehende Arbeit selbständig und ohne fremde Hilfe angefertigt und alle Stellen, die ich wörtlich dem Sinne nach aus Veröffentlichungen entnommen habe, als solche kenntlich gemacht habe, mich auch keiner anderen als der angegebenen Literatur oder sonstiger Hilfsmittel bedient habe.
Ich versichere an Eides Statt, dass ich die vorgenannten Angaben nach bestem Wissen und Gewissen gemacht habe und dass die Angaben der Wahrheit entsprechen und ich nichts verschwiegen habe.
Die Strafbarkeit einer falschen eidesstattlichen Versicherung ist mir bekannt, namentlich die Strafandrohung gemäß § 156 StGB bis zu drei Jahren Freiheitsstrafe oder Geldstrafe bei vorsätzlicher Begehung der Tat bzw. gemäß § 161 Abs. 1 StGB bis zu einem Jahr Freiheitsstrafe oder Geldstrafe bei fahrlässiger Begehung.

_____
Ort, Datum / Unterschrift

Universität Bremen

Ort, Datum: _____

.

Erklärungen zur elektronischen Version und zur Überprüfung einer Dissertation

Hiermit betätige ich gemäß §7, Abs. 7, Punkt 4, dass die zu Prüfungszwecken beigelegte elektronische Version meiner Dissertation identisch ist mit der abgegebenen gedruckten Version.

Ich bin mit der Überprüfung meiner Dissertation gemäß §6 Abs. 2, Punkt 5 mit qualifizierter Software im Rahmen der Untersuchung von Plagiatsvorwürfen einverstanden.

_____

Unterschrift